A SMALL STRAIN LARGE ROTATION THEORY AND FINITE ELEMENT FORMULATION OF THIN CURVED BEAMS

A THESIS SUBMITTED FOR THE DEGREE OF DOCTOR OF PHILOSOPHY IN THE DEPARTMENT OF CIVIL ENGINEERING AT THE CITY UNIVERSITY

BY

ABDELRAHMAN ELZUBEIR MOHAMED BSc, MSc

THE CITY UNIVERSITY APRIL 1983

To my Parents

ABSTRACT

In this thesis a theory for the geometrically nonlinear analysis of thin curved beam-type structures is proposed and an associated displacement finite element formulation developed.

An exact two-dimensional large rotation theory, which is based on an intrinsic coordinate system, has been developed. Four alternative Lagrangian formulations of the theory have been presented for comparison.

A family of two-dimensional thin curved beam elements has been developed by using the constraint technique to include the convective coordinate system. The elements are relatively simple and the minimum number of degrees of freedom necessary has been used.

The Total Lagrangian formulation has been shown to be numerically more effective than the Updated Lagrangian formulation. A new Total Lagrangian formulation that includes the effect of curvature change on axial force in the incremental equilibrium equations has been developed. The formulation is based on the geometric strains and has the capability of predicting true axial force values in large rotation and curvature problems. This approach can be used in the general continuum mechanics large deformation formulations.

A large rotation theory for three-dimensional beams and Total Lagrangian formulations of the theory, which are based on the Green strains and the geometric strains, have been developed. The theory correctly describes the large rotation elastic response of a thin eccentric curved beam of rectangular cross-section. Material nonlinearity, which is based on the von-Mises yield function and the Prandtl-Reuss flow rule and in which isotropic hardening is assumed, has been included in the formulation.

A family of three-dimensional beam elements, that can accurately accommodate the theory, has been developed by the constraint technique. The elements are suitable for use as stiffeners in the analysis of stiffened shell structures.

The elements, which have been developed, have been implemented in the LUSAS finite element system. The accuracy of the results obtained has been demonstrated by comparison with published results.

ACKNOWLEDGEMENTS

The research described herein was undertaken in the Department of Civil Engineering of The City University. During the course of the research the author received valuable advice and helpful suggestions from many persons. In particular the author wishes to express his gratitude to the following:

To Professor J. E. Gibson, Head of the Department, for the helpful way in which the project was accommodated.

To Dr. L. F. Boswell, who supervised this work, for his constant encouragement, his valuable advice and his guidance throughout the duration of the project, without which the effective fulfilment of this work would not have been possible.

To Dr. L. P. R. Lyons for his kind help, his constant supervision and his helpful suggestions which directly contributed to the formulation of the ideas in this study. His help and advice regarding the use of the LUSAS finite element system is greatly appreciated.

To Dr. S. H. Zhang, Dr. D. Irving, Mr. A. M. Kareem and Mr. N. El-Kaddah for their generous help in many ways.

To the staff of The City University Computer Centre whose effort is appreciated.

To Mrs Calda Petrie who typed the manuscript.

To The Sudan Government for providing financial support.

Last, but not least, to my family and friends for their love and encouragement.

NOTATION

Only the main symbols are listed here. Other symbols are defined as they first appear in the text:

A	Cross-sectional Area
Ae	First moment of area about the reference line
A_θ	Matrix of displacement gradients obtained from the nonlinear strains
a_t^i	Wanted element variables up to the i^{th} iteration referred to the configuration at time t(t = O or t)
a_c^i	Wanted element variables from the beginning of an increment up to the i^{th} iteration
B	Strain matrix relating the variation in the continuum mechanics strains to the variation in displacements
$\bar{B}$	Strain matrix relating to the variation in the strain resultants to the variation in the nodal variables
B_t^o, $\bar{B}_t^o$	Infinitesimal strain matrix with reference to the configuration at time t (t = O or t)
$B_L(u_t)$, $\bar{B}_L(a_t)$	Linear strain matrix with reference to the configuration at time t (t = O or t)

b	Breadth of the cross-section
b	Unwanted element variables
$[cs]_i$	Matrix of direction cosines at point i
D, $\mathbf{D}^e$	Elastic modulus matrices
$\bar{\mathbf{D}}$, $\bar{\mathbf{D}}^e$	Elastic rigidity matrices
D(σ,k),**D**(**s**,k)	Elasto-plastic modulus matrices
$\bar{\mathbf{D}}$(**s**,k)	Elasto-plastic rigidity matrix
d	Depth of the cross-section
$\underset{\sim}{d}$	Displacement vector of a general point
E	Young's modulus of elasticity
e	Green strain measure of the reference line
e	Strains referred to spatial coordinates in the deformed geometry
e_y, e_z	Eccentricities along the local y, z axes respectively
F, f	Yield functions
F_{yz}	Shear stress resultant
$\underset{\sim}{f}$	Vector of uniformly distributed loads acting in a fixed direction
G_t	Matrix relating the variation of the vector of the generalised strain resultants to the variation in the nodal variables with reference to the configuration at time t (t = O or t)
G	Shear modulus
$\hat{\mathbf{g}}$	Natural base vector in two dimensions

g_x, g_y, g_z	Displacement gradient vectors
g^y, g^z	Vectors normal to the convected x surface in the deformed configuration
$\mathbf{H}$	Matrix relating the Green strains or the geometric strains to generalised strain resultants
$\mathbf{H}^*$	Matrix relating the variation in the geometric strains to the variation in the Green strains
I	Second moment of area about the reference line
$[I]$	Unit matrix
I_{yy}, I_{zz}	Second moments of area about the centroidal axes of the cross-section
$\hat{i}, \hat{j}, \hat{k}$	Unit vectors in the global X,Y,Z directions respectively
J	Torsional rigidity
$K_o, K_L(a_t)$	Infinitesimal strain and initial displacement stiffness matrices respectively
K_T	Tangent stiffness matrix
K_σ	Initial stress stiffness matrix
K_σ^*	Additional initial stress stiffness matrix
K	Physical curvature in two dimensions
K_{xy}, K_{xz}	Measures of bending curvatures about the local y and z axes respectively

k	Strain hardening parameter
k_1, k_2	Factors included in the shear rigidity terms to describe the torsion of a solid rectangular cross-section
k_s	Factor included in the shear modulus terms to improve the shear displcement approximation
L	Length
M, M^*	Constraint matrix in terms of the initial total element variables
M_A, M_B	Partitions of the constraint matrix with reference to the wanted and unwanted variables respectively
M	Bending moment
M_t	Bending moment with reference to the configuration at time t (t = 0 or t)
M_{xy}, M_{xz}	Bending moments about the local y, z axes respectively
$\vec{N}$	Vector normal to the natural base vector in the deformed geometry
N_i	Heirarchical shape functions
$\bar{N}_i$	Parabolic interpolation functions
$\bar{\bar{N}}_i$	Cubic interpolation functions
$\hat{n}$	Unit vector normal to the natural base vector in the deformed geometry
$\hat{n}_y, \hat{n}_z$	Unit vectors normal to the convected x surface in the deformed configuration

$\bar{P}_{ti}$	The initial stress matrix with reference to the configuration at time t (t = O or t)
$\bar{P}^*_{ti}$	Additional initial stress matrix with reference to the configuration at time t (t = O or t)
P	Applied load
P_t	Axial force with reference to the configuration at time t (t = O or t)
$\vec{p}$	Vector of follower pressure loads
$\vec{q}$	Vector of total uniformly distributed load per unit undeformed length
R	Vector of conservative equivalent nodal forces
R_d	Vector of deformation dependent nodal forces
$\vec{R}$	Position vector of a general point before deformation
$\bar{R}$	Position vector of a general point after deformation
$\vec{r}$	Position vector of a point on the beam reference line before deformation
$\bar{r}$	Position vector of a point on the beam reference line after deformation
S, S_t	2nd piola-Kirchoff stresses with reference to the configuration at time t(t = O or t)

$\bar{S}_t, \bar{S}_t^i$	Vector of stress resultants with reference to configuration at time t (t = 0 or t), for the i^{th} iteration
$\bar{S}^*$	Vector of modified initial stress resultants obtained from the geometric strains
T	Transformation matrix
T	Total torsional moment
T_y, T_z	Torsional moments due to the torsions of the y and the z normals respectively
U,V,W	Displacement components in the global X, Y and Z directions respectively
u,v,w	Displacement components in the local x, y and z directions respectively
u_t	Vector of continuum mechanics displacements relative to the configuration at time t (t = 0 or t)
$\vec{V}$	Displacement vector of a point on the beam reference line
V_t	Volume in the configuration at time t (t = 0 or t)
v	Volume in the deformed configuration
W	Constrained shape function array
WN, WN*	Unconstrained shape function array in terms of the initial total element variables
W_A, W_B	Partitions of the shape function array with reference to the wanted and the unwanted variables respectively

X, Y, Z	Global coordinates
x, y, z	Local material coordinates
$\hat{x}, \hat{y}, \hat{z}$	Unit vectors in the local x, y and z directions respectively
α_i	Generalised variables defining the displacement variation
α, β, θ	Measures of rotation about the global X, Y and Z axes respectively
γ	Variables defined by the shape function array
$\gamma_{xy}, \gamma_{xz}, \gamma_{yz}$	Shear strains
δ, δ^*	Initial total element variables
δW	External virtual work
δW_{int}	Internal virtual work
$\varepsilon_t, \varepsilon_t^i$	Vector of strain measures which are explicit functions of the displacement gradients with reference to the configuration at time t (t = O or t), for the i^{th} iteration
ε_t'	Green-Lagrange strains or geometric strains with reference to the configuration at time t (t = O or t)
ε_t^*	Generalised strain measures of the reference line obtained from the geometric strains with reference to the configuration at time t (t = O or t)
ε_t^o	Infinitesimal strains with reference to configuration at time t (t = O or t)

ε_t^L	Nonlinear strains with reference to configuration at time t (t = O or t)
$\varepsilon_{xx}, \varepsilon_{yy}$	Direct strain components
θ_t	Vector of displacement gradients with reference to the configuration at time t (t = O or t)
$\theta_x, \theta_y, \theta_z$	Measures of rotation about the local x, y and z axes respectively
λ	plastic strain rate multiplier
ν	Poisson's ratio
ξ	Natural coordinate
σ	True Cauchy stresses or nominal stresses
$\bar{\sigma}$	effective stress
σ_{xx}, σ_{yy}	Stress components in the x and y directions respectively
σ_y	Uniaxial yield stress
$\tau_{xy}, \tau_{xz}, \tau_{yz}$	Shear stresses
τ_y, τ_z	Torsions about the local x axis of the local y and z normals respectively
ϕ_j	Rotation of node point j
ϕ_y	Angle between the local y axes in the deformed and undeformed configurations
ϕ_z	Angle between the local z axes in the deformed and undeformed configurations
ψ^i	Nonlinear equilibrium equations
$\vec{\Omega}$	Rotation vector (for small displacement displacements)

CONTENTS

CHAPTER 1

GENERAL INTRODUCTION

1.1 INTRODUCTORY REMARKS

Modern developments in design and construction have lead to the increasing use of slender structural members. Typical examples of these are the stiffened plated box girders which are used in bridge structures and the stiffened shell constructions used in offshore structures.

The evolution of such complex structures has resulted in the establishment of extensive research and development programmes to improve the knowledge of the behaviour of these structures when they are subjected to load.

A well established method for the study of structural behaviour is structural testing. The size of the structural members may be so large, however, that full scale testing becomes impractical. Thus, there are two alternative approaches available for structural testing. The first is model testing (1), which has limitations due to the difficulty of accurately scaling down the prototype including all factors affecting performance, such as initial imperfections and initial stresses. The second approach requires the testing of panels with the same geometry and support conditions as that of the

complete member (2). This approach needs a knowledge of the panel width required and boundary conditions to be used for the panels. There are obvious advantages if the results obtained from structural testing could be compared with those obtained from theoretical analysis.

The development of powerful computers has resulted in the application of numerical methods to solve structural problems. These methods have been shown to be very effective and to give extremely good results. To define the special features required for the analysis of stiffened structures it is necessary to state the main modes of failure of these structures. Due to their slenderness the failure of these structures is predominantly by buckling (3 - 7). Depending on the relative sizes of shells and stiffeners, failure may occur by local buckling of panels and stiffeners while their junctions remain straight and while the shell is still elastic, by overall buckling in the form of significant radial movements of stiffeners or as a complex interaction of the two modes. In some cases these may also be combined with lateral torsional instability (tripping) of the stiffeners. It is usual not to include tripping in an analysis and the present design procedures adopt the criterion of limiting the depth of the stiffener in order to preclude the tripping effect (6, 8). An additional factor which must be taken into account in the analysis is that the fabrication of such structures results in initial imperfections and introduces residual

stresses. Hence, the behaviour of these structures is such that large displacements and rotations can develop. This, coupled with the need to make use of the full load carrying capacity, may also lead to plastic deformation. Thus the analysis procedure must take into account both geometric and material nonlinearity. Since these structures are normally constructed using steel, however, the strains can be assumed to be small.

This nonlinear behaviour is best treated incrementally especially because of the incremental nature of the laws governing plastic deformation. Originally the effect of stiffeners was taken into account employing the concept of smeared stiffeners, thus ignoring the possibility of local buckling (3). A study of the behaviour of stiffened cylinders under moderately large rotations has been carried out by Bushnell (4, 5, 9) using a double loop iteration subincremental technique and the finite difference energy method taking into account the discrete form of the stiffeners. He concludes that agreement between test and theory is improved if the analytical model reflects the discrete behaviour of stiffeners. For stiffened plates, Webb and Dowling (7) have presented solutions for flat, angle and Tee section stiffeners by applying dynamic relaxation to the finite difference equivalents of the governing equations.

The significant features of the stiffened structures, namely the interaction of the buckling modes, the yielding and discrete behaviour of the stiffeners and the influence of initial imperfections and residual stresses, are more effectively considered using the finite element method (10 - 14). Crisfield (6) has used the finite element method to obtain solutions for eccentrically stiffened steel plates for moderately large displacements. Plasticity is considered by using approximate yield criteria that are direct functions of the stress resultants and plastic curvatures, obtained from a modification of Ilyshin's yield function by making some allowance for yield in the fibres before full section yield. The stiffeners are modelled as two uniaxial line elements and a central rectangular bar element. Bathe and Bolourchi (15) have presented compatible shell and bending elements formulated by interpolating the element geometry using the mid-surface nodal point coordinates and mid-surface nodal point normals. Ferguson and Clark (16) have developed two- and three-dimensional super-parametric eccentric beam elements suitable for use as stiffeners based on relaxing the Kirclhoff hypothesis by assuming that plane sections remain plane, but not necessarily normal to the beam axis. Both formulations, however, include shear deformation and the performance of such elements is known to deteriorate for very thin beams especially for large rotation problems (11, 17).

Curved beam element formulations have attracted considerable interest due to their relative simplicity while giving insight to the more complex problems of shell elements. This accounts for the large number and different types of beam elements presented in the literature (16 - 32). However, to the author's knowledge, a generally curved eccentric beam element formulation that can accommodate large rotations is not yet available.

1.2 SCOPE AND OUTLINE OF THESIS

For large deformation analysis of beam and shell type problems two alternative approaches are generally adopted (15). In the classical approach, a plate or shell theory, which has been developed from the three-dimensional continuum mechanics equations by incorporating various assumptions appropriate to the structural behaviour, is used as a starting point of the element formulation (10, 30). The alternative approach uses the continuum mechanics equations and then introduces approximations in the element formulation (10, 15, 35, 36). The latter approach amounts to using a general shell or plate theory. In this thesis an approach similar to the classical one is adopted. Using the Kirchhoff hypothesis the shape of the element is defined before and after deformation. This definition of geometry is used to obtain exact strain displacement relations. Elements that can correctly accommodate these relations are then developed.

Generally a small strain large rotation formulation for beam and shell type problems is best treated by using a frame indifferent measure of strains. Hence the most accurate approach is to develop the theory using an intrinsic coordinate system. The strains obtained from such a description of motion are the Green-Lagrange strains. In a displacement finite element model for generally curved thin beam and shell type elements such a coordinate system can be defined accurately using the constraint technique. In the constraint technique geometric relations are used to correctly define the shape of the element and the variation of the local variables. In fact the technique can be used to develop completely conforming elements if required.

A further point of importance is the definition of the stress-strain relations to be used in the virtual work expression in a Total Lagrangian frame of reference. This is necessary when attempting to obtain the same results for both stresses and displacements using either the Total Lagrangian or Updated Lagrangian formulation. Taking into account the added numerical effort required to calculate the shape function array for elements based on the constraint technique, the Total Lagrangian formulation will be numerically more effective than the Updated Lagrangian formulation. The displacements of a structure, which have been obtained using an objective

theory as a basis for the formulation, will be exactly the same using either formulation. For the calculation of stresses, however, for large rotation large curvature problems a difference in the response obtained using either formulation can be expected unless appropriate material constants are used. Hence, a transformation of the modulus matrix will be necessary when a Total Lagrangian formulation is used. To avoid this and at the same time reduce the computer time required for solution, a combined Total plus Updated Lagrangian formulation can be used.

Alternatively, the conventional or geometric measure of strains can be used since the stresses calculated using these measures of strain can be assumed to be equal to the true stresses if the strains are small. Thus the nominal stress and the conventional strain can be used as work conjugate variables in the virtual work equation. Such an approach is equivalent to assuming a strain energy function in terms of the Green's deformation tensor and satisfies the requirement of frame indifference (37). For beam and shell type elements this approach takes into account the effect of curvature on the axial force thus resulting in true axial force values. The approach is general, however, and may be used in continuum mechanics based formulations (see Appendix II).

The objective of this thesis is:

1. To develop a small strain large rotation exact theory for curved two-dimensional beam type structures in Total, Updated and Combined Lagrangian frames of reference based on the Green strain measure.

2. To develop a general incremental formulation for geometric nonlinearity based on the conventional definition of strains as the change in length per unit initial length and the change in the right angle, and to show the capability of this theory to evaluate correctly the stresses using the Total Lagrangian formulation.

3. To demonstrate the possibility of obtaining non-conforming and exactly conforming curved elements using the constraint technique.

4. To examine the effectiveness of these elements in correctly dealing with the objective theory developed with a special reference to the convergence requirements.

5. To present comparisons between the Lagrangian formulations developed and hence decide on the numerical effectiveness of either formulation.

6. To examine the possibility of extending the small strain large rotation theory to three dimensions for thin curved beam elements including material nonlinearity and hence develop thin generally curved eccentric three-dimensional beam elements using the constraint technique. Such elements would be suitable for use as stiffeners.

Outline of Thesis:

Sections 1.3 to 1.5 of this chapter give a brief general account of the conditions and difficulties encountered in developing small strain large rotation finite element formulations based on beam type elements and suitable for use in the analysis of stiffened shell constructions. The remedies suggested in the literature to overcome these difficulties are also outlined. In Section 1.6 a summary of the mathematical formulation based on the Lagrangian description of motion is given.

Chapter 2 presents the exact two-dimensional large rotation theory for thin curved beam elements. Incremental equilibrium equations which are based on four alternative descriptions of deformation are given and these are:

i. Total Lagrangian formulation based on the Green strain measure (TLG).

ii. Updated Lagrangian formulation based on the Green strain measure (ULG).

iii. Combined Total and Updated Lagrangian formulation based on the Green strain measure (UTLG).

iv. Total Lagrangian formulation based on the conventional strain measure (TLC).

Chapter 3 deals with the development of curved two-dimensional beam elements which can represent the theory presented in Chapter 2. The elements are formulated using the constraint technique.

Chapter 4 examines the convergence requirements, gives an assessment of the performance of the elements and demonstrates the possibility of obtaining exactly the same results for both displacements and stresses, using the alternative descriptions of deformation. The results obtained are compared with published results.

Chapter 5 presents the three-dimensional large rotation theory which is an extension of the two-dimensional theory. Neglecting distorsion, the theory exactly represents the deformation of a beam of eccentric solid rectangular cross-section. Material nonlinearity based on the von-Mises yield criterion and the Prandtl-Reuss flow rule with isotropic hardening is also included in

the formulation. For beams under torsion, however, the material nonlinearity presented is only correct for concentric square cross-sections.

Chapter 6 presents the formulation and application of the three-dimensional thin eccentric beam elements. The elements are developed using the constraint technique. The applications presented are intended to show the excellent capabilities of the theory and elements which have been developed.

Chapter 7 presents general discussions and conclusions with some suggestions for possible future work.

One of the advantages of the finite element method is that once a general purpose program comprising input, assembly and solution facilities is written, it becomes a relatively simple task to add new elements. One such very efficient general purpose finite element program is LUSAS (38, 39). The elements and theory developed were implemented in the LUSAS system. In this presentation, however, attention is focused on operations to be performed on a single element.

1.3 LARGE DEFORMATION THEORY

The nonlinear equilibrium equations for almost any structure can be obtained using a variational principle and such an approach is basic to the finite element formulation [10, 11]. Mainly there are three types of finite element formulations:

a) The displacement method: based on minimizing the total potential energy where the displacements are the unknowns.

b) The equilibrium method: based on minimizing the complementary energy where the stresses are the unknowns.

c) Mixed finite element models: based on the Riessener variational principle where both displacements and stresses constitute the unknowns.

The displacement finite element method is the most widely used because of its simplicity and sound theoretical basis. The virtual work principle, which is suitable for both linear and nonlinear problems, is the basis of the finite element displacement formulation [10, 11].

1.3.1 Geometric Nonlinearity

The virtual work principle can either be formulated in terms of variables in the deformed configuration or in terms of variables referred to the undeformed configuration. For the first approach the work conjugate variables are the true Cauchy stresses and the strains referred to a spatial coordinate system and measured in the deformed configuration. For the second approach the work conjugate variables are the second Piola-Kirchhoff stresses and the Green-Lagrange strains referred to referential or material coordinates in the undeformed configuration [37]. These alternative descriptions of deformation are termed Eulerian or Lagrangian respectively. The Kirchhoff stresses and the Cauchy stresses are related by the ratio of the volume in the reference state to the ratio of the volume in the current state [12, 40]. Thus, for small strains these stress measures are equal.

1.3.2 The Eulerian Formulation

The virtual work principle is written in terms of the unknown deformed configuration for the Eulerian formulation. Thus a solution is only possible by assuming that the reference configuration instantaneously coincides with the current state. McMeeking and Rice [40] have presented an Eulerian formulation based on Hill's variational principle. The special feature of

their formulation is the additional term in the initial stress stiffness matrix. The term is a function of the strain matrix and the initial Cauchy stresses and results from relating the nominal stress to a spin-invariant stress rate. The authors also point out, however, the possibility of obtaining the same results when work conjugate measures of stress and strain are used in the virtual work equation.

1.3.3 The Lagrangian Formulation

The Lagrangian approach is more suitable for use in continuum mechanics since one can always assume the existence of an undeformed configuration for many structures. An important point to note here, however, is that the equilibrium equations while written in the undeformed configuration must be satisfied in the deformed configuration [37]. This implies that the stresses are measured relative to material coordinates in the deformed configuration. Also, their directions are always normal to the cross-sectional areas in the deformed configuration, to which the respective axes that the stresses are referred to are normal in the undeformed configuration. Hence, if a stress-strain relationship is to be written, either the stresses, which are measured in the deformed configuration, must be referred back to the undeformed configuration or the strains must be referred to the deformed configuration so that both tensors in the

virtual work principle are referred to the same axes. This fact is basic to all the difficulties in the geometric nonlinear formulations presented in the literature.

Thus, in the Lagrangian description of deformation two alternatives are possible in order to relate the work conjugate stresses and strains. In the first, which is known as the Total Lagrangian approach the stresses must be referred back to the undeformed configuration. This requires the use of appropriate material constants. For finite elasticity Oden (12, 41) has used a strain energy function to define the stress-strain relations. Hibbitt et al (42) have given the transformation necessary for the constitutive relations for metal structures. This is obtained by adopting a linear relation between true stress and strain increments which is necessary because the measure of stress and strain increments must be independent of the current rate of rigid body motion when using the Prandtl-Reuss flow rule (defined in true stress vs logarithmic strain) together with the von Mises yield criterion (43). Hence, the transformation of the modulus matrix is necessary in a Total Lagrangian formulation. In almost all the Total Lagrangian formulations presented in literature, however, this transformation is neglected (10, 15, 20, 44, 45).

The second approach using the Lagrangian formulation refers the strains to the deformed configuration by considering that this configuration coincides instantaneously with the current state (20, 44 - 47). This approach, termed the Updated Lagrangian, is equivalent to the Eulerian formulation. Hence, for the Updated Lagrangian formulation direct proportionality between the stresses and strains in the virtual work principle can be assumed for large rotation problems without introducing errors.

Thus, provided that appropriate material constants are used the results obtained using either the Total Lagrangian or the Updated Lagrangian should be identical. The question, which formulation to be used, now arises. An answer to this is that the choice of method should only depend on the relative numerical effectiveness and ease of implementation of either method. Clearly the computer time required for an Updated Lagrangian solution will be considerably more than that required for a Total Lagrangian solution. This is basically due to the necessity of recalculating the element shape functions each time the geometry is updated. Bathe and Bolourchi (20) have concluded that for three-dimensional beam elements the Updated Lagrangian formulation is numerically more effective than the Total Largangian formulation. This is because their Total Lagrangian formulation requires a transformation

of the interpolation functions as a consequence of the definition of the axes they use.

Most researchers agree that the difference between the Total and Updated Lagrangian results, if any, will be due to the choice of material constants (15, 20, 44, 45). It has been previously stated that the modulus matrix transformation required by the Total Lagrangian formulation is always neglected. This approximation is valid for small strains and small rotations. For large rotations and/or plastic deformations, however, such an approximation is invalid and large errors will result if the transformation is neglected (42). The approximation amounts to assuming direct proportionality between the 2nd Piola-Kirchhoff stresses and the Green-Lagrange strains in the virtual work equations. Thus, neglecting the transformation, the Total Lagrangian formulation while giving correct displacement estimations for large rotation problems will result in the wrong stresses. This is the only serious disadvantage of the general Total Lagrangian formulation. The remedy to this problem is provided in this thesis (see Section 1.3.5).

1.3.4 Large Deformation in Beam and Shell Type Problems

The continuum mechanics nonlinear Green strain-displacement relations are exact (37). For beam and shell type problems approximations, such as the Kirchhoff hypothesis, are used to describe the deformation at a general point within an element in terms of the deformation of the neutral surface. This introduces curvature terms which can be extremely complex. In fact, one of the main difficulties in dealing with beam and shell type problems is accounting for the effects of curvature. In a finite element context this difficulty is pronounced for elements which include rotations as degrees of freedom in the non-conservative nature of moments which are referred to fixed axes (48). This is due to the fact that finite rotations referred to fixed axes are not vectors (37) and hence not commutative even for small strain formulations (see Figure 1.1). Thus, as has been stated by Argyris et al (48), the strains must be expressed as at least second order functions in the non-commutative nodal rotations.

Frey and Cescotto (27) and Surana (49) have eliminated the restriction on rotation magnitude by defining the displacement field as a nonlinear function of the nodal rotations and basing the derivation of the element properties on this displacement field (Figure 1.3).

Argyris et al [48] have adopted the "natural method" where separate rigid body displacements and natural deformations are used for the description of the current state of the finite element. Thus, to avoid the non-commutative nature of finite rotations referred to fixed axes they use semi-tangential rotations, which correspond to semi-tangential torques (Figure 1.2) and are commutative even when large.

Bathe and Bolourchi [20] have used Euler angle transformations (Figure 1.5) to take into account the effect of finite rotations. This method has some serious shortcomings, however, [21] and these include:

i. The Euler angle transformation is not linearly dependent for all values of Euler angles.

ii. The generalised moments corresponding to Euler angles cannot be easily interpreted in a physical sense.

iii. The transformations are complex and computationally demanding since they involve many trigonometric functions.

Hence, as an alternative Belytschko et al (21) have used a rigid-convected or a co-rotational coordinate formulation, where each element is associated with a cartesian coordinate system that rotates and translates with the element (Figure 1.4). Such a formulation involves an approximation, however, because it places a limitation on the amount of rotation within the element which might be large (12, 42).

Epstein and Murray (25) have presented a Total Lagrangian formulation for straight two-dimensional beam elements using convected coordinates. The formulation is exact and results in an objective measure of curvature. Taking into account the fact that during rigid body motion a finite element remains unchanged with respect to a following (convective) coordinate system (48), it is possible to extend this formulation to curved two- and three-dimensional beams. This can be achieved by describing the deformation in terms of an intrinsic coordinate system for each material point within the finite element. In practice this means defining these coordinates at each integration point in the element. This is the approach adopted in this thesis.

Epstein and Murray [25] have also stated the importance of the additional term, which includes a second order derivative of the in-plane displacement, in the curvature definition. They have shown that neglecting this term results in a relative error in curvature which is equal to the square of the sine of the angle of rotation. Hence, it is necessary to retain this term for large rotation and curvature problems.

The main disadvantage of this formulation is the assumption of direct proportionality between the generalised strains and the stress resultants in the virtual work equation. If this assumption is not made, the formulation results in unsymmetrical incremental equations. In effect the coupling between axial force and bending moment, and hence the effect of the curvature on the axial force, is neglected. This approximation is the same as neglecting the modulus matrix transformation required by the general Total Lagrangian formulation (Section 1.3.3).

Hibbitt et al [28] have presented a hybrid small strain large rotation beam element formulation with a hermite cubic interpolation of position of a point and a quadratic interpolation of the axial force. By regarding the axial force as an independent variable they formulate an augmented virtual work equation based on the first order bending theory. Using the

axial force and bending moment values obtained from this principle the true axial force and bending moments are then calculated, thus taking into account the effect of curvature on axial force. Hence, the modification needed to obtain the true axial force is still not included in the principle. It is apparent from this formulation, however, that when calculating the strains incrementally the strain increments must add up to the total strain values obtained by substituting the total displacements in the strain displacement relations. In the displacement finite element formulation this can be achieved by using the incremental strains (44) rather than the total differential of strains (which is required in forming the tangent stiffness matrix) to calculate the stress increments.

1.3.5 The Geometric or Conventional Strains

It has been previously stated that the material strain measure, the Green strain, is to be used in the Lagrangian formulation. The Green strain is a function of the stretch ratio (37, 46). To obtain exact strain displacement relations for beam and shell type structures Donnell (50) has used the geometric or conventional strains namely the unit stretch and angle change. To obtain explicit relations for strains in terms of displacement gradients he has used a binomial series expansion neglecting third and higher order terms in displacement gradients. Similar strain-

displacement relations can be obtained for flexible bodies such as plates and shells by expressing the Green strains in terms of deformation and rotation tensors and then neglecting second order terms in Green strain measures of the middle surface. Oden (12) has stated that this results in an improvement of the performance of plate and shell type elements. Thus the possibility of using the conventional strains in their exact form (37) and nominal stresses as work conjugate variables in the virtual work principle for beam and shell type elements needs to be considered. A total Lagrangian formulation obtained in this manner results in symmetrical incremental equations and true stress resultant values.

1.3.6 Material Nonlinearity

The small displacement nonlinear material analysis of structures using the finite element method is well established (10, 51 - 54). The basic ingredients of the analysis are (45):

i. the elastic stress-strain relations,

ii. a yield condition that specifies the state of stress corresponding to the start of plastic flow,

iii. a flow rule that relates plastic strain increments to the current stresses and stress increments subsequent to yielding,

iv a hardening rule that specifies how the yield condition is modified during plastic flow.

For metal type structures assuming isotropic hardening the von-Mises yield criterion and the Prandtl-Reuss flow rule are commonly used (33, 42, 45). An approximate yield function based on stress resultants and plastic curvature is used by some investigators in the analysis of plates and stiffened plates (6, 7, 55, 56).

The Prandtl-Reuss flow rule is defined in terms of the true stress and logarithmic strain. The stress and strain increments used in the rule must be independent of the current rate of rigid body motion (42, 43). For large rotation problems it is necessary to adopt a frame indifferent measure of variables. Once such a measure is adopted, for example by the use of a convective coordinate system, the same formulation for the small displacement analysis can be used (33, 42). The combined geometric and material nonlinear analysis is best dealt with by the use of the double loop iteration subincremental technique thus relaxing the limitation on load increment size (4, 5, 33).

1.4 THE INCREMENTAL EQUILIBRIUM EQUATIONS

The nonlinear equilibrium equations are obtained by substituting the finite element representation of strains and displacements, in terms of the nodal degrees of freedom, in the virtual work expression. To obtain a solution it is necessary to write these equations in an incremental form adopting an adequate solution procedure.

1.4.1 Solution Procedures (57 - 60)

Basically there are two classes of solution procedures, namely, methods which are incremental in nature and which do not necessarily satisfy equilibrium and iterative methods which tend to follow the equilibrium path. Examples of the first class are (57):

1. The pure incremental approach where the equations are assumed to be linear within each increment with no correction applied to satisfy equilibrium. The main advantage of this approach is the ease of application. The solutions obtained by this method tend to drift from the true solution.

2. The perturbation method where the displacements are expanded in a series form with respect to an incremental load parameter at some equilibrium state. Depending on the number of terms retained in the series, several sets of linear equations are formed and solved. Errors resulting from this approach tend to accumulate and the solution drifts from the true solution. The amount of drifting is dependent on the load increment size and the number of terms retained in the series.

3. The initial value formulation in which the displacements are written as functions of a load parameter. By differentiating the equilibrium equations with respect to this parameter, a set of differential equations, in terms of displacement rates with respect to the load parameter and normalised generalised forces, is obtained. Hence, the displacement values are calculated by numerical integration from a known initial displacement value. Using Euler's method for this integration results in the pure incremental approach stated above. More accurate integration schemes such as the Runge-Kutta method (58) can be used to reduce drifting.

There are mainly two versions of iteration techniques and these are the direct iteration and the Newton-Raphson methods. In the direct iteration technique, starting from an initial estimate of displacements, the nonlinear effects are calculated and an improved solution of a linear set of equations obtained. This solution is then back-substituted into the nonlinear equations and the iteration continued until convergence of successive iterations is obtained. The success of this procedure depends primarily on the initial estimate of displacements. The serious disadvantage of this method is that it will only converge for moderately nonlinear problems.

The most widely used iteration solution technique is the Newton-Raphson method [10, 28, 61]. This is because it is extremely accurate and converges quite rapidly. The main disadvantage of this method is the excessive computational effort required since the stiffness matrix is formed and inverted.at each cycle of iteration. Hence, an alternative modified Newton-Raphson method may be used [10, 44, 45]. In this method the stiffness matrix is held constant for a number of iterations and then updated after the convergence rate has begun to deteriorate. Various acceleration procedures can also be used to ensure and accelerate convergence [10, 59, 60]. The Newton-Raphson method has been adopted in this thesis.

1.4.2 The Tangent Stiffness Matrix

Using the Newton-Raphson method, a Taylor's series expansion of the equilibrium equations about an equilibrium position, neglecting second and higher order terms in displacement increments, gives the incremental equations as linearised functions of the displacement increments [10, 49, 61, 62]. Once the linearised equations are solved for the increments the total displacements are obtained as the accumulation of the increments. Using the total displacements the gradient of the equilibrium equations, which is the tangent stiffness matrix, and the out-of-balance forces, or residuals, are recalculated, thus giving a new set of linearised equations. This iteration procedure is repeated till a specified convergence limit is achieved. The convergence control criteria commonly used are [52]:

1. The maximum absolute residual limit.
2. The limit for the norm of the residual forces.
3. The limit for the norm of the displacement increments.

To obtain an expression for the external work in the virtual work equation an assumption has to be made regarding the effect of deformation on the generalised forces. These forces may change in both magnitude

and direction as the body deforms and in general must be expressed in terms of the displacements and their gradients (12). For small strains and small rotations it is reasonable to assume that these forces are conservative. For large rotations the effect of deformation on the generalised forces must be taken into account (42). This is particularly important in the case of follower loads such as pressure loads. Inclusion of this effect results in a slight modification in the incremental equations in the form of an additional contribution to the tangent stiffness matrix, generally known as the load correction matrix (41, 42). The load correction matrix is however, usually unsymmetrical. Frey and Cescotto (27) have presented a study of the effects of including and neglecting this matrix. This contribution is usually negelcted (44, 45) due to the difficulties in dealing with unsymmetrical matrices. Such an approximation amounts to assuming that the externally applied loads are conservative. Bathe et al (44) and Epstein and Murray (25), while neglecting the unsymmetrical contribution to the tangent stiffness, have presented a modification to the load vector for deformation dependent loads. This is the approach which has been followed in this thesis.

The form of the tangent stiffness matrix is now well established (10, 15, 42, 44, 45, 61). For the Total Lagrangian formulation the tangent stiffness matrix is composed of three matrices. These are the infinitesimal strain, the initial displacement and the initial stress stiffness matrices. For the Updated Lagrangian formulation, assuming the reference configuration instantaneously coincides with the current configuration, the tangent stiffness matrix is composed of two matrices, the infinitesimal strain stiffness matrix and the initial stress stiffness matrix (15, 20, 44, 45, 46).

The form of the initial stress stiffness matrix is, however, still a matter of controversy. Frey and Cescotto (27) and Surana (49) by using a displacement field which is a nonlinear function of the nodal rotations have obtained a Total Lagrangian formulation in which the initial stress stiffness matrix contains two additional terms. It has been pointed out previously that such a displacement field description is necessary to take account of the noncommutative nature of finite rotations referred to fixed axes. Thus, once a measure of variables which is frame indifferent is adopted, say by using a convective coordinate system, these modifications to the stiffness matrix will not be needed. McMeeking and Rice (40) have presented an Eulerian formulation (which is equivalent to the

Updated Lagrangian formulation) in which the initial stress stiffness matrix includes an additional term resulting from the use of a frame indifferent stress rate. A similar additional initial stress stiffness matrix has been obtained in this thesis in the Total Lagrangian formulation based on the geometric strains.

1.5 ELEMENT GEOMETRY AND DEGREES OF FREEDOM

The requirements for monotonic convergence of the finite element idealisation are that the elements should be complete and compatible (10, 11). For the completeness requirement the displacement functions must be able to represent rigid body displacements and constant strain states. This is due to the fact that as the number of elements is increased the state of strain within each element approaches a state of constant strain. The compatibility requirement is essentially that the displacements within elements and across element boundaries are continuous so that no gaps may develop between elements. As a consequence of this, the highest order displacement derivative present in the virtual work expression must be finite thus requiring the continuity between elements of the derivative one order lower. If the elements are only complete and not compatible i.e. nonconforming the analysis result may still converge with no guarantee of monotonic convergence.

Originally finite element formulations were based on using generalised coordinates in defining the approximating polynomials which is known as generalised coordinate finite elements (11, 14). The major difficulties encountered were the fact that these generalised coordinates are functions of the local coordinates, and hence difficult to define for curved elements, and the need for inverting the generalised coordinate matrix, which relates the variables to the coordinates, with no guarantee of the existence of an inverse. Another factor of importance, especially for beam and shell type elements, is that the displacements of the element need to be independent of the orientation of the local element coordinate system i.e. geometric invariance or spatial istropy (11). Generally a displacement model is geometrically invariant if the same order polynomial terms are used for all displacement components with appropriate interchange of coordinates. For some elements it is difficult to obtain spatially isotropic generalised coordinate formulations.

These difficulties have enhanced the development of element formulations in which interpolation functions are used. These developments lead to the formulation of the more general and versatile isoparametric finite elements and associated element families. An essential ingredient of the isoparametric formulations is the

necessity of evaluating all the integrals within the element using numerical integration. The most widely used numerical integration technique is the Gauss quadrature (10, 11).

There is no need for the inversion of a matrix in the isoparametric element formulation since both geometry and approximating function are interpolated using the same shape functions. An important concept to consider, specially for beam and shell type problems, is interpolation directionality (20). This makes it necessary to ensure that the interpolated nodal variables and coordinates are both referred to the same coordinate system either local or global. For the isoparametric elements this results in no difficulties, since it is always possible to interpolate the known global nodal coordinates and the unknown global nodal variables using the same shape functions. The required variables can then be obtained by transformation, whenever that is necessary [10, 49, 61]. Thus the isoparametric element formulation can be understood as a means of defining material coordinates in the global axes directions at each of the integration points, and this is a factor which contributes to their success in both linear and nonlinear analyses [10, 11, 44, 52].

1.5.1 Nonconforming Elements

The basic problems when using isoparametric elements to analyse beam and shell type structures are two fold. Firstly excessive shear strain energy is stored in the element and secondly as the element becomes thinner the stiffness coefficients corresponding to the transverse displacement degrees of freedom are considerably larger than those corresponding to the longitudinal displacements which results in numerical ill-conditioning (10, 11).

To eliminate numerical ill-conditioning superparametric elements, wherein a linear variation of the displacement in the thickness direction is assumed, are used (10, 61). Such elements, however, while resulting in an improvement, still suffer from aspect ratio problems (49, 61). Thus, the use of relative degrees of freedom or matrix conditioning schemes may be necessary (11, 61). As an alternative one of the following two approaches has been suggested:

i. The use of degenerate isoparametric elements, wherein the strain in the transverse direction is neglected and, as a relaxation to the Kirchhoff hypothesis, plane sections are assumed to remain plane, but necessarily normal to the middle surface (10, 16, 36).

ii. The use of element models based on independent interpolation for the displacements and rotations (11, 17, 20).

For beam type problems the second approach is preferred due to the simplicity of such element models and their ability to reproduce shear deformation.

The performance of the independent interpolation models, wherein low order interpolation functions are used is known to degenerate rapidly as the beam becomes thin due to an overestimation of shear stiffness (10, 11). Also, inextensional deformations are poorly represented by these models (17). Hence, the following actions are proposed as a remedy to these difficulties:

a) The use of substitute shape functions which smooth appropriate derivatives (10, 63).

b) The use of reduced integration where a lower order integration rule is used for the transverse shear strain energy and for the extensional energy in the case of inextensional deformation (10, 17, 64).

c) The use of a penalty function approach, wherein conditions of zero or negligible transverse shear and extensional strains can be treated as the limiting cases when the penalty numbers reach infinity. Reduced integration is required to achieve the condition of zero or negligible transverse shear and extensional strains in the numerical implementation of penalty finite elements (10).

d) The direct application of constraints in the generation of incompatible elements. For thin elements internally applied constraints enforcing the Kirchhoff conditions at certain points within the element result in effectively excluding shear strains (10, 35, 38, 65, 66).

e) The use of mixed finite element models with independent interpolation for displacements and stresses (17).

For plate bending problems the use of reduced integration has been shown to be equivalent to the application of discrete Kirchhoff constraints or the use of smoothed derivatives (10, 63). Reduced integration or derivative smoothing often result in element forms which are equivalent to those which can be derived by hybrid formulations (10, 17).

The direct application of discrete constraints has been shown to be very effective. In fact, some of the most successful shell and plate bending elements, such as the SEMILOOF shell element (35) and the ISOFLEX plate bending element (38), have been developed using this technique. In the constraint technique, geometric relations are used to eliminate relevant degrees of freedom with the added advantage of there being no need to store the eliminated variables. Such an interpretation of the constraint technique leads to the introduction of a "second generation of isoparametric elements" with the possibility of developing compatible thin shell and beam elements such as the ISOBEND element presented by Irons (35). In this element a side is treated as a thin beam, thus imposing on the midside of a shell element the displacement and the slope characteristics of a thin beam.

The constraint technique can also be used to avoid the problem of interpolation directionality in curved beam and shell type elements. It has been stated by Bathe and Bolourchi (20) that because of interpolation directionality the Hermite interpolation functions, which are necessary for compatibility in beam elements, can be correctly used only for straight elements. In the constraint technique, starting with an isoparametric type interpolation of the global coordinates and

variables, it is possible to define local material coordinates and form constraint equations. The local coordinates correctly follow the curved element geometry. The constraint equations are essentially geometric relations in terms of the local variables at any point within the element. These equations relate the required local variables to the interpolated global variables. An additional advantage of this technique is, that once a shape function array containing all the displacements and derivatives required for the calculation of element characteristics is written in terms of the final or "wanted" variables, no transformation either from local to global of the stress-strain relations or from global to local of displacements and/or their derivatives, required by some element formulations [10, 49, 61], would be necessary. The constraint technique has been used in developing the elements presented in this thesis.

1.5.2 Convergence and the Patch Test

The elements developed using the constraint technique are usually nonconforming thus violating the requirement of compatibility necessary for monotonic convergence [35, 38, 66]. Such elements can be understood as being based on a modified virtual work principle thus making them of the mixed finite elements class [11]. It is necessary, however, to ensure that

the essential ingredients of completeness are not lost for convergence of analyses by such elements. Hence, it is important that an assemblage of incompatible elements can represent constant strain conditions. This completeness condition on an element assemblage is achieved by using the patch test (10, 11, 38).

In a geometrically nonlinear context Oden (41) has stated that the convergence criteria are the same as those required for linear solutions, namely, completeness and compatibility. For beam type problems, however, Crisfield (6, 56) has used smoothed derivatives in the nonlinear relations only as an extension of the patch test. Thus, while it is possible to obtain complete compatibility using the constraint technique it might be of advantage in some cases to use nonconforming elements.

1.5.3 Displacement Approximation within Elements

In linear elastic two-dimensional finite element analysis using beam elements the compatibility criterion requires continuity of the displacements and the first derivative of the transverse displacement only. Hence, a linear variation of the in-plane displacement and a cubic variation of the out-of-plane displacement will be sufficient. It has been

stated by Dawe (22, 23, 24), Popov and Sharifi (67) and Crisfield (56) that such a displacement variation does not accurately represent the inter-element equilibrium of forces. Dawe (23) has shown that there is no advantage in increasing the order of the out-of-plane displacement unless the variation of the in-plane displacement is similarly increased.

An important consideration for beam elements with eccentricity is the elimination of the error that results from an incompatibility in the in-plane displacements of the reference line and the centroid of the cross-section (68, 69). Thus, the variation of the in-plane displacement must be at least of the same order as that of the gradient of the out-of-plane displacement. Hence, it is necessary in such a case to use a parabolic-cubic variation of displacements.

It has been pointed out earlier that as a result of adopting a frame indifferent measure of curvature the second order derivative of the in-plane displacement is included in the nonlinear curvature term (35). For problems where both rotation and curvature are large, thus increasing the importance of this additional term, the continuity of the first derivative of the in-plane displacement will be necessary and a cubic-cubic variation of the displacements must be used.

Since the first derivative of the in-plane displacement is used as a measure of strain, such a displacement variation may sometimes be undesirable.

In the case of three-dimensional beams, two main additional factors appear and these are, the non-commutative nature of finite rotations and torsion. The noncommutative finite rotations are avoided by using a convective coordinate system. For solid cross-sections the linear st. Venant torsion [70, 71, 72] is usually assumed and the continuity of the angle of twist is necessary for compatibility [64, 65]. The effect of distorsional warping for thin walled beams is effectively treated using Vlasov's theory [73, 74, 75], in which case a continuity of at least the gradient of the angle of twist will be necessary [26, 76, 77, 78]. By assuming that the elements are of solid rectangular cross-sections the effect of distorsion can be neglected and the assumption that plane sections remain plane used [71, 73, 74]. Thus, thin walled beams can be treated approximately as a combination of eccentric beam elements of solid cross-sections with a common reference nodal line [33].

1.6 SUMMARY OF LAGRANGIAN FORMULATION

The principle of of virtual work is written in terms of the true Cauchy stresses σ and strains $\mathbf{e}$ as:

$$\int_v \delta \mathbf{e}^T \sigma \, dv = \delta W \quad \ldots \quad \ldots \quad \ldots \quad \ldots \quad \ldots \quad \ldots \quad (1.1)$$

where v is the volume in the deformed configuration and δW is the virtual external work.

In a Lagrangian coordinate system the principle is defined in terms of the 2nd Piola-Kirchhoff stresses S_t and the Green-Lagrange strains ϵ'_t with reference to the configuration at time t as

$$\int_{V_t} \delta \epsilon'^T_t \, S_t \, dV_t = \delta W \quad \ldots \quad \ldots \quad \ldots \quad \ldots \quad \ldots \quad (1.2)$$

In a finite element displacement formulation the Green-Lagrange strains are defined in terms of the total displacements u_t as

$$\epsilon'_t = \left[B_t + \frac{1}{2} B_L(u_t)\right] u_t \quad \ldots \quad \ldots \quad \ldots \quad \ldots \quad (1.3)$$

Thus the variations in strain $\delta\epsilon'_t$ can be defined as

$$\delta\epsilon'_t = \left[B_t + B_L(u_t)\right] \delta u_t = B \, \delta u_t \quad \ldots \quad \ldots \quad \ldots \quad (1.4)$$

The external virtual work is written in terms of the generalised nodal forces R and the virtual nodal displacements δu_t as

$$\delta W = \delta u_t^T R \quad \ldots \quad \ldots \quad \ldots \quad \ldots \quad \ldots \quad \ldots \quad (1.5)$$

Substituting from (1.4) and (1.5) into (1.2) gives the nonlinear equilibrium equations as

$$\psi = \int_{V_t} B^T S_t \, dV_t - R = 0 \quad \ldots \quad \ldots \quad \ldots \quad \ldots \quad (1.6)$$

Using the Newton-Raphson method a Taylor's series expansion of (1.6) about an equilibrium position ψ^{i+1} gives

$$\psi^{i+1} = \psi^i + \frac{\partial \psi}{\partial u} \Delta u_t^i + \ldots = 0 \quad \ldots \quad \ldots \quad \ldots \quad \ldots \quad (1.7)$$

Neglecting second and higher order terms in displacement increments in (1.7) gives incremental relations of the form

$$\frac{\partial \psi}{\partial u} \Delta u_t^i = - \psi^i \quad \ldots \quad \ldots \quad \ldots \quad \ldots \quad \ldots \quad \ldots \quad (1.8)$$

where $\frac{\partial \psi}{\partial u}$ is the tangent stiffness matrix and

$- \psi^i$ is the vector of residual nodal forces.

Equation (1.8) can be solved for the displacement increments Δu_t^i and the total displacements obtained as

$$u_t^{i+1} = u_t^i + \Delta u_t^i \quad \ldots \quad \ldots \quad \ldots \quad \ldots \quad \ldots \quad (1.9)$$

By assuming that the applied loads are conservative, the tangent stiffness matrix is defined from (1.6) as

$$K_T = \frac{\partial \psi}{\partial u} = \int_{V_t} \frac{\partial B^T}{\partial u} S_t \, dV_t + \int_{V_t} B^T \frac{\partial S_t}{\partial u} \, dV_t \quad (1.10)$$

and also assuming proportionality between stresses and strains, the stresses are defined in terms of the total displacements as

$$S_t = D \, \epsilon'_t = D \left[B_t + \frac{1}{2} B_L(u_t)\right] u_t \quad \ldots \quad (1.11)$$

Hence, the variations in stress are defined from (1.11) and (1.4) as

$$\delta S_t = D \, \delta \epsilon'_t = D \, B \, \delta u_t \quad \ldots \quad \ldots \quad \ldots \quad \ldots \quad (1.12)$$

The modulus matrix D in (1.12) can be modified to take account of material nonlinearity as is shown in Section 1.6.3.

1.6.1 The Total Lagrangian Formulation

Referring all the variables to the undeformed configuration at time O, the strain displacement matrix B (Equation (1.4)) is given by

$$B = B_o + B_t(u_o) \quad \ldots \quad \ldots \quad \ldots \quad \ldots \quad \ldots \quad (1.13)$$

The tangent stiffness matrix is defined from (1.10) and (1.12) as

$$K_T = \int_{V_o} B^T D\, B\, dV_o + \int_{V_o} \frac{\partial B^T}{\partial u} S_o\, dV_o \quad \ldots \quad (1.14)$$

The first term in (1.14) represents the infinitesimal strain and the initial displacement stiffness matrices and the second term is the initial stress stiffness matrix.

The incremental strains are defined from (1.3) and (1.9) as

$$\Delta\varepsilon_o^i = [B_o + B_L(u_o^i) + \frac{1}{2} B_L(\Delta u_o^i)]\{\Delta u_o^i\} \quad \ldots \quad (1.15)$$

from which the stress increments can be obtained as

$$\Delta S_o^i = D\, \Delta\, \varepsilon_o^i \quad \ldots \quad \ldots \quad \ldots \quad \ldots \quad \ldots \quad \ldots \quad (1.16)$$

and the total stresses are defined as

$$S_o^{i+1} = S_o^i + \Delta S_o^i \quad \ldots \quad \ldots \quad \ldots \quad \ldots \quad \ldots \quad (1.17)$$

Hence, the residuals are obtained from (1.17), (1.13) and (1.6) as

$$-\psi^{i+1} = R - \int_{V_o} B^T S_o^{i+1} \, dV_o \quad \ldots \quad \ldots \quad \ldots \quad (1.18)$$

1.6.2 The Updated Lagrangian Formulation

With reference to the configuration at time t the strain displacement matrix is given from (1.4) by

$$B = B_t + B_L(u_t) \quad \ldots \quad \ldots \quad \ldots \quad \ldots \quad \ldots \quad (1.19)$$

Assuming that the reference configuration instantaneously coincides with the current configuration, the tangent stiffness matrix is given from (1.10) and (1.12) as

$$K_T = \int_{V_t} B_t^T D B_t \, dV_t + \int_{V_t} \frac{\partial B^T}{\partial u} S_t \, dV_t \quad \ldots \quad (1.20)$$

wherein the initial displacement matrix, being a function of the unknown displacements u_t, has to be neglected.

The incremental strains are defined from (1.3) as

$$\Delta\epsilon_t^i = [B_t + \frac{1}{2} B_L(\Delta u_t^i)]\Delta u_t^i \quad \ldots \quad \ldots \quad \ldots \quad (1.21)$$

The stress increments are then obtained as

$$\Delta S_t^i = D\,\Delta\,\epsilon_t^i \quad \ldots \quad \ldots \quad \ldots \quad \ldots \quad \ldots \quad \ldots \quad (1.22)$$

and the total stresses are given by

$$S_t^{i+1} = S_t^i + \Delta S_t^i \quad \ldots \quad \ldots \quad \ldots \quad \ldots \quad \ldots \quad (1.23)$$

The nodal residuals are then defined from (1.23), (1.19) and (1.6) as

$$-\psi^{i+1} = R - \int_{V_t} B_t^T S_t^{i+1}\, dV_t \quad \ldots \quad \ldots \quad \ldots \quad (1.24)$$

1.6.3 Stress-Strain Relations

The constitutive law relating stresses to strains for elastic materials can be written as

$$\sigma = D^e e \quad \ldots \quad \ldots \quad \ldots \quad \ldots \quad \ldots \quad \ldots \quad \ldots \quad (1.25)$$

For an elastic-plastic material the constitutive law relates stress increments to strain increments as

$$\Delta\sigma = D\,\Delta e \quad \ldots \quad \ldots \quad \ldots \quad \ldots \quad \ldots \quad \ldots \quad (1.26)$$

Using the von Mises yield criterion with the Prandtl-Reuss flow rule the yield surface is defined as

$$F = \left[\frac{1}{2}(\sigma_1 - \sigma_2)^2 + \frac{1}{2}(\sigma_2 - \sigma_3)^2 + \frac{1}{2}(\sigma_3 - \sigma_1)^2 + 3\sigma_4^2 + 3\sigma_5^2 + 3\sigma_6^2\right]^{1/2} - \sigma_y$$

$$\equiv \bar{\sigma} - \sigma_y \quad \ldots \quad \ldots \quad \ldots \quad \ldots \quad \ldots \quad \ldots \quad (1.27)$$

where $\sigma_1, \sigma_2, \sigma_3$ are the normal stress components,

$\sigma_4, \sigma_5, \sigma_6$ are the shear stress components,

$\bar{\sigma}$ is the effective stress and

σ_y is the uniaxial yield stress.

The elasto-plastic modulus matrix is then defined as

$$D(\sigma,k) = D^e - D^e\{\frac{\partial F}{\partial \sigma}\}\{\frac{\partial F}{\partial \sigma}\}^T D^e / r \quad \ldots \quad \ldots \quad \ldots \quad (1.28)$$

where the vector $\{\frac{\partial F}{\partial \sigma}\}$ can be obtained from (1.27)

and the value of r is given for isotropic hardening by

$$r = \{\frac{\partial F}{\partial \sigma}\}^T D^e \{\frac{\partial F}{\partial \sigma}\} + \{\frac{4\ E\ k\ \bar{\sigma}^2}{\sigma_y^2}\} \quad \ldots \quad \ldots \quad (1.29)$$

where E is the elastic modulus, $k = E_p/(E - E_p)$ is the hardening parameter and E_p is the post-yield uniaxial modulus for a bilinear strain hardening material.

Once yielding has occurred the plastic strain rate multiplier λ is used to test for plastic loading ($\lambda > 0$) or elastic unloading ($\lambda < 0$) and is given by

$$\lambda = \frac{1}{r} \{\frac{\partial F}{\partial \sigma}\}^T D^e \Delta \mathbf{e} \quad \ldots \quad \ldots \quad \ldots \quad \ldots \quad \ldots \quad (1.30)$$

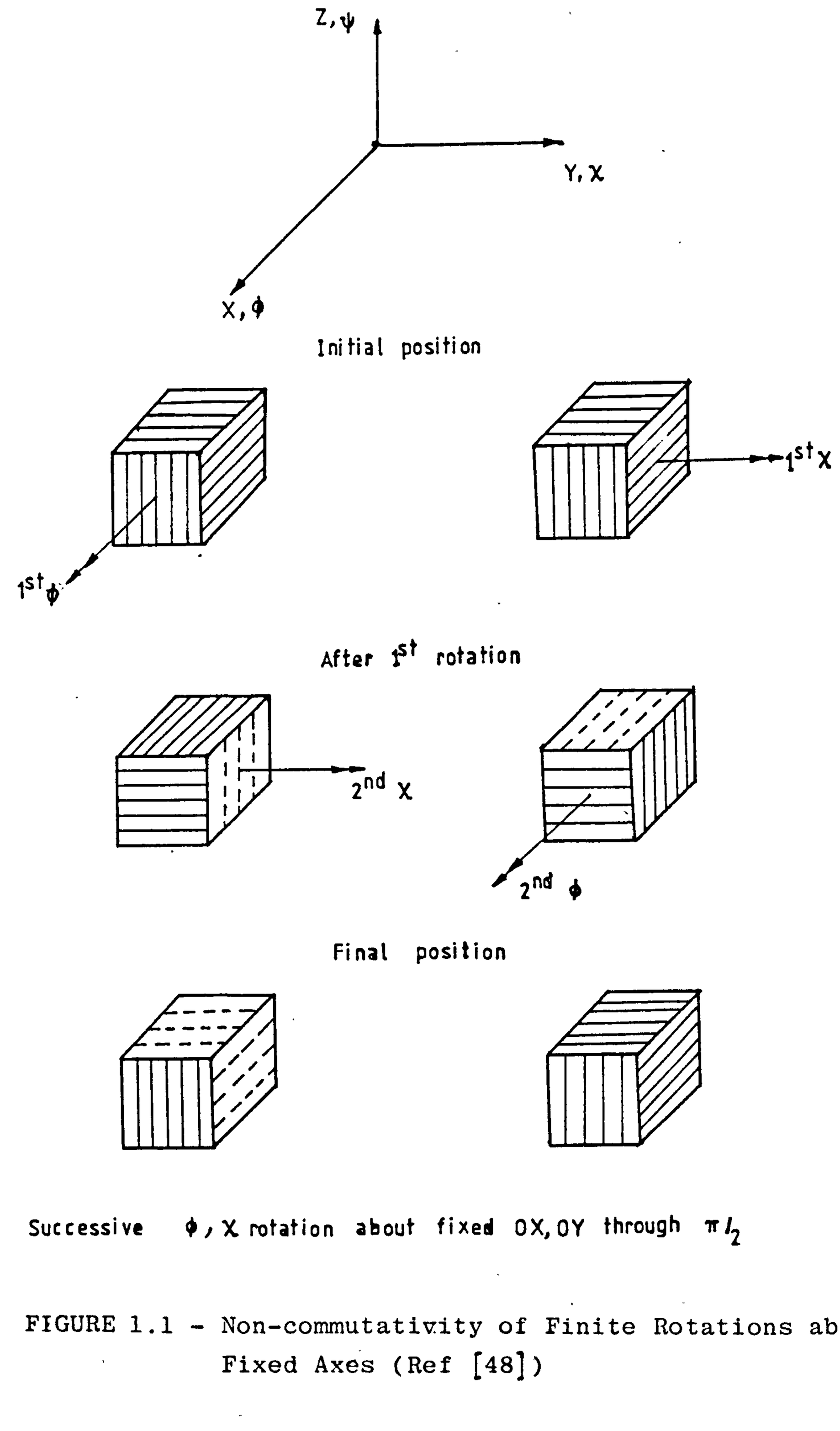

FIGURE 1.1 - Non-commutativity of Finite Rotations about Fixed Axes (Ref [48])

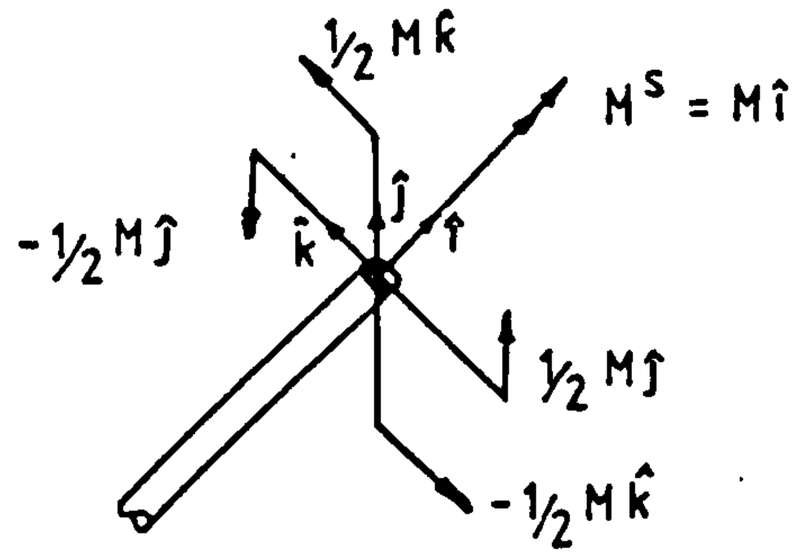

Levers (unit lengths) $\hat{\jmath}$ and $\hat{k}$

Forces (fixed directions) $\pm \frac{1}{2} M \hat{k}$ and $\pm \frac{1}{2} M \hat{\jmath}$

$$M^S = \hat{\jmath} \times \tfrac{1}{2} M \hat{k} - \hat{k} \times \tfrac{1}{2} M \hat{\jmath} = M \hat{\imath}$$

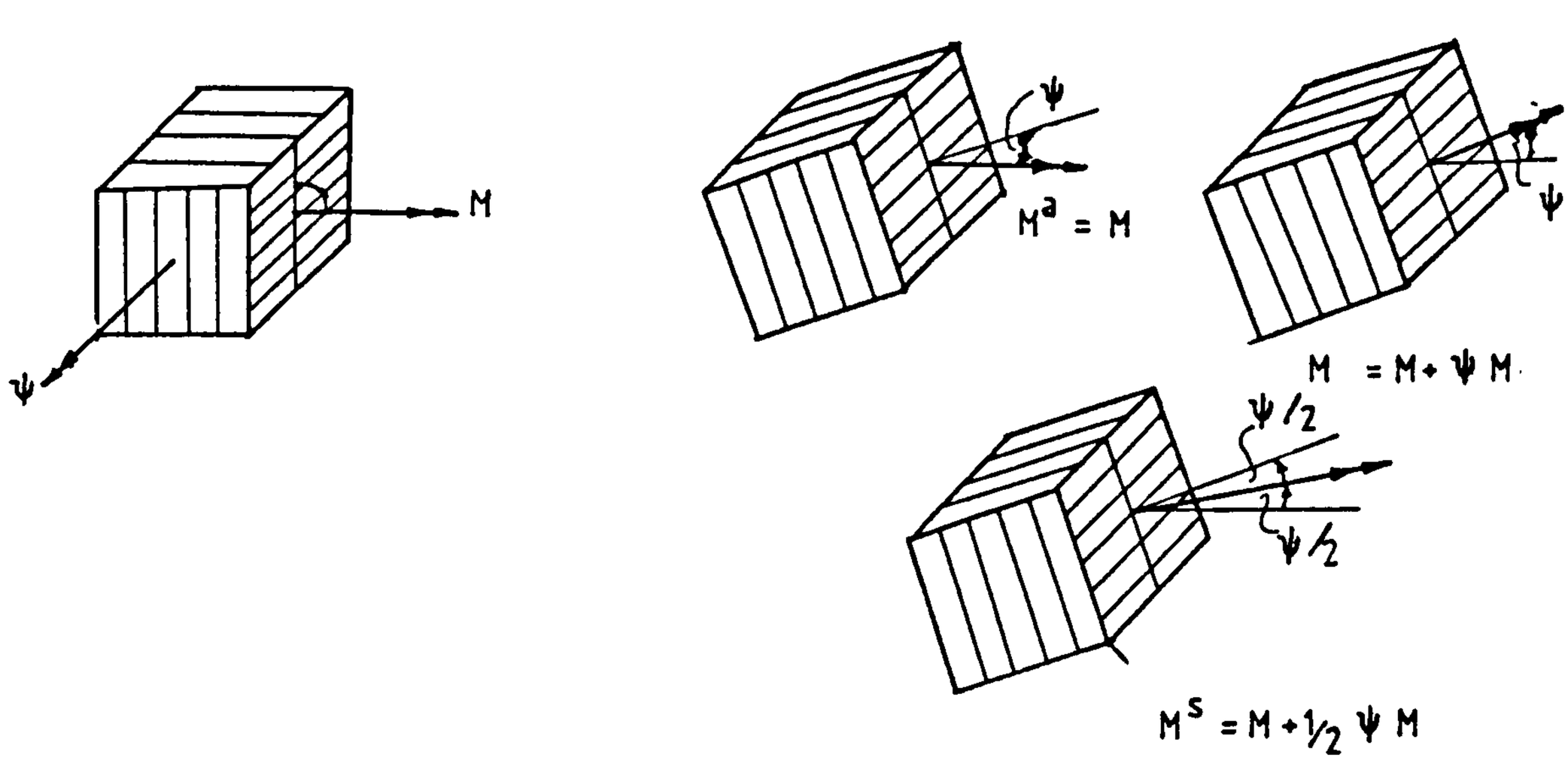

FIGURE 1.2 - Semitangential Moments

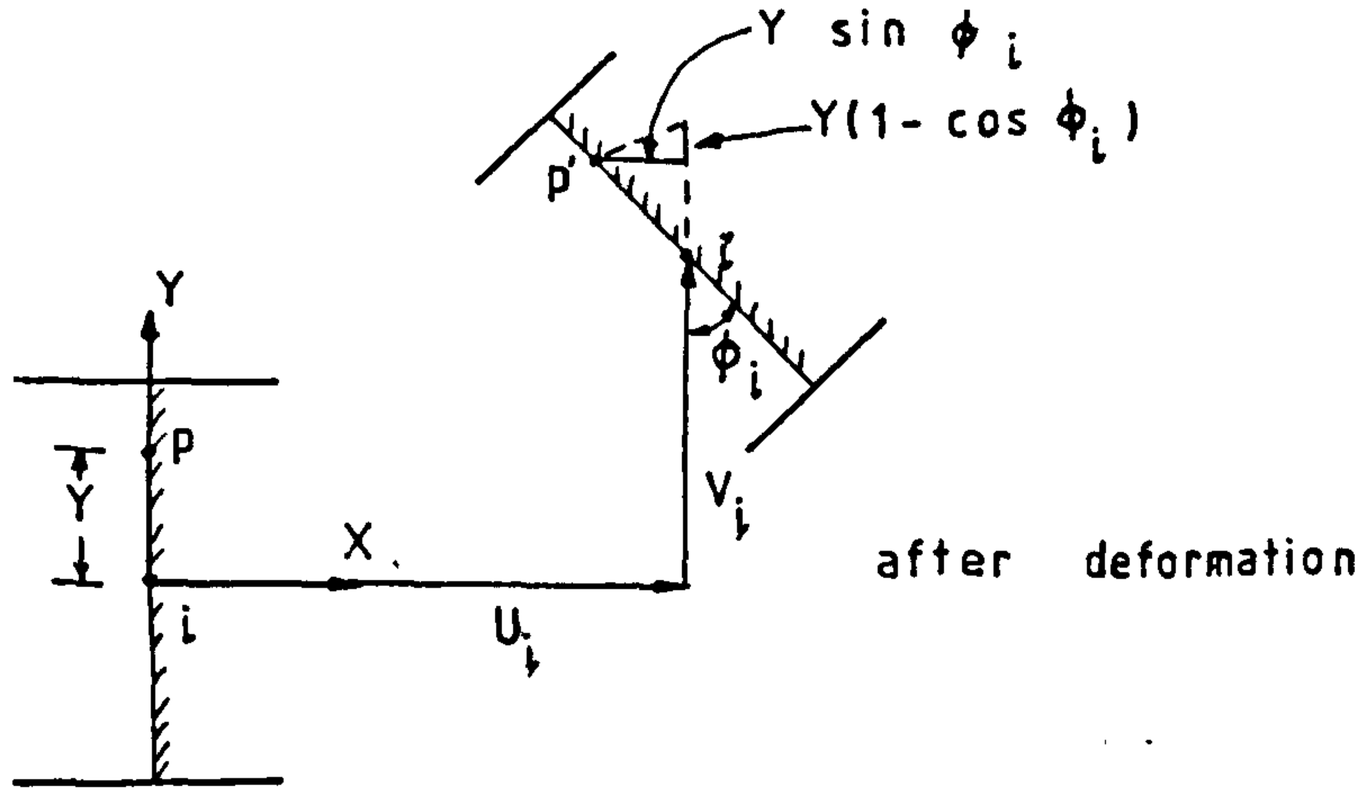

$$U_p = U_i - Y \sin \phi_i$$

$$V_p = V_i - Y(1 - \cos \phi_i)$$

FIGURE 1.3 - Large Displacement Field as a nonlinear Function of Nodal Variables

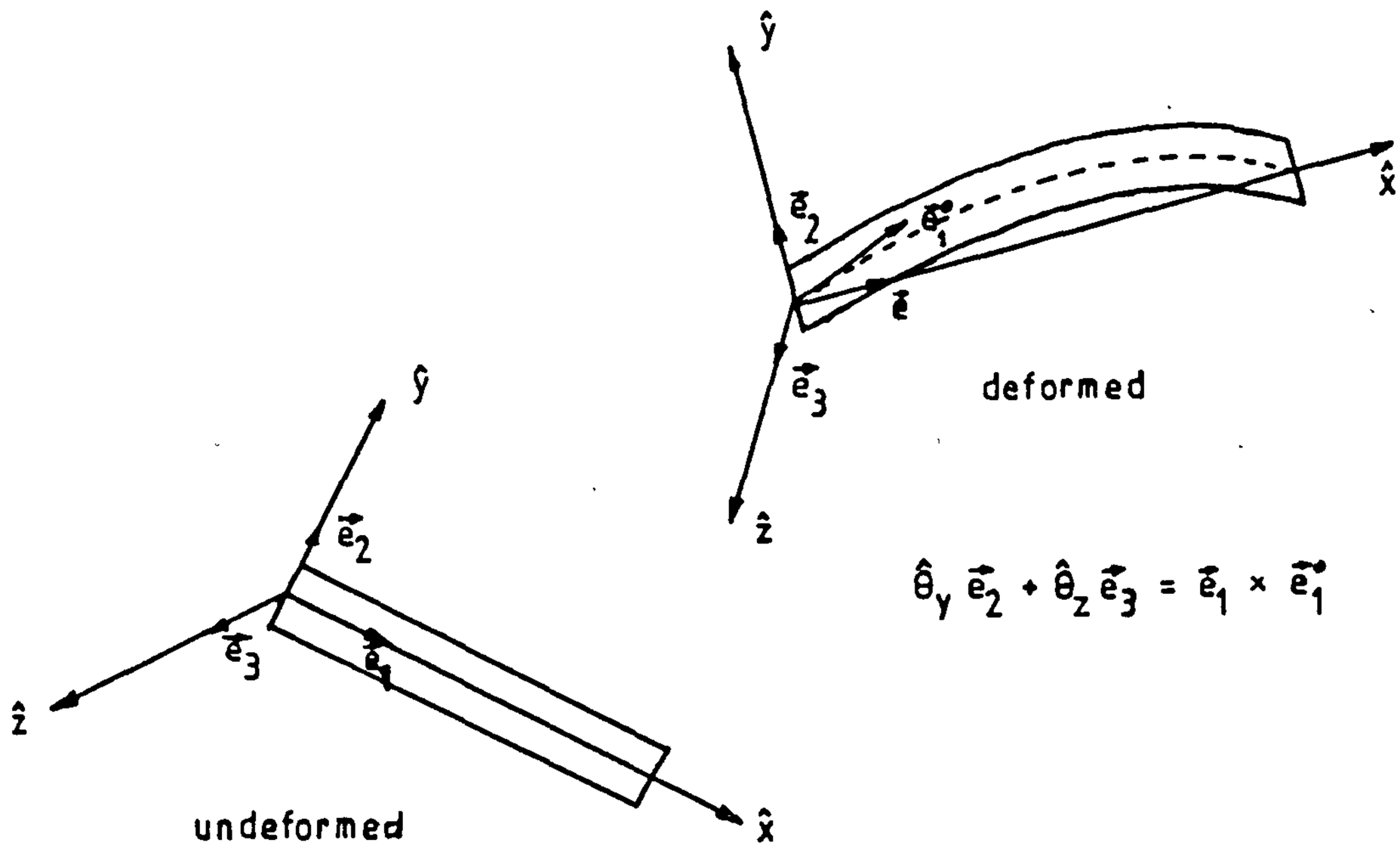

FIGURE 1.4 - Rigid Convected Coordinates ($\hat{x}$, $\hat{y}$, $\hat{z}$)

(Ref [21])

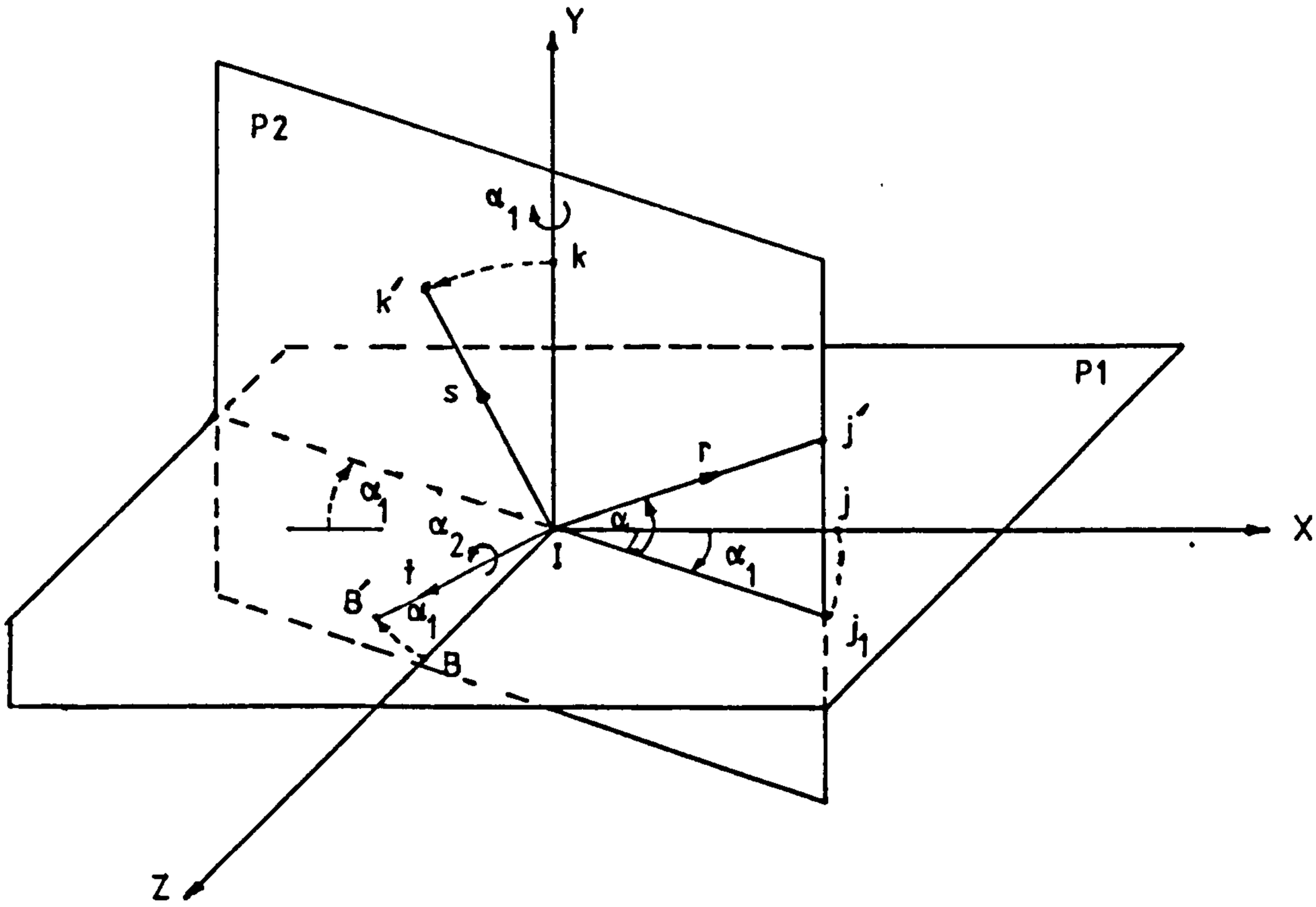

(a) First Step

α_1 = rotation of coordinate axes about Y axis:(X,Y,Z) to (Ij_1,Y,t)

α_2 = rotation of coordinate axes about t axis:(Ij_1,Y,t) to (r,s,t)

Plane P1 is perpendicular to Plane P2

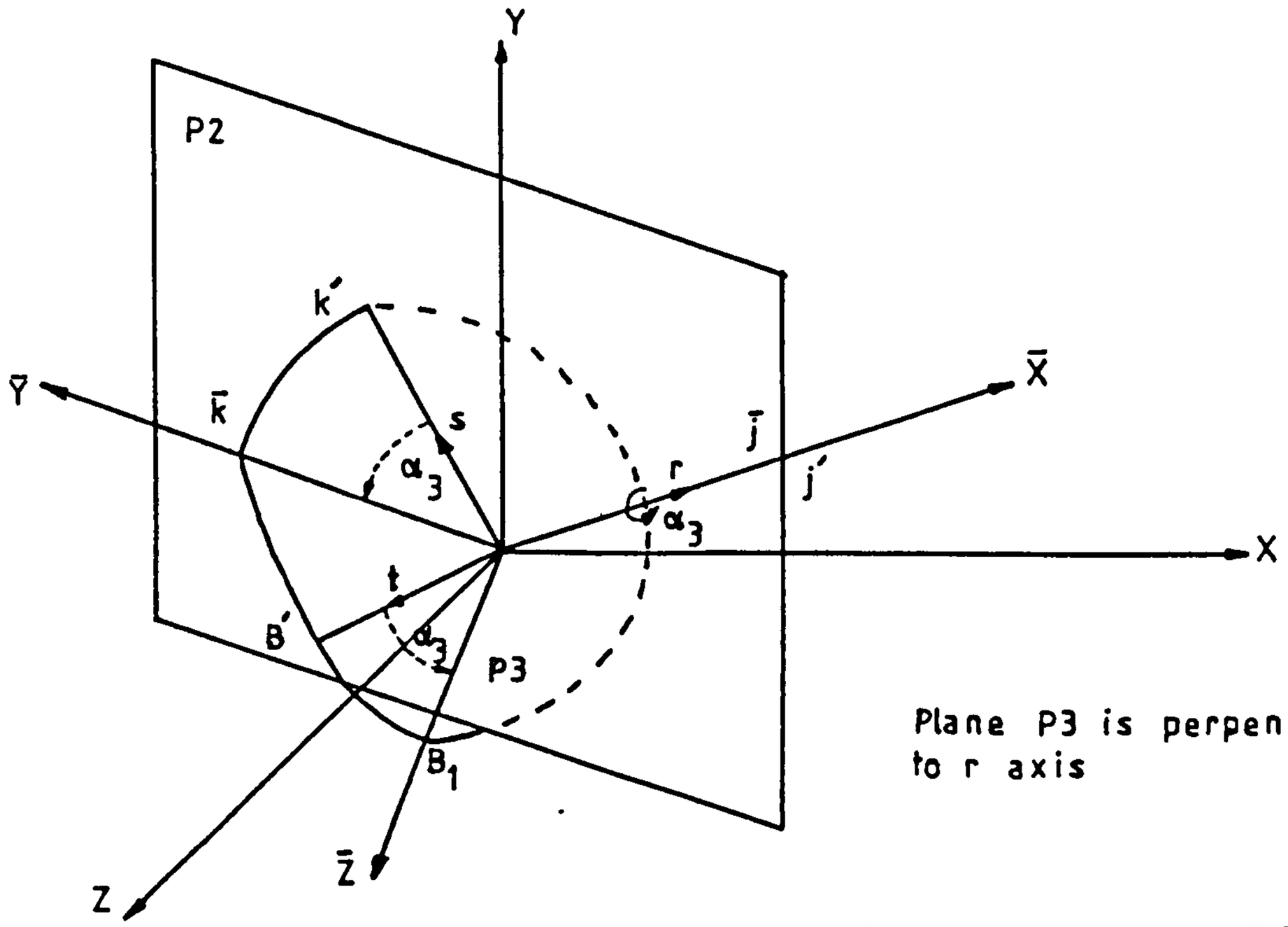

Plane P3 is perpendicular to r axis

α_3 = rotation of coordinate axes about r(≡$\bar{X}$) axis:(r,s,t) to ($\bar{X}$,$\bar{Y}$,$\bar{Z}$)

(b) Final Step

FIGURE 1.5 - Euler Angle Transformations: (X, Y, Z) to ($\bar{X}$, $\bar{Y}$, $\bar{Z}$)

C H A P T E R 2

TWO-DIMENSIONAL LARGE DEFORMATION CURVED BEAM THEORY

2.1 INTRODUCTION

One of the important features of the curved beam problem is the coupling that exists between the displacement components in the definition of strains. In order to describe the large deformations in such a problem it is necessary to use a frame indifferent measure of strains. The Green-Lagrange strain obtained using convective differentiation is such a strain measure. A consequence of using the Green-Lagrange strains is the necessity of defining local coordinate axes for each material point within the element. Whilst the Green-Lagrange strain-displacement relations are generally exact, approximations are usually introduced for beam and shell type problems. These approximations become necessary as a result of attempting to relate the deformation of a general point within the element to the deformation of the neutral surface.

An exact large rotation formulation for two-dimensional straight beam elements based on the Green-Lagrange strains has been presented by Epstein and Murray [25].

The general idea behind this formulation is that the Kirchhoff hypothesis, which assumes that plane sections remain plane and normal to the beam axis after deformation, is used to define the geometric shape of the element after deformation. The geometry after deformation is defined using position vectors and convected coordinates. The Green-Lagrange strain-displacement relations are then obtained from the relations defining geometry after deformation. A generalised approach which is applicable to curved beams is adopted in this chapter by using an intrinsic coordinate system at each material point within an element.

There is a disadvantage, however, in using the Green-Lagrange strains for beam type large rotation, large curvature problems. This is the necessity of assuming direct proportionality between the Green-Lagrange strains and the 2nd Piola-Kirchhoff stresses in the virtual work expression. For beams this amounts to neglecting the effect of curvature on axial force. An attempt to include such an effect using the approach presented by Epstein and Murray [25] results in unsymmetrical matrices (Section 2.2.1). A Total Lagrangian formulation based on such an approximation will result on giving wrong axial force values while predicting the displacements correctly for large rotation and curvature problems.

A remedy to this difficulty is the use of an Updated Lagrangian formulation. This is because in an Updated Lagrangian formulation one can reasonably assume that the 2nd Piola-Kirchhoff stresses are directly proportional to the Green-Lagrange strains in the virtual work expression. The main disadvantage of the Updated Lagrangian formulation, however, is that the element shape functions must be recalculated every time the coordinates are updated. This requires considerable additional computer time compared to a Total Lagrangian solution. Thus, the alternative of a combined Updated and Total Lagrangian formulation has to be considered. In the combined approach the geometry is updated at the beginning of each load increment only. The equilibrium iterations within the increment are based on the Total-Lagrangian formulation.

One approach commonly used in engineering is to assume proportionality between the nominal stress and the conventional strain (50). The assumption that third and higher order terms in displacement gradients are negligible is frequently used to obtain explicit relations, in terms of displacement gradients, for these strain measures. It is possible, however, to obtain exact incremental equilibrium equations for two-dimensional beams, in terms of strain measures, which are explicit functions of displacement gradients,

by using the conventional strains and the nominal stress in the virtual work equation. In a Total Lagrangian formulation this approach includes the effect of curvature on axial force thus making it suitable for large rotation and curvature problems wherein the axial force is of importance.

In this chapter four alternative formulations of the incremental equilibrium equations for small strain large rotation two-dimensional curved beams are presented for comparison. These are:

1. A Total Lagrangian formulation based on the Green strains (TLG).

2. An Updated Lagrangian formulation based on the Green strains (ULG).

3. A combined Updated and Total Lagrangian formulation based on the Green strains (UTLG).

4. A Total Lagrangian formulation based on the conventional strains (TLC).

The contribution to the tangent stiffness matrix due to deformation dependent forces is neglected. The effect of such forces is taken into account, however, by modifying the applied load vector.

2.2. TWO-DIMENSIONAL LARGE ROTATION THEORY

Referring to Figure 2.1 the position vector of any point P on the beam reference axis before deformation is defined in terms of the global coordinates as

$$\vec{r} = X\,\hat{i} + Y\,\hat{j} \quad \ldots \quad \ldots \quad \ldots \quad \ldots \quad \ldots \quad \ldots \qquad (2.1)$$

where X and Y are functions of the natural coordinate ξ.

The local x axis is defined to be tangential to the reference line. A unit vector in the local x direction is defined from (2.1) by

$$\hat{x} = \frac{d\vec{r}/d\xi}{|d\vec{r}/d\xi|} \quad \ldots \quad \ldots \quad \ldots \quad \ldots \quad \ldots \quad \ldots \qquad (2.2)$$

A unit vector in the local y direction is then given by

$$\hat{y} = \hat{k}X\hat{x} \quad \ldots \quad \ldots \quad \ldots \quad \ldots \quad \ldots \quad \ldots \quad \ldots \qquad (2.3)$$

The position vector of a point at distance y from the reference line before deformation is

$$\vec{R} = \vec{r} + y\,\hat{y} \quad \ldots \quad \ldots \quad \ldots \quad \ldots \quad \ldots \quad \ldots \qquad (2.4)$$

After deformation, the position vector of point P on the reference line is

$$\bar{r} = \vec{r} + \vec{V} \quad \ldots \quad \ldots \quad \ldots \quad \ldots \quad \ldots \quad \ldots \quad \ldots \qquad (2.5)$$

where $\vec{V}$ is the displacement vector and is given in terms of the components u and v in the local coordinate directions by

$$\vec{V} = u\,\hat{x} + v\,\hat{y} \quad \ldots \quad \ldots \quad \ldots \quad \ldots \quad \ldots \quad \ldots \qquad (2.6)$$

Since convected coordinates are assumed, using convective differentiation, the natural base vector after deformation is defined as

$$\hat{g} = \frac{d\bar{r}}{dx} = (1 + \frac{du}{dx})\hat{x} + \frac{dv}{dx}\,\hat{y} \quad \ldots \quad \ldots \quad \ldots \quad \ldots \qquad (2.7)$$

The vector $\vec{N}$ normal to $\hat{g}$ is

$$\vec{N} = \hat{k} \times \hat{g} = -\frac{dv}{dx}\,\hat{x} + (1 + \frac{du}{dx})\hat{y} \quad \ldots \quad \ldots \quad \ldots \qquad (2.8)$$

Since plane sections are assumed to remain plane and normal to the reference axis, the vector $\vec{N}$ is used to define the local y direction after deformation. The unit vector $\hat{n}$ in the direction of $\vec{N}$ is given from (2.8) by

$$\hat{n} = \frac{\vec{N}}{|\vec{N}|} = \frac{-\,dv/dx\ \hat{x} + (1 + du/dx)\hat{y}}{(1 + 2e)^{1/2}} \quad \ldots \quad \ldots \quad (2.9)$$

where e is the Green strain measure of the reference line given by

$$e = \frac{du}{dx} + \frac{1}{2}\left(\frac{du}{dx}\right)^2 + \frac{1}{2}\left(\frac{dv}{dx}\right)^2 \quad \ldots \quad \ldots \quad \ldots \quad \ldots \quad (2.10)$$

Assuming that the strain normal to the beam reference axis is negligible, the position vector after deformation of point distant y from the reference line can be written as

$$\bar{R} = \bar{r}(x) + y\,\hat{n} \quad \ldots \quad \ldots \quad \ldots \quad \ldots \quad \ldots \quad \ldots \quad (2.11)$$

From (2.7), (2.9) and (2.11) the derivatives of $\bar{R}$ with respect to the convected x and y coordinates are

$$\frac{\partial \bar{R}}{\partial x} = \hat{g} + y\,\frac{d\hat{n}}{dx}$$

$$\frac{\partial \bar{R}}{\partial y} = \hat{n} \quad \ldots \quad \ldots \quad \ldots \quad \ldots \quad \ldots \quad \ldots \quad (2.12)$$

The vector $\frac{d\hat{n}}{dx}$ is normal to $\hat{n}$ and parallel to the convected x coordinate. Thus

$$\frac{d\hat{n}}{dx} = -\,K\,\hat{g} \quad \ldots \quad \ldots \quad \ldots \quad \ldots \quad \ldots \quad \ldots \quad (2.13)$$

where K is a measure of the physical curvature.

Substituting from (2.13) into (2.12) gives

$$\frac{\partial \bar{R}}{\partial x} = (1 - K\ y)\hat{g}$$

$$\frac{\partial \bar{R}}{\partial y} = \hat{n} \qquad \ldots \quad \ldots \quad \ldots \quad \ldots \quad \ldots \qquad (2.14)$$

Therefore from (2,14), (2.10), (2.9) and (2.7)

$$\frac{\partial \bar{R}}{\partial x} \cdot \frac{\partial \bar{R}}{\partial x} = (1 - K\ y)^2\ \hat{g}.\hat{g} = (1 - K\ y)^2\ (1 + 2e)$$

$$\frac{\partial \bar{R}}{\partial x} \cdot \frac{\partial \bar{R}}{\partial y} = (1 - K\ y)\hat{g}.\hat{n} = 0$$

$$\frac{\partial \bar{R}}{\partial y} \cdot \frac{\partial \bar{R}}{\partial y} = \hat{n}.\hat{n} = 1 \qquad \ldots \quad \ldots \quad \ldots \qquad (2.15)$$

2.2.1 Internal Virtual Work in Terms of The Green Strain

The Green Strain tensor in two dimensions is

$$\epsilon = \frac{1}{2}\left(\begin{bmatrix} \frac{\partial \bar{R}}{\partial x} \cdot \frac{\partial \bar{R}}{\partial x} & \frac{\partial \bar{R}}{\partial x} \cdot \frac{\partial \bar{R}}{\partial y} \\ \frac{\partial \bar{R}}{\partial y} \cdot \frac{\partial \bar{R}}{\partial x} & \frac{\partial \bar{R}}{\partial y} \cdot \frac{\partial \bar{R}}{\partial y} \end{bmatrix} - \begin{bmatrix} 1 & 0 \\ 0 & 1 \end{bmatrix} \right) \quad \ldots \qquad (2.16)$$

Substituting from (2.15) into (2.16) provides only one non-zero strain component ε_{xx} which is defined as

$$\varepsilon'_t = \varepsilon_{xx} = \frac{1}{2}\left(\frac{\partial \bar{R}}{\partial x} \cdot \frac{\partial \bar{R}}{\partial x} - 1\right)$$

$$= (1 - K\,y)^2 \left(\frac{1}{2} + e\right) - \frac{1}{2} \quad \ldots \quad \ldots \quad \ldots \quad (2.17)$$

The internal virtual work expression in a Lagrangian frame of reference at time t is given by the following definition

$$\delta W_{int} = \int_{V_t} \delta \varepsilon'^{T}_t \, S_t \, dV_t \quad \ldots \quad \ldots \quad \ldots \quad \ldots \quad (2.18)$$

If it is assumed that the area A remains constant, the volume increment dV_t is defined in terms of the initial dimensions as [25]

$$dV_t = (1 + 2e)^{1/2} \, dA \, dL_o \quad \ldots \quad \ldots \quad \ldots \quad \ldots \quad (2.19)$$

Hence, in a Total Lagrangian frame of reference the internal virtual work expression is given from (2.18) and (2.19) by

$$\delta W_{int} = \int_{L_o} \int_{A} \delta \varepsilon'^{T}_o \; S_o (1 + 2e)^{1/2} \, dA \, dL_o$$

$$\ldots \quad \ldots \quad \ldots \quad \ldots \quad \ldots \quad (2.20)$$

where S_o is the 2nd Piola-Kirchhoff *stress. The* integration is over the initial area A and the initial length L_o.

From (2.17) the variation in strain is

$$\delta\varepsilon'_t = (1 - K\,y)(1 + 2e)(-y\,\delta K) + (1 - Ky)^2\delta e \qquad (2.21)$$

Defining a new curvature term χ which is an explicit function of the displacement gradients as

$$\chi = -(1 + 2e)^{3/2} K \quad \ldots \quad \ldots \quad \ldots \quad \ldots \quad \ldots \qquad (2.22)$$

and substituting for δK from (2.22) into (2.21) gives

$$\delta\varepsilon'_t = (1 - K\,y)(1 + 2e)^{-1/2}\, y\,\delta\chi +$$

$$+ (1 - K\,y)(1 + 2\,K\,y)\delta e \quad \ldots \quad \ldots \quad \ldots \qquad (2.23)$$

The strain variation is then substituted from (2.23) into (2.20) to give

$$\delta W_{int} = \int_{L_o} M\,\delta\chi + [(1 + 2e)^{1/2} P_o +$$

$$+ 2K(1 + 2e)^{1/2} M)\delta e]\, dL_o$$

$$= \int_{L_o} M\delta\chi + \tilde{N}\,\delta e \quad \ldots \quad \ldots \quad \ldots \quad \ldots \qquad (2.24)$$

where the stress resultants P_o and M are given by

$$P_o = \int_A (1 - K\,y) S_o \, dA$$

$$M = \int_A (1 - K\,y) y \, S_o \, dA \qquad \ldots \quad \ldots \quad \ldots \qquad (2.25)$$

and

$$\tilde{N} = (1 + 2e)^{1/2} P_o + 2K(1 + 2e)^{1/2} M \quad \ldots \quad \ldots \qquad (2.26)$$

The internal virtual work expression of (2.24) is exact and the strain measures e and χ are explicit functions of the displacement gradients and are given from (2.9), (2.10), (2.13) and (2.22) by

$$e = \frac{du}{dx} + \frac{1}{2}\left(\frac{du}{dx}\right)^2 + \frac{1}{2}\left(\frac{dv}{dx}\right)^2$$

$$\chi = (1 + 2e)^{3/2} \frac{d\hat{n}}{dx} \cdot \hat{g}/(\hat{g}.\hat{g})$$

$$= - \frac{d^2v}{dx^2}\left(1 + \frac{du}{dx}\right) + \frac{dv}{dx} \frac{d^2u}{dx^2} \quad \ldots \quad \ldots \quad \ldots \qquad (2.27)$$

It can be seen from (2.24) that the axial force measure $\tilde{N}$ which is work conjugate to the Green strain measure of the reference axis e is a function of both the strain e and the curvature K. While e can be assumed small compared to unity for small strains and hence neglected, the curvature K cannot always be neglected

without introducing an error. This is particularly so for problems where both curvatures and rotations are large and wherein the effect of axial force is of importance. Retaining this term in the virtual work expression, however, results in an unsymmetrical tangent stiffness matrix and hence it is neglected. This amounts to assuming direct proportionality between the 2nd Piola-Kirchhoff stress and the Green-Lagrange strain in the virtual work expression and neglecting the coupling between the axial and bending stress resultants. Thus, the strain at any point is defined in terms of the generalised strain resultants as

$$\varepsilon'_o \simeq \begin{bmatrix} 1 & y \end{bmatrix} \begin{Bmatrix} e \\ \chi \end{Bmatrix} = H\varepsilon_o \quad \ldots \quad \ldots \quad \ldots \quad (2.28)$$

and the stress is

$$S_o = E\,\varepsilon'_o = E\,H\,\varepsilon_o \quad \ldots \quad \ldots \quad \ldots \quad \ldots \quad (2.29)$$

where E is Young's modulus.

The internal virtual work expression (2.20) now takes the following form

$$\delta W_{int} = \int_A \delta\varepsilon_o^T \int_A H^T E H \, dA \, \varepsilon_o \, dL_o$$

$$= \int_{L_o} \varepsilon_o^T \bar{D} \varepsilon_o dL_o \quad \ldots \quad \ldots \quad \ldots \quad \ldots \quad \ldots \qquad (2.30)$$

in which $\bar{D}$ is the modulus matrix.

2.2.2 Internal Virtual Work in Terms of The Conventional Strain

The geometric measures of strain as unit stretch and angle change are

$$\varepsilon_{ii} = \left(\frac{\partial \bar{R}}{\partial x_i} \cdot \frac{\partial \bar{R}}{\partial x_i}\right)^{1/2} - 1$$

$$i = 1, 3; \; j = 1, 3$$

$$\gamma_{ij} = \frac{\partial \bar{R}}{\partial x_i} \cdot \frac{\partial \bar{R}}{\partial x_j} \quad i \neq j \quad \ldots \quad \ldots \quad \ldots \quad \ldots \qquad (2.31)$$

where in (2.31) the shear strains γ_{ij} are assumed to be small. This assumption is valid for the thin beams considered here for which the shear strain is actually assumed to be zero. For the general case, however, the change in the right angle can be used as the definition of the shear (see Appendix II).

From (2.31) and (2.15) it can be seen that the only non-zero strain term is ε_{xx}, as before, and is given by

$$\varepsilon'_t = \varepsilon_{xx} = \left(\frac{\partial \bar{R}}{\partial x} \cdot \frac{\partial \bar{R}}{\partial x}\right)^{1/2} - 1$$

$$= (1 - K\,y)\,(1 + 2e)^{1/2} - 1 \qquad \ldots \quad \ldots \qquad (2.32)$$

and its variation is

$$\delta\varepsilon'_t = -\,y(1 + 2e)^{1/2}\,\delta K +$$

$$+ (1 - K\,y)\,(1 + 2e)^{-1/2}\delta e \qquad \ldots \quad \ldots \qquad (2.33)$$

The strain displacement relations can be approximated from (2.32) by using the binomial series expansion and neglecting third and higher order terms in displacement gradients, so that

$$\varepsilon'_t \simeq \begin{bmatrix} 1 & y \end{bmatrix} \begin{Bmatrix} \frac{du}{dx} + \frac{1}{2}\left(\frac{dv}{dx}\right)^2 \\ -\frac{d^2v}{dx^2}\left(1 - \frac{du}{dx}\right) + \frac{dv}{dx}\,\frac{d^2u}{dx^2} \end{Bmatrix} \ldots \qquad (2.32a)$$

These relations are similar to those which have been presented by Donnell [50] for plates. Relations (2.32a) can also be obtained by writing the Green strains in terms of deformation and rotation tensors and neglecting second and higher order terms in strains

as suggested by Oden [12]. However, in what follows relations (2.32) are used in their exact form.

The strain components are redefined as follows:

$$\varepsilon_t^* = \begin{Bmatrix} e^* \\ \chi^* \end{Bmatrix} = \begin{Bmatrix} (1 + 2e)^{1/2} - 1 \\ -(1 + 2e)^{1/2} K \end{Bmatrix} \quad \ldots \quad \ldots \quad (2.34)$$

Taking variations of (2.34) and substituting into (2.33) gives

$$\delta\varepsilon_t' = \delta e^* + y\,\delta\varepsilon^* = \begin{bmatrix} 1 & y \end{bmatrix} \begin{Bmatrix} \delta e^* \\ \delta\chi^* \end{Bmatrix}$$

$$= H\delta\varepsilon_t^* \quad \ldots \quad \ldots \quad \ldots \quad (2.35)$$

The stress S_t is assumed to be proportional to the strain ε_t'. Therefore, from (2.32) and (2.34):

$$S_t = E\,\varepsilon_t' = E((1 + 2e)^{1/2} - 1 - K(1 + 2e)^{1/2} y)$$

$$= E \begin{bmatrix} 1 & y \end{bmatrix} \begin{Bmatrix} e^* \\ \chi^* \end{Bmatrix} = EH\varepsilon_t^*$$

$$\ldots \quad \ldots \quad \ldots \quad (2.36)$$

The curvature term χ^* is then defined in terms of the explicit function of displacement gradients χ. From (2.34), (2.22) and (2.13) we have

$$\chi^* = -K(1+2e)^{1/2} = \frac{d\hat{n}}{dx}\cdot\hat{g}\,(1+2e)^{1/2}$$

$$= \frac{\chi}{1+2e} \qquad \ldots\ \ldots\ \ldots\ \ldots\ \ldots\ \ldots \qquad (2.37)$$

Therefore from (2.34) and (2.37)

$$\delta\varepsilon^* = \begin{Bmatrix} \delta e^* \\ \delta\chi^* \end{Bmatrix} = \begin{bmatrix} \frac{1}{(1+2e)^{1/2}} & 0 \\ \frac{-2\chi}{(1+2e)^2} & \frac{1}{(1+2e)} \end{bmatrix} \begin{Bmatrix} \delta e \\ \delta\chi \end{Bmatrix}$$

$$= H^*\delta\varepsilon \qquad \ldots\ \ldots\ \ldots\ \ldots\ \ldots\ \ldots \qquad (2.38)$$

From (2.35) and (2.36) the internal virtual work expression (2.18) now takes the form

$$\delta W_{int} = \int_{V_t} \delta\varepsilon_t'^{T}\, S_t\, dV_t$$

$$= \int_{L_t} \delta\varepsilon_t^T H^{*T} \int_{A_t} H^T E H\, dA_t\, \varepsilon_t^*\, dL_t$$

$$= \int_{L_t} \delta\varepsilon_t^T H^{*T} \bar{D}\, \varepsilon_t^*\, dL_t \qquad \ldots\ \ldots\ \ldots \qquad (2.39)$$

where $\bar{D}$ is the modulus matrix.

This virtual work expression is equally applicable to both the Updated and Total Lagrangian formulations. This expression is used for the Total Lagrangian formulation however, because its advantage is clearly pronounced in this formulation with the additional benefit of economy in computer time.

2.3 STRESS-STRAIN RELATIONS

Since the strains are assumed to be small the constitutive relations used for small displacement formulations are included in all formulations developed.

There is only one non-zero stress term which is defined in terms of Young's modulus E and the strain ε' (Equations (2.9) and (2.36)) as

$$S = E \varepsilon' = D \varepsilon' \quad \ldots \quad \ldots \quad \ldots \quad \ldots \quad \ldots \quad (2.40)$$

From (2.30) and (2.39) the rigidity matrix $\bar{D}$ which relates the stress resultants, i.e. axial force and bending moment, to the generalised strains is defined as follows

$$\bar{D} = \int_A H^T E H \, dA$$

$$= \int_A \begin{bmatrix} E & Ey \\ Ey & Ey^2 \end{bmatrix} dA \quad \ldots \quad \ldots \quad \ldots \quad \ldots \qquad (2.41)$$

Assuming that the cross-sectional area A remains constant, the integration is carried out explicitly to give

$$\bar{D} = \begin{bmatrix} EA & EAe \\ EAe & EI \end{bmatrix} \quad \ldots \quad \ldots \quad \ldots \qquad (2.42)$$

where Ae is the first moment of area and I is the second moment of area about the reference axis.

2.4 THE INCREMENTAL EQUILIBRIUM EQUATIONS

During the development of the incremental equilibrium equations the applied loads are assumed to be conservative. In this section the tangent stiffness matrix and the incremental stress and strain relations are developed for each of the four formulations adopted.

2.4.1 Total Lagrangian Formulation Based on Green Strain Measure (TLG)

The strains at a general point are given in terms of the displacement gradients from (2.27) and (2.28) by

$$\varepsilon'_o = H\left(\begin{Bmatrix} \frac{du_o}{dx} \\ -\frac{d^2v_o}{dx^2} \end{Bmatrix} + \begin{Bmatrix} \frac{1}{2}\left(\frac{du_o}{dx}\right)^2 + \frac{1}{2}\left(\frac{dv_o}{dx}\right)^2 \\ \frac{dv_o}{dx}\frac{d^2u_o}{dx^2} - \frac{du_o}{dx}\frac{d^2v_o}{dx^2} \end{Bmatrix}\right)$$

$$= H\{\varepsilon_o^o + \varepsilon_o^L\} \quad \ldots \quad \ldots \quad \ldots \quad \ldots \quad \ldots \quad (2.43)$$

in which ε_o^o is the infinitesimal strain and is written, in a finite element representation, in terms of the nodal variables $\mathbf{a}_o$ as

$$\varepsilon_o^o = \begin{Bmatrix} \frac{du_o}{dx} \\ -\frac{d^2v_o}{dx^2} \end{Bmatrix} = \bar{B}_o\, \mathbf{a}_o \quad \ldots \quad \ldots \quad \ldots \quad \ldots \quad (2.44)$$

and ε_o^L is the nonlinear strain which can be written as

$$\varepsilon_o^L = \frac{1}{2}\begin{bmatrix} \frac{du_o}{dx} & \frac{dv_o}{dx} & 0 & 0 \\ -\frac{d^2v_o}{dx^2} & \frac{d^2u_o}{dx^2} & \frac{du_o}{dx} & \frac{dv_o}{dx} \end{bmatrix} \begin{Bmatrix} \frac{du_o}{dx} \\ \frac{dv_o}{dx} \\ -\frac{d^2v_o}{dx^2} \\ \frac{d^2u_o}{dx^2} \end{Bmatrix}$$

$$= \frac{1}{2}\bar{B}_L(a_o)a_o = \frac{1}{2} A_\theta \theta_o \quad \ldots \quad \ldots \quad \ldots \quad (2.45)$$

In a finite element representation defining the vector θ_o in terms of the nodal degrees of freedom a_o we have

$$\theta_o = \{\frac{du_o}{dx}, \frac{dv_o}{dx}, -\frac{d^2v_o}{dx^2}, \frac{d^2u_o}{dx^2}\}^T = G_o a_o \quad \ldots \quad (2.46)$$

Taking variations of (2.43) with respect to the nodal variables, the strain-displacement matrix B (Equation (1.13)) is given by

$$B = B_o + B_L(u_o) = H[\bar{B}_o + \bar{B}_L(a_o)]$$

$$= H\bar{B} \quad \ldots \quad \ldots \quad \ldots \quad \ldots \quad \ldots \quad \ldots \quad \ldots \quad (2.47)$$

From (2.47), (2.41) and (2.40) the tangent stiffness matrix (Equation (1.14)) now takes the following form

$$K_T = \int_{V_o} B^T D B \, dV_o + \int_{V_o} \frac{\partial B}{\partial u} S_o \, dV_o$$

$$= \int_{L_o} \bar{B}^T \left(\int_{A_o} H^T D H \, dA_o \right) \bar{B} \, dL_o$$

$$+ \int_{L_o} \frac{\partial \bar{B}^T}{\partial a} \int_{A_o} H^T S_o \, dA_o \, dL_o$$

$$= \int_{L_o} \bar{B}^T \bar{D} \bar{B} \, dL_o + \int_{L_o} \frac{\partial \bar{B}^T}{\partial a} \bar{S}_o \, dL_o$$

$$= (K + K_L(a_o)) + K_\sigma \quad \ldots \quad \ldots \quad \ldots \quad \ldots \quad (2.48)$$

where

$$\bar{S}_o = \int_{A_o} H^T S_o \, dA_o = \{P_o, M_o\}^T \quad \ldots \quad \ldots \quad \ldots \quad (2.49)$$

is the vector of initial stress resultants composed of an axial force P_o and a bending moment M_o.

The explicit form of the initial stress stiffness matrix K_σ (Equation (2.48)) is obtained from (2.46), (2.45) and (2.44) as follows:

$$K_\sigma = \int_{L_o} \frac{\partial \bar{B}^T}{\partial a} \bar{S}_o \, dL_o = \int_{L_o} \frac{\partial \bar{B}_L}{\partial a} \bar{S}_o \, dL_o$$

$$= \int_{L_o} G_o^T \frac{\partial A_\theta^T}{\partial a} \bar{S}_o \, dL_o$$

$$= \int_{L_o} G_o^T \frac{\partial}{\partial a} \begin{bmatrix} \frac{du_o}{dx} & -\frac{d^2 v_o}{dx^2} \\ \frac{dv_o}{dx} & \frac{d^2 u_o}{dx^2} \\ 0 & \frac{du_o}{dx} \\ 0 & \frac{dv_o}{dx} \end{bmatrix} \begin{Bmatrix} P_o \\ M_o \end{Bmatrix} dL_o$$

$$= \int_{L_o} G_o^T \begin{bmatrix} P_o [I] & M_o [I] \\ M_o [I] & 0 \end{bmatrix} \frac{\partial \theta_o}{\partial a} \, dL_o$$

$$= \int_{L_o} G_o^T \bar{P}_{oi} G_o \, dL_o \quad \ldots \quad \ldots \quad \ldots \quad \ldots \quad (2.50)$$

where $\bar{P}_{oi}$ is the initial stress resultant matrix and $[I]$ is a two by two unit matrix.

Using the tangent stiffness matrix and the residual nodal forces, the displacement increments Δa_o^i are evaluated. The total displacements are then obtained as

$$a_o^{i+1} = a_o^i + \Delta a_o^i \quad \ldots \quad \ldots \quad \ldots \quad \ldots \quad \ldots \quad (2.51)$$

The incremental strain resultants (Equation (1.15)) are defined by

$$\Delta \varepsilon_o^i = [\bar{B}_o + \bar{B}_L(a_o^i) + \frac{1}{2} \bar{B}_L(\Delta a_o^i)] \{\Delta a_o^i\} \quad \ldots \quad \ldots \quad (2.52)$$

From (2.30) and (2.52) the increments of the stress resultants (Equation (1.16)) are given by

$$\Delta \bar{S}_o^i = \bar{D} \Delta \varepsilon_o^i \quad \ldots \quad \ldots \quad \ldots \quad \ldots \quad \ldots \quad \ldots \quad (2.53)$$

and the total stress resultants are

$$\bar{S}_o^{i+1} = \bar{S}_o^i + \Delta \bar{S}_o^i \quad \ldots \quad \ldots \quad \ldots \quad \ldots \quad \ldots \quad \ldots \quad (2.54)$$

From which the nodal residual forces are evaluated as follows

$$- \psi^{i+1} = R - \int_{L_o} \bar{B}^T \bar{S}_o^{i+1} \, dL_o \quad \ldots \quad \ldots \quad \ldots \quad (2.55)$$

where R is the vector of applied equivalent nodal forces and

$$\bar{B} = \bar{B}_o + \bar{B}_L(a_o^{i+1})$$

Using the new total displacements (Equation (2.51)) and the new total stress resultants (Equation (2.54)), the tangent stiffness matrix can be reformed and hence used with the residuals given by (2.55) to obtain a new set of displacement increments.

2.4.2 Updated Lagrangian Formulation Based on Green Strain Measure (ULG)

With reference to the configuration at time t the strains are defined from (2.27) and (2.28) as

$$\varepsilon'_t = H\left(\begin{Bmatrix} \frac{du_t}{dx} \\ -\frac{d^2v_t}{dx^2} \end{Bmatrix} + \begin{Bmatrix} \frac{1}{2}\left(\frac{du_t}{dx}\right)^2 + \frac{1}{2}\left(\frac{dv_t}{dx}\right)^2 \\ \frac{dv_t}{dx}\ \frac{d^2u_t}{dx^2} - \frac{du_t}{dx}\ \frac{d^2v_t}{dx^2} \end{Bmatrix}\right)$$

$$= H(\varepsilon_t^o + \varepsilon_t^L) \qquad \ldots \quad \ldots \quad \ldots \quad \ldots \quad \ldots \qquad (2.56)$$

where

$$\varepsilon_t^o = \begin{Bmatrix} \frac{du_t}{dx} \\ -\frac{d^2v_t}{dx^2} \end{Bmatrix} = B_t^o\, a_t \qquad \ldots \quad \ldots \quad \ldots \quad \ldots \qquad (2.57)$$

and

$$\varepsilon_t^L = \begin{bmatrix} \frac{du_t}{dx} & \frac{dv_t}{dx} & 0 & 0 \\ -\frac{d^2v_t}{dx^2} & \frac{d^2u_t}{dx^2} & \frac{du_t}{dx} & \frac{dv_t}{dx} \end{bmatrix} \begin{Bmatrix} \frac{du_t}{dx} \\ \frac{dv_t}{dx} \\ -\frac{d^2v_t}{dx^2} \\ \frac{d^2u_t}{dx^2} \end{Bmatrix}$$

$$= \frac{1}{2} B_L(a_t) a_t = \frac{1}{2} A_\theta \theta_t \quad \ldots \quad \ldots \quad \ldots \qquad (2.58)$$

where θ_t is given in a finite element representation by

$$\theta_t = \{\frac{du_t}{dx}, \frac{dv_t}{dx}, -\frac{d^2v_t}{dx^2}, \frac{d^2u_t}{dx^2}\}^T = G_t a_t \qquad (2.59)$$

a_t being the vector of nodal variables.

Taking variations of (2.56), the strain displacement matrix **B** (Equation (1.19)) is given by

$$\mathbf{B} = \mathbf{B}_t + \mathbf{B}_L(u_t) = \mathbf{H}\left[\bar{\mathbf{B}}_t + \mathbf{B}_L(a_t)\right]$$

$$= \mathbf{H}\,\bar{\mathbf{B}} \quad \ldots \quad \ldots \quad \ldots \quad \ldots \quad \ldots \quad \ldots \quad \ldots \qquad (2.60)$$

Assuming that the reference configuration instantaneously coincides with the current configuration at time t, the tangent stiffness matrix (Equation (1.20)) is of the form

$$\mathbf{K}_T = \int_{V_t} \mathbf{B}_t^T \mathbf{D} \mathbf{B}_t \, dV_t + \int_{V_t} \frac{\partial \mathbf{B}^T}{\partial \mathbf{u}} \mathbf{S}_t \, dV_t$$

$$= \int_{L_t} \bar{\mathbf{B}}_t^T \left(\int_{A_t} \mathbf{H}^T \mathbf{D} \mathbf{H} \, dA_t \right) \bar{\mathbf{B}}_t \, dL_t + \int_{L_t} \frac{\partial \bar{\mathbf{B}}^T}{\partial \mathbf{a}} \int_{A_t} \mathbf{H}^T \mathbf{S}_t \, dA_t \, dL_t$$

$$= \int_{L_t} \bar{\mathbf{B}}_t^T \bar{\mathbf{D}} \bar{\mathbf{B}}_t \, dL_t + \int_{L_t} \frac{\partial \bar{\mathbf{B}}^T}{\partial \mathbf{a}} \bar{\mathbf{S}}_t \, dL_t = \mathbf{K}_t + \mathbf{K}_\sigma \quad \ldots \quad \ldots \quad \ldots \quad (2.61)$$

where

$$\bar{\mathbf{S}}_t = \int_{A_t} \mathbf{H}^T \mathbf{S}_t \, dA_t = \{P_t , M_t\}^T \quad \ldots \quad \ldots \quad (2.62)$$

is the vector of initial stress resultants.

The initial stress stiffness matrix $\mathbf{K}_\sigma$ is obtained in a manner which is similar to (2.50) i.e.

$$\mathbf{K}_\sigma = \int_{L_t} \frac{\partial \bar{\mathbf{B}}^T}{\partial \mathbf{a}} \bar{\mathbf{S}}_t \, dL_t = \int_{L_t} \mathbf{G}_t^T \frac{\partial \mathbf{A}_\theta}{\partial \mathbf{a}} \bar{\mathbf{S}}_t \, dL_t$$

$$= \int_{L_t} \mathbf{G}_t \bar{\mathbf{P}}_{ti} \mathbf{G}_t \, dL_t \quad \ldots \quad \ldots \quad \ldots \quad \ldots \quad (2.63)$$

in which the initial stress matrix $\bar{P}_{ti}$ is given by

$$\bar{P}_{ti} = \begin{bmatrix} P_t\ [I] & M_t\ [I] \\ \\ M_t\ [I] & O \end{bmatrix} \quad \ldots \quad \ldots \quad \ldots \quad \ldots \qquad (2.64)$$

where [I] is a two by two unit matrix.

On forming the incremental equilibrium equations and solving for the displacement increments $\Delta\ a_t^i$, the total displacements are obtained as

$$a_t^{i+1} = a_t^i + \Delta\ a_t^i \quad \ldots \quad \ldots \quad \ldots \quad \ldots \quad \ldots \qquad (2.65)$$

The incremental strain resultants (Equations (1.21)) are defined by

$$\Delta\ \epsilon_t^i = [\bar{B}_t + \frac{1}{2}\ \bar{B}_L(\Delta\ a_t^i)]\ \{\Delta\ a_t^i\} \quad \ldots \quad \ldots \qquad (2.66)$$

The stress resultant increments and the total stress resultants are then given by

$$\Delta\ \bar{S}_t^i = \bar{D}\ \Delta'\epsilon_t^i$$

$$\bar{S}_t^{i+1} = \bar{S}_t^i + \Delta\ \bar{S}_t^i \quad \ldots \quad \ldots \quad \ldots \quad \ldots \quad \ldots \qquad (2.67)$$

The nodal residuals to be used to evaluate a new set of displacement increments are

$$-\psi^{i+1} = R - \int_{L_t} \bar{B}_t^T \bar{S}_t^{i+1} \, dL_t \quad \ldots \quad \ldots \quad \ldots \quad (2.68)$$

2.4.3 Combined Updated and Total Lagrangian Formulation Based on Green Strain Measure ($\bar{U}TLG$)

In this formulation the coordinates are updated at the beginning of each load increment only. The iterations within the increment are carried out using the Total Lagrangian formulation. As a consequence of this, the displacements from the beginning of the increment until convergence (a_c) must be stored.

Thus, the strain displacement matrix is defined as

$$B = B_t + B_L(u_c) = H\left[\bar{B}_t + \bar{B}_L(a_c)\right]$$

$$= H \; \bar{B}_c \quad \ldots \quad \ldots \quad \ldots \quad \ldots \quad \ldots \quad \ldots \quad (2.69)$$

where t refers to the beginning of a new increment.

The tangent stiffness matrix now takes the following form

$$K_T = \int_{L_t} \bar{B}_c^T \bar{D} \bar{B}_c \, dL_t + \int_{L_t} G_t^T \bar{P}_{ti} G_t \, dL_t$$

$$= (K_t + K_L(a_c)) + K_\sigma \quad \ldots \quad \ldots \quad \ldots \quad \ldots \qquad (2.70)$$

The matrix G_t is given by (2.59) but is evaluated at the beginning of a new increment only. The initial stress matrix $\bar{P}_{ti}$ is given by (2.64) and the total displacements are given by (2.65).

The displacements a_c are evaluated as follows

$$a_c^{i+1} = a_c^i + \Delta a_t^i \quad \ldots \quad \ldots \quad \ldots \quad \ldots \quad \ldots \quad \ldots \qquad (2.71)$$

with their value being zero at the beginning of each load increment.

The incremental strain resultants are defined as

$$\Delta \epsilon_t^i = [\bar{B}_t + \bar{B}_L(a_c^i) + \frac{1}{2} \bar{B}_L(\Delta a_t^i)] \{\Delta a_t^i\} \quad \ldots \qquad (2.72)$$

From which the stress resultants increments and the total stress resultants are given by (2.67). The nodal residuals are then obtained as follows

$$-\psi^{i+1} = R - \int_{L_t} \bar{B}_c^T \bar{S}_t^{i+1} \, dL_t \quad \ldots \quad \ldots \quad \ldots \qquad (2.73)$$

2.4.4 Total Lagrangian Formulation Based on Conventional Strain Measure (TLC)

The variation in stress is defined from (2.36) and (2.38) as

$$\delta \mathbf{S}_o = \mathbf{E}\ \mathbf{H}\ \mathbf{H}^*\ \delta\boldsymbol{\varepsilon}_o = \mathbf{D}\ \mathbf{H}\ \mathbf{H}^*\ \delta\boldsymbol{\varepsilon}_o \quad \ldots \quad \ldots \quad \ldots \quad (2.74)$$

The strain resultant measures $\boldsymbol{\varepsilon}_o$ and their variations $\delta\boldsymbol{\varepsilon}_o$ are given in terms of the displacement gradients and the nodal variables $\mathbf{a}_o$ by

$$\boldsymbol{\varepsilon}_o = \begin{Bmatrix} \dfrac{du_o}{dx} \\ -\dfrac{d^2v_o}{dx^2} \end{Bmatrix} + \begin{Bmatrix} \frac{1}{2}\left(\dfrac{du_o}{dx}\right)^2 + \left(\dfrac{dv_o}{dx}\right)^2 \\ \dfrac{dv_o}{dx}\ \dfrac{d^2u_o}{dx^2} - \dfrac{du_o}{dx}\ \dfrac{d^2v_o}{dx^2} \end{Bmatrix}$$

$$= \boldsymbol{\varepsilon}_o^O + \boldsymbol{\varepsilon}_o^L$$

$$= \bar{\mathbf{B}}_o\ \mathbf{a}_o + \frac{1}{2}\ \bar{\mathbf{B}}_L(\mathbf{a}_o)\mathbf{a}_o = \bar{\mathbf{B}}_o\mathbf{a}_o + \frac{1}{2}\ \mathbf{A}_\theta\ \boldsymbol{\theta}_o$$

$$\delta\boldsymbol{\varepsilon}_o = \bar{\mathbf{B}}_o\ \delta\mathbf{a}_o + \bar{\mathbf{B}}_L(\mathbf{a}_o)\delta\mathbf{a}_o = \bar{\mathbf{B}}\ \delta\mathbf{a}_o \quad \ldots \quad \ldots \quad (2.75)$$

where

$$A_\theta = \begin{bmatrix} \frac{du_o}{dx} & \frac{dv_o}{dx} & 0 & 0 \\ -\frac{d^2v_o}{dx^2} & \frac{d^2u_o}{dx^2} & \frac{du_o}{dx} & \frac{dv_o}{dx} \end{bmatrix}$$

$$\theta_o = \{\frac{du_o}{dx}, \frac{dv_o}{dx}, -\frac{d^2v_o}{dx^2}, \frac{d^2u_o}{dx^2}\}^T \ldots \quad \ldots \qquad (2.76)$$

Thus, from these relations and (2.39) the nonlinear equilibrium equations are

$$\psi = \int_{L_o} \bar{B}^T H^{*T} \int_{A_o} H^T D H \, dA_o \, \epsilon_o^* \, dL_o - R$$

$$= \int_{L_o} \bar{B}^T H^{*T} \bar{S}_o \, dL_o - R = 0 \quad \ldots \quad \ldots \qquad (2.77)$$

in which $\bar{S}_o$ is the vector of stress resultants given by

$$\bar{S}_o = \bar{D} \, \epsilon_o^* = \{P_o, M_o\}^T \quad \ldots \quad \ldots \quad \ldots \quad \ldots \qquad (2.78)$$

Assuming that the equivalent nodal forces R are conservative, the tangent stiffness matrix, $K_T = \frac{\partial \psi}{\partial a}$, is obtained from (2.77) as

$$K_T = \int_{L_o} \bar{B}^T H^{*T} \bar{D} \frac{\partial \epsilon^*}{\partial a} dL_o + \int_{L_o} \frac{\partial \bar{B}^T}{\partial a} H^{*T} \bar{S}_o dL_o$$

$$+ \int \bar{B}^T \frac{\partial H^{*T}}{\partial a} \bar{S}_o dL_o$$

$$= (K_o + K_L(a)) + K_\sigma + K_\sigma^* \quad \ldots \quad \ldots \quad \ldots \quad (2.79)$$

The special feature of this formulation is the additional term K_σ^* in Equation (2.79). The contribution of this term to the stiffness matrix can be understood as an additional initial stress stiffness matrix.

The linear strain stiffness matrix, which includes both the the infinitesimal strain and the initial displacement stiffness matrices, is defined from (2.79), (2.75) and (2.38) as:

$$K_o + K_L(a_o) = \int_{L_o} \bar{B}^T H^{*T} \bar{D} H^* \bar{B} dL_o$$

$$= \int_{L_o} B^{*T} \bar{D} B^* dL_o \quad \ldots \quad \ldots \quad \ldots \quad \ldots \quad (2.80)$$

where $B^* = H^* \bar{B}$ $\ldots \quad \ldots \quad \ldots \quad \ldots \quad \ldots \quad (2.81)$

The geometric stiffness matrix K_σ can be defined from (2.79), (2.76) and (2.75) as follows

$$K_\sigma = \int_{L_o} \frac{\partial \bar{B}^T}{\partial a} H^{*T} \bar{S}_o \, dL_o = \int_{L_o} G_o^T \frac{\partial A_\theta^T}{\partial a} S^* \, dL_o$$

$$= \int G_o^T \bar{P}_{oi} G_o \, dL_o \quad \ldots \quad \ldots \quad \ldots \quad \ldots \quad (2.82)$$

in which

$$S^* = H^{*T} \bar{S}_o = \{P_o^* \quad M_o^*\}^T \quad \ldots \quad \ldots \quad \ldots \quad \ldots \quad (2.83)$$

and $\bar{P}_{oi}$, the initial stress matrix, is given by

$$\bar{P}_{oi} = \begin{bmatrix} P_o^* [I] & M_o^* [I] \\ M_o^* [I] & O \end{bmatrix} \ldots \quad \ldots \quad \ldots \quad (2.84)$$

From (2.83), (2.78) and (2.38) S^* is defined as

$$S^* = H^{*T} \bar{S}_o = \begin{Bmatrix} \frac{P_o}{(1 + 2e)^{1/2}} - \frac{2\chi M_o}{(1 + 2e)^2} \\ \frac{M_o}{(1 + 2e)} \end{Bmatrix} \ldots \quad (2.85)$$

Hence, from (2.85) and (2.75)

$$d\ H^{*T}\ \bar{S}_o = dS^* = \begin{bmatrix} \dfrac{-P_o}{(1+2e)^{3/2}} + \dfrac{8\chi M_o}{(1+2e)^3} & \dfrac{-2M_o}{(1+2e)^2} \\ \dfrac{-2M_o}{(1+2e)^2} & 0 \end{bmatrix} \begin{Bmatrix} \delta e \\ \delta \chi \end{Bmatrix}$$

$$= \bar{P}_i^*\ \bar{B}\ d\ a \quad \ldots \quad \ldots \quad \ldots \quad \ldots \quad \ldots \quad (2.86)$$

Therefore, from (2.79) and (2.86) the additional initial stress stiffness matrix K_σ^* takes the following form

$$K_\sigma^* = \int_{L_o} \bar{B}^T\ \bar{P}_i^*\ \bar{B}\ dL_o \quad \ldots \quad \ldots \quad \ldots \quad \ldots \quad \ldots \quad (2.87)$$

From (2.80), (2.82) and (2.87) it can be clearly seen that all three components of the tangent stiffness matrix are symmetrical.

Upon solving the incremental equilibrium equations for the displacement increments $\Delta\ a_o^i$ and evaluating the total displacements a_o^{i+1} (Equation (2.51), the incremental strains are obtained as

$$\Delta\epsilon_o^{*i} = [H^*][\bar{B}_o + \bar{B}_L(a_o^i) +$$

$$+ \frac{1}{2}\ \bar{B}_L(\Delta\ a_o^i)] \quad \{\Delta\ a_o^i\} \quad \ldots \quad \ldots \quad \ldots\ldots \quad (2.88)$$

The incremental stress resultants are given from (2.78) and (2.88) by

$$\Delta \bar{S}_o^i = \bar{D} \Delta \epsilon_o^{*i} \quad \ldots \quad \ldots \quad \ldots \quad \ldots \quad \ldots \quad (2.89)$$

and the total stress resultants are

$$\bar{S}_o^{i+1} = \bar{S}_o^i + \Delta \bar{S}_o^i \quad \ldots \quad \ldots \quad \ldots \quad \ldots \quad \ldots \quad (2.90)$$

The residual nodal forces are given from (2.77), (2.78), (2.81) and (2.90) by

$$-\dot{\psi}^{i+1} = R - \int_{L_o} \bar{B}^T H^{*T} \bar{D} \epsilon^* \, dL_o$$

$$= R - \int_{L_o} B^{*T} \bar{S}_o^{i+1} \, dL_o \quad \ldots \quad \ldots \quad \ldots \quad (2.91)$$

Now the assumption that the strains are small can be introduced into the formulation by neglecting e in Equations (2.38), (2.85) and (2.86), so that

$$H^* = \begin{bmatrix} 1 & 0 \\ -2\chi & 1 \end{bmatrix} \quad \ldots \quad \ldots \quad \ldots \quad \ldots \quad \ldots \quad (2.38a)$$

$$S^* = \begin{Bmatrix} P_o - 2\chi M_o \\ M_o \end{Bmatrix} \quad \ldots \quad \ldots \quad \ldots \quad \ldots \quad \ldots \quad (2.85a)$$

and

$$\bar{P}_i^* = \begin{bmatrix} -P_o + 8\chi M_o & --2M_o \\ -2M_o & 0 \end{bmatrix} \quad \ldots \quad \ldots \quad \ldots \quad \ldots \qquad (2.86a)$$

2.4.5 The External Virtual Work and Equivalent Nodal Forces

So far the applied loads have been assumed to be conservative. Thus, the effect of deformation on the generalised nodal forces R was neglected and the well established form [10] assumed. To take into account the effect of follower pressure loads and applied concentrated moments a modification of the equivalent nodal forces is necessary for a Total Lagrangian formulation.

Consider the two types of uniformly distributed loads, namely those acting in a fixed direction and independent of deformation given by

$$\vec{f} = f_x \hat{x} + f_y \hat{y} \quad \ldots \quad \ldots \quad \ldots \quad \ldots \quad \ldots \qquad (2.92)$$

per unit undeformed length of the reference line and the follower pressure loads acting normally to the reference line after deformation defined as

$$\vec{p} = p\,\hat{n} \quad \ldots \quad \ldots \quad \ldots \quad \ldots \quad \ldots \quad \ldots \quad (2.93)$$

per unit deformed length.

The total force per unit underformed length is given from (2.9), (2.18), (2.92) and (2.93) by

$$\vec{q} = \vec{f} + \vec{p}$$

$$= f_x\hat{x} + f_y\hat{y} + (1 + 2e)^{1/2}\, p\left(\frac{-\frac{dv}{dx}\,\hat{x} + (1 + \frac{du}{dx})\hat{y}}{(1 + 2e)^{1/2}}\right)$$

$$= (f_x - \frac{dv}{dx}\,p)\hat{x} + (f_y + (1 + \frac{du}{dx})\,p)\hat{y} \quad \ldots \quad (2.94)$$

The external virtual work due to this load is

$$\delta W_q = \int_{L_o} \delta\vec{V} \cdot \vec{q}\; dL_o$$

$$= \delta\, a_o^T \int_{L_o} N_o^T \begin{Bmatrix} f_x - \frac{dv}{dx}\,p \\ f_y + (1 + \frac{du}{dx})p \end{Bmatrix} dL_o \quad \ldots \quad (2.95)$$

where the shape functions N_o are given by

$$N_o = \frac{\partial}{\partial a} \begin{Bmatrix} u \\ v \end{Bmatrix} \quad \ldots \quad \ldots \quad \ldots \quad \ldots \quad \ldots \quad \ldots \quad (2.96)$$

in which u and v are the components of the displacement of the reference line in the local axes directions (Equation (2.6)).

Assuming that a concentrated moment M_j is applied at node point j, the external virtual work due to this moment is

$$\delta W_m = \delta \phi_j M_j \quad \ldots \quad \ldots \quad \ldots \quad \ldots \quad \ldots \quad \ldots \quad (2.97)$$

where the angle of rotation ϕ is obtained from the unit vectors $\hat{y}$ (Equation (2.3)) and $\hat{n}$ (Equation (2.9)).

Thus

$$\cos \phi = \hat{y} \cdot \hat{n} = \frac{(1 + du_o/dx)}{(1 + 2e)^{1/2}}$$

$$\sin \phi = |\hat{y} \times \hat{n}| = \frac{dv_o/dx}{(1 + 2e)^{1/2}} \quad \ldots \quad \ldots \quad \ldots \quad (2.98)$$

Therefore

$$\phi = \arctan \frac{dv_o/dx}{(1 + du_o/dx)}$$

and its vatiation is

$$\delta\phi = \frac{1}{1 + 2e}\left[\left(1 + \frac{du_o}{dx}\right)\delta\frac{dv_o}{dx} - \frac{dv_o}{dx}\,\delta\frac{du_o}{dx}\right] \qquad (2.99)$$

The strain e is assumed to be small compared to unity and hence negligible. Substituting from (2.99) into (2.97) gives

$$\delta W_m = \delta a_o^T N_j^T \begin{Bmatrix} -\frac{dv_o}{dx} M \\ \\ (1 + \frac{du_o}{dx})M \end{Bmatrix}_j \quad \ldots \qquad (2.100)$$

in which the shape functions N_j are given by

$$N_j = \frac{\partial}{\partial a_o} \begin{Bmatrix} \frac{du_o}{dx} \\ \\ \frac{dv_o}{dx} \end{Bmatrix}_j \quad \ldots \quad \ldots \quad \ldots \quad \ldots \quad \ldots \qquad (2.101)$$

The total external virtual work is then obtained as

$$\delta W = \delta\, a_o^T(R + R_d) \quad \ldots \quad \ldots \quad \ldots \quad \ldots \quad \ldots \qquad (2.102)$$

where R is the conservative vector of equivalent nodal forces and R_d is the vector of deformation dependent nodal forces given from (2.95) and (2.100) by

$$R_d = \int_{L_o} N_o^T \begin{Bmatrix} -\frac{dv_o}{dx} p \\ \\ \frac{du_o}{dx} p \end{Bmatrix} dL_o + N_j^T \begin{Bmatrix} -\frac{dv_o}{dx} M \\ \\ \frac{du_o}{dx} M \end{Bmatrix}_j \quad \ldots \qquad (2.103)$$

From (2.98) for small strains

$$\frac{dv_o}{dx} = \sin \phi$$

and

$$1 + \frac{du_o}{dx} = \cos \phi \quad \ldots \quad \ldots \quad \ldots \quad \ldots \quad \ldots \quad \ldots \qquad (2.104)$$

For axial deformation only ($\frac{dv_o}{dx} = 0$)

$$\cos \phi = \frac{1 + du/dx}{(1 + 2e)^{1/2}} = 1 \quad \ldots \quad \ldots \quad \ldots \qquad (2.105)$$

2.5 CONCLUSIONS

1. The Lagrangian method for describing geometric nonlinearity has been used to develop a small strain large rotation theory for thin curved two-dimensional beam finite elements.

2. The theory has been based on an intrinsic coordinate system defined at each material point within an element.

3. Four alternative formulations of the incremental equilibrium equations have been presented for comparison in an attempt to correctly evaluate both displacements and stresses.

4. The applied concentrated loads have been assumed to be conservative during the formulation of the incremental equilibrium equations. However, the effect of deformation dependent loads has been taken into account by modifying the equivalent nodal loads for the Total Lagrangian formulations.

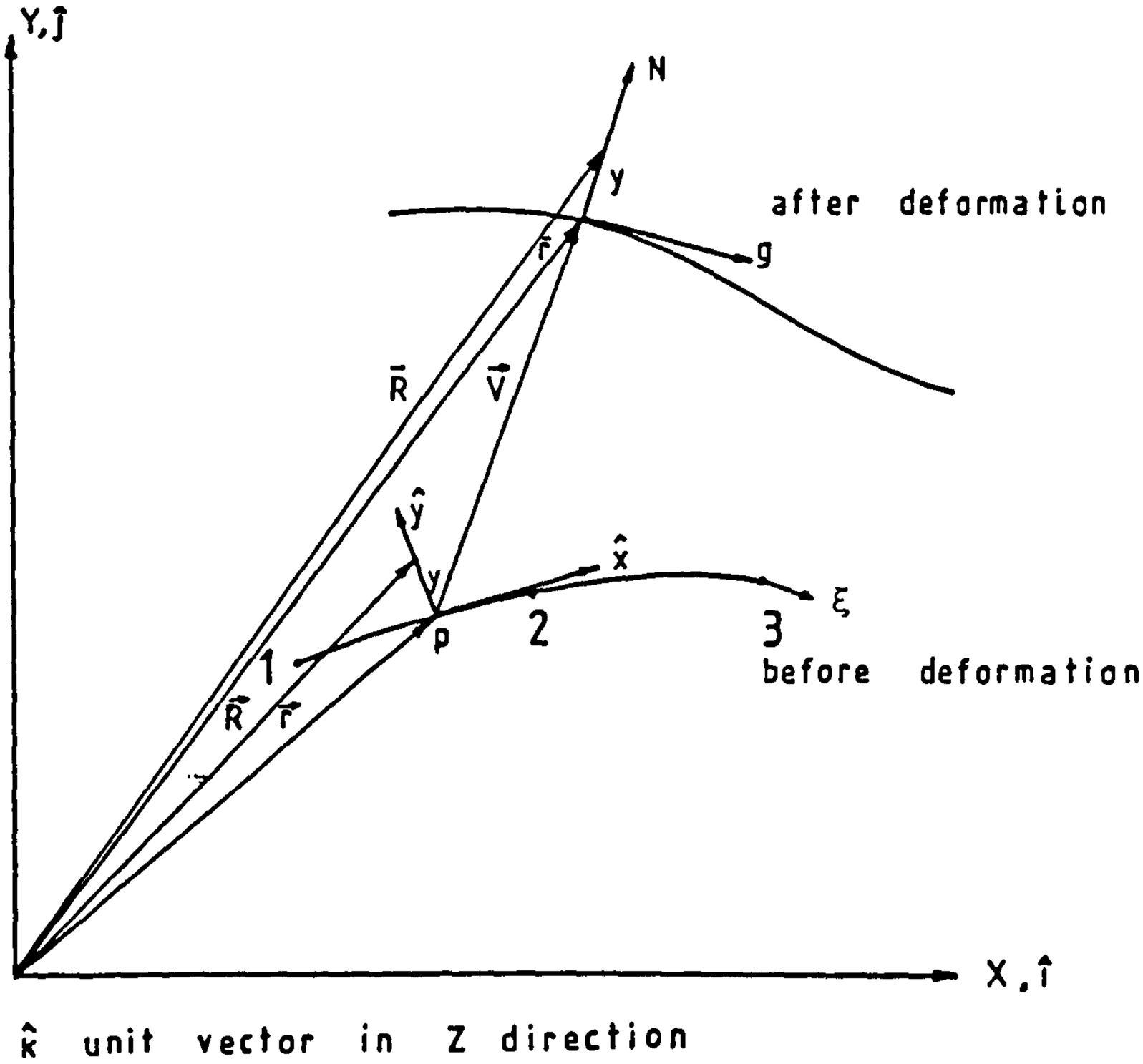

$$\vec{r} = X\,\hat{i} + Y\,\hat{j}$$

Local Axes

$$\hat{x} = \frac{dr/d\xi}{|dr/d\xi|}$$

$$\hat{y} = \hat{k} \times \hat{x}$$

$$\vec{R} = \vec{r} + y\,\hat{y}$$

$$\vec{r} = \vec{r} + \vec{V}$$

$$\vec{V} = u\,\hat{x} + v\,\hat{y}$$

$$\vec{R} = \vec{r} + y\,\hat{n}$$

FIGURE 2.1 - Geometry of Deformation

CHAPTER 3

FORMULATION OF THIN CURVED TWO-DIMENSIONAL BEAM FINITE ELEMENTS

3.1 INTRODUCTION

The formulations presented in Chapter 2 are based on the use of convected coordinates and associated element formulations must include these coordinates. Whilst the theory is based on material coordinates at every point along element reference line, the intrinsic coordinates need to be defined only at the integration points.

The correct definition of such a coordinate system is achieved by using the constraint technique. In the constraint technique geometric relationships are used to define discretely the shape of the element before deformation and the variation of variables referred to the intrinsic coordinate system. The elements presented in this chapter are based on the constraint technique applied to displacement finite element models, in which independent interpolation of the displacements and rotations (or displacement derivatives) is used .

3.2 THE REQUIREMENTS FOR THE ELEMENTS

The choice of element degrees of freedom should be based on the convergence criteria of compatibility and completeness. For beam type problems in linear elastic solutions C^0 continuity of the in-plane displacements and C^1 continuity of the out-of-plane displacements is required. For eccentric beam element formulations the variation of the in-plane displacement must be at least of the same order as that of the gradient of the out-of-plane displacement. Hence, a parabolic-cubic variation of displacements is necessary.

For improved element performance, however, the same order of variation must be used for both displacement components [22, 23, 24, 56, 67]. The same convergence criteria of compatibility and completeness are applicable for geometric nonlinearity. It can be seen from the nonlinear strain displacement relations (Equation (2.27)) that C^1 continuity is required for both displacement components. An objection to such a displacement variation which is often put forward is that the continuity of the gradient of the in-plane displacement, which is a measure of the axial strain, will contradict the physical laws of equilibrium when there is an abrupt change in thickness. The second order in-plane term contributes only to the nonlinear part of curvature. Epstein and Murray [25] have shown that by neglecting this term a relative error in curvature of $\sin^2\phi$ (ϕ being

the angle of rotation) results. Therefore, the effect of this term is substantial when both rotation and curvature are large, in which case a cubic-cubic variation of displacements is necessary. It is possible to obtain both conforming and non-conforming elements by the constraint technique depending on the choice of the initial displacement variations and the constraint equations applied (Section 3.3.1).

Hence, three curved beam elements have been developed using the constraint technique. These are:

1. ISOBEM1 element (Figure 3.1) which is a non-conforming curved beam element with C^o continuity of in-plane displacement and C^1 continuity of the out-of-plance displacement. An additional internal degree of freedom is introduced to ensure continuity between the reference line and the cross-section centroid for eccentric elements.

2. ISOBEM2 element (Figure 3.2) which is a non-conforming beam element with C^1 continuity of both displacement components.

3. SUBBEAM element (Figure 3.3) which is a beam element with C^1 continuity for both displacement components and complete conformity of the displacement field.

For all three elements a parabolic variation of the initial geometry is assumed.

3.3 THE CONSTRAINT TECHNIQUE

In the original constraint technique the Kirchhoff conditions of zero shear strains are applied directly at the elements' Gauss points to effectively exclude shear strain [10, 35, 38, 66]. The technique can be interpreted, however, as a means of defining the element geometry and the assumed variation of the local displacements correctly for generally curved beam and shell type elements. Thus, by using this technique it is possible to avoid the problem of interpolation directionality. This objective can be achieved as follows:

i. The known global coordinates are independently interpolated to the required order.

ii. The global displacements and their derivatives are independently interpolated using the same natural coordinates.

iii. The local (intrinsic) coordinates are defined at any point in terms of the interpolated coordinates.

iv. The constraint technique is used to define correctly the variation of variables referred to the local axes in terms of the independently interpolated global variables.

3.3.1 Non-conforming and Conforming Displacement Variations within Elements

The constraint equations are applied at certain points within the element, thus, resulting in non-conforming element formulations. It is possible, however, to obtain completely conforming elements using the constraint technique provided that the correct variation of displacements is postulated initially and the constraints are applied at enough points.

To illustrate this let us assume a parabolic variation of both a displacement v and its derivative θ for the straight beam of Figure 3.4a in terms of the natural coordinate ξ and generalised variables α_i as

$$v = \alpha_1 + \alpha_2\xi + \alpha_3\xi^2$$

$$\theta = \alpha_4 + \alpha_5\xi + \alpha_6\xi^2 \quad \ldots \quad \ldots \quad \ldots \quad \ldots \quad (3.1)$$

To obtain the variables α_i in terms of the nodal variables six equations are required. Using the two conditions at each of the two ends gives four equations. The two additional equations required are obtained by applying the condition that the derivative of v with respect to the local (intrinsic) coordinate x is equal to θ at the two Gauss points $\xi = \pm 1/\sqrt{3}$. Solving these equations and substituting for α_i in (3.1) gives

$$v = (\frac{1}{2} - \frac{1}{2}\xi)v_1 + (\frac{1}{2} + \frac{1}{2}\xi)v_2 +$$

$$+ \frac{c}{4}(1 - \xi^2)\theta_1 - \frac{c}{4}(1 - \xi^2)\theta_2$$

$$\theta = -\frac{3}{4c}(1 - \xi^2)v_1 + \frac{3}{4c}(1 - \xi^2)v_2 +$$

$$\frac{1}{4}(-1 - 2\xi + 3\xi^2)\theta_1 + \frac{1}{4}(-1 + 2\xi + 3\xi^2)\theta_2 \qquad (3.2)$$

where $c = \frac{dx}{d\xi}$

The same results may be obtained by starting with the independent interpolation of v and θ, assuming parabolic interpolation functions, and then using the condition $\frac{dv}{dx} = \theta$ at the two points $\xi = \pm 1/\sqrt{3}$ to eliminate the two internal degrees of freedom v_3 and θ_3 (Figure 3.4b).

Differentiating v in (3.2) with respect to x gives

$$\frac{dv}{dx} = -\frac{1}{2c} v_1 + \frac{1}{2c} v_2 - \frac{1}{2} \xi\theta_1 + \frac{1}{2} \xi\theta_2 \quad \ldots \quad (3.3)$$

which is clearly incompatible with θ in (3.2).

Crisfield [6] has used a smoothed derivative the same as (3.3) in evaluating the derivatives of the transverse displacements in the nonlinear part of the strain-displacement relations as an extension of the path test. Beam elements based on displacement variations which are the same as that in (3.2) are known to behave as if a cubic vatiation of displacements is used [10, 38, 66].

Instead of the parabolic initial variation of (3.1) a cubic variation of both v and θ can be assumed giving

$$v = \alpha_1 + \alpha_2\xi + \alpha_3\xi^2 + \alpha_4\xi^3$$

$$\theta = \alpha_5 + \alpha_6\xi + \alpha_7\xi^2 + \alpha_8\xi^3 \quad \ldots \quad \ldots \quad \ldots \quad (3.4)$$

Besides the four equations which are obtained from end conditions, four additional equations are required to solve for α_i. These are obtained by applying the condition $\frac{dv}{dx} = \theta$ at four points within the element. These points are chosen to be the four equidistant

points $\xi = \pm \frac{3}{5}$; $\pm \frac{1}{5}$ (Figure 3.4c). Hence, forming the eight equations required, solving these for α_i and substituting in (3.4) gives

$$v = (\frac{1}{2} - \frac{3}{4}\xi + \frac{1}{4}\xi^3)v_1 + (\frac{1}{2} + \frac{3}{4}\xi - \frac{1}{4}\xi^3)v_2 +$$

$$+ \frac{c}{4}(1 - \xi - \xi^2 + \xi^3)\theta_1 + \frac{c}{4}(-1 - \xi + \xi^2 + \xi^3)\theta_3$$

$$\theta = -\frac{3}{4c}(1 - \xi^2)v_1 + \frac{3}{4c}(1 - \xi^2)v_2 +$$

$$\frac{1}{4}(-1 - 2\xi + 3\xi^2)\theta_1 + \frac{1}{4}(-1 + 2\xi + 3\xi^2)\theta_2 \qquad (3.5)$$

which is clearly a completely compatible displacement field. In fact, the interpolation functions in (3.5) are the same as the well known Hermitian interpolation functions. The same relations as those in (3.5) can be obtained by applying the constraint technique to an independently interpolated displacement field (Figure 3.4d), wherein a cubic variation is assumed, to eliminate the four internal degrees of freedom. Appendix I gives the complete derivations for the two examples considered with the first example presented using both alternative approaches.

The advantage of the constraint approach is that it can be easily extended to include curved elements. The technique is best carried out numerically. The global displacements and their derivatives with respect to the

global coordinates (or rotations) are interpolated independently to the required order. By applying the constraint equations in the local element axes certain degrees of freedom are eliminated. The order of interpolation is limited by the final or "wanted" degrees of freedom.

3.3.2 Outline of the Constraint Technique

a) Referring to Figure 3.5 the global coordinates of any point P(X,Y) on the beam reference line are given in terms of the coordinates of the nodes by

$$\begin{Bmatrix} X \\ \\ Y \end{Bmatrix} = \sum_{i=1}^{n} N_i \begin{Bmatrix} X \\ \\ Y \end{Bmatrix}_i \quad \ldots \quad \ldots \quad \ldots \quad \ldots \quad (3.6)$$

where n is the number of points defining geometry and N_i are the shape functions. Since a parabolic variation of geometry is assumed for all elements n is equal to three. The shape functions N_i are the heirarchial shape functions, which consider the variables as departures from linearity and are given by

$$N = \frac{1}{2} - \frac{1}{2}\xi$$

$$N_2 = 1 - \xi^2$$

$$N_3 = \frac{1}{2} + \frac{1}{2}\xi \quad \ldots \quad \ldots \quad \ldots \quad \ldots \quad \ldots \quad (3.7)$$

From (2.1), (2.2) and (3.6) the unit vector $\hat{x}$ defining the local x axis is obtained as

$$\hat{x} = \frac{dX/d\xi \ \hat{i} + dY/d\xi \ \hat{j}}{((dX/d\xi)^2 + (dY/d\xi)^2)^{1/2}} \quad \ldots \quad \ldots \quad (3.8)$$

The unit vector $\hat{y}$ defining the local y direction is given from (2.3) and (3.8) by

$$\hat{y} = \hat{k} \times \hat{x} = \frac{-dY/d\xi \ \hat{i} + dX/d\xi \ \hat{j}}{((dX/d\xi)^2 + (dY/d\xi)^2)^{1/2}} \quad (3.9)$$

b) The global displacements U, V and the rotation θ (or the displacement gradient) of point P are independently interpolated to the required order as follows

$$\begin{Bmatrix} U \\ V \\ \theta \end{Bmatrix} = \sum_{j=1}^{m} N_j \begin{Bmatrix} U \\ V \\ \theta \end{Bmatrix}_j$$

where m is the number of points defining the displacement approximation and N_j are the shape functions.

The displacement vector $\vec{V}$ of a point on the beam reference line (Figure 3.5) is defined in terms of the components in the global axes directions U, V as

$$\vec{V} = U\,\hat{i} + V\,\hat{j} \qquad \ldots \quad \ldots \quad \ldots \quad \ldots \qquad (3.11)$$

From (3.10) and (3.11) the components of the displacement in the local axes directions are obtained as follows

$$\begin{Bmatrix} u \\ v \end{Bmatrix} = \begin{Bmatrix} \vec{V}.\hat{x} \\ \vec{V}.\hat{y} \end{Bmatrix} = \begin{bmatrix} \hat{i}.\hat{x} & \hat{j}.\hat{x} \\ \hat{i}.\hat{y} & \hat{j}.\hat{y} \end{bmatrix} \begin{Bmatrix} U \\ V \end{Bmatrix}$$

$$= \begin{bmatrix} \hat{i}.\hat{x} & \hat{j}.\hat{x} \\ \hat{i}.\hat{y} & \hat{j}.\hat{y} \end{bmatrix} \sum_{j=1}^{m} N_j \begin{Bmatrix} U \\ V \end{Bmatrix} \qquad (3.12)$$

where from (3.8) and (3.9)

$$\hat{i}.\hat{x} = \hat{j}.\hat{y} = (dX/d\xi)/((dX/d\xi)^2 + (dY/d\xi)^2)^{1/2}$$

$$\hat{j}.\hat{x} = -\hat{i}.\hat{y} = (dY/d\xi)/((dX/d\xi)^2 + (dY/d\xi)^2)^{1/2}$$

... ... (3.13)

c) Enforcing the Kirchhoff hypothesis of zero shear strain (or the condition that the gradient of the independently interpolated displacement is equal to the independently interpolated derivative in the local element axes) at discrete points within an element gives constraint equations of the form

$$\mathbf{M}\ \delta = 0 \quad \ldots \ldots \ldots \ldots \ldots \ldots \quad (3.14)$$

where δ is the vector of the total initial nodal variables.

These constraint equations are used to relate the unwanted element variables to the required final variables. If some of the variables to be eliminated are in the local axes directions a transformation of the relevant global nodal variables in δ will be necessary. From (3.12) the global displacement components are defined in terms of the local components as

$$\begin{Bmatrix} U \\ \\ V \end{Bmatrix} = \begin{bmatrix} \hat{i}.\hat{x} & \hat{i}.\hat{y} \\ \\ \hat{j}.\hat{x} & \hat{j}.\hat{y} \end{bmatrix} \begin{Bmatrix} u \\ \\ v \end{Bmatrix} \quad \ldots \quad \ldots \quad \ldots \qquad (3.15)$$

If such a transformation of the nodal variables is required, the constraint equations (3.14) are modified using (3.15) to give equations of the form

$$M^* \delta^* = O \qquad \ldots \quad \ldots \quad \ldots \quad \ldots \quad \ldots \qquad (3.16)$$

which can be written in terms of the wanted variables a and the variables to be eliminated b as follows

$$\left[M_A \,\vdots\, M_B \right] \left\{ \begin{matrix} a \\ \cdots \\ b \end{matrix} \right\} = C \qquad \ldots \quad \ldots \quad \ldots \quad \ldots \qquad (3.17)$$

solving (3.17) for b in terms of a gives

$$b = - M_B^{-1} M_A \, a \qquad \ldots \quad \ldots \quad \ldots \quad \ldots \quad \ldots \qquad (3.18)$$

d) one of the most efficient computational arrangements for displacement finite elements is to write a shape function array relating all the displacements and gradients required for the element formulation to the nodal variables of the element. Thus, such an unconstrained shape function array is defined in terms of the original total variables in the following form

$$\gamma = WN\ \delta = WN^*\ \delta^*$$

$$= \left[W_A \vdots\ W_B \right] \left\{ \begin{matrix} a \\ --- \\ b \end{matrix} \right\} \quad \ldots \quad \ldots \quad (3.19)$$

Substituting for b from (3.18) into (3.19) gives the constrained shape function array in terms of the final wanted element variables as

$$\gamma = \left[W_A - W_B\ M_B^{-1}\ M_A \right] a \quad \ldots \quad \ldots \quad \ldots \quad \ldots \quad (3.20)$$

Figure 3.6 gives a schematic diagram of the constraint technique outlined above. The technique is general and hence applicable to all elements. Individual elements differ in the form of the displacement interpolation, the constraint equations and the shape function array. These are presented in the following sections for each of the three elements which have been developed.

3.4 ISOBEM1 ELEMENT

The element (Figure 3.1) is a thin curved non-conforming beam element with C^o continuity of the in-plane displacement. Two integration points are used to evaluate all integrals required.

The variation of the global displacements and rotation is assumed to be initially parabolic. These are independently interpolated as follows

$$\begin{Bmatrix} U \\ V \\ \theta \end{Bmatrix} = \sum_{i=1}^{3} N_i \begin{Bmatrix} U \\ V \\ \theta \end{Bmatrix}_i \quad \ldots \quad \ldots \quad \ldots \quad \ldots \quad \ldots \qquad (3.21)$$

in which N_i are the hierarchial shape functions given by (3.7).

The Kirchhoff condition of zero shear strain is applied at the two Gauss points $\xi = \pm 1/\sqrt{3}$, thus making the rotation θ equal to the derivative with respect to the local x of the local transverse displacement at these points. The condition is defined by the relation

$$\frac{du}{dy} + \frac{dv}{dx} = -\theta + \frac{dv}{dx} = 0 \qquad \ldots \quad \ldots \quad \ldots \qquad (3.22)$$

which can be written in terms of the total nodal variables from (3.12) and (3.21) as

$$\sum_{i=1}^{3} \left[\frac{dN_i}{dx} \hat{i}.\hat{y} \quad \frac{dN_i}{dx} \hat{j}.\hat{y} \quad - N_i \right] \begin{Bmatrix} U \\ V \\ \theta \end{Bmatrix}_i = 0 \qquad \ldots \qquad (3.23)$$

Evaluating (3.23) at the two Gauss points $\xi = \pm 1/\sqrt{3}$ gives the constraint matrix **M** of (3.14) and the total nodal variables δ (Figure 3.1a) are given by

$$\delta = \{U_1, V_1, \theta_1, \Delta U_2, \Delta V_2, \Delta\theta_2, U_3, V_3, \theta_3\}^T \qquad (3.24)$$

The two constraint equations are used to eliminate two of the element's variables. These are chosen to be the local transverse displacement and the rotation at the middle node. The remaining internal in-plane degree of freedom ensures a parabolic variation of the in-plane displacement. This is necessary for eccentric elements to avoid an incompatibility between the reference line and the centroid of the cross-section. Hence, the variables at the middle node are transformed to the local axes directions by using the transformation Equation (3.15). This gives, after rearrangement, $\mathbf{M}^*$ of (3.16) with δ^* defined as

$$\delta^* = \begin{Bmatrix} a \\ --- \\ b \end{Bmatrix} = \{U_1,\ V_1,\ \theta_1,\ \Delta u_2,\ U_3,\ V_3,\ \theta_3 \,\vdots\, \Delta v_2,\ \Delta\theta_2\}^T$$

... ... (3.25)

The unconstrained shape function array is given from (3.12) and (3.21) by

$$\gamma = \begin{Bmatrix} u \\ v \\ \\ \frac{du}{dx} \\ \frac{du}{dy} \\ \\ \frac{dv}{dx} \\ \\ \frac{d^2u}{dxdy} \\ \\ \frac{d^2u}{dx^2} \end{Bmatrix} = \sum_{i=1}^{3} \begin{bmatrix} N_i\ \hat{i}.\hat{x}, & N_i\ \hat{j}.\hat{x}, & 0 \\ N_i\ \hat{i}.\hat{y}, & N_i\ \hat{j}.\hat{y}, & 0 \\ \\ \frac{dN_i}{dx}\ \hat{i}.\hat{x}, & \frac{dN_i}{dx}\ \hat{j}.\hat{x} & 0 \\ 0\ , & 0\ , & -\ N_i \\ \frac{dN_i}{dx}\ \hat{i}.\hat{y}, & \frac{dN_i}{dx}\ \hat{j}.\hat{y}, & 0 \\ \\ 0\ , & 0\ , & -\ \frac{dN_i}{dx} \\ \\ \frac{d^2N_i}{dx^2}\ \hat{i}.\hat{x} & \frac{d^2N_i}{dx^2}\ \hat{j}.\hat{x}\ , & 0 \end{bmatrix} \begin{Bmatrix} U \\ V \\ \\ \theta \end{Bmatrix}_i \qquad (3.26)$$

OR

$$\gamma = WN\ \delta = WN^*\ \delta^*$$

$$= \left[W_A \,\vdots\, W_B\right] \begin{Bmatrix} a \\ --- \\ b \end{Bmatrix} \quad \ldots \quad \ldots \quad \ldots \qquad (3.27)$$

from which the constrained shape function array is obtained in terms of the "wanted" variables **a** by eliminating the "unwanted" variables **b** (Equation (3.20)).

3.5 ISOBEM2 ELEMENT

For this element, (Figure 3.2), C^1 continuity of both displacement components is assumed. The global displacements and the first derivatives of displacements with respect to the local x are interpolated independently assuming a parabolic variation. The derivatives with respect to the local x of the local displacements, which are obtained from the independently interpolated displacements, are made equal to the independently interpolated gradients at the two Gauss points $\xi = \pm 1/\sqrt{3}$. The constraint equations thus formed are used to eliminate the degrees of freedom at the middle node.

The resulting displacement field is incompatible with two variations of the displacement derivatives. In order to avoid the development of spurious mechanisms in the in-plane direction, three integration points must be used to evaluate the different integrals required. Also the axial strain in linear analysis must be defined by the independently interpolated gradient rather than the derivative of the independently interpolated in-plane displacement.

The global displacements U, V and the gradients θ, ε are independently interpolated as follows

$$\begin{Bmatrix} U \\ V \\ \\ \\ \theta \\ \\ \varepsilon \end{Bmatrix} = \sum_{i=1}^{3} N_i \begin{Bmatrix} U \\ V \\ \\ \\ \theta \\ \\ \varepsilon \end{Bmatrix}_i \quad \ldots \quad \ldots \quad \ldots \quad \ldots \quad \ldots \qquad (3.28)$$

wherein N_i are the hierarchical shape functions (Equation (3.7)).

The constraint equations are obtained from the relations

$$- \theta + \frac{dv}{dx} = 0$$

$$- \varepsilon + \frac{du}{dx} = 0 \quad \ldots \quad \ldots \quad \ldots \quad \ldots \quad \ldots \qquad (3.29)$$

which are given in terms of the element variables from (3.12) and (3.28) by

$$\sum_{i=1}^{3} \begin{bmatrix} \frac{dN_i}{dx}\,\hat{i}.\hat{y} & \frac{dN_i}{dx}\,\hat{j}.\hat{y} & -N_i & 0 \\ \\ \frac{dN_i}{dx}\,\hat{i}.\hat{x} & \frac{dN_i}{dx}\,\hat{j}.\hat{x} & 0 & -N_i \end{bmatrix} \begin{Bmatrix} U \\ V \\ \\ \theta \\ \\ \varepsilon \end{Bmatrix}_i = 0 \quad \ldots \qquad (3.30)$$

Evaluating (3.30) at the two Gauss points $\xi = \pm 1/\sqrt{3}$ results in the constraint matrix **M** of (3.14) and the total variables δ are defined as

$$\delta = \{U_1,\ V_1,\ \theta_1,\ \varepsilon_1,\ \Delta U_2,\ \Delta V_2,\ \Delta\theta_2,\ \Delta\varepsilon_2,\ U_3,\ V_3,\ \theta_3,\ \varepsilon_3\}^T$$

Rearranging the variables we have

$$\delta^* = \left\{\begin{array}{c} \mathbf{a} \\ \hline \\ \mathbf{b} \end{array}\right\} = \{U_1,\ V_1,\ \theta_1,\ \varepsilon_1,\ U_3,\ V_3,\ \theta_3,\ \varepsilon_3 \vdots$$

$$\vdots \Delta U_2,\ \Delta V_2,\ \Delta\theta_2, \Delta\varepsilon_2\}^T \qquad \ldots \quad \ldots \qquad (3.32)$$

The unconstrained shape function array is given for this element by the following definition

$$\gamma = \begin{Bmatrix} u \\ v \\ \varepsilon \\ \frac{du}{dy} \\ \frac{d^2u}{dxdy} \\ \frac{d^2u}{dx^2} \\ \frac{du}{dx} \end{Bmatrix} = \sum_{i=1}^{3} \begin{bmatrix} N_i\ \hat{i}.\hat{x}, & N_i\ \hat{j}.\hat{x}, & 0 & 0 \\ N_i\ \hat{i}.\hat{y}, & N_i\ \hat{j}.\hat{y} & 0 & 0 \\ 0 & 0 & 0 & N_i \\ 0 & 0 & -\frac{dN_i}{dx} & 0 \\ 0 & 0 & 0 & \frac{dN_i}{dx} \\ \frac{dN_i}{dx}\ \hat{i}.\hat{x} & \frac{dN_i}{dx}\ \hat{j}.\hat{x} & 0 & 0 \end{bmatrix} \begin{Bmatrix} U \\ V \\ \theta \\ \varepsilon \end{Bmatrix}_i$$

$$= WN\ \delta = WN^*\ \delta^*$$

$$= \left[W_A \vdots W_B \right] \begin{Bmatrix} a \\ \cdots \\ b \end{Bmatrix} \quad \ldots \quad \ldots \quad \ldots \qquad (3.33)$$

3.6 SUBBEAM ELEMENT

The element (Figure 3.3) is completely conforming with C^1 continuity of both displacement components. The final degrees of freedom are the same as those for ISOBEM2. The initial variation of displacements is assumed to be cubic and hence four points are required to define this variation (Figure 3.3a). Thus eight internal degrees of freedom are introduced. The eight constraint equations required for the elimination of the internal degrees of freedom are obtained by

evaluating two constraint conditions at four points within the element. The final variation of displacements is an exact cubic and it becomes necessary to use at least three integration points to evaluate the element characteristics.

The global displacements U, V and the gradients θ, ε are now interpolated as follows

$$\begin{Bmatrix} U \\ V \\ \\ \theta \\ \varepsilon \end{Bmatrix} = \sum_{i=1}^{4} \bar{\bar{N}}_i \begin{Bmatrix} U \\ V \\ \\ \theta \\ \varepsilon \end{Bmatrix}_i \quad \ldots \quad \ldots \quad \ldots \quad \ldots \quad (3.34)$$

The internal degrees of freedom are defined at the third points $\xi = \pm \frac{1}{3}$ and $\bar{\bar{N}}_i$ are the cubic interpolation functions given by

$$\bar{\bar{N}}_1 = \frac{1}{16}(-1 + \xi + 9\xi^2 - 9\xi^3)$$

$$\bar{\bar{N}}_2 = \frac{9}{16}(1 - 3\xi - \xi^2 + 3\xi^3)$$

$$\bar{\bar{N}}_3 = \frac{9}{16}(1 + 3\xi - \xi^2 - 3\xi^3)$$

$$\bar{\bar{N}}_4 = \frac{1}{16}(-1 - \xi + 9\xi^2 + 9\xi^3) \quad \ldots \quad \ldots \quad (3.35)$$

The constraint equations are the same as for ISOBEM2 (Equation (3.29)), but the conditions are in terms of the cubic interpolation functions $\bar{\bar{N}}_i$ (Equation (3.35)) and are defined in terms of the nodal variables as follows

$$\sum_{i=1}^{4} \begin{bmatrix} \frac{d\bar{\bar{N}}_i}{dx}\,\hat{i}.\hat{y} & \frac{d\bar{\bar{N}}_i}{dx}\,\hat{j}.\hat{y} & -\bar{\bar{N}}_i & 0 \\ \frac{d\bar{\bar{N}}_i}{dx}\,\hat{i}.\hat{x} & \frac{d\bar{\bar{N}}_i}{dx}\,\hat{j}.\hat{x} & 0 & -\bar{\bar{N}}_i \end{bmatrix} \begin{Bmatrix} U \\ V \\ \theta \\ \varepsilon \end{Bmatrix}_i = 0$$

These are applied at the four equidistant points $\xi = \pm \frac{3}{5}, \pm \frac{1}{5}$ to obtain the constraint matrix M (Equation (3.14)).

The total variables δ (Figure 3.3a) are defined as

$$\delta = \{U_1, V_1, \theta_1, \varepsilon_1, U_2, V_2, \theta_2, \varepsilon_2, U_3, V_3, \theta_3, \varepsilon_3, U_4, V_4, \theta_4, \varepsilon_4\}^T \quad \ldots \quad \ldots \quad \ldots \quad \ldots \quad (3.37)$$

and

$$\delta^* = \begin{Bmatrix} a \\ --- \\ b \end{Bmatrix} = \{U_1, V_1, \theta_1, \varepsilon_1, U_4, V_4, \theta_4, \varepsilon_4 \,|\, U_2, V_2, \theta_2, \varepsilon_2, U_3, V_3, \theta_3, \varepsilon_3\}^T \quad \ldots \quad \ldots \quad \ldots \quad (3.38)$$

The unconstrained shape function array is given by

$$\gamma = \begin{Bmatrix} u \\ v \\ \varepsilon \\ \frac{du}{dy} \\ \frac{dv}{dx} \\ \frac{d^2u}{dxdy} \\ \frac{d^2u}{dx^2} \end{Bmatrix} = \sum_{i=1}^{4} \begin{bmatrix} \bar{\bar{N}}_i\ \hat{i}.\hat{x} & \bar{\bar{N}}_i\ \hat{j}.\hat{x} & 0 & 0 \\ \bar{\bar{N}}_i\ \hat{i}.\hat{y} & \bar{\bar{N}}_i\ \hat{j}.\hat{y} & 0 & 0 \\ 0 & 0 & 0 & \bar{\bar{N}}_i \\ 0 & 0 & -\bar{\bar{N}}_i & 0 \\ \frac{d\bar{\bar{N}}_i}{dx}\ \hat{i}.\hat{y} & \frac{d\bar{\bar{N}}_i}{dx}\ \hat{j}.\hat{y} & 0 & 0 \\ 0 & 0 & -\frac{d\bar{\bar{N}}_i}{dx} & 0 \\ 0 & 0 & 0 & \frac{d\bar{\bar{N}}_i}{dx} \end{bmatrix} \begin{Bmatrix} U \\ V \\ \theta \\ \varepsilon \end{Bmatrix}_i$$

$$= \quad WN\ \delta \quad = \quad WN^*\ \delta^*$$

$$= \begin{bmatrix} W_A \vdots W_B \end{bmatrix} \begin{Bmatrix} a \\ --- \\ b \end{Bmatrix} \quad \ldots \quad \ldots \qquad (3.39)$$

3.7 COMPUTATIONAL IMPLEMENTATION

The elements presented above and which incorporate the theory presented in Chapter 2 were implemented in the general purpose finite element program LUSAS. Simplified schematic diagrams of the computational procedure which has been used for the pre-solution and post-solution element calculations are presented in Figures 3.7 and 3.8 respectively. In what follows,

brief comments on the special features of the computational implementation are presented.

The special requirements of the constraint technique (Figure 3.6)are:

a) a matrix partitioning scheme in order to rearrange variables

b) a matrix inversion routine to form the constraint matrix C (Figure 3.6).

In addition to the computations needed for small displacement analyses, the nonlinear solutions require the calculation of the nodal residuals for each element.

For the Total Largangian solutions, the shape function array is formed only once and written on to disc. For all subsequent solutions the array is read from the disc and used in the element computations.

The Total Lagrangian formulation based on the Green strains (TLG), requires only two additional subroutines to be added to the small displacement calculations. These are:

i. A subroutine to form the linear strain matrix B_L and to add it to the infinitesimal strain matrix B_o.

ii. A subroutine to form the geometric stiffness matrix K_σ and add it to the tangent stiffness matrix.

The Total Lagrangian formulation based on the conventional strains (TLC) needs two more routines, namely:

i. A subroutine to form the H^* matrix.

ii. A subroutine to form the additional geometric stiffness matrix K^*_σ and add it to the tangent stiffness matrix.

The Updated Lagrangian formulation (ULG) requires a routine to update the coordinates plus the two subroutines required by the TLG formulation.

The geometry is always assumed to be parabolic and hence is defined by three nodes when updating the coordinates. For the two end element nodes the global displacements, which are degrees of freedom, are added to the initial global coordinates to obtain the updated coordinates. The coordinates of the internal node are computed as follows:

a) The local displacement components are obtained by interpolation using the initial geometry and the shape function array.

b) The displacements are transformed into the global directions.

c) The global displacements are added to the initial global coordinates.

Therefore, it is necessary to reform the shape function array for the elements whenever one of the following is required:

a) Computation of the updated coordinates.

b) Recalculation of the new shape functions which are needed to form the element characteristics.

The additional requirement of the combined Updated plus Total Lagrangian formulation (UTLG) is the necessity of storing the displacements from the beginning of the load increment $\mathbf{a}_c$. Once the solution has converged, the displacements $\mathbf{a}_c$ are used to obtain the new updated geometry.

The modification necessary for deformation dependent nodal forces must be included for the TLG, TLC and UTLG formulations.

Clearly the Total Lagrangian formulations are easier to implement than the Updated Lagrangian formulations.

3.8 CONCLUSIONS

1. The possibility of obtaining non-conforming and exactly conforming elements by using the constraint technique has been demonstrated.

2. Non-conforming and exactly conforming elements have been developed using the constraint technique.

3. The choice of the degrees of freedom for the elements has been based on the convergence requirements of completeness and compatibility taking into consideration the two following factors:

   (i) The possibility of the elements being eccentric.

   (ii) The capability of the elements to represent correctly the large rotation theory presented in Chapter 2.

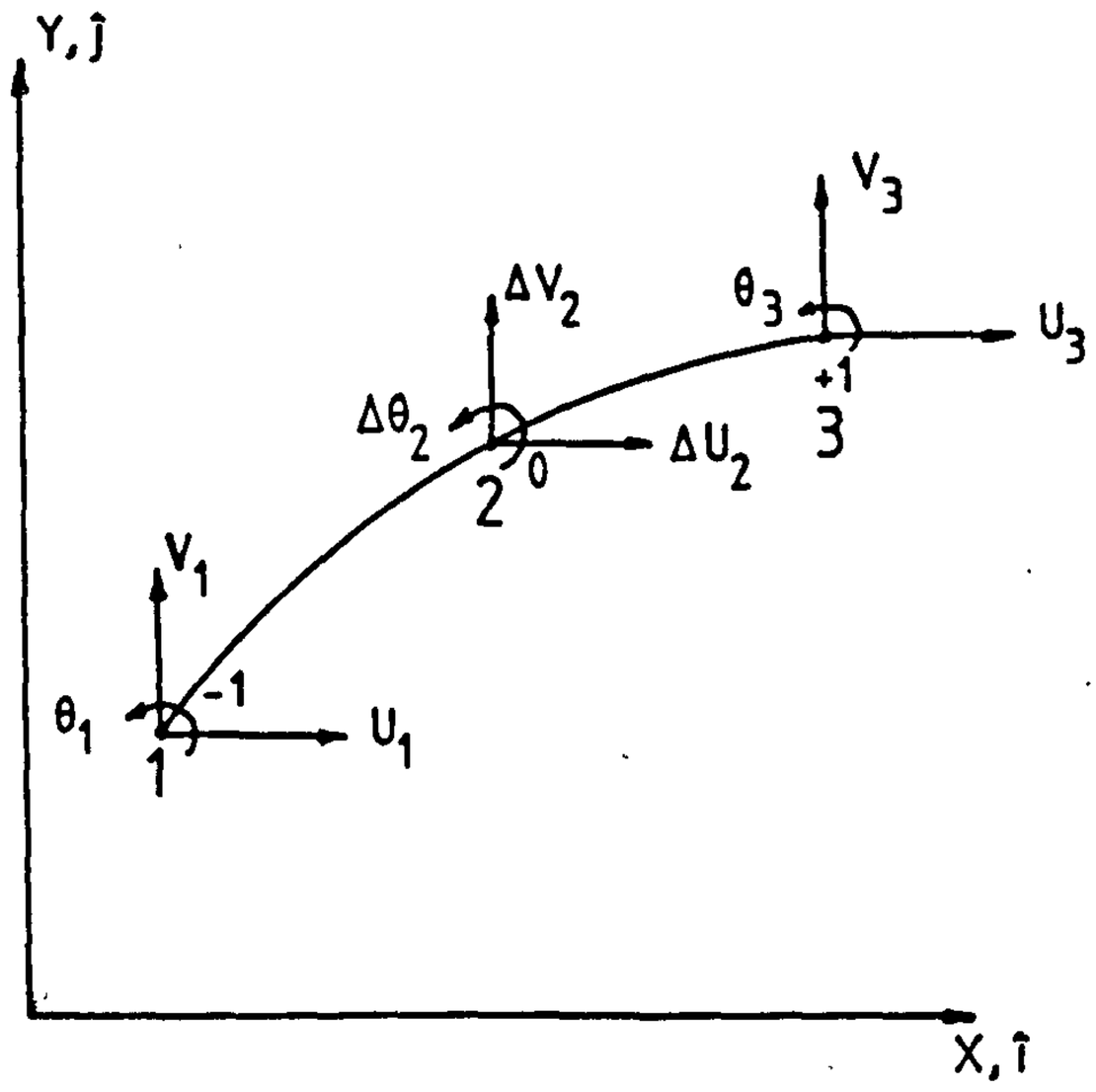

(a) Original element

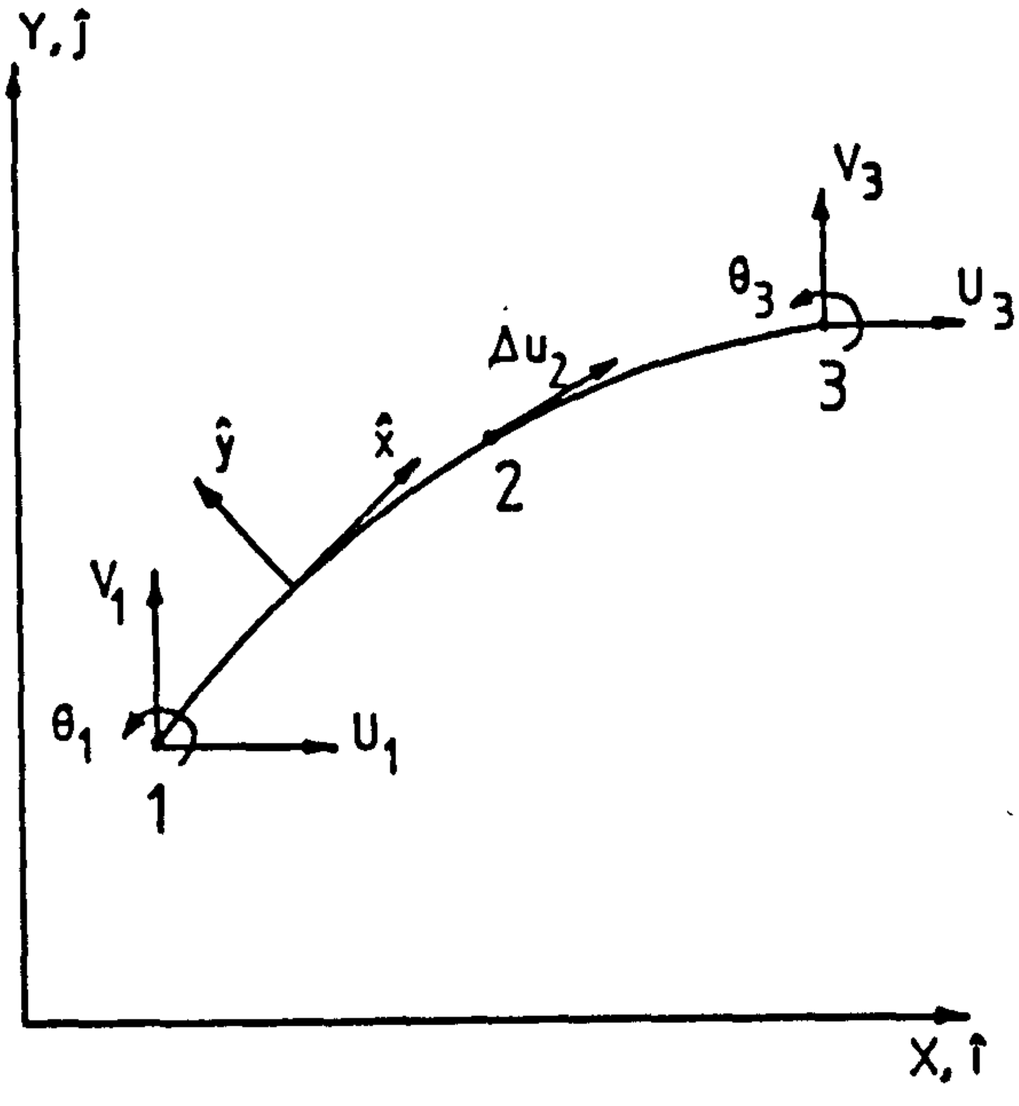

(b) Final element

FIGURE 3.1 - ISOBEM 1 Nodal Variables

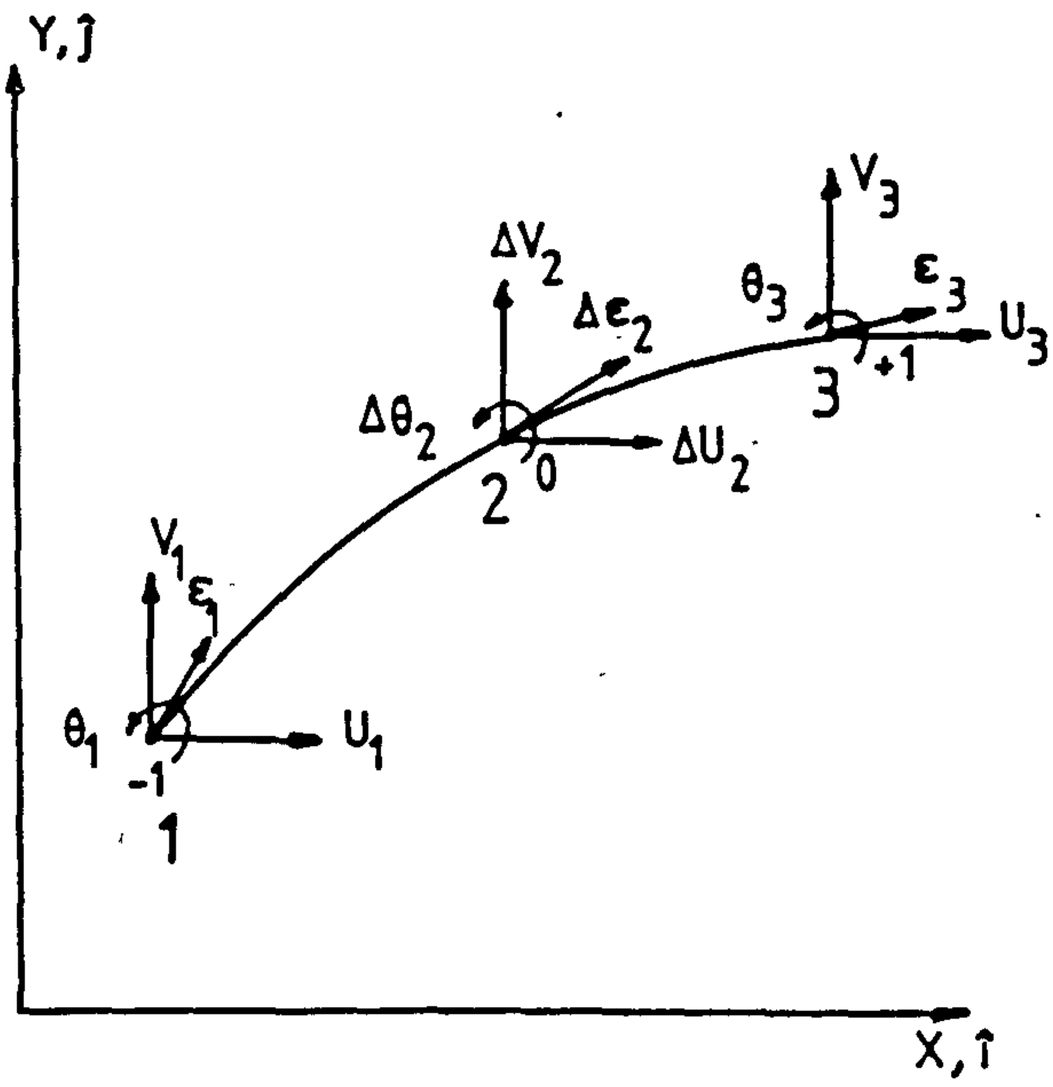

(a) Original element

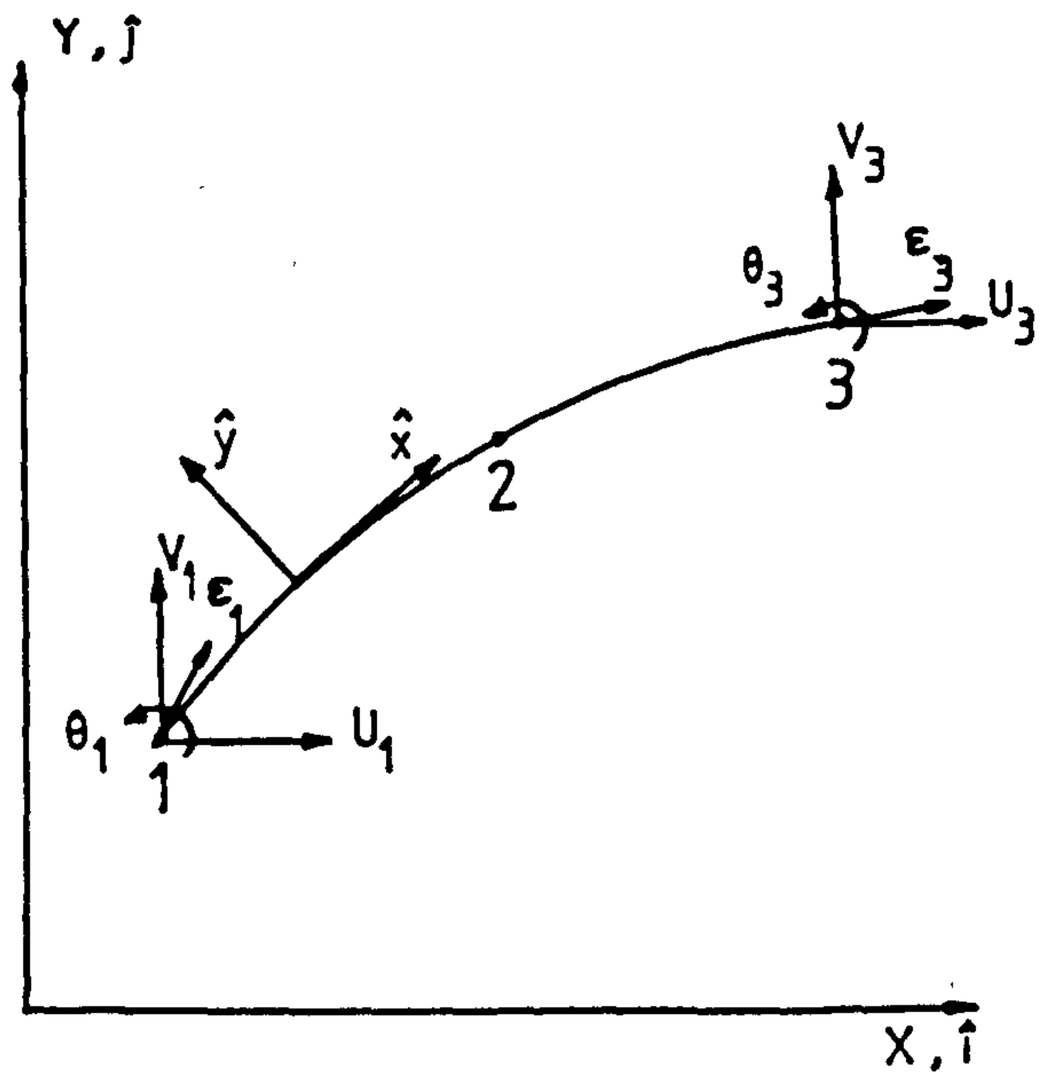

(b) Final element

FIGURE 3.2 - ISOBEM 2 Nodal Variables

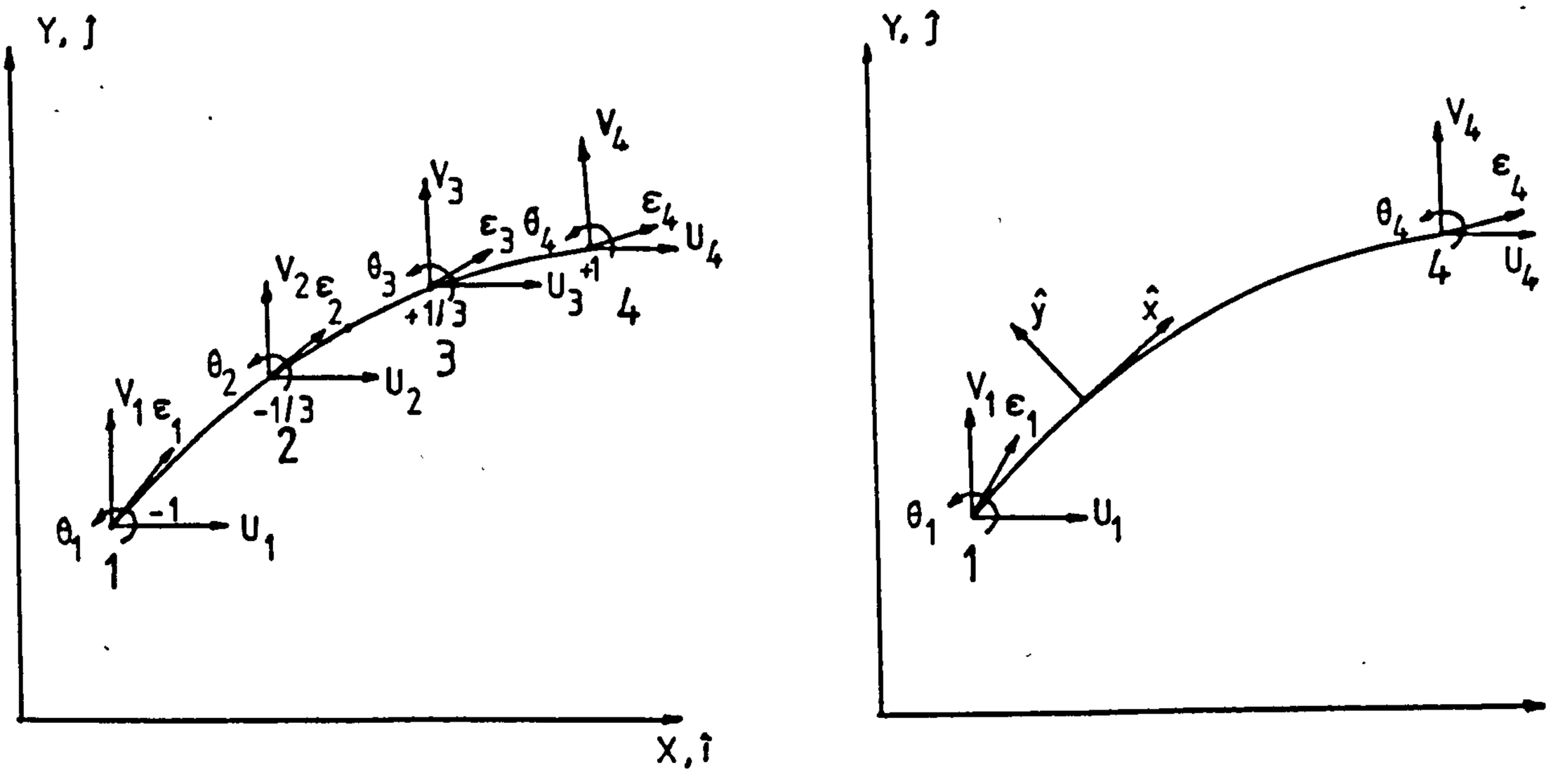

(a) Original element

(b) Final element

FIGURE 3.3 - SUBBEAM nodal Variables

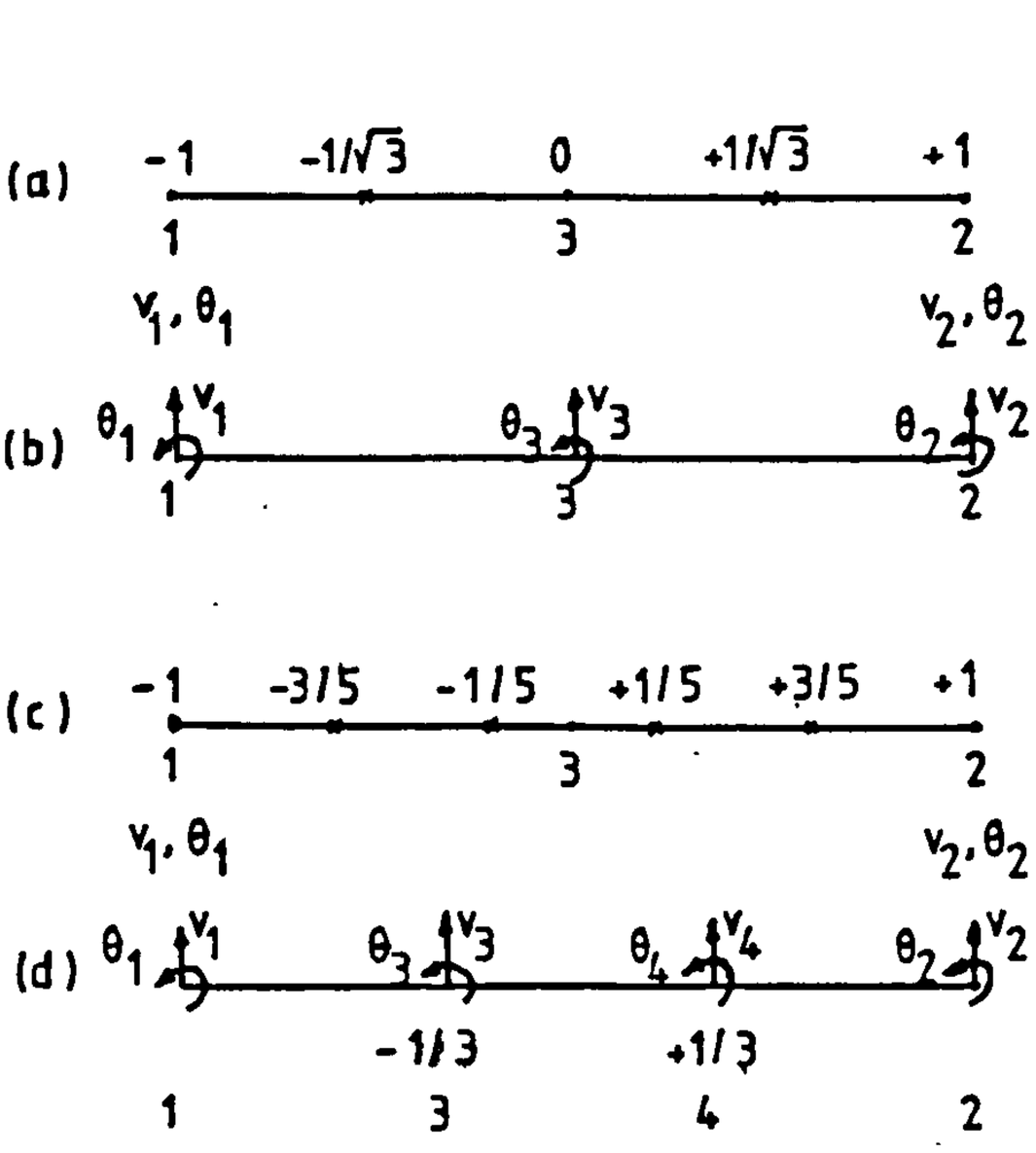

FIGURE 3.4 - Non-conforming and Conforming Displacement

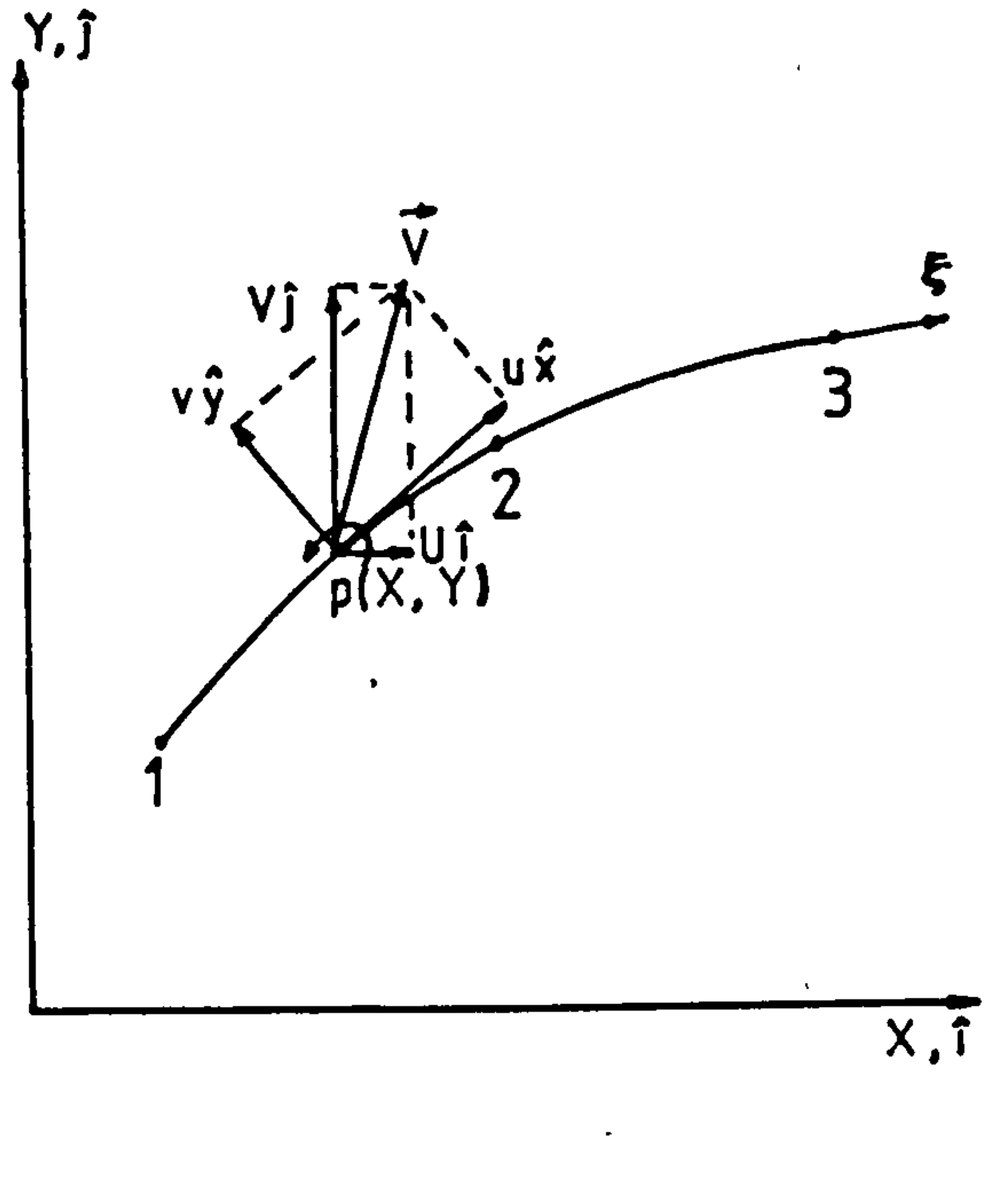

FIGURE 3.5 - Element Geometry and Displacement

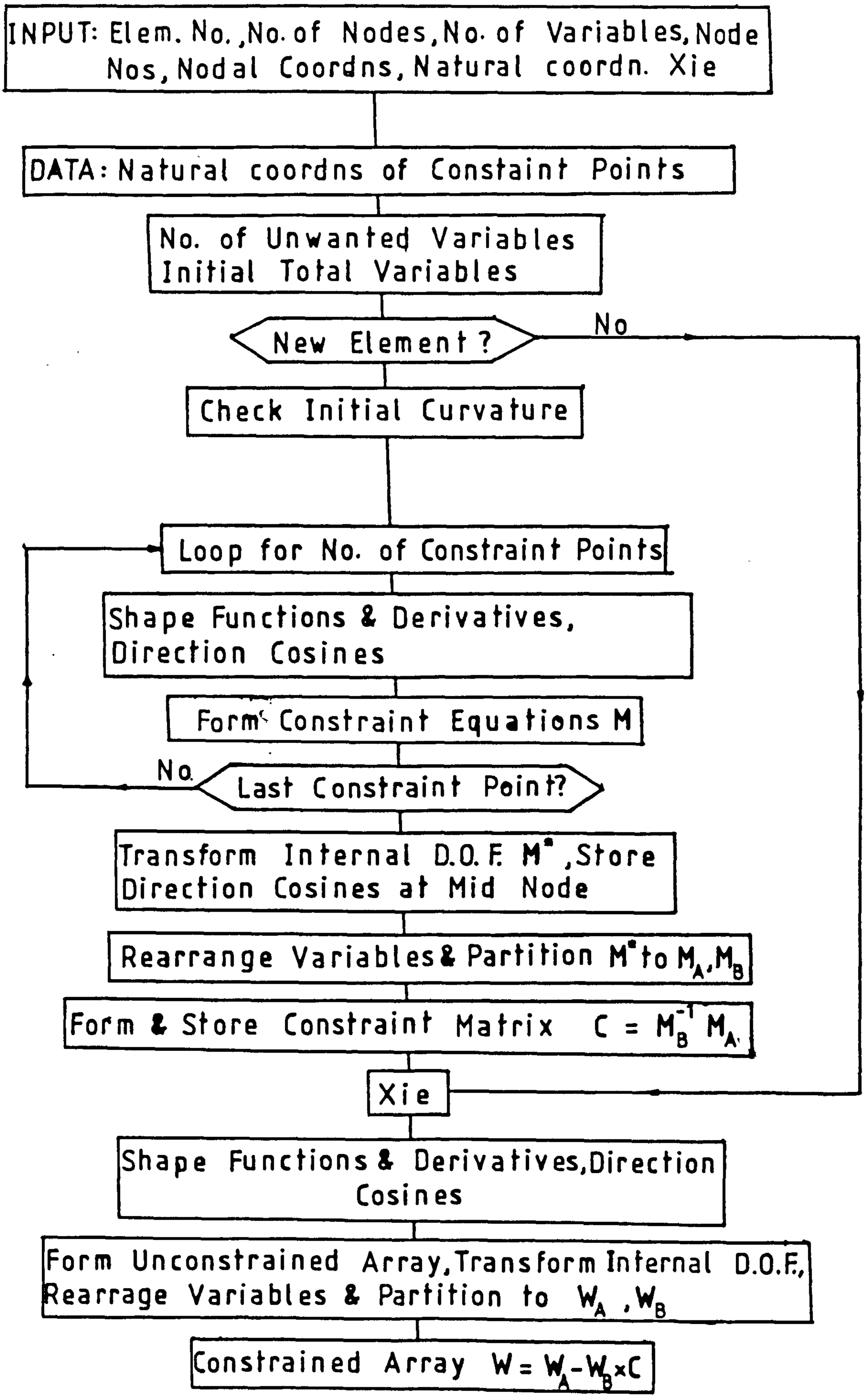

FIGURE 3.6 - 2-D Beam Element Computations - The Constrained Shape Function Array

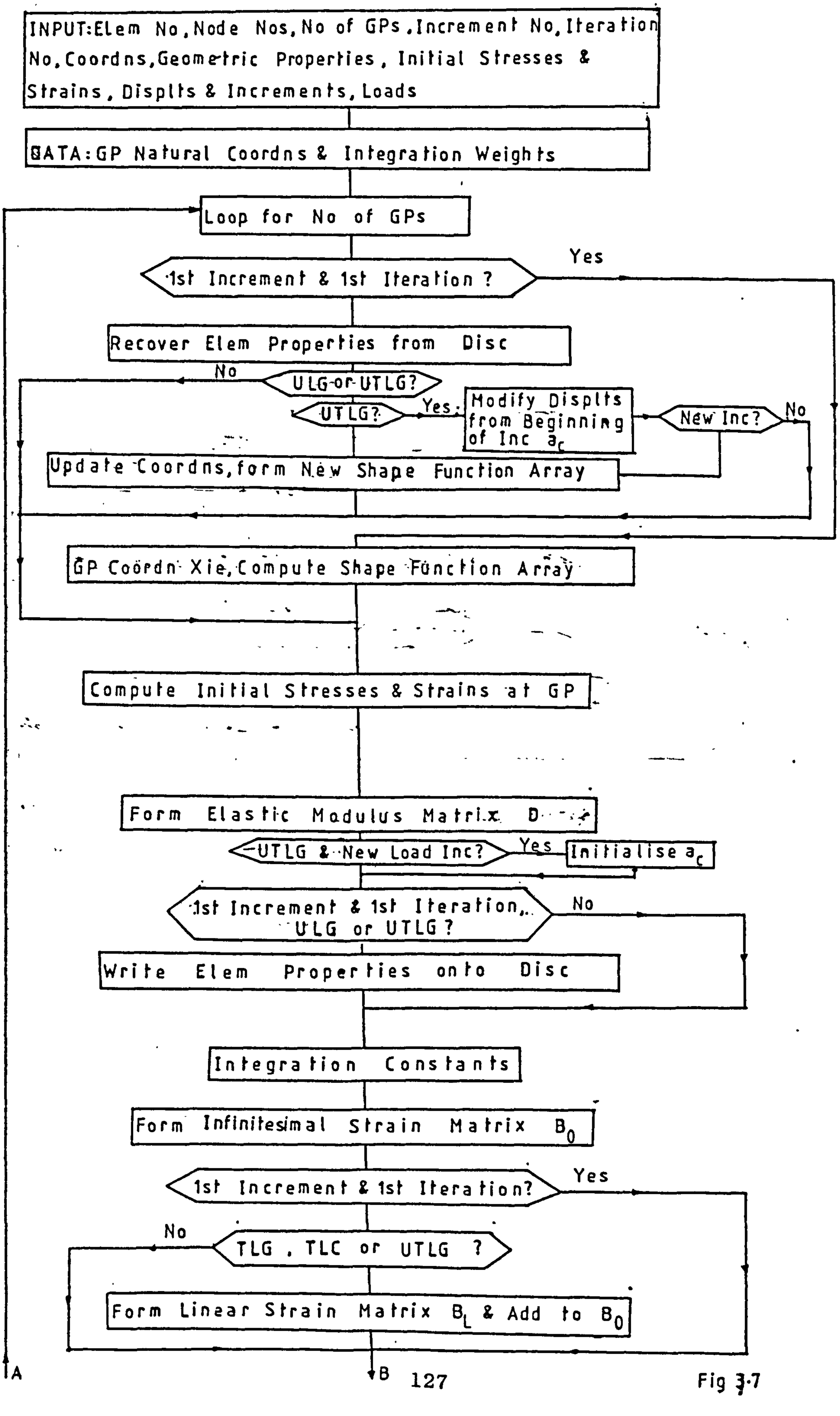
INPUT:Elem No,Node Nos,No of GPs,Increment No,Iteration No,Coordns,Geometric Properties, Initial Stresses & Strains, Displts & Increments, Loads
DATA:GP Natural Coordns & Integration Weights
Loop for No of GPs
1st Increment & 1st Iteration ?
Yes
Recover Elem Properties from Disc
No
ULG or UTLG?
UTLG?
Yes
Modify Displts from Beginning of Inc a_c
New Inc?
No
Update Coordns, form New Shape Function Array
GP Coordn Xie, Compute Shape Function Array
Compute Initial Stresses & Strains at GP
Form Elastic Modulus Matrix D
UTLG & New Load Inc?
Yes
Initialise a_c
1st Increment & 1st Iteration, ULG or UTLG ?
No
Write Elem Properties onto Disc
Integration Constants
Form Infinitesimal Strain Matrix B_0
1st Increment & 1st Iteration?
Yes
No
TLG , TLC or UTLG ?
Form Linear Strain Matrix B_L & Add to B_0
A
B

Fig 3.7

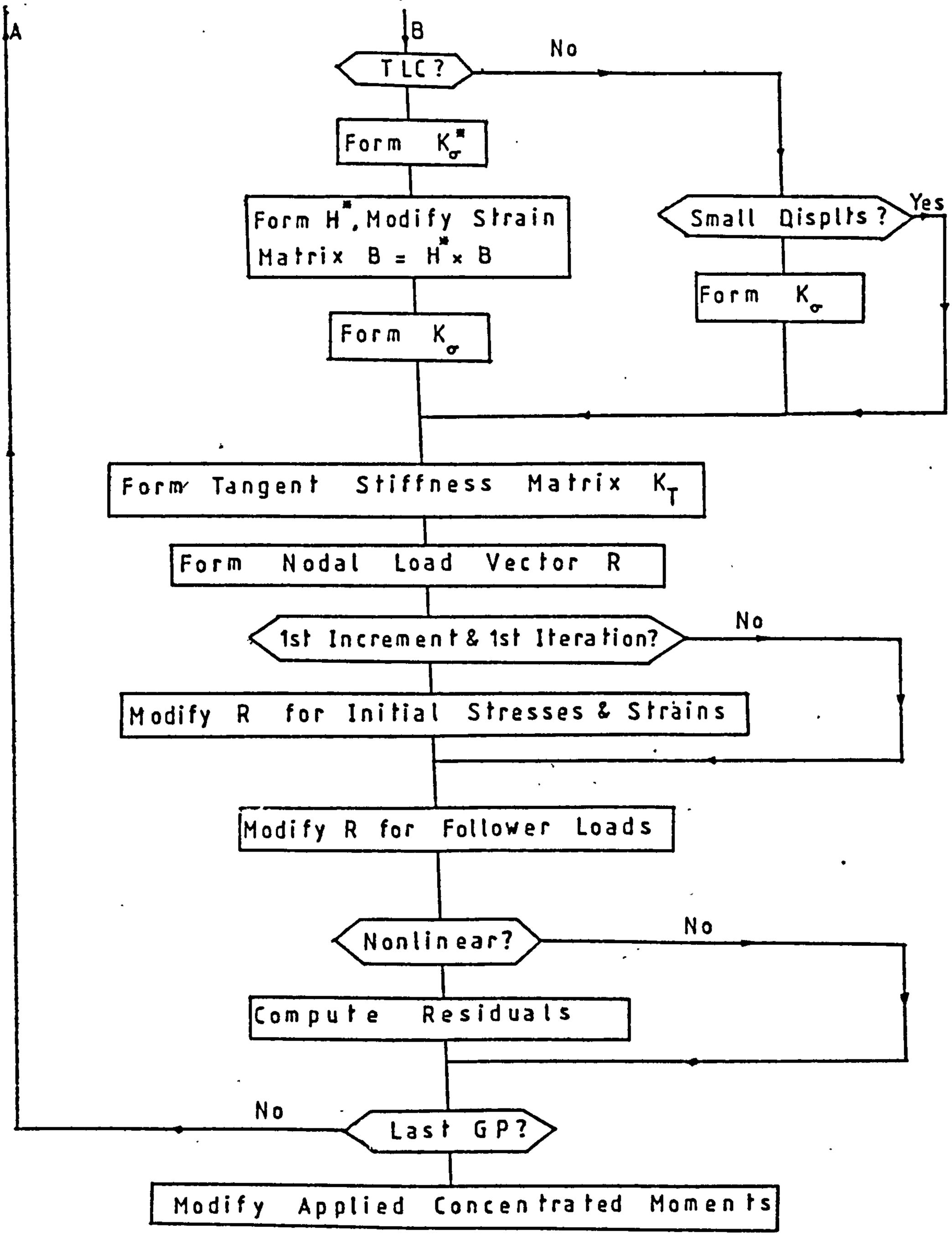

FIGURE 3.7 - 2-D Beam Element Pre-solution Computations - The Tangent Stiffness Matrix and the Nodal Residuals

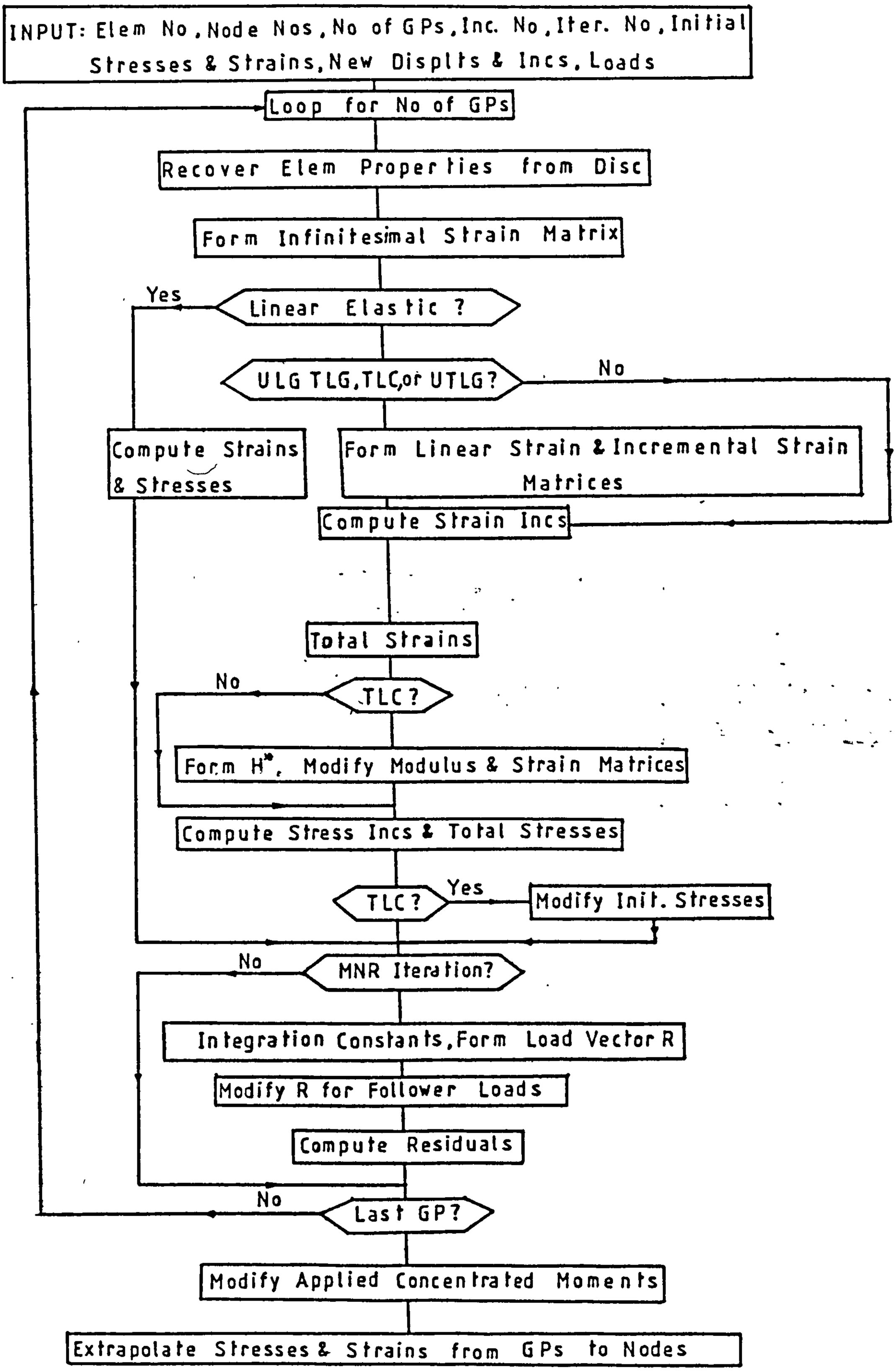

FIGURE 3.8 - 2-D Beam Element Post-solution Computations - Calculation of strains and stresses

CHAPTER 4

TWO-DIMENSIONAL CURVED BEAM APPLICATIONS

4.1 INTRODUCTION

The main objectives of the numerical results which are presented in this chapter are:

1. To assess the performance of the three elements, ISOBEM 1 (Figure 3.1), ISOBEM 2 (Figure 3.2) and SUBBEAM (Figure 3.3), as beam finite elements in linear applications.

2. To examine the performance of the three elements in geometrically nonlinear solutions and to assess their ability to represent correctly the large rotation theory which has been presented in Chapter 2.

3. To present a comparison in order to determine the numerical effectiveness of the four formulations for geometric nonlinearity, namely:

   (i) The Total Lagrangian formulation based on the Green strains (TLG)

   (ii) The Updated Lagrangian formulation based on the Green strains (ULG)

(iii) The combined Updated and Total Lagrangian formulation (UTLG)

(iv) The Total Lagrangian formulation based on the conventional strain (TLC)

Despite the fact that the elements are relatively simple with a small number of degrees of freedom they possess excellent capabilities. This is demonstrated clearly in the range of examples presented in the following sections. It should be noted that imperial units have been used in some examples instead of the SI system to conform with published results.

4.2 LINEAR SOLUTIONS

4.2.1 Straight Cantilever Beam

A straight cantilever beam was modelled by one element and solutions were obtained for different load cases using the three elements. It is apparent from the results which are given in Table 4.1 that all three elements give exact results when they are compared to the exact beam theory.

4.2.2 Curved Cantilever Beam

A curved cantilever beam problem (Figure 4.1) was solved employing each of the three curved elements and straight ISOBEM 1 elements to study the convergence characteristics of the curved beam elements. Solutions were obtained by one, two, four, eight and sixteen element idealisations for the following two load cases:

(a) vertical load at the free end

(b) concentrated moment at the free end.

The results are presented in Tables 4.2 and 4.3 and are compared with the beam theory (taking into account the effect of both bending and axial force (Figure 4.1)). The displacements of the curved element idealisations converge to the exact solution faster than the displacements of the straight elements. This is clearly seen from Figure 4.2 in which the percentage errors in end displacements on a logarithmic scale are plotted for different degrees of freedom.

The stress resultants obtained are presented in Figures 4.3a-b and 4.4. The results of the idealisations using the two non-conforming elements, i.e. ISOBEM 1 and ISOBEM 2, converge rapidly to the correct values. The SUBBEAM element idealisations, however, while converging

to the correct values show some oscillation in the axial force results from coarse meshes.

The maximum errors in displacements to seven significant figures when using one element only are as follows:

(a) Vertical load at free end:

Element	% Error	Displacement Component
ISOBEM 1	2.1	Vertical
ISOBEM 2	1.79	Vertical
SUBBEAM	4.47	Horizontal
Straight elements	39.96	Vertical

(b) Moment at free end:

Element	% Error	Displacement Component
ISOBEM 1	0.6	Horizontal
ISOBEM 2	1.68	Horizontal
SUBBEAM	1.65	Horizontal
Straight elements	29.29	Vertical

This firmly establishes the superior performance of the curved beam elements.

4.2.3 Shallow Clamped Arch

The complete arch (Figure 4.5) sub-tends an angle of 30^{o} and has a base length of 34 in (863.6 mm). The arch carries a central normal load and the following two arch thicknesses are considered:

(a) thick arch - t = 1 in (25.4 mm)

(b) thin arch - t = $\frac{1}{16}$ in (1.6 mm)

Half the arch was modelled by one, two, four, eight and sixteen elements. Solutions were obtained considering the two arch thicknesses and employing each of the three elements. The arches were also analysed by thirty-two ISOBEM 1 elements idealisations.

The crown displacement convergence curves on a logarithmic scale are given in Figure 4.6. All three elements give exact results for the thick arch to six significant figures on using sixteen or more elements. The non-conforming ISOBEM 1 and ISOBEM 2 elements perform better than the completely conforming SUBBEAM element for the thin arch.

The results for the stress resultants for the thick arch are presented in Figures 4.7a-b. The results from idealisations by each of the three elements converge rapidly to the exact values. Figures 4.8a-b give the

stress resultants for the thin arch. It can be seen from these figures that the results from idealisations by the two non-conforming elements are not affected by the thickness change. The results for the axial stress resultants from the SUBBEAM element idealisations, however, show some oscillations for the thin arch.

4.2.4 Deep Clamped Arch

The arch (Figure 4.9) is semi-circular with clamped ends and the radius of the centreline is 17 in (431.8 mm). The arch carries a central normal load. The same two thicknesses of 1 in (25.4 mm) and $\frac{1}{16}$ in (1.6 mm) are considered.

Half the arch was idealised by one, two, four, eight and sixteen elements. Solutions were obtained considering the two arch thicknesses and employing each of the three elements. Idealisations by thirty-two ISOBEM 1 elements were also used to obtain solutions. These represented the converged answers.

The convergence curves for the crown displacement are given on a logarithmic scale in Figure 4.10. For the thick arch the performance of the non-conforming elements is better than the SUBBEAM element performance when coarser meshes are used. But the latter element idealisation still converges to the same answer as

that obtained from the non-conforming elements' idealisations by the sixteen element mesh. The results of the non-conforming elements are not affected by the thickness change. The convergence of the SUBBEAM element results, however, is not monotonic and is slower for the thin arch.

The convergence of the stress resultants (Figures 4.11a-b and 4.12a-b) from the ISOBEM 1 and ISOBEM 2 element idealisations is very rapid. Also the thickness change does not affect the performance of these elements. The bending moments from the SUBBEAM element idealisations converge to the correct values for the thick arch. The thin arch bending moment results show slight oscillations. However, the average nodal values (Figure 4.12b) coverage to the correct answers. The axial stress resultants, however, show some oscillations. The average nodal values coverage to the correct values for the thick arch (Figure 4.11a). The fluctuations in axial stress resultants for the thin arch are considerable with values many times the order of the correct answers.

To conclude the convergence of the two non-conforming elements is very fast and is independent of the problem geometry and thickness. The SUBBEAM element results while being convergent for the thick arch, show some

oscillations in the axial force results. The performance of the element seems to be dependent on the problem geometry and thickness. Similar behaviour has been reported by Dawe [22, 23, 24] for curved elements with a cubic-cubic variation in displacements. The axial force resultants only, however, are affected considerably for the very thin deep arch. Since the deformation in such a case is nearly inextensional, the axial force will not be of importance [24].

4.3 GEOMETRICALLY NON-LINEAR SOLUTIONS

In all the geometrically nonlinear applications the loads were applied incrementally with complete Newton-Raphson iterations within each increment until convergence. The overall convergence control limits of the residual norm and the displacement norm were used in conjunction with the local convergence control of maximum absolute residual. A value of 1% was assumed for the two norms. Thus, the convergence was effectively controlled by the maximum absolute residual value.

4.3.1 Cantilever Under Vertical Load at Free End

This is an example which is commonly used as a test problem. Exact solutions and numerical results have been obtained for this problem by means of elliptic integrals [79, 80], dynamic relaxation based on

equilibrium equations written in the updated geometry [79] and hybrid finite elements [28].

The main characteristics of this cantilever problem are as follows:

i. Both the curvature and rotation can be large.

ii. The interaction between axial force and bending moment is clearly demonstrated and both of these are of equal importance.

iii. The deformation is inextensional.

Thus this problem is used to test the accuracy of both the theory and the elements which have been developed. This is achieved by comparing the results for displacements and stresses. The displacement values obtained are compared with published numerical results. Since there are no published values for the stresses, however, the Updated Lagrangian results, which represent the true stresses, are considered to be the correct stress resultant values. Also, from equilibrium considerations the axial stress resultant should be equal to zero at the support. A value of 10^{-2} was assumed for the maximum absolute residual convergence control in all the cantilever solutions.

The cantilever was modelled by sixteen equal elements. The load was applied in forty increments, with Newton-Raphson iterations within each increment, up to a maximum load of 10 $\frac{EI}{L^2}$. Solutions were obtained by the ULG, UTLG, TLG and TLC formulations employing each of the three elements. The Total Lagrangian formulations and the combined formulation required for convergence a maximum of four iterations per increment. The convergence rate of the complete Updated Lagrangian formulation (ULG) was slower. A maximum of fifteen iterations for the ISOBEM 1 idealisation and six iterations for the ISOBEM 2 and SUBBEAM idealisations were required for convergence.

The tip displacement results from the four ISOBEM 1 element idealisation solutions are given in Table 4.4 and Figure 4.13 and are compared with values from ref. [79]. The ULG and UTLG formulations are in close agreement with the exact values. The TLG results, however, show considerable variation from the correct values, especially for large rotations. The TLC formulation, while giving an improvement on the TLG results, is still in error. Figures 4.14a-b present a comparison between the stress resultants from the four formulations. The values from the Total Lagrangian solutions are clearly in error. The errors increase with the increase in curvature and rotation.

The failure of the two Total Lagrangian formulations was found to be primarily as a result of the equations becoming indefinite (with negative pivots), when the rotations exceed one radian. To investigate this problem further it is worth noting that in the original ISOBEM 1 element formulation the rotation is taken as a degree of freedom. Also, the element degrees of freedom are arranged so that the rotation is obtained first in the solution process.

Thus, for inextensional (or nearly inextensional) deformation, the axial strain is equal to zero (or a very small value) when the solution converges to the exact answer. Therefore,

$$e = \frac{du}{dx} + \frac{1}{2}\left(\frac{du}{dx}\right)^2 + \frac{1}{2}\left(\frac{dv}{dx}\right)^2 = 0 \quad \ldots \quad \ldots \quad (4.1)$$

Due to the arrangement of the element variables the values of $\frac{dv}{dx}$ are obtained first in the solution scheme. Hence, taking (4.1) as a quadratic equation in $\frac{du}{dx}$ and solving gives

$$\frac{du}{dx} = -1 \pm \left(1 - \left(\frac{dv}{dx}\right)^2\right)^{1/2} \quad \ldots \quad \ldots \quad \ldots \quad \ldots \quad (4.2)$$

The roots in (4.2) are real if

$$\left(\frac{dv}{dx}\right)^2 \leq 1 \quad \ldots \quad \ldots \quad \ldots \quad \ldots \quad \ldots \quad \ldots \quad (4.3)$$

The incremental in-plane strains add up to e when the Total Lagrangian formulations are used. Since $\frac{dv}{dx}$ represents the rotation for the ISOBEM 1 element, the rotation cannot exceed one radian for the inextensional cantilever example. Therefore, the equations become indefinite on attempting to solve for rotations that exceed one radian.

For the Updated Lagrangian solutions on the other hand the incremental axial strains are defined as follows

$$e = \frac{d\Delta u}{dx} + \frac{1}{2}(\frac{d\Delta u}{dx})^2 + \frac{1}{2}(\frac{d\Delta v}{dx})^2 \quad \ldots \quad \ldots \quad \ldots \quad (4.4)$$

Thus, the condition for real roots in an inextensional deformation is

$$(\frac{d\Delta v}{dx})^2 \leqslant 1 \quad \ldots \quad \ldots \quad \ldots \quad \ldots \quad \ldots \quad \ldots \quad (4.4)$$

This places a limit on the size of the rotation increment and hence introduces a limit on the load increment value.

Clearly condition (4.3) does not apply for the approximate theory based on the conventional strains (Equation (2.32a)) in which the axial strains are given by

$$e = \frac{du}{dx} + \frac{1}{2}\left(\frac{dv}{dx}\right)^2 \quad \ldots \quad \ldots \quad \ldots \quad \ldots \quad \ldots \quad (4.6)$$

Strain-displacement relations similar to those given by Equation (2.32a) are commonly used in the analysis of plate and shell type problems [6, 10, 50, 55, 56]. Thus, Total and Updated Lagrangians solutions were obtained for the cantilever example to test the accuracy of the approximate theory. Sixteen element ISOBEM 1 idealisations, in which the approximate theory was employed,were used. It can be seen from the results, which are presented in Figure 4.15, that the limitation on the rotation size has been removed. The Total Lagrangian results are, however, still in error compared to the exact and the Updated Lagrangian solutions.

The disadvantage of the Updated Lagrangian solutions is that considerably more computer time is required by these compared to the Total Lagrangian solutions. It will be of great advantage therefore if correct Total Lagrangian solutions are developed. The difficulty outlined above can be avoided by taking into account the following two facts.

(a) Condition (4.3) can be satisfied by the use of the displacement derivatives (which are rotation measures) rather than the rotations as degrees of freedom.

(b) The convergence criteria for a geometrically nonlinear solution are the same as those for linear finite element solutions i.e. compatibility and completeness [41].

These factors lead to the development of the ISOBEM 2 element by adopting an alternative interpretation of the constraint technique. In the ISOBEM 2 element the constraint equations are obtained by making the gradients of the independently interpolated displacements equal to the independently interpolated displacement derivatives. The SUBBEAM element was formulated by the same procedure to eliminate the incompatibility in displacement gradients within the ISOBEM 2 element.

The displacement results obtained by these elements for the cantilever example are exact for all four formulations. Idealisations by both the ISOBEM 1 and SUBBEAM elements give almost identical results, Tables 4.5 and 4.6. Figures 4.16 and 4.17 give plots of these results. The rotations obtained by all four formulations are in very good agreement. The sine of the angle of rotation is equal to the derivative of the out-of-plane displacement with respect to the in-plane coordinate for the two Total Lagrangian formulations (Equation (2.104)).

Considering the variation of the stress resultants along the length, however, the difference between the four formulations is clearly apparent. The bending moments obtained from all four formulations are almost identical. These are presented in Figure 4.18a. The axial force results are shown in Figure 4.18b. The TLG formulation results are obviously wrong since the values at the support are expected to be zero from equilibrium considerations. The error in these results increases with the increase in curvature (along the beam) and rotation. Hence, it results from neglecting the effect of bending on the axial force (Equation (2.26)) when using the Green strains.

It can be seen from Figure 4.19 that the correct axial force values are obtained if Equation (2.26) is used to calculate the true axial force. A similar procedure for the evaluation of the true stress resultants has been suggested by Hibbitt et al [28]. It is only possible, however, to evaluate the total true axial forces by this procedure. The true increments in axial stress resultants, which might be required in a materially nonlinear problem, are not available. This is where the TLC formulation provides an advantage. While retaining the advantages of the Total Lagrangian formulation, mainly the saving in computer time, the TLC formulation gives the true stress resultants (Figure 4.18) and in incremental form if required.

The UTLG formulation, which initiates as the TLG formulation for the first load increment, tends to correct itself and thus gives correct displacements and stresses (Figures 4.16, 4.17 and 4.18). The use of the UTLG formulation saves computer time compared to the use of a complete ULG solution.

The cantilever example was solved applying twenty and ten load increments with Newton-Raphson equilibrium iterations up to a total load of 10 $\frac{EI}{R^2}$ to study the effect of load increment size on the performance of the four formulations. The tip displacement results are presented in Figures 4.20 and 4.21. It can be seen from these figures that the TLG solution is not affected by the increment size. The other three formulations are affected slightly by the increment size. The apparent slight dependence of the TLC formulation results on the increment size can be attributed to the fact that the Green strain measure of the centreline e, which is included in the incremental formulation (Equations (2.38), (2.85) and (2.86)), was assumed small and neglected. Hence, it may be of advantage to retain this term in the formulation.

The axial force results are shown in Figures 4.22 and 4.23 for the twenty increments and ten increments solutions respectively. The TLG results being wrong

are not shown in the figures. It can be seen from these results that the TLC formulation gives values which are almost identical to the correct ULG formulation results. The UTLG formulation axial force results depend on the increment size and are wrong initially. This result was expected and is mainly due to the error introduced from the complete TLG solution for the first load increment.

Thus, the UTLG formulation needs to be modified to eliminate the error in the first increment. This may be achieved by adopting one of the following two alternatives:

(a) The use of a complete Updated Lagrangian solution for the first increment.

(b) The use of a combined formulation based on the conventional strains.

Generally the UTLG formulation is more complex, relatively difficult to implement and requires more storage compared to the other three formulations.

4.3.2 Symmetrical Buckling of Two-hinged Deep Arch

Wood and Zienkiewicz [61] have obtained the buckling response of a two-hinged deep arch (Figure 4.24) by using the Total Lagrangian formulation and paralinear elements. This example was chosen to test the accuracy of the curved elements in nonlinear solutions, especially when employing the Total Lagrangian formulations.

Half the arch was idealised with eight elements. Sixty equal displacement increments with Newton-Raphson iterations were applied up to a total crown displacement of 0.36 R. Solutions were obtained by the four formulations using each of the three elements. Since the rotations are only moderately large and the curvatures are relatively small, all solutions are expected to be in close agreement. The maximum number of iterations required for convergence with a relative error (maximum absolute residual) of 10^{-4} was four for the ULG formulation and three for the other three formulations. The results of the central load versus deflection and central load versus horizontal reaction from each element idealisation are compared with results from ref. [61].

Figures 4.25a-b give the results from the ISOBEM 1 idealisation. These show close agreement. There is a difference, however, in the post-buckling response between the Total and Updated Lagrangian results. This is due to the fact that the rotation and curvature become large in the post buckling phase.

The results from the ISOBEM 2 (Figure 4.26a-b) and the SUBBEAM (Figure 4.27a-b) idealisations are in very close agreement for all formulations. Table 4.7 gives the ISOBEM 2 element idealisation results.

The values of the buckling loads obtained from all solutions are as follows:

Element Type	Buckling Load (x $\frac{EI}{R^2}$)			
	ULG	UTLG	TLC	TLG
ISOBEM 1	15.23	15.31	15.06	15.04
ISOBEM 2	15.23	15.23	15.31	15.29
SUBBEAM	15.25	15.25	15.26	15.25

These closely agree with the value of 15.3 $\frac{EI}{R^2}$ (and 15.2 $\frac{EI}{R^2}$) given in ref. [61].

4.3.3 Cantilever Under Pure Moment

This example was chosen to demonstrate the capability of the theory and of the elements to deal with very large rotations (up to 2π radians). To obtain a solution by the Total Lagrangian formulations (TLG and TLC) and the combined formulation (UTLG), the modification of the applied load vector (Equation (2.103)) must be included in the computations. This modification, being a function of the displacement derivatives at a node point, is included in the computations for the two C^1 continuous elements, ISOBEM 2 and SUBBEAM only.

The cantilever (Figure 4.28) was modelled by six equal elements. The moments were applied in thirty increments to bend the cantilever into a complete circle. Newton-Raphson equilibrium iterations were used within each increment to achieve convergence.

The four solutions obtained from the SUBBEAM element idealisation are in close agreement. The average number of iterations required for convergence, within an increment with a relative error of 10^{-4}, was six. Comparative results for values at the free end obtained by the TLG formulation and exact values from ref. [25] are presented in Table 4.8. These show very good

agreement. Figure 4.28 gives some sample deformed configurations obtained by the TLG solution compared with the exact deformed configurations, which are circular segments of radius $\frac{EI}{M}$ for sufficiently large area [25].

Figures 4.29a and 4.29b give plots in a non-dimensional form of the displacements and the displacement derivatives of the free end, respectively. The two Total Lagrangian formulations give almost identical results. This is to be expected since the axial force is zero. The derivative of the local transverse displacement with respect to the in-plane coordinate is equal to the sine of the angle of rotation from the ULG and UTLG solutions. The UTLG results show a slight departure from the exact curves for very large rotations. The two Updated Lagrangian solutions, being a function of the developing element curvature result for large rotations, in elements which are too curved to be correctly defined by the assumed parabolic variation of element geometry. This is an idication that the use of more elements is required in these formulations.

The Total Lagrangian solutions are clearly in very good agreement with the exact solution. A drift from the exact curves occurs for large rotations, however, on applying these formulations and the six ISOBEM 2

element idealisation to solve the cantilever under pure moment problem. This can be seen from the results presented in Figures 4.30a-b. This is due in part to the incompatibility in the displacement gradients within the ISOBEM 2 element. The incompatibility effect can be reduced by increasing the number of elements used. An improved response, therefore, is to be expected if the number of elements is increased. Closer agreement with the exact curves is obtained by both formulations for the cantilever example by increasing the number of ISOBEM 2 elements used to twelve (Figure 4.31a-b).

4.3.4 Numerical Effectiveness of Formulations

Sample relative computer times which were required for solution are given in Table 4.9 to examine the numerical effectiveness of the four formulations. The Total Lagrangian solutions are clearly numerically more effective than the Updated Lagrangian solutions. Generally, using the Total Lagrangian formulations can save up to 50% or more in computer time compared to the ULG formulation.

The ULG formulation always results in correct answers, but requires considerably more computer time compared to the other three formulations.

The UTLG formulation can save in computer time compared to a complete ULG solution. It is worth noting, however, that the UTLG solution computer time was more than the ULG solution time for the cantilever under pure moment.

The TLG formulation gives exact displacement predictions and is independent of the load increment size.

The TLC formulation gives true incremental stress resultants for problems in which both rotation and curvature are large and in which the axial force is of importance.

The TLC approach is general and can be applied to all large deformation problems. To demonstrate this point, the two-dimensional theory which is presented in Appendix II was introduced into isoparametric element computations. The cantilever beam under vertical load at the free end was modelled by four 8-noded isoparametric elements (Figure 4.32). A single load increment of $\frac{EI}{L^2}$ was applied with Newton-Raphson equilibrium iterations. Two solutions were obtained by the TLG and TLC formulations. The results obtained for the axial stresses along the centreline of the cantilever are presented in Figure 4.32. The TLC formulation gives the correct stress results at the support where the TLG results are obviously wrong. This demonstrates the superiority of

the TLC formulation in predicting the true stresses. The isoparametric elements, however, were numerically ill-conditioned in both solutions. These elements are, therefore, unsuitable for use in the analysis of very thin structures.

4.3.5 Cantilever Under Uniformly Distributed Load and Follower Pressure Loading

A cantilever beam (L = 5 m, EI = 833.4 kNm^2, EA = 10^6 kN) was modelled by eight elements. Ten uniformly distributed load increments with Newton-Raphson equilibrium iterations within each increment, were applied up to a total load of $10\frac{EI}{L^3}$ per unit length. The load was kept in a fixed direction. The two Total Lagrangian formulations TLG and TLC were used to obtain solutions by each of the three elements. The good agreement between all solutions was expected since the rotations are only moderately large and the axial forces are small.

The ISOBEM 2 element idealisation results are presented in Table 4.10. Figures 4.33, 4.34 and 4.35 give the results from the ISOBEM 1, ISOBEM 2 and SUBBEAM element idealisations respectively. The results are compared with the analytical solution presented in ref. [81]. These show very close agreement.

The modification which is required for follower pressure loading (Equation (2.103)) was included in the computations for the two C^1 continuous elements. The cantilever beam idealised by eight elements was subjected to a follower pressure loading. The load was applied in ten increments up to a total load of $10\frac{EI}{L^3}$ per unit length. Newton-Raphson equilibrium iterations were used within each increment to achieve convergence. The ULG and TLG formulations were used to obtain solutions for comparison. The results for the tip displacements of the cantilever are presented in Table 4.11 and Figure 4.36. These show very good agreement between the two formulations. The ratio of the computer time required for the TLG solution to that required for the ULG solution is 0.3456. This is further evidence of the numerical effectiveness of the Total Lagrangian formulation.

4.3.6 The Post-bifurcation of a Simply Supported Beam

This problem which has been presented by Hibbitt et al [28] is one of the classical elastica problems. The problem consists of a force in a constant direction applied to the beam so that the beam buckles at a load $P_{cr} = \pi^2 EI/(4L^2)$, where L is the original beam half length. The simply supported beam (Figure 4.37) has a slenderness ratio L/R of 2.81×10^3.

Half the beam was modelled by ten equal elements. Ten equal displacement increments of L/5, with Newton-Raphson equilibrium iterations were applied at the pinned end.

An initial imperfection was assumed in order to initiate buckling. The undeformed geometry was defined by a sine curve. Two values of 2L/1000 and L/1000 were assumed for the maximum imperfection at mid-span. A third approach in which an eccentricity in the form of a sine curve was introduced in the modulus matrix (Equation (2.42)) was used to check the eccentric element formulation. A maximum value of L/10000 was assumed for the eccentricity at mid-span.

The results from the three solutions obtained by using the SUBBEAM element idealisation and the TLG formulation are presented in Table 4.12. The TLG formulation was used since it is not affected by the increment size.

The three solutions are in very close agreement. The number of iterations which were required for convergence within each increment with a relative error of 10^{-6} is given in Table 4.12. A maximum of thirty, thirty-two and twenty-nine iterations were required in the first increment for each of the three solutions respectively.

The position of the beam centreline is shown in Figure 4.37 at various loads during flexure. A plot of the load obtained from these solutions as a function of the position of the end of the beam compared with the results from ref. [28] is presented in Figure 4.38. This shows that the results which have been obtained are in excellent agreement with those from ref. [28].

The same beam was analysed using ten ISOBEM 2 elements. The results, which closely agree with those from ref. [28], are presented in Figure 4.39.

4.4 CONCLUSIONS

1. The results obtained by using each of the three elements have been shown to be exact when they are compared to the results obtained from the beam theory for straight elements in linear elastic solutions. The elements have been proven to be very accurate when used as curved beam elements. The performances of the ISOBEM 1 element and ISOBEM 2 element have been shown to be independent of problem geometry and thickness. The SUBBEAM element results have been found to be slightly dependent on the problem geometry and thickness.

2. The Total Lagrangian formulations TLG and TLC have been proven to be numerically more effective than the Updated Lagrangian formulation ULG and the combined formulation UTLG.

3. It has been demonstrated that for problems in which both curvature and rotation are large the TLC formulation is more suitable if incremental true axial stress resultants are required. The TLG formulation has been proven to be very effective in predicting the correct displacements for any size of load increment.

4. It has been found that the element used in large rotation and curvature problems must be C^1 continuous in both displacement components for the TLG and TLC formulations to converge to the correct answers. This requirement of the theory (Chapter 2) results from adopting the Kirchhoff hypothesis which states that plane sections remain plane and normal to the beam axis after deformation. This point has been proven by the excellent results obtained by the ISOBEM 2 and SUBBEAM element idealisations. The ISOBEM 1 element on the other hand has been found to be unsuitable for use in the analysis of large rotation and curvature problems when a Total Lagrangian solution is adopted.

5. The ISOBEM 1 element can be used with either the ULG or the UTLG formulation if C^1 continuity is physically objectionable. It has been shown that the UTLG formulation can save in computer time compared to the ULG formulation. It has been found, however, that the UTLG formulation should be modified to use large increments and at the same time predict correct stress values.

6. The load vector modification, which is necessary for the convergence to the exact answers of large rotation Total Lagrangian solutions of structures under applied concentrated moment, is a function of the displacement derivatives. It has been found that the incompatibility of these derivatives in the ISOBEM 2 element can affect the performance of this element in the analysis of such problems. It has been demonstrated, however, that such an effect can be reduced by increasing the number of elements.

7. It has been shown that follower pressure loading can be successfully dealt with in a Total Lagrangian formulation by modifying the applied load vector.

8. It has been proven that eccentric beam problems and beams with initial imperfections can be successfully included in a large deformation formulation by introducing the eccentricity (or imperfection) into the modulus matrix.

$A = 0.25\ m^2$

$I = 0.02083\ m^4$

$E = 0.2 \times 10^9\ kN/m^2$

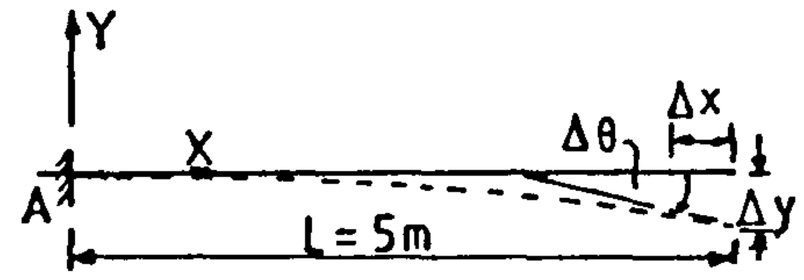

Load Case	Description of Value	Finite Element Solution using Thin Beam Elements						Beam Theory
		ISOBEM 1 Value	(Element/Theory)	ISOBEM 2 Value	(Element/Theory)	SUBBEAM Value	(Element/Theory)	
Vertical load at free end $P_y = -30$	$\Delta y \times 10^4$	-3.000	(1)	-3.000	(1)	-3.000	(1)	-3.000
	$\Delta\theta \times 10^4$	-0.900	(1)	-0.900	(1)	-0.900	(1)	-0.9
	M_A	150.0	(1)	150.0	(1)	150.0	(1)	150
Axial load at free end $P_x = 30$	$\Delta x \times 10^4$	0.03	(1)	0.03	(1)	0.03	(1)	0.03
	P_A	30.00	(1)	30.00	(1)	30.00	(1)	30
Concentrated moment at free end $M = 30$	$\Delta y \times 10^4$	0.900	(1)	0.900	(1)	0.900	(1)	0.9
	$\Delta\theta \times 10^4$	0.360	(1)	0.360	(1)	0.360	(1)	0.36
	M_A	-30.00	(1)	-30.00	(1)	-30.00	(1)	-30
Uniformly distributed load $w_y = -16$	$\Delta y \times 10^4$	-3.000	(1)	-3.000	(1)	-3.000	(1)	-3.0
	$\times 10^4$	-0.800	(1)	-0.800	(1)	-0.800	(1)	-0.800
	M_A	166.7	(1.0)	166.7	(1.0)	166.7	(1.0)	166.7

TABLE 4.1 Straight Cantilever Beam Results (One Element).

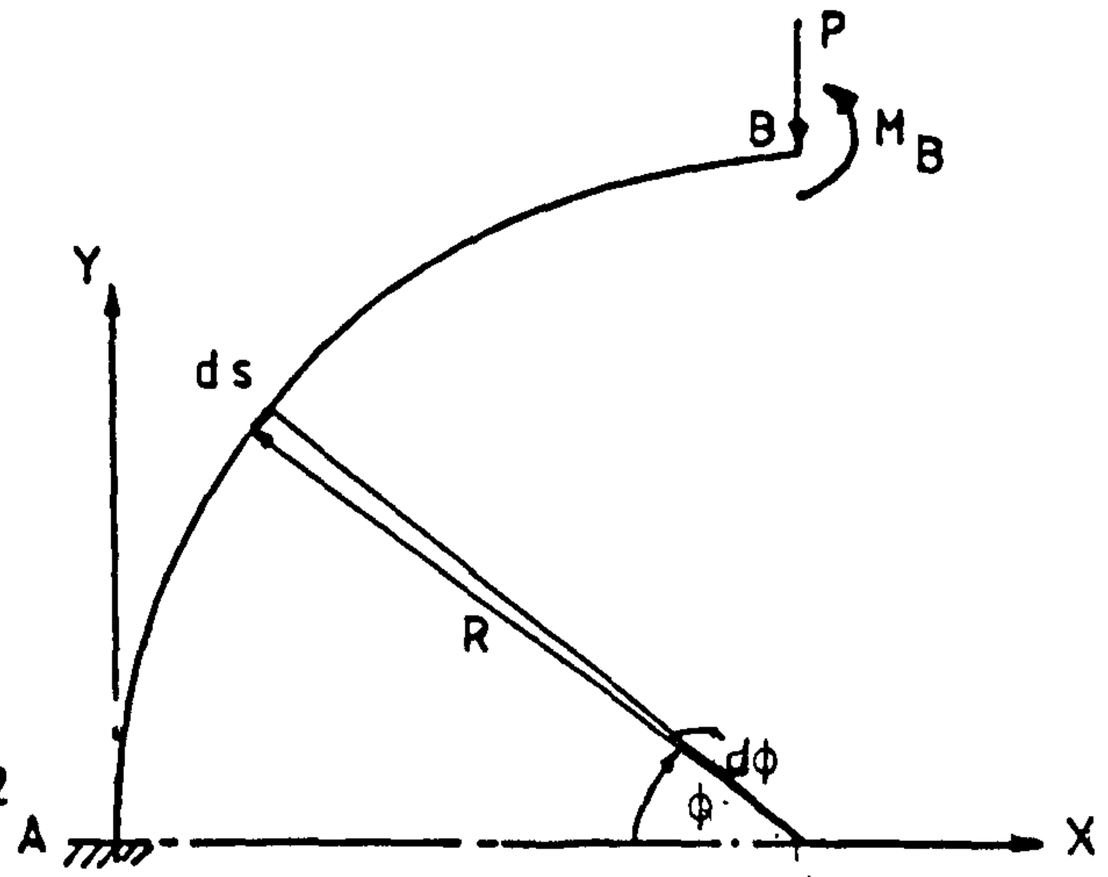

R = 10 m
b = 0·5 m
d = 1·0 m
$E = 2 \times 10^8 KN/m^2$

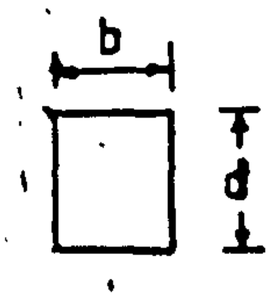

Beam Theory:

$$\Delta_i = \int_0^L \frac{M m_i}{EI} ds + \int_0^L \frac{N n_i}{EA} ds$$

Displacements at free end :

a- unit vertical load at free end : P = - 1

$$\Delta_y = -\frac{\pi}{4}\left[\frac{R^3}{EI} + \frac{R}{EA}\right] = -\cdot 00009433$$

$$\Delta_x = \frac{R^3}{2EI} - \frac{R}{2EA} = \cdot 0005995$$

$$\Delta_\theta = -\frac{R^2}{EI} = -\cdot 00012$$

b- moment at free end : M = - 10

$$\Delta_y = -\frac{10 R^2}{EI} = -\cdot 0012$$

$$\Delta_x = \frac{10 R^2}{EI}\left[\frac{\pi}{2} - 1\right] = \cdot 0006850$$

$$\Delta_\theta = -\frac{10R}{EI} \times \frac{\pi}{2} = -\cdot 0001885$$

FIGURE 4.1 - Curved Cantilever Beam

Description of Value	Number of Elements along Length	FINITE ELEMENT ANALYSIS USING THIN BEAM ELEMENTS								Beam Theory
		Curved ISOBEM 1 Elements		Curved ISOBEM 2 Elements		Curved SUBBEAM Elements		Straight ISOBEM 1 Elements		
		Value	(Element/Theory)	Value	(Element/Theory)	Value	(Element/Theory)	Value	(Element/Theory)	
Vertical deflection at free end	1	-.9235	(.9790)	-.9264	(.9821)	-.9557	(1.0131)	-.5664	(.6004)	
	2	-.9420	(.9986)	-.9422	(.9988)	-.9321	(.9881)	-.8296	(.8795)	
	4	-.9432	(.9999)	-.9432	(.9999)	-.9428	(.9995)	-.9135	(.9684)	-.9433
	8	-.9433	(1.0000)	-.9433	(1.0000)	-.9433	(1.0000)	-.9358	(.9920)	
$\Delta y \times 10^4$	16	-.9433	(1.0000)	-.9433	(1.0000)	-.9433	(1.0000)	-.9414	(.9980)	
Horizontal deflection at free end	1	.5907	(.9853)	.9573	(.9963)	.6263	(1.0447)	.5650	(.94245)	
	2	.5991	(.9993)	.5993	(.9997)	.5886	(.9818)	.5855	(.9766)	
	4	.5995	(1.0000)	.5995	(1.0000)	.5992	(.9995)	.5957	(.9937)	.5995
	8	.5995	(1.0000)	.5995	(1.0000)	.5995	(1.0000)	.5986	(.9985)	
$\Delta x \times 10^4$	16	.5995	(1.0000)	.5995	(1.0000)	.5995	(1.0000)	.5993	(.9997)	
Relation at free end	1	-.12004	(1.0003)	-.1187	(.9892)	-.1187	(.9892)	-.08486	(.7071)	
	2	-.1200	(1.0000)	-.1199	(.9992)	-.1199	(.9992)	-.1109	(.9242)	
	4	-.1200	(1.0000)	-.1200	(1.0000)	-.1200	(1.0000)	-.1177	(.9808)	-.12
$\theta \times 10^4$	8	-.1200	(1.0000)	-.1200	(1.0000)	-.1200	(1.000)	-.1194	(.9950)	
	16	-.1200	(1.0000)	-.1200	(1.0000)	-.1200	(1.0000)	-.1199	(.9992)	
Axial stress resultant at support	1	-1.166	(1.166)	-1.013	(1.013)	-.7063	(.7063)	-.7071	(.7071)	
	2	-1.049	(1.049)	-1.000	(1.000)	1.397	(-1.397)	-.9239	(.9239)	
	4	-1.013	(1.013)	-1.000	(1.000)	-.6734	(.6734)	-.9808	(.9808)	-.9239
	8	-1.003	(1.003)	-1.000	(1.000)	-.9727	(.9727)	-.9952	(.9952)	
	16	-1.001	(1.001)	-1.000	(1.000)	-.9972	(.9972)	-.9988	(.9988)	

TABLE 4.2 Curved Cantilever Beam Results
Unit Vertical Load at Free End.

Description of Value	Number of Elements along Length	FINITE ELEMENT RESULTS USING THIN BEAM ELEMENTS Curved ISOBEM 1 Elements Value (Element/Theory)	Curved ISOBEM 2 Elements Value (Element/Theory)	Curved SUBBEAM Elements Value (Element/Theory)	Curved ISOBEM 1 Elements Value (Element/Theory)	Beam Theory
Vertical deflection at free end $\Delta y \times 10^4$	1	-1.2004 (1.0003)	-1.1874 (.9895)	-1.1873 (.9894)	-0.8486 (.7071)	-1.2
	2	-1.2000 (1.0000)	-1.1991 (.99925)	-1.1991 (.99925)	-1.1087 (.9239)	
	4	-1.2000 (1.0000)	-1.2000 (1.0000)	-1.2000 (1.0000)	-1.1770 (.9808)	
	8	-1.2000 (1.0000)	-1.2000 (1.0000)	-1.2000 (1.0000)	-1.1943 (.99525)	
	16	-1.2000 (1.0000)	-1.2000 (1.0000)	-1.2000 (1.0000)	-1.1986 (.9988)	
Horizontal deflection at free end $\Delta x \times 10^4$	1	.6809 (.9940)	.6735 (.9832)	.6737 (.9835)	.8486 (1.2388)	.6850
	2	.6847 (.99956)	.6842 (.9988)	.6842 (.9988)	.7283 (1.0632)	
	4	.6850 (1.0000)	.6849 (.99985)	.6849 (.99985)	.6960 (1.0161)	
	8	.6850 (1.0000)	.6850 (1.0000)	.6850 (1.0000)	.6877 (1.0039)	
	16	.6850 (1.0000)	.6850 (1.0000)	.6850 (1.0000)	.6857 (1.0010)	
Rotation at free end $\theta \times 10^4$	1	-.1881 (.9979)	-.1861 (.9873)	-.1861 (.9873)	-.1697 (.9003)	- .1885
	2	-.1885 (1.0000)	-.1883 (.9989)	-.1883 (.9989)	-.1837 (.9745)	
	4	-.1885 (1.0000)	-.1885 (1.0000)	-.1885 (1.0000)	-.1873 (.9936)	
	8	-.1885 (1.0000)	-.1885 (1.0000)	-.1885 (1.0000)	-.1882 (.9984)	
	16	-.1885 (1.0000)	-.1885 (1.0000)	-.1885 (1.0000)	-.1884 (.9995)	

TABLE 4.3 Curved Cantilever Beam Results

Concentrated Moment at Free End.

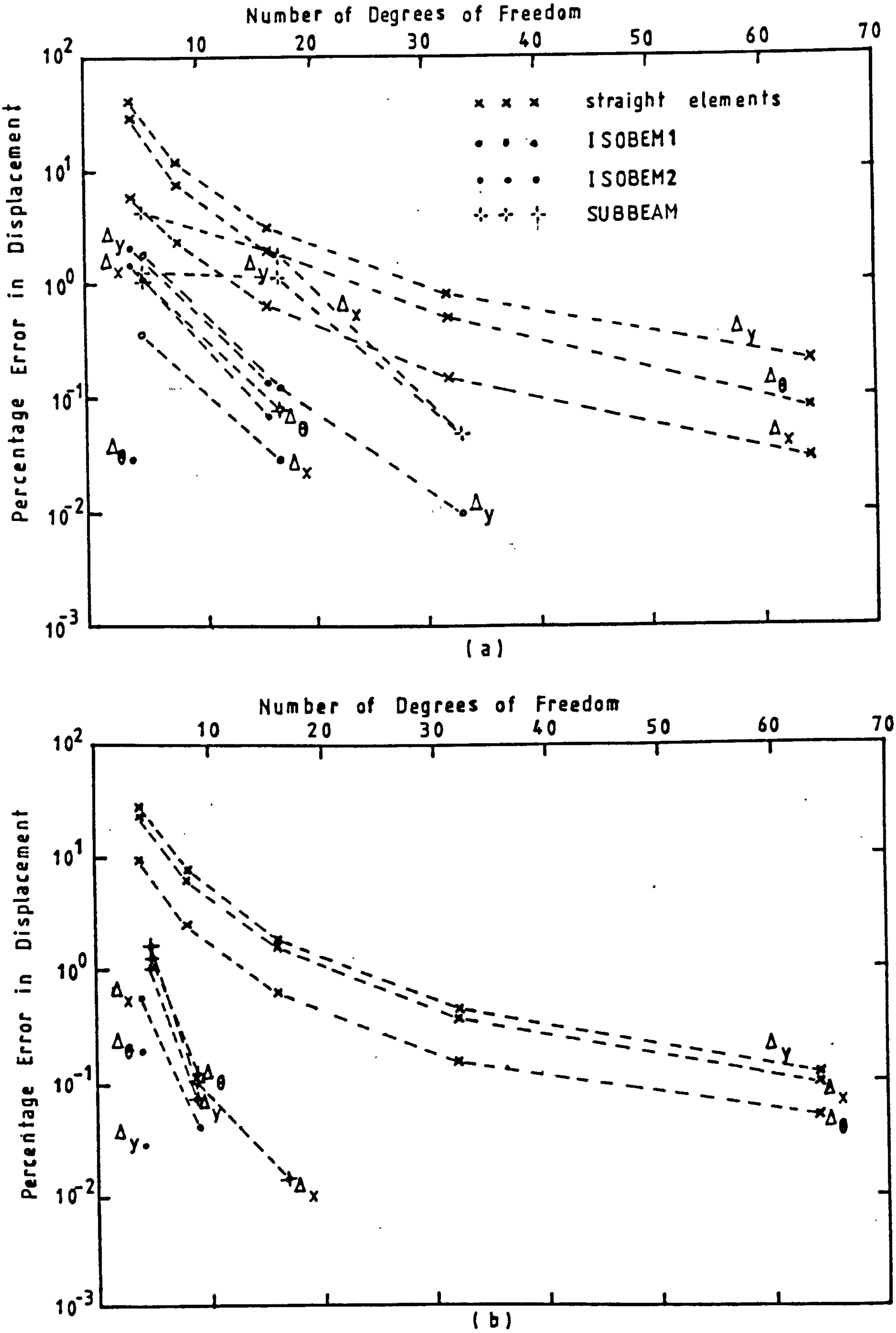

FIGURE 4.2 - Curved Cantilever Beam - Percentage Error in Displacement for Different Numbers of Elements

(a) Unit Load at Free End

(b) Moment at Free End

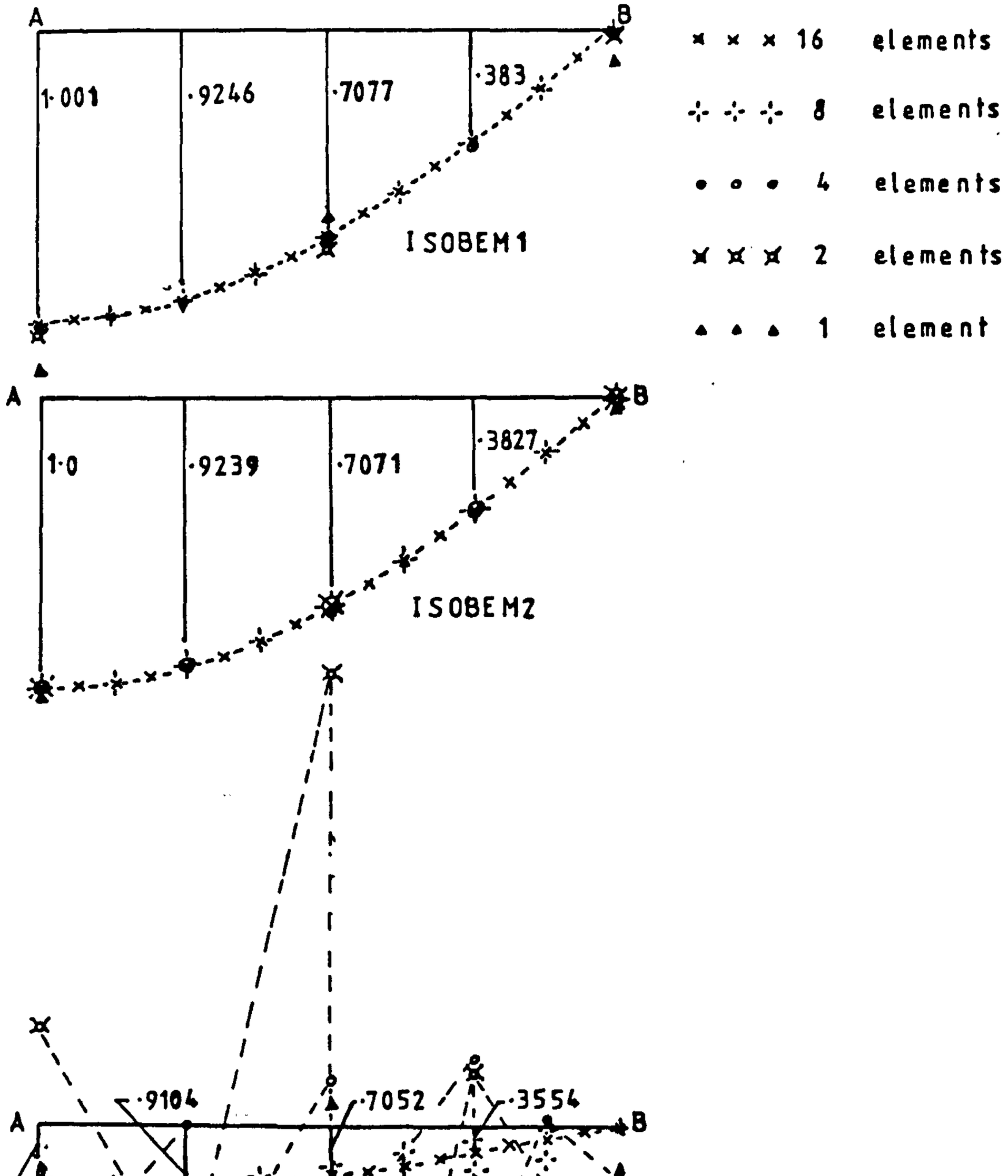

FIGURE 4.3a - Curved Cantilever under Vertical Load at Free End - Variation of Axial Force Along Length

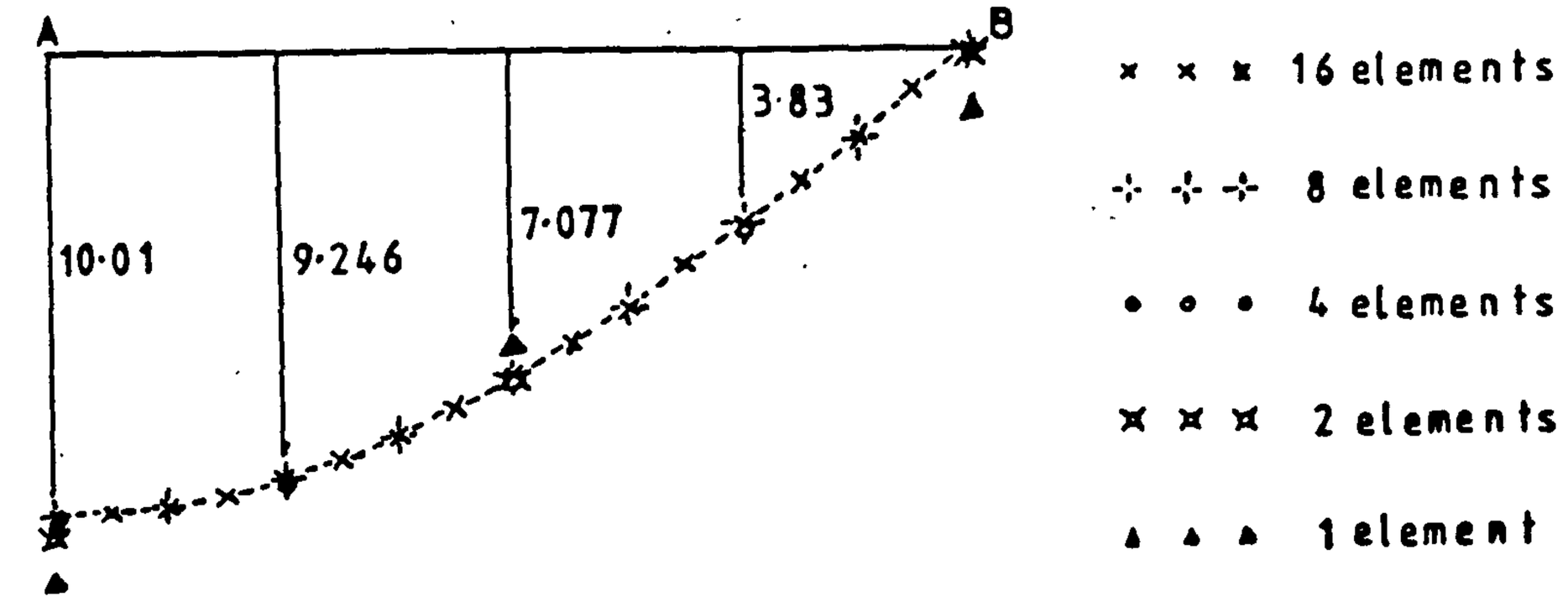

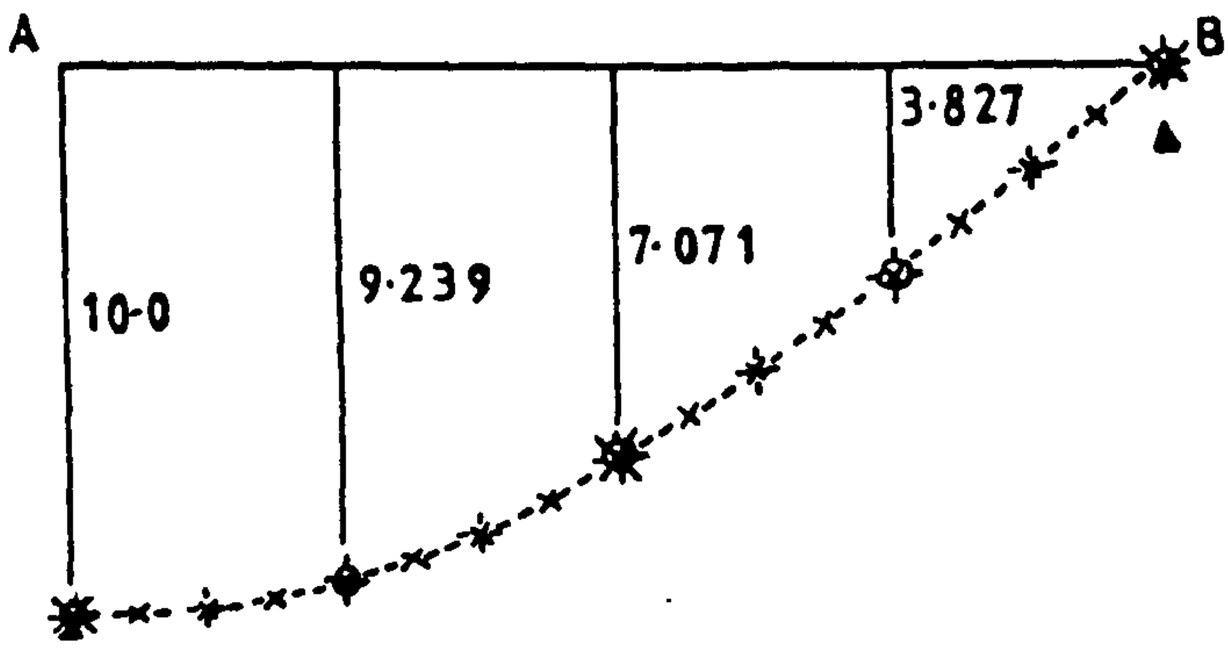

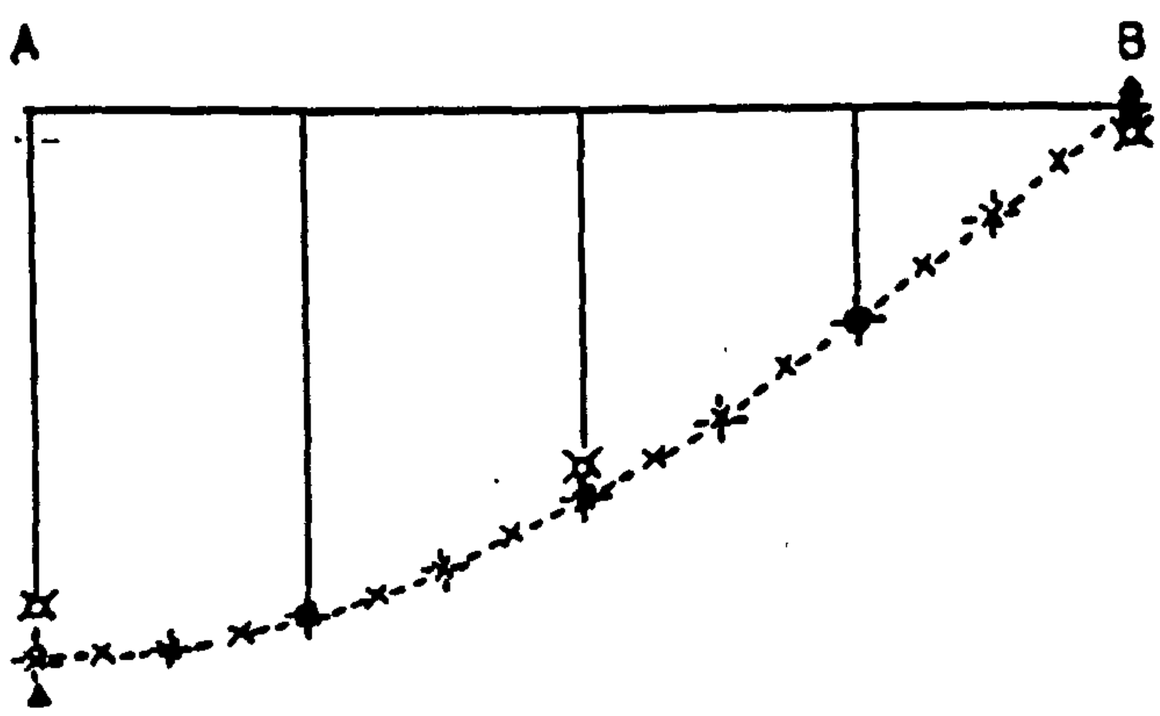

FIGURE 4.3b - Curved Cantilever under Vertical Load at Free End - Variation of Bending Moment Along Length

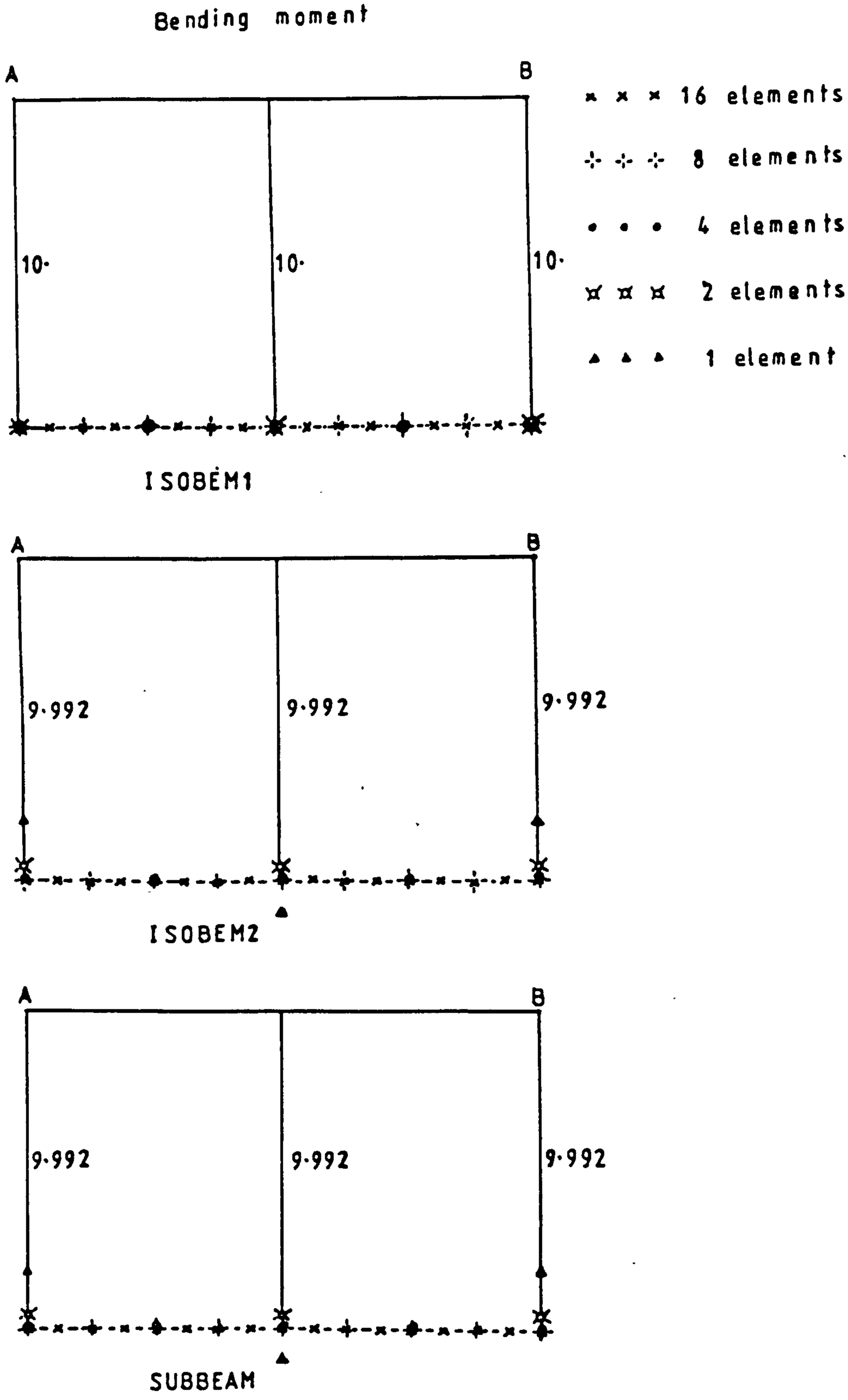

FIGURE 4.4 - Curved Cantilever under Moment at Free End
- Variation of Bending Moment Along Length

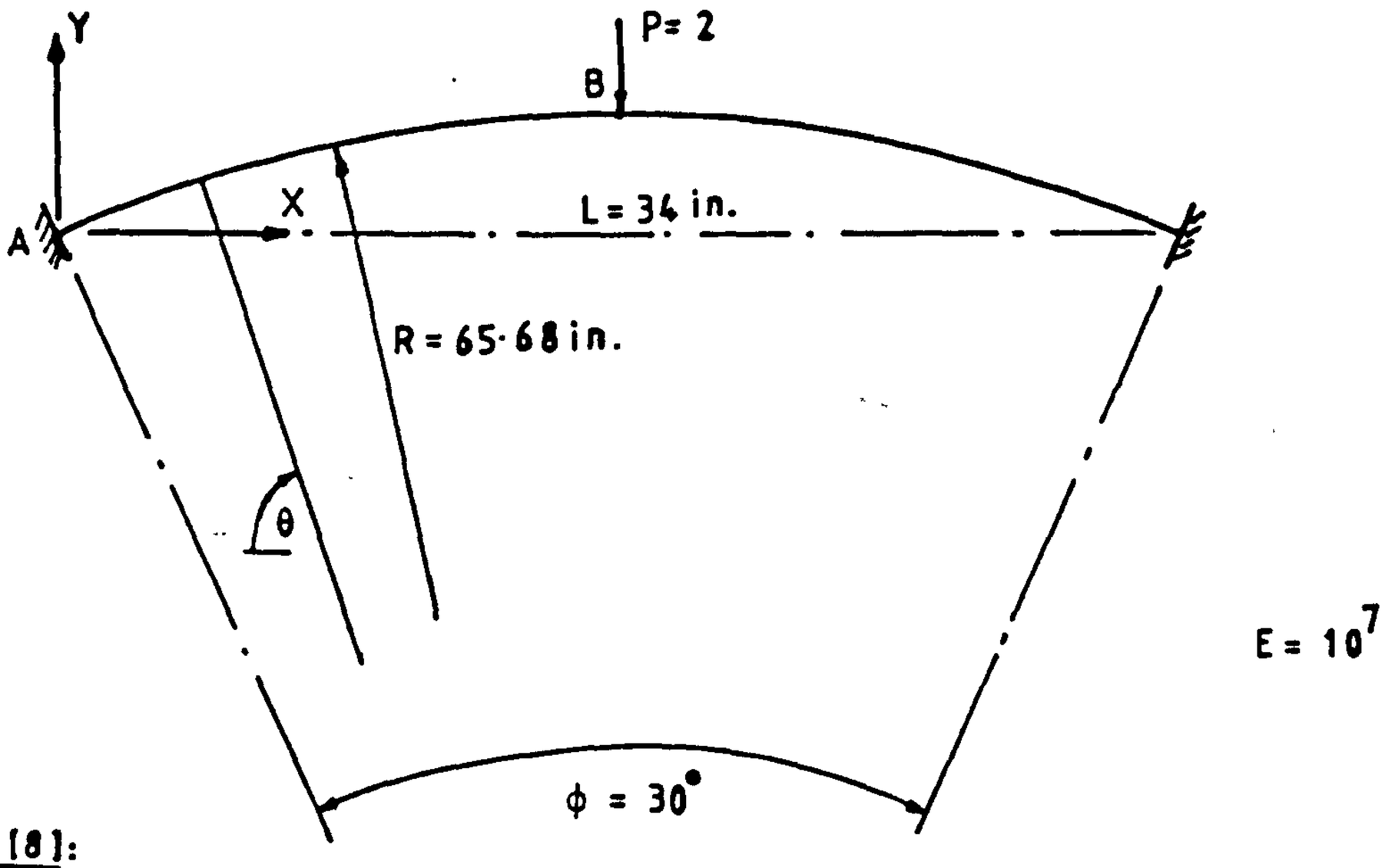

Ref.[8]:

$$H_A = 2{\cdot}9975\,P \quad , \quad V_A = 0{\cdot}5P \quad , \quad M_A = {\cdot}006653L \times P$$

$$M_x = -0{\cdot}4524 - 17 + 65{\cdot}68\cos\theta + 5{\cdot}995 \times (65{\cdot}68\sin\theta - 63{\cdot}44)$$

$$P_x = \cos\theta - 5{\cdot}995\sin\theta$$

FIGURE 4.5 - Shallow Clamped Arch

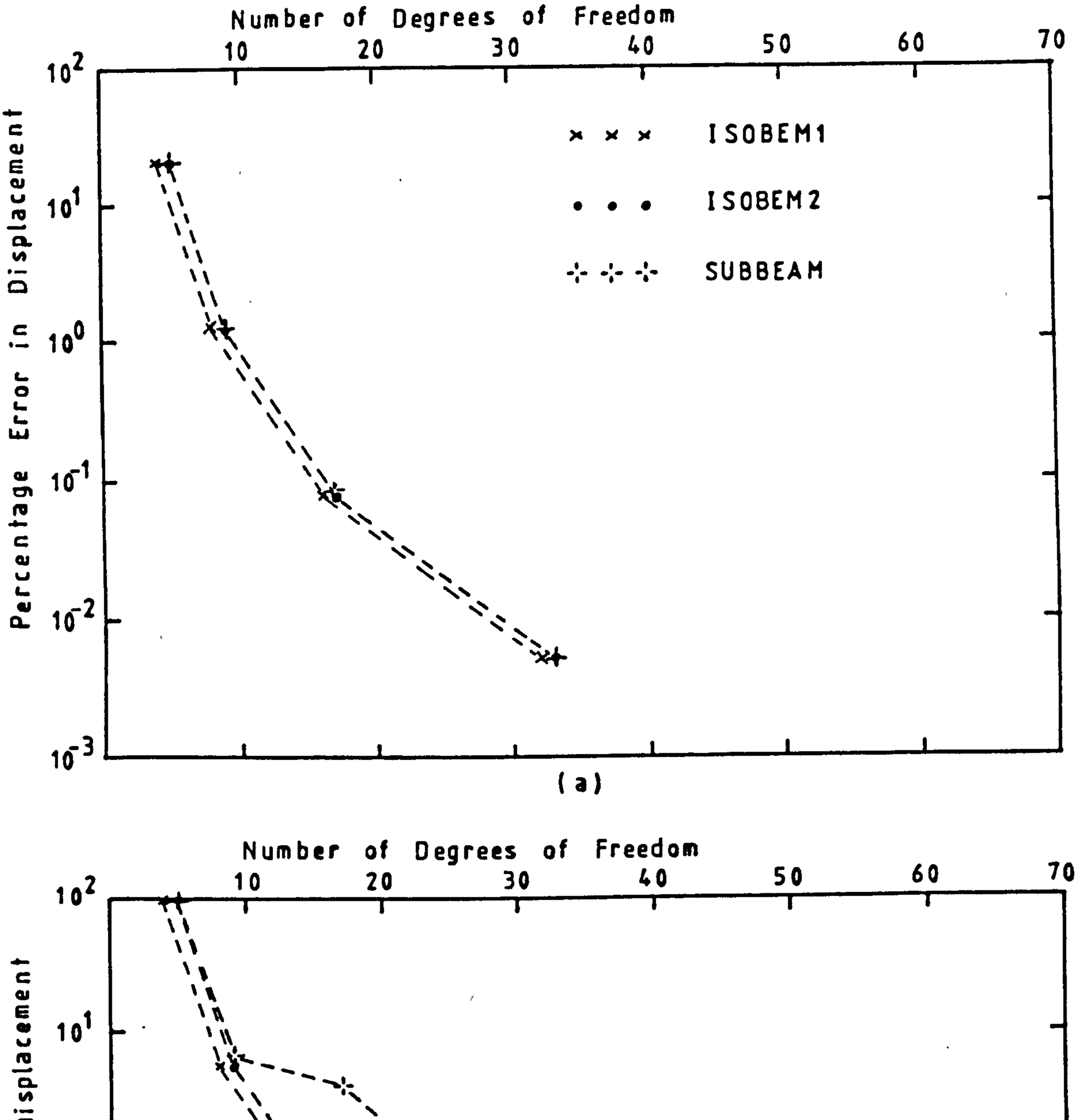

FIGURE 4.6 - Shallow Arch - Percentage Error in Displacement for Different Numbers of Elements

(a) Thick Arch

(b) Thin Arch

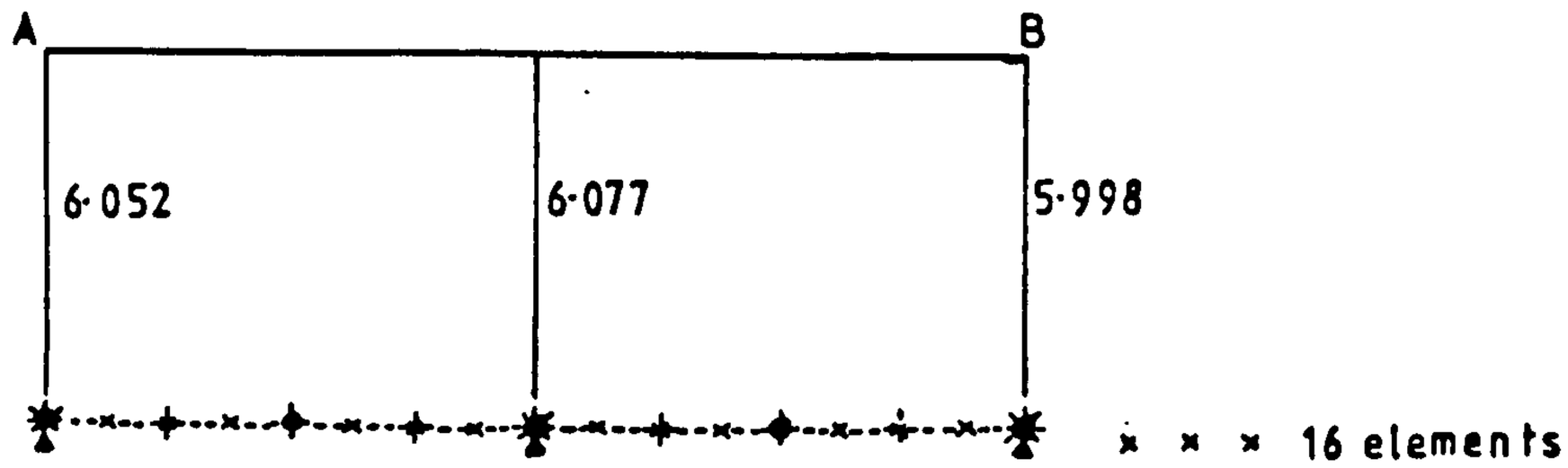

ISOBEM 1

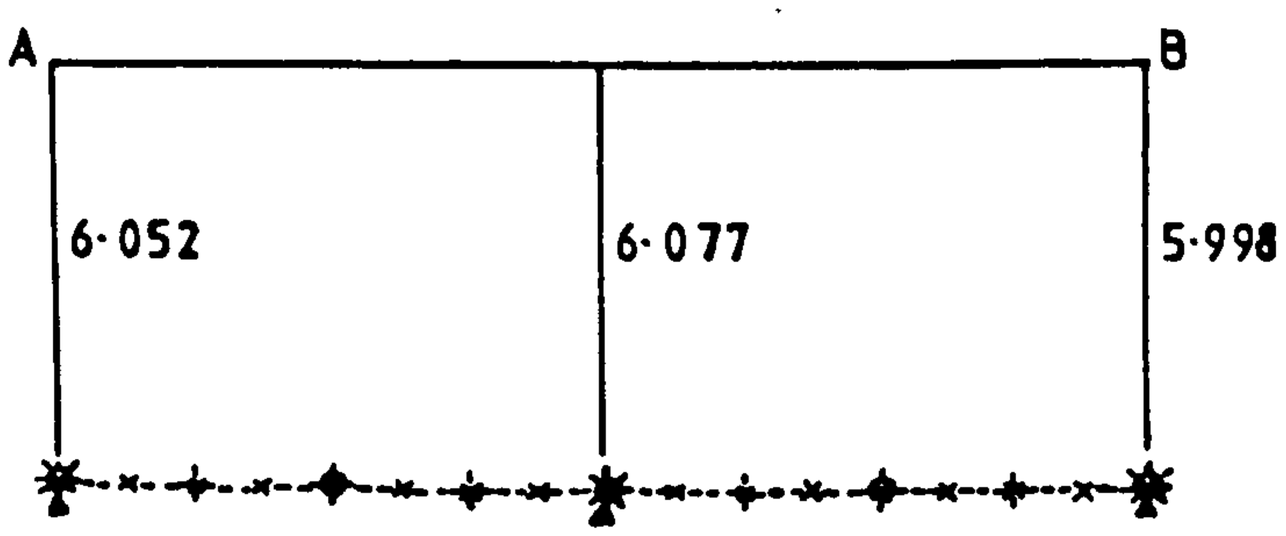

ISOBEM 2

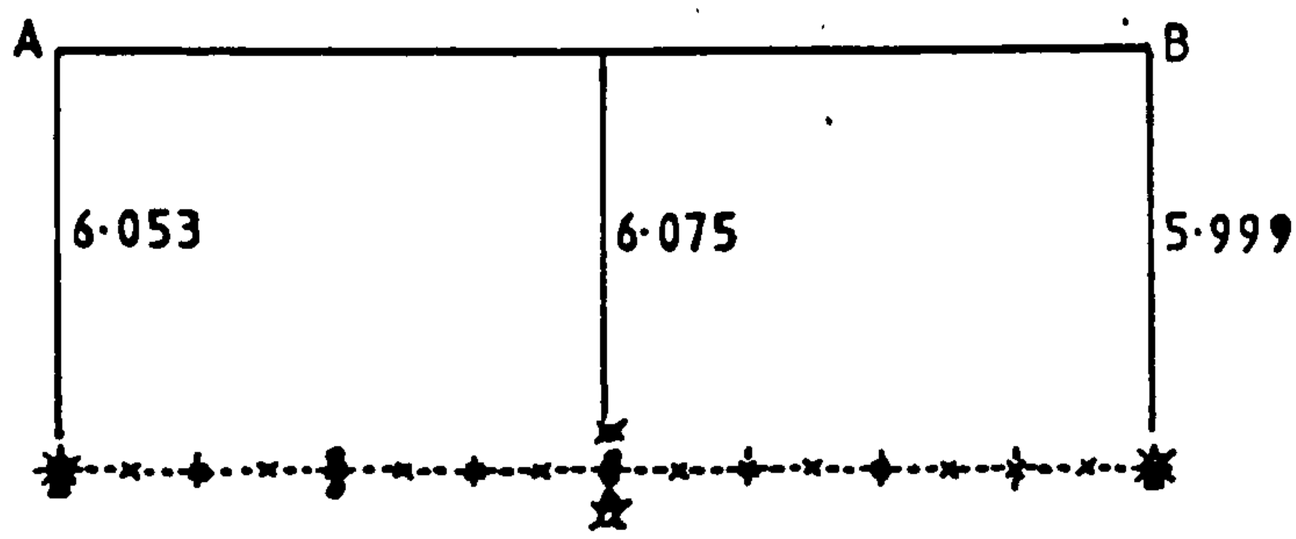

SUBBEAM

FIGURE 4.7a - Thick Shallow Arch - Variation of Axial Force along Length

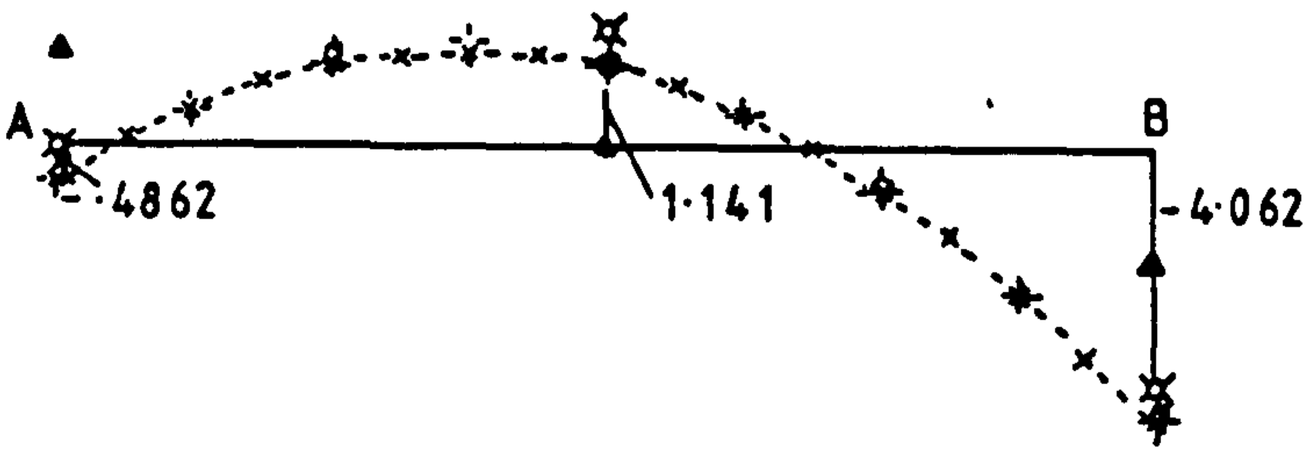

ISOBEM 1

× × × 16 elements

-⊹- -⊹- -⊹- 8 elements

• • • 4 elements

⨯ ⨯ ⨯ 2 elements

▲ ▲ ▲ 1 element

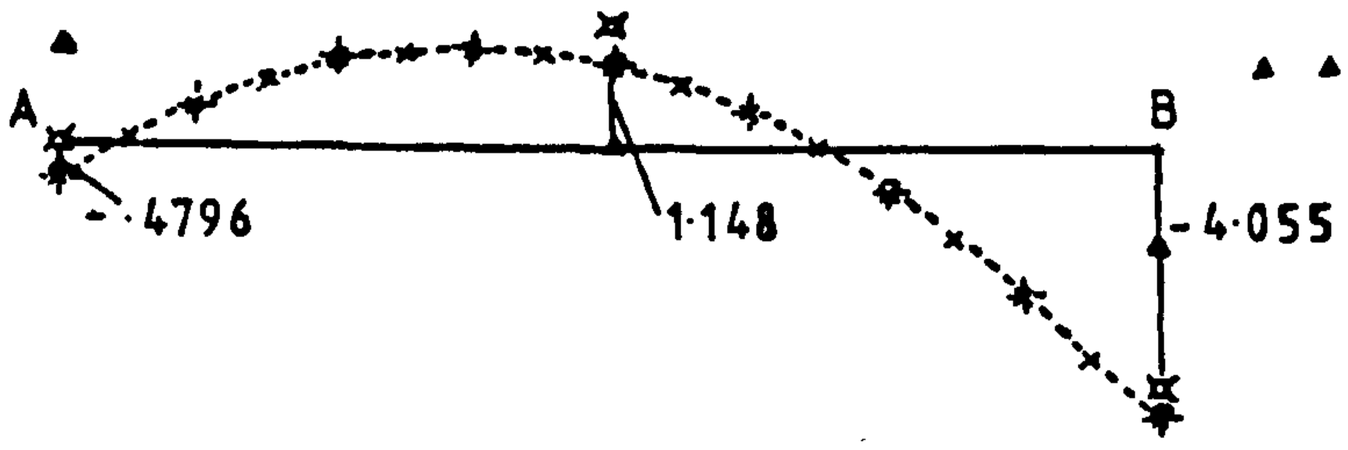

ISOBEM 2

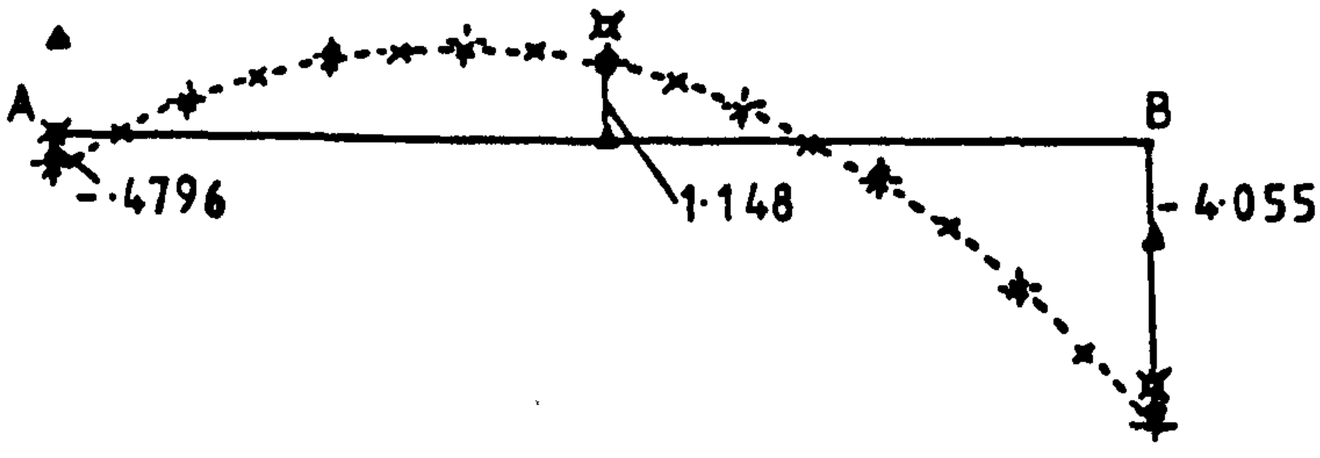

SUBBEAM

FIGURE 4.7b - Thick Shallow Arch - Variation of Bending Moment along Length

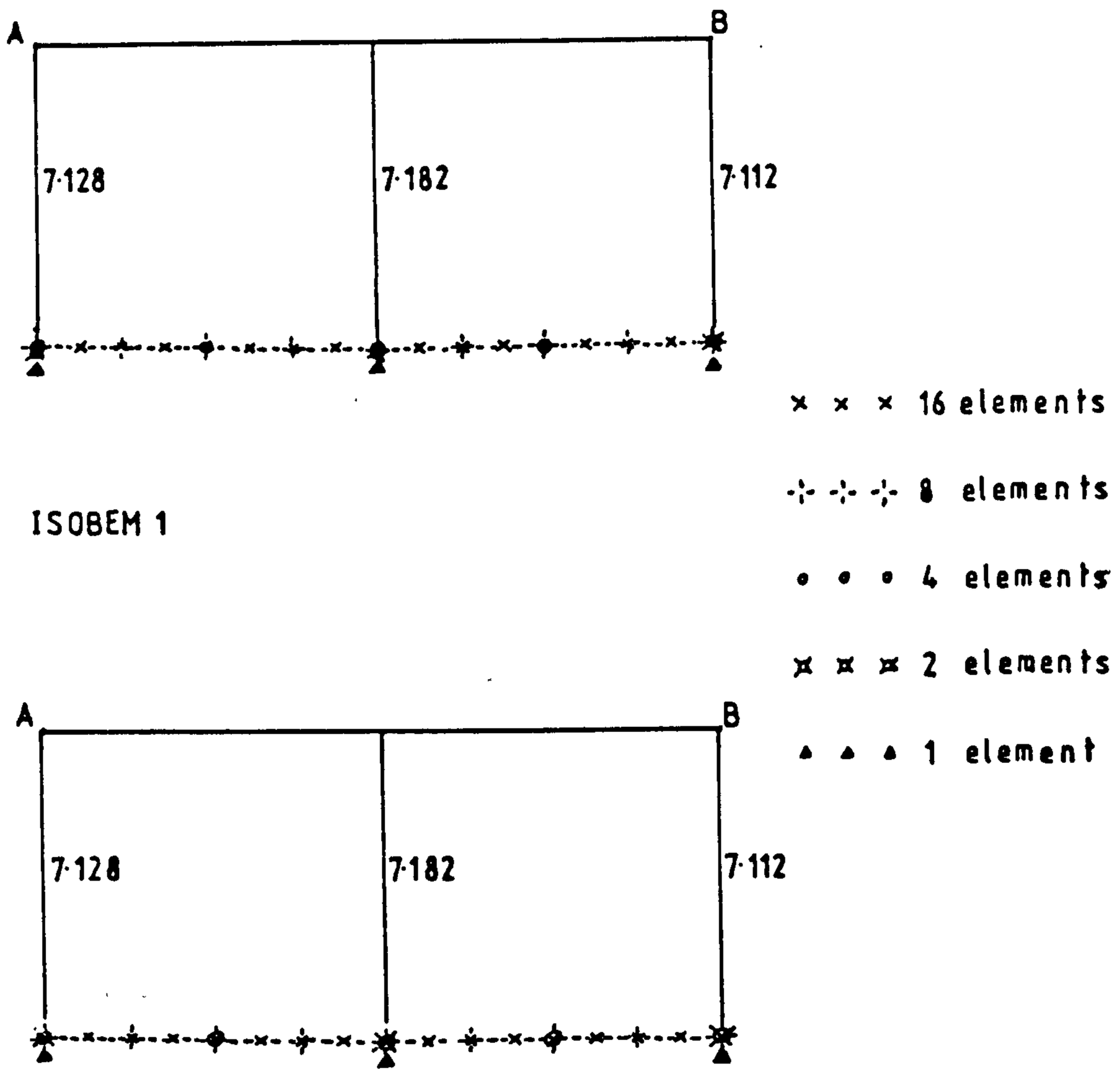

FIGURE 4.8a - Thin Shallow Arch - Variation of Axial Force along Length

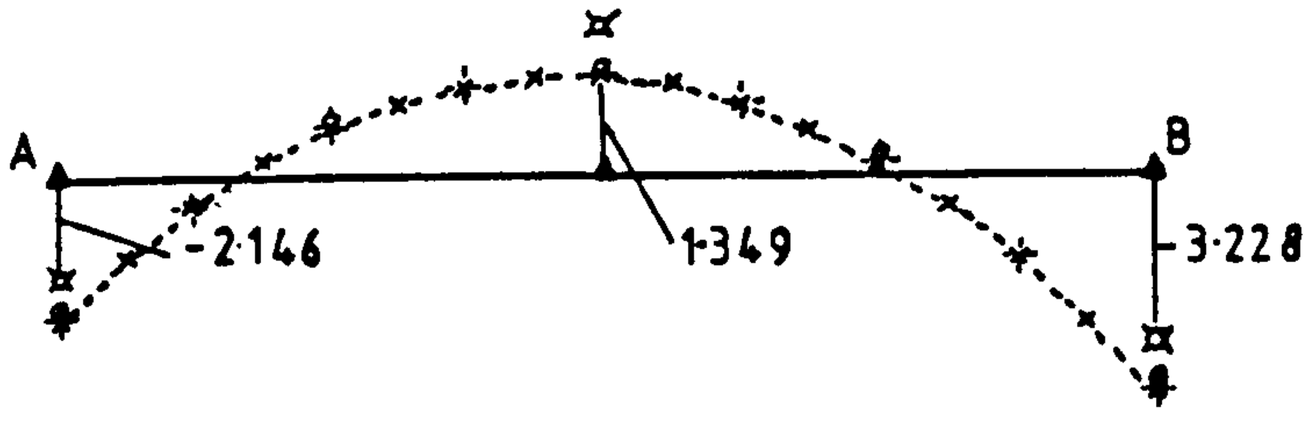

ISOBEM 1

× × × 16 elements

⊹ ⊹ ⊹ 8 elements

• • ○ 4 elements

✕ ✕ ✕ 2 elements

▲ ▲ ▲ 1 element

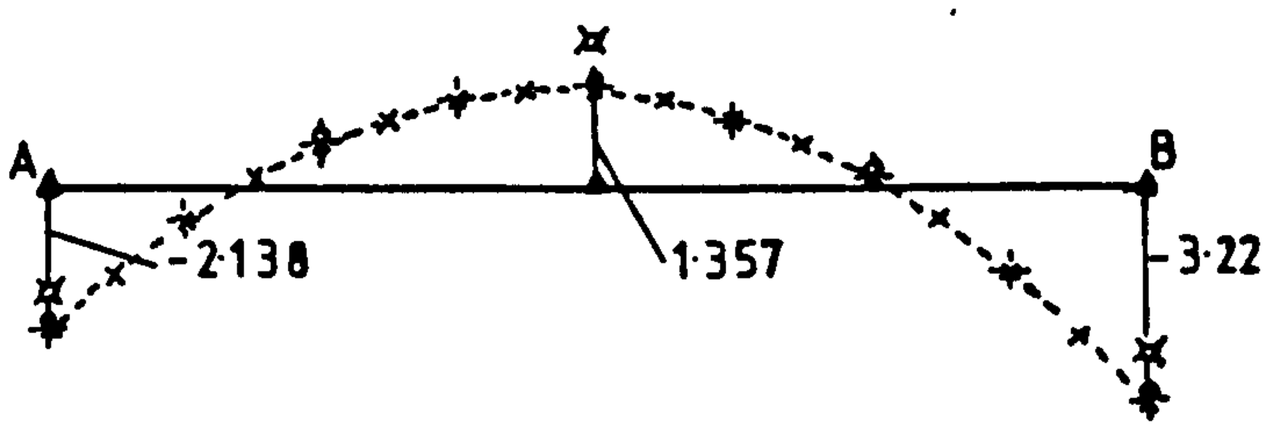

ISOBEM 2

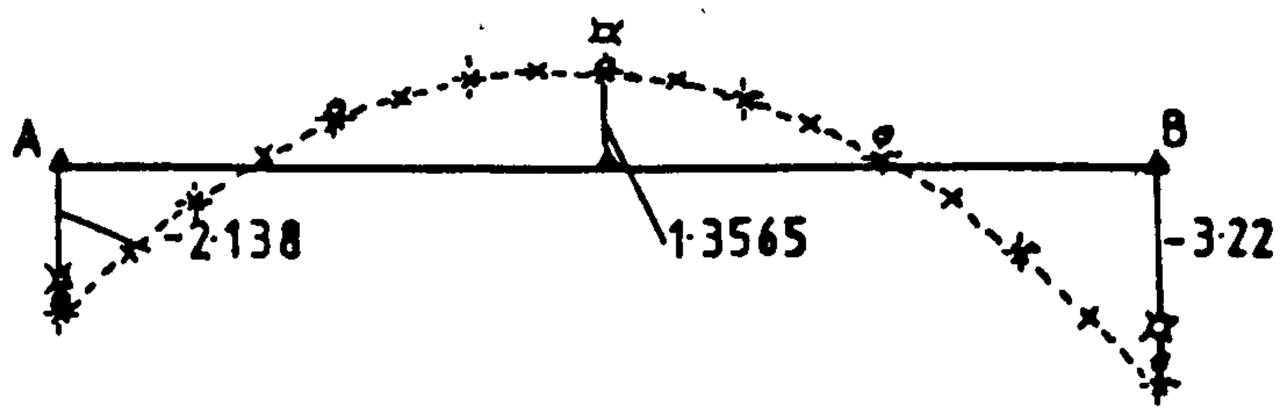

SUBBEAM

FIGURE 4.8b - Thin Shallow Arch - Variation of Bending Moment along Length

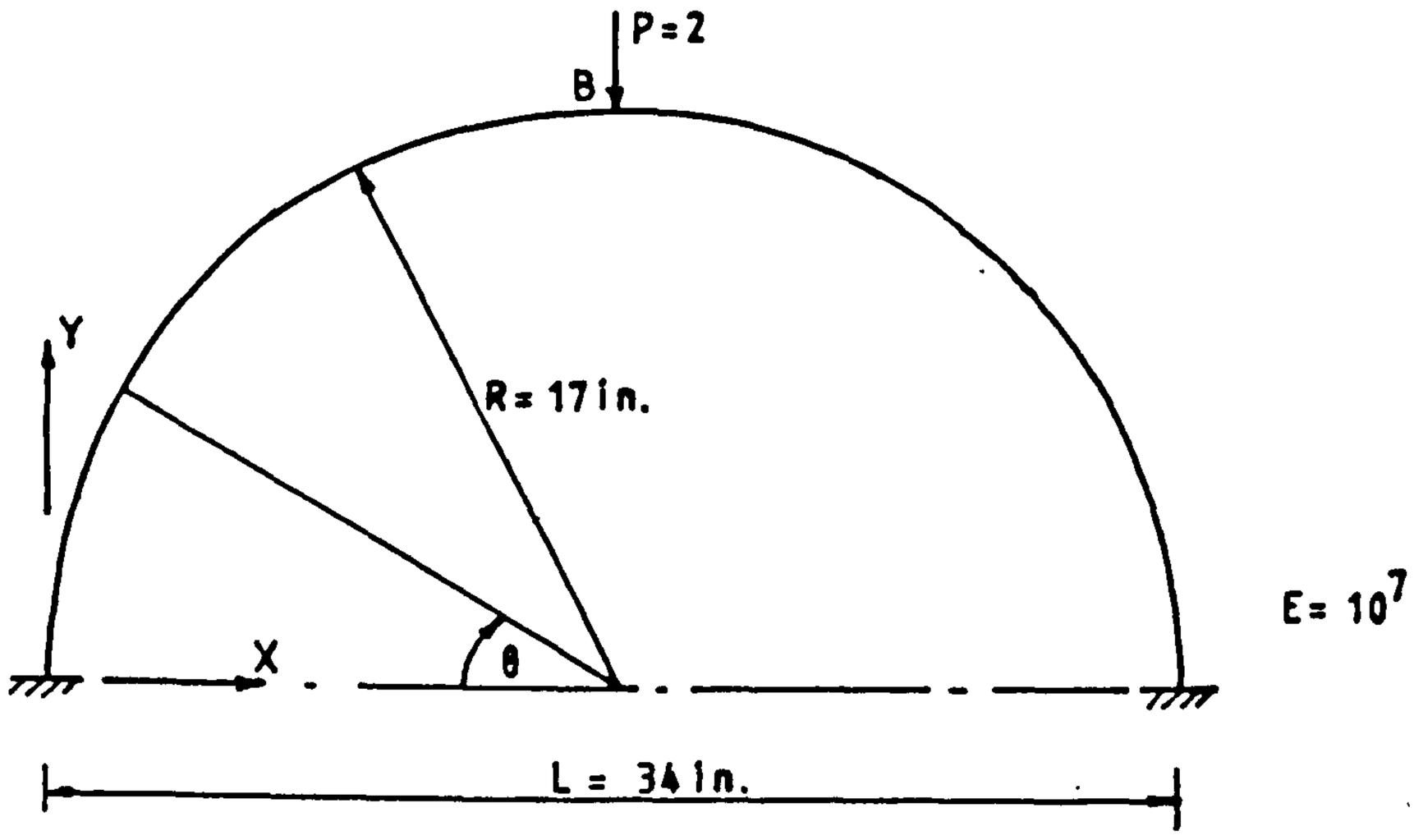

Ref.[8]:

$H_A = 0.4591P$, $V_A = 0.5P$, $M_A = .0553L \times P$

$M_x = -3.7604 - 17 \times (1 - \cos\theta) + .9182 \times 17 \sin\theta$

$P = -\cos\theta - .9182 \sin\theta$

FIGURE 4.9 – Deep Clamped Arch

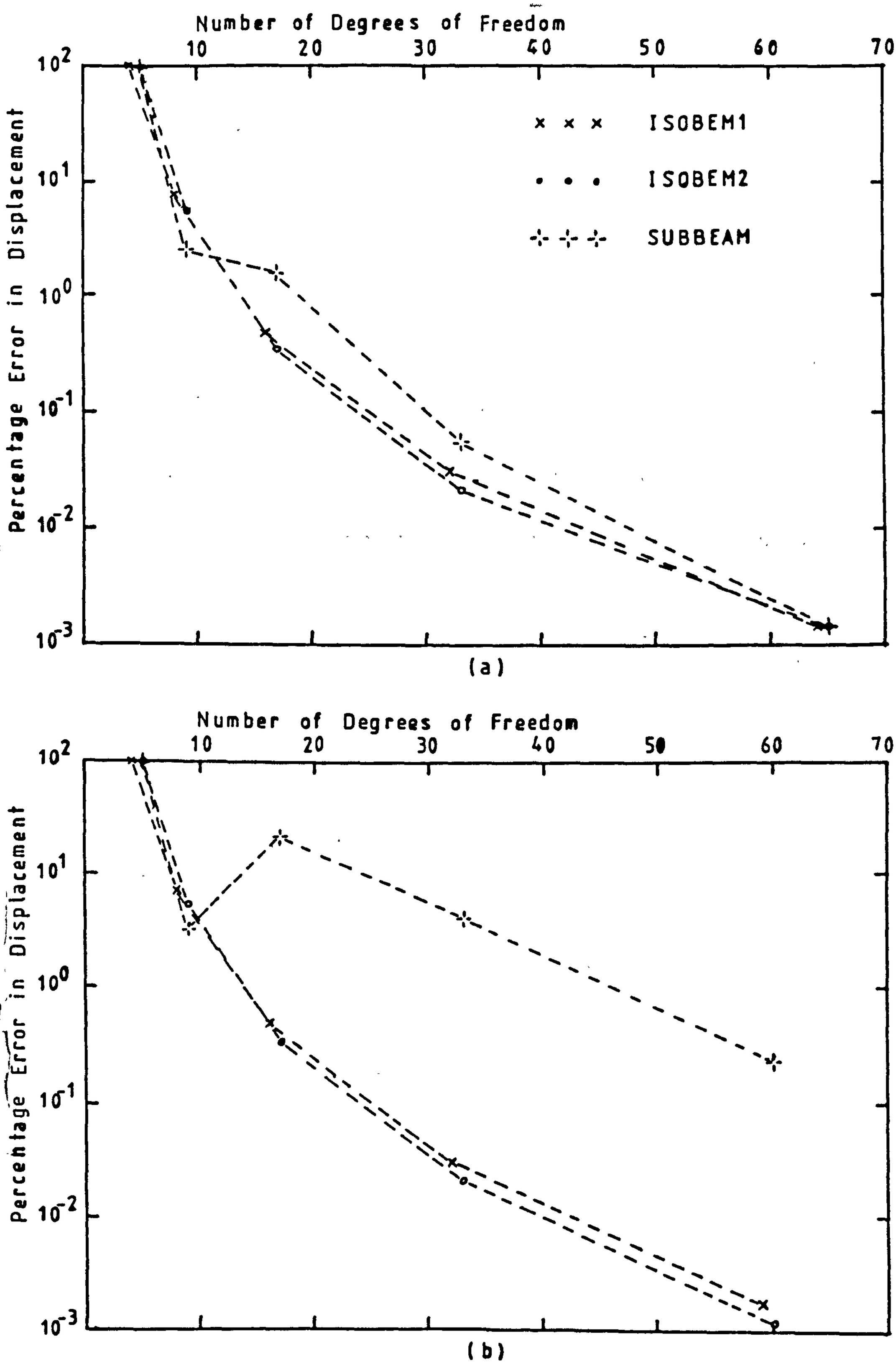

FIGURE 4.10 - Deep Arch - Percentage Error in Displacement for Different Numbers of Elements

(a) Thick Arch

(b) Thin Arch

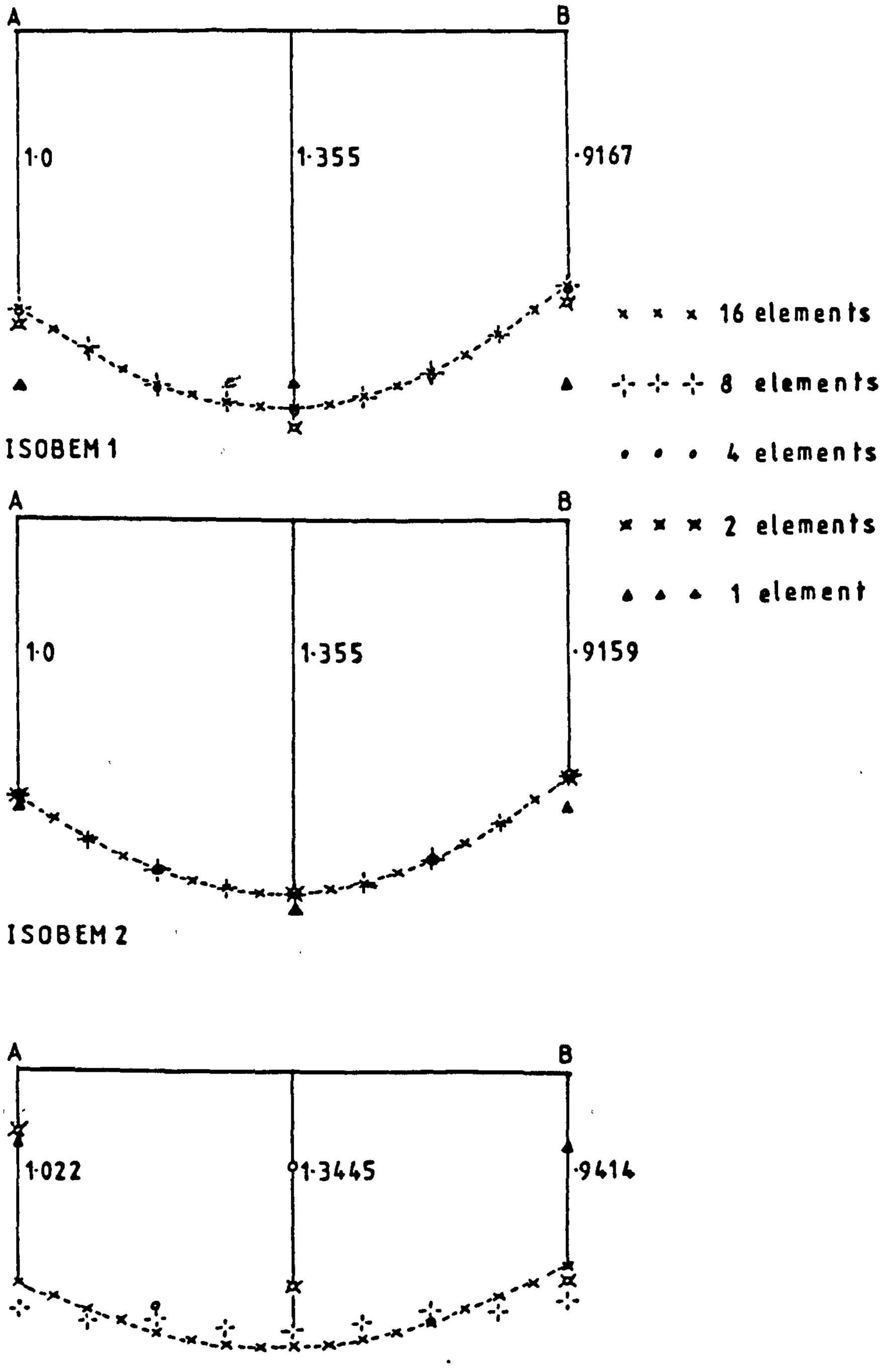

FIGURE 4.11a - Thick Deep Arch - Variation of Axial Force along Length

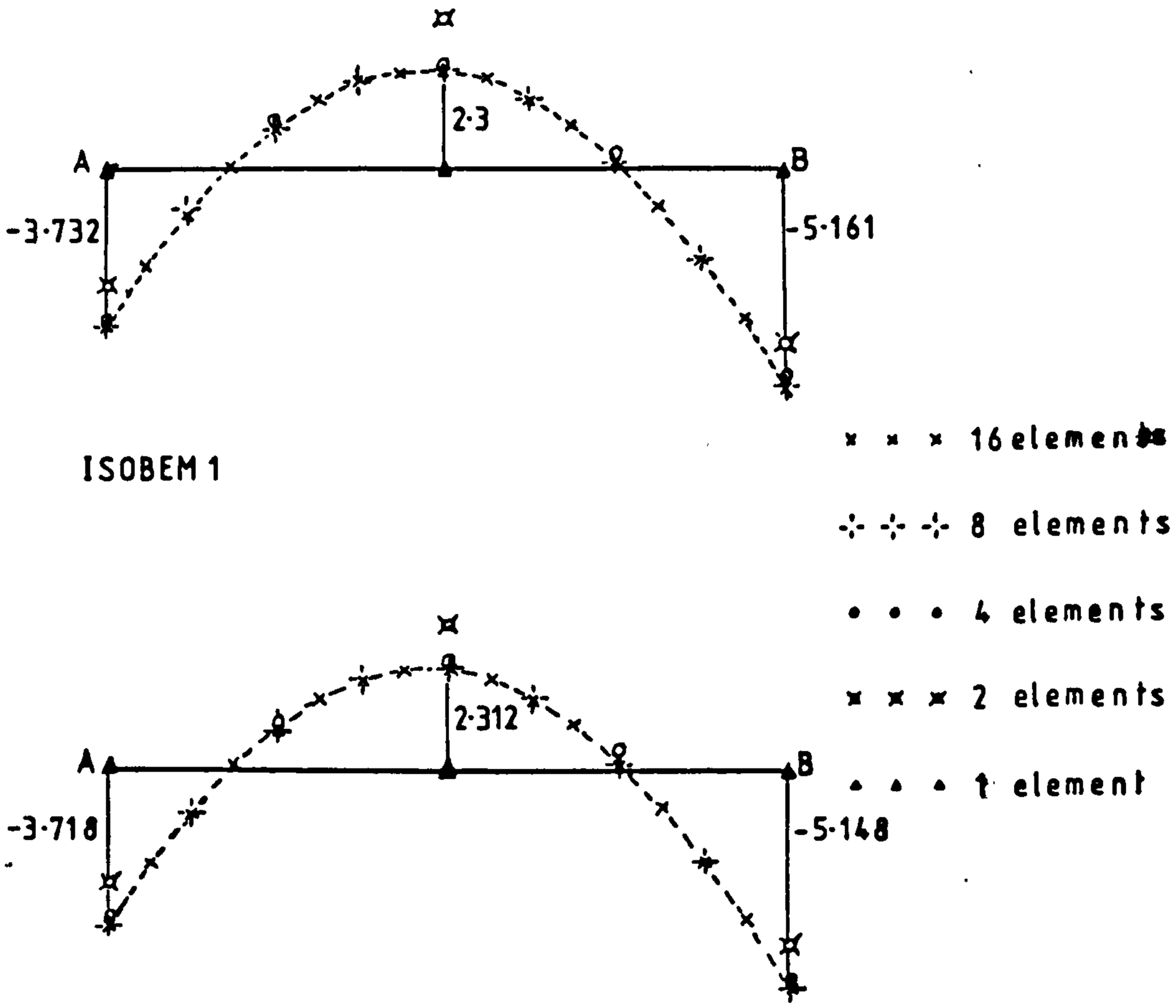

FIGURE 4.11b - Thick Deep Arch - Variation of Bending Moment along Length

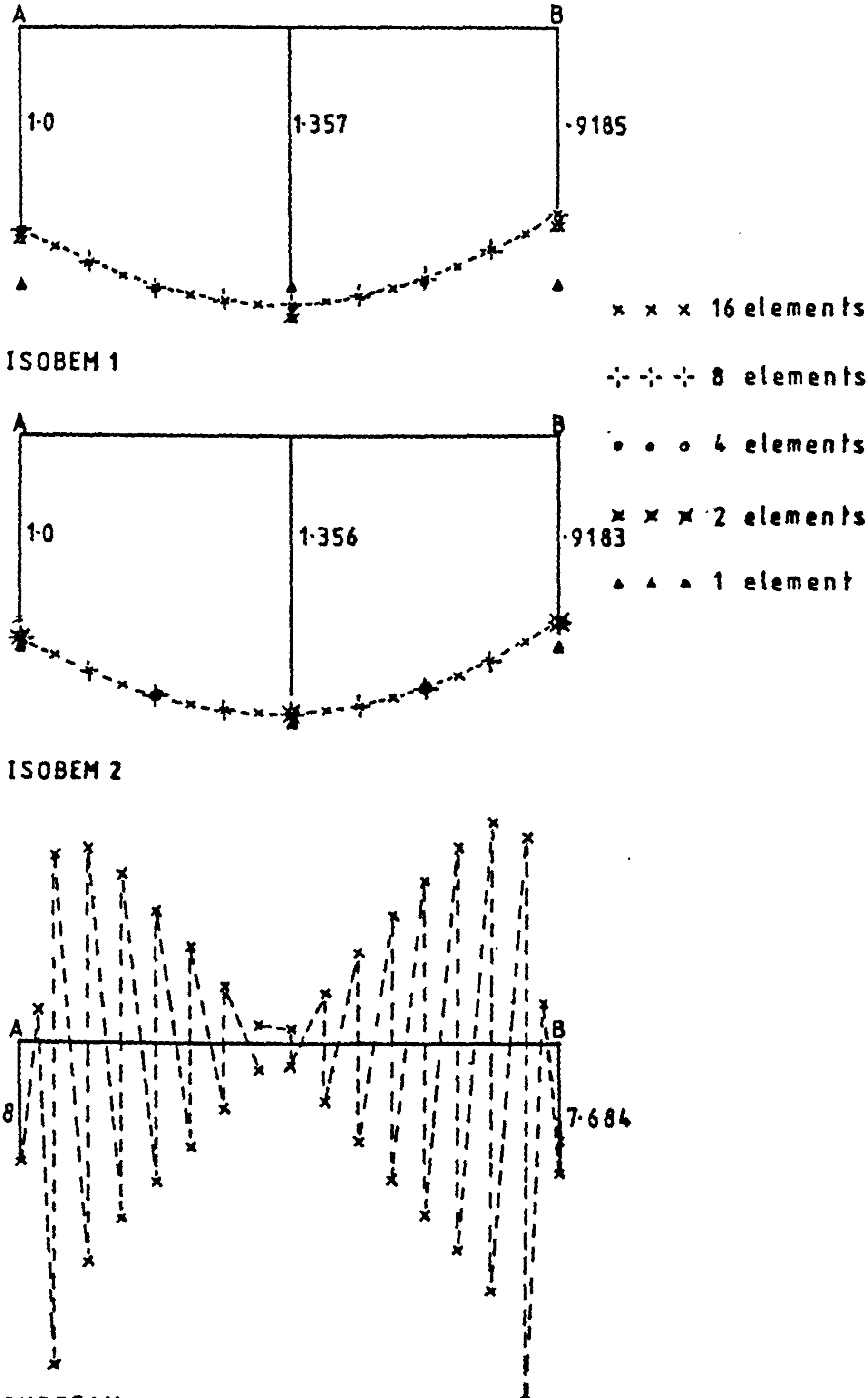

FIGURE 4.12a - Thin Deep Arch - Variation of Axial Force along Length

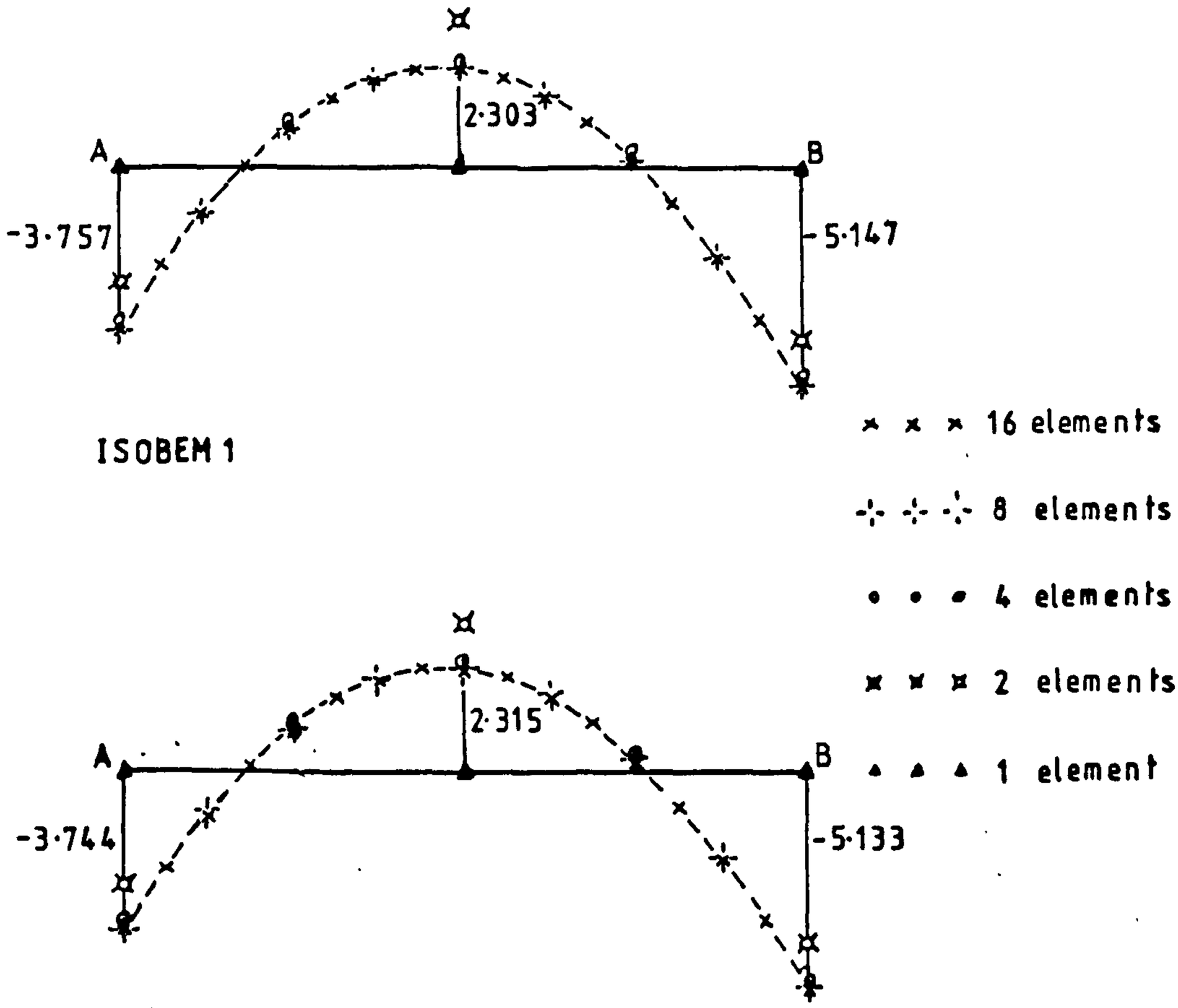

FIGURE 4.12b - Thin Deep Arch - Variation of Bending Moment along Length

$\frac{PL^2}{EI}$	V/L					$\frac{L-U}{L}$					2θ/π			
	TLG	TLC	UTLG	ULG	Ref(79)	TLG	TLC	UTLG	ULG	Ref(79)	TLG	TLC	UTLG	ULG
1	.3135	.2923	.2972	.3021	.302	.9386	.9474	.9453	.9438	.944	.2963	.2735	.2886	.2954
2	.5454	.4782	.4857	.4936	.494	.7940	.8510	.8450	.8399	.840	.5030	.4346	.4880	.4990
3	.6283	.6045	.5969	.6035	.603	.5699	.7432	.7524	.7463	.745	.5002	.5378	.6181	.6288
4	.7160	.7050	.6655	.6704	.670	.5021	.6035	.6774	.6719	.671	.5868	.6190	.7055	.7148
5	.7344	.7485	.7108	.7145	.714	.4974	.5033	.6179	.6132	.612	.5586	.6373	.7667	.7747
6	.7352	.7713	.7426	.7454	.744	.2919	.4567	.5702	.5662	.566	.4878	.6374	.8111	8183
7	.7696	.7884	.7662	.7684	.767	.2869	.4230	.5312	.5277	.528	.5385	.6375	.8445	.8510
8	.7749	.8031	.7844	.7862	.785	.3206	.3928	.4988	.4958	.496	.5101	.6376	.8702	.8762
9	.8016	.8101	.7989	.8004	.799	.3083	.3745	.4714	.4688	.469	.5561	.6376	.8904	.8960
10	.8420	.8265	.8108	.8121	.811	.2540	.3576	.4479	.4456	.445	.5903	.6377	.9065	.9118

TABLE 4.4 Cantilever under Point Loat at Free End

ISOBEM 1 Results.

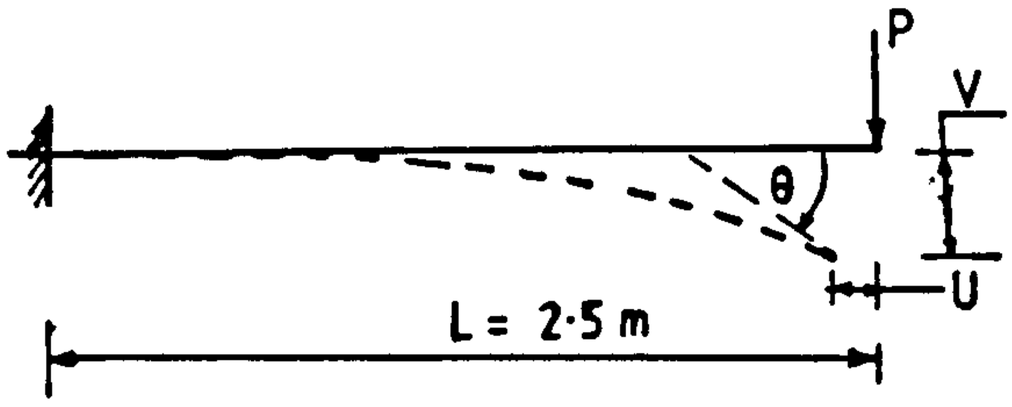

EI = 16666 KN-m^2

EA 2×10^7 KN

16 elements

40 load increments

FIGURE 4.13 - Cantilever under Vertical Load at Free End - ISOBEM 1 Resutls

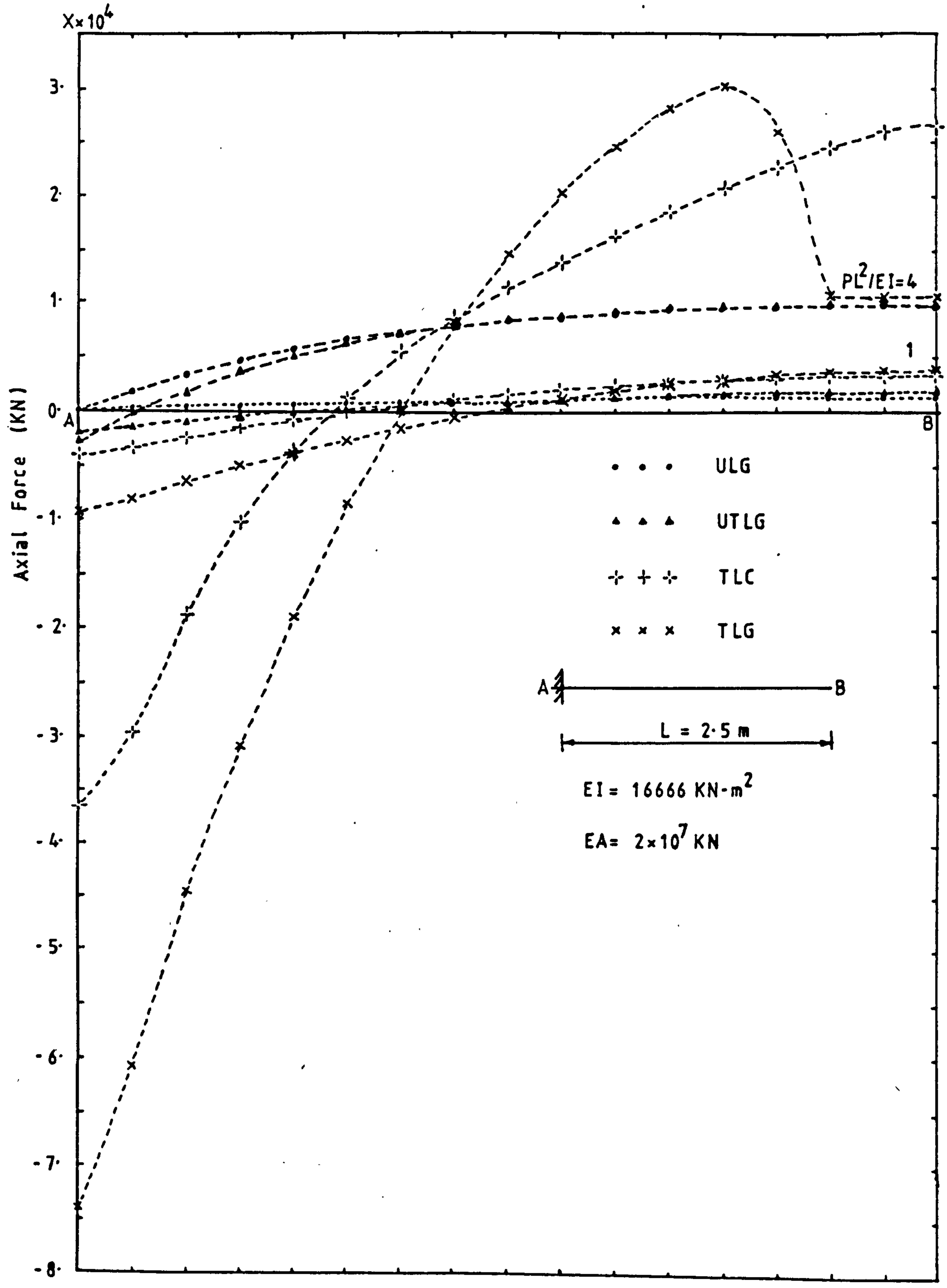

FIGURE 4.14a - Cantilever under Vertical Load at Free End - Variation of Axial Force along Length - ISOBEM 1 Resutls (average nodal values)

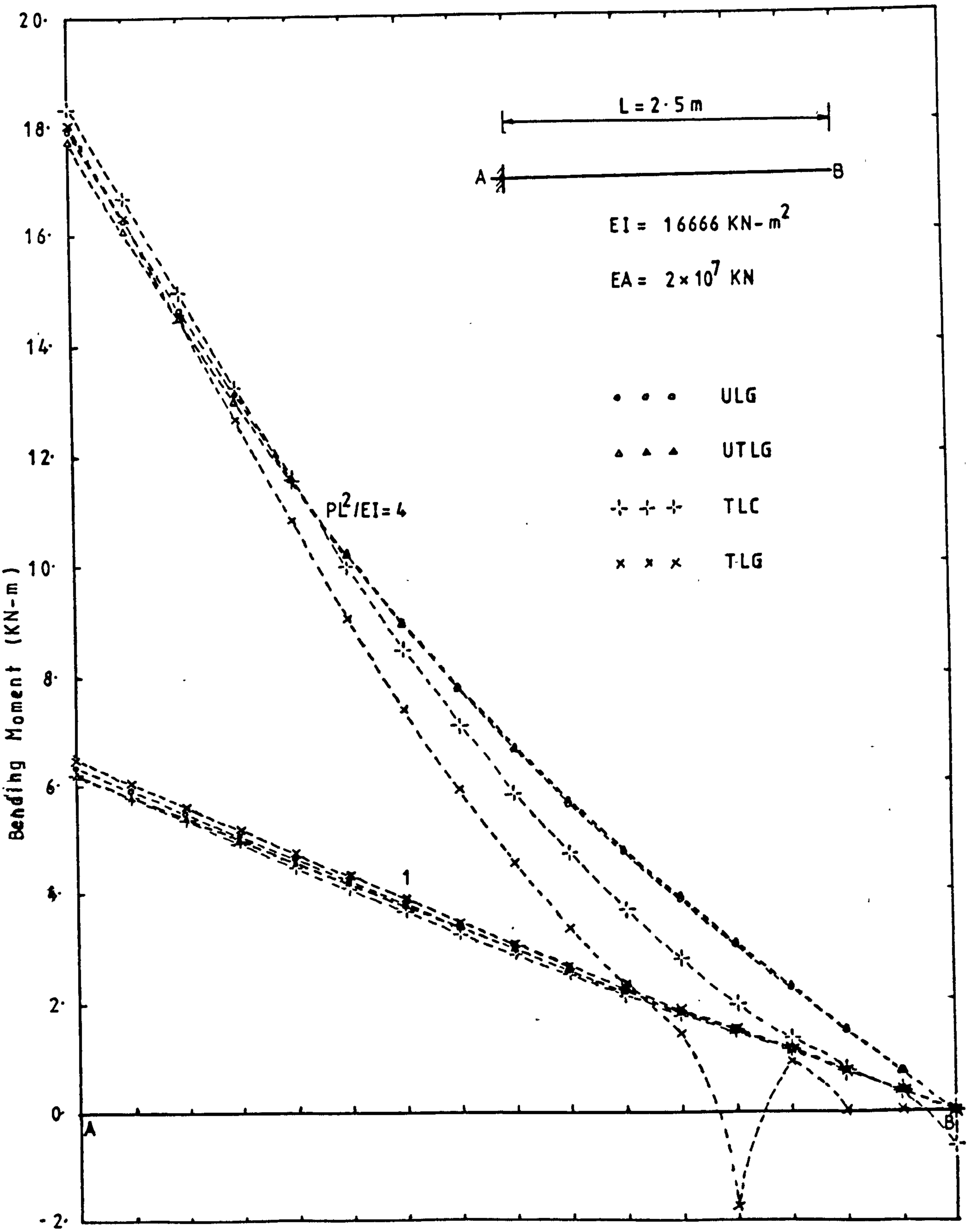

FIGURE 4.14b - Cintilever under Vertical Load at Free End - Approximate Theory - ISOBEM 1 Results

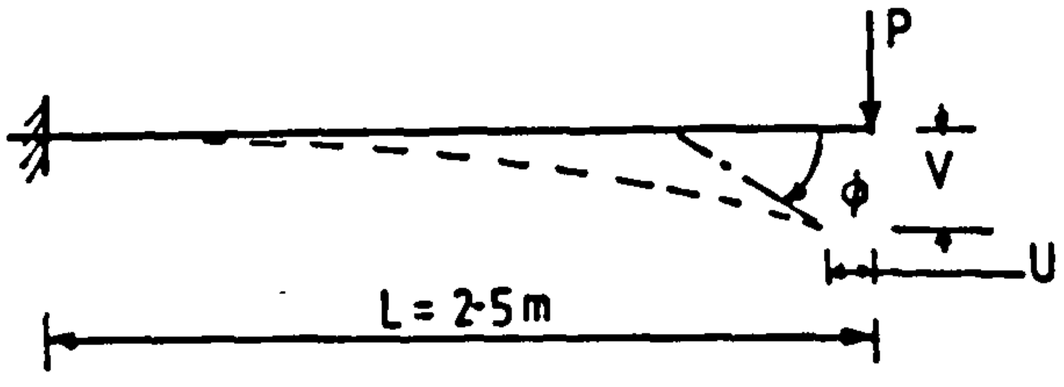

EI = 16666 KN-m²

EA = 2 × 10⁷ KN

16 elements

40 load increments

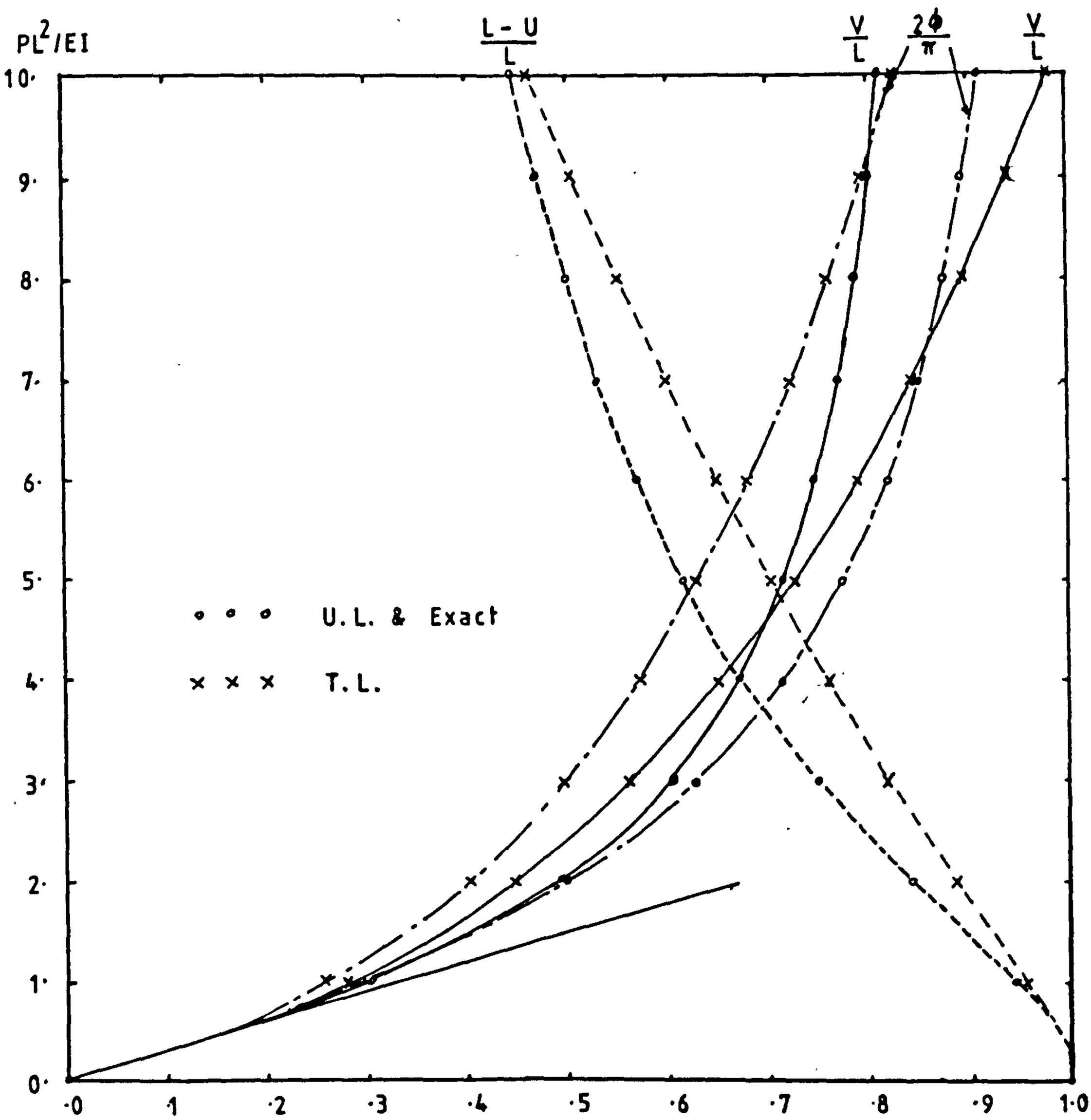

FIGURE 4.15 - Cantilever under Vertical Load at Free End - Approximate Theory - ISOBEM 1 Results

$\frac{PL^2}{EI}$	V/L					$\frac{L-U}{L}$					$2\phi/\pi$			
	TLG	TLC	UTLG	ULG	Ref(79)	TLG	TLC	UTLG	ULG	Ref(79)	TLG*	TLC*	UTLG	ULG
1	.3019	.3018	.3018	.3009	.302	.9435	.9436	.9436	.9438	.944	.2938	.2937	.2931	.2939
2	.4939	.4936	.4936	.4928	.494	.8390	.8394	.8394	.8399	.840	.4979	.4976	.4969	.4983
3	.6040	.6035	.6035	.6029	.603	.7448	.7457	.7456	.7462	.745	.6278	.6273	.6269	.6287
4	.6709	.6703	.6703	.6699	.670	.6700	.6713	.6711	.6716	.671	.7134	.7128	.7130	.7150
5	.7150	.7142	.7143	.7139	.714	.6110	.6126	.6125	.6129	.612	.7727	.7721	.7729	.7751
6	.7459	.7451	.7452	.7449	.744	.5638	.5657	.5655	.5659	.566	.8152	.8146	.8164	.8187
7	.7689	.7680	.7681	.7678	.767	.5253	.5274	.5272	.5275	.528	.8466	.8460	.8491	.8514
8	.7866	.7857	.7858	.7856	.785	.4932	.4956	.4953	.4956	.496	.8700	.8695	.8742	.8766
9	.8009	.7999	.8000	.7998	.799	.4661	.4686	.4683	.4686	.469	.8878	.8873	.8940	.8964
10	.8126	.8116	.8117	.8115	.811	.4428	.4455	.4451	.4454	.445	.9011	.9007	.9098	.9122

* $\phi = \sin^{-1} \frac{du}{dx}$

TABLE 4.5 Cantilever under Point Load at Free End

ISOBEM 2 Results.

$\frac{PL^2}{EI}$	V/L					$\frac{L-U}{L}$					2φ/π			
	TLG	TLC	UTLG	ULG	Ref(79)	TLG	TLC	UTLG	ULG	Ref(79)	TLG*	TLC*	UTLG	ULG
1	.3019	.3026	.3018	.3009	.302	.9435	.9433	.9436	.9438	.944	.2938	.2951	.2931	.2939
2	.4939	.4944	.4936	.4928	.494	.8390	.8389	.8394	.8399	.840	.4982	.4995	.4969	.4983
3	.6040	.6041	.6035	.6029	.603	.7448	.7451	.7456	.7462	.745	.6286	.6297	.6269	.6287
4	.6710	.6707	.6703	.6699	.670	.6700	.6706	.6711	.6716	.671	.7150	.7160	.7130	.7150
5	.7150	.7146	.7143	.7139	.714	.6110	.6120	.6125	.6129	.612	.7754	.7764	.7729	.7751
6	.7459	.7454	.7452	.7449	.744	.5638	.5651	.5655	.5659	.566	.8195	.8205	.8165	.8187
7	.7689	.7683	.7681	.7678	.767	.5253	.5268	.5272	.5275	.528	.8528	.8540	.8491	.8514
8	.7866	.7860	.7858	.7856	.785	.4932	.4950	.4953	.4956	.496	.8789	.8802	.8742	.8766
9	.8009	.8001	.8000	.7998	.799	.4661	.4680	.4683	.4686	.469	.8998	.9013	.8940	8964
10	.8126	.8118	.8117	.8115	.811	.4428	.4449	.4451	.4454	.445	.9171	.9189	.9098	.9122

* = $\sin^{-1} \frac{dv}{dx}$

TABLE 4.6 Cantilever under Point load at Free End

SUBBEAM Result.

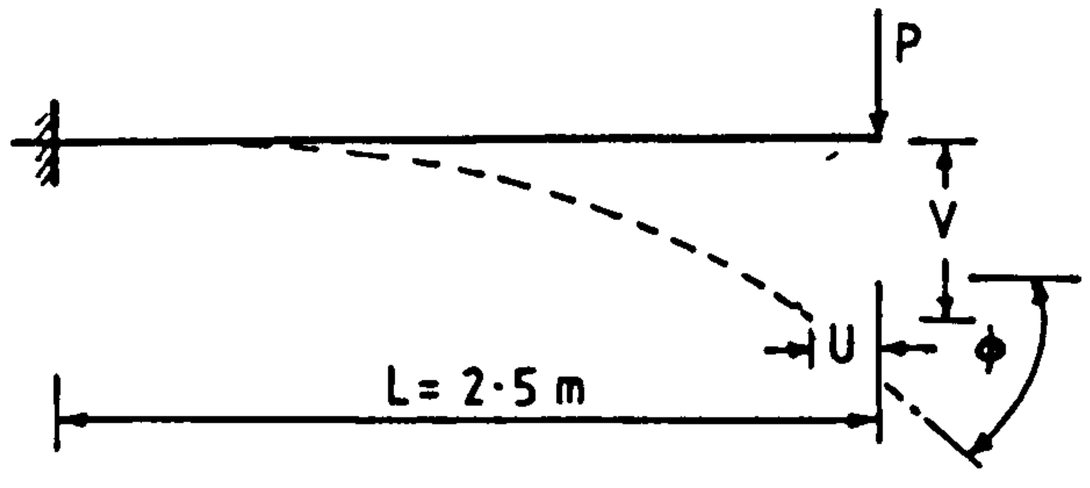

EI = 16666 KN-m^2

EA = 2×10^7 KN

16 elements

40 load increments

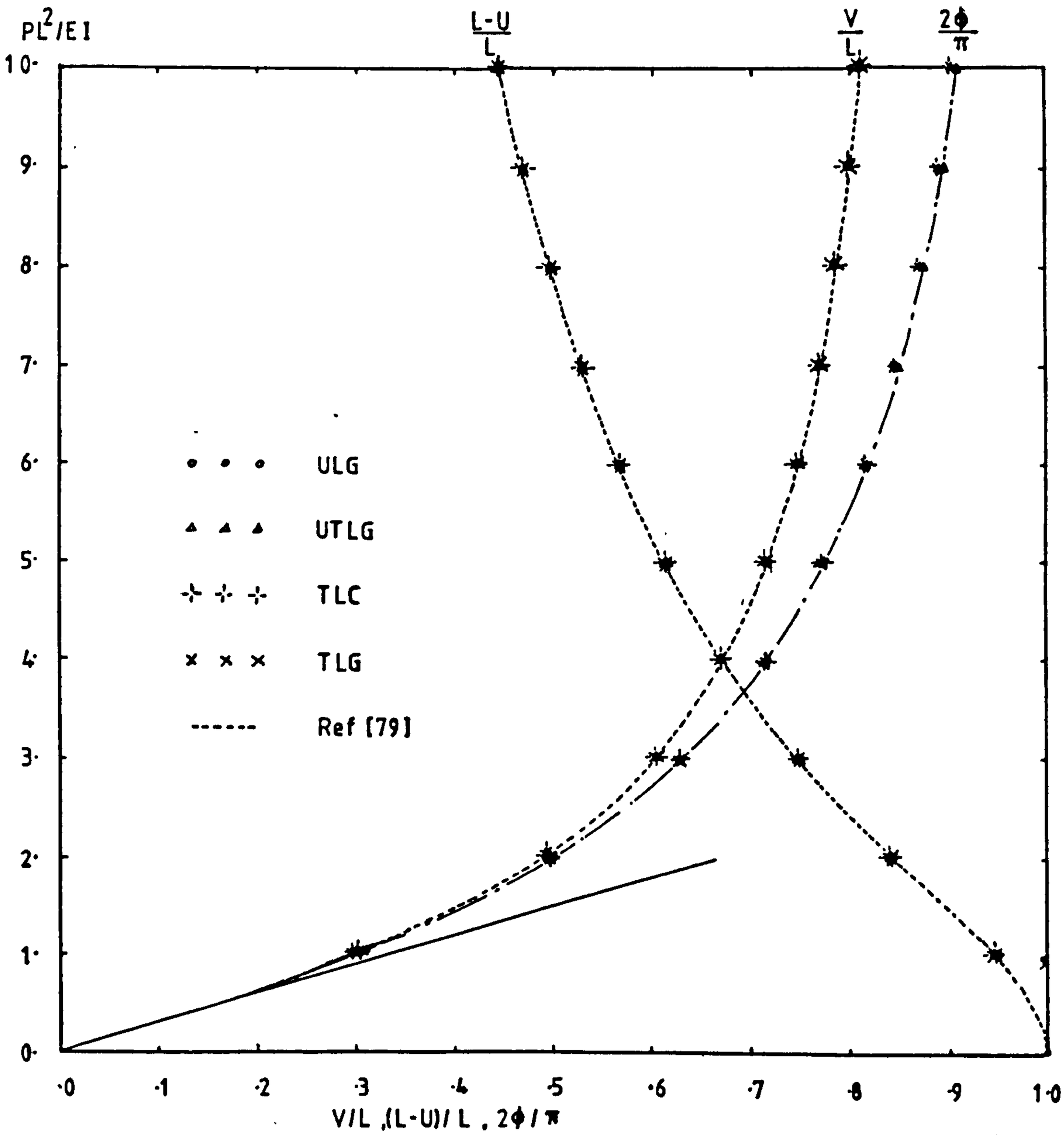

FIGURE 4.16 - Cantilever under Vertical Load at Free End - ISOBEM 2 Resutls

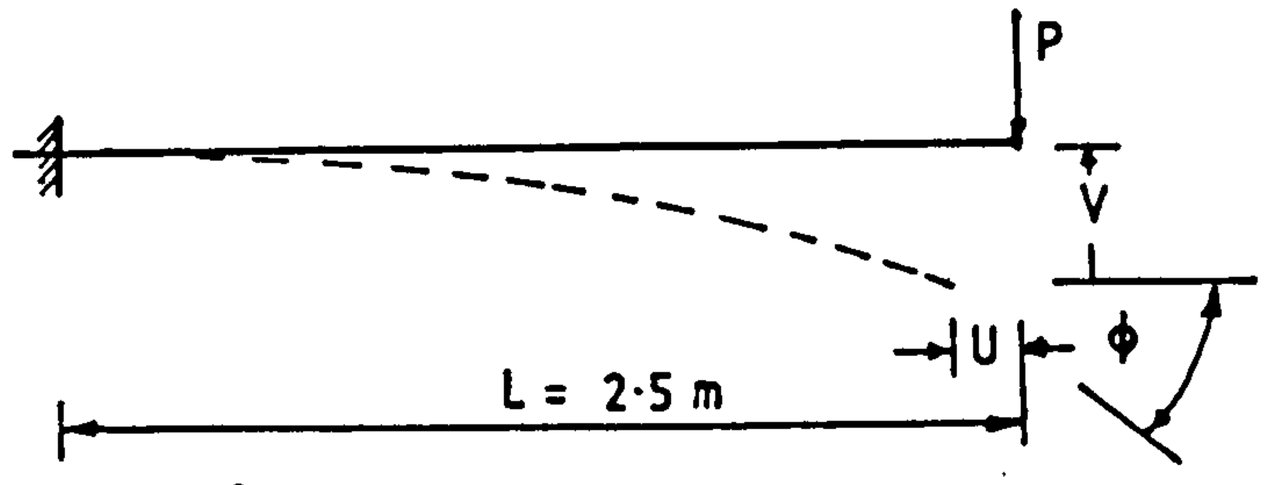

EI = 16666 KN-m^2 16 elements

EA= 2×10^7 KN 40 load increments

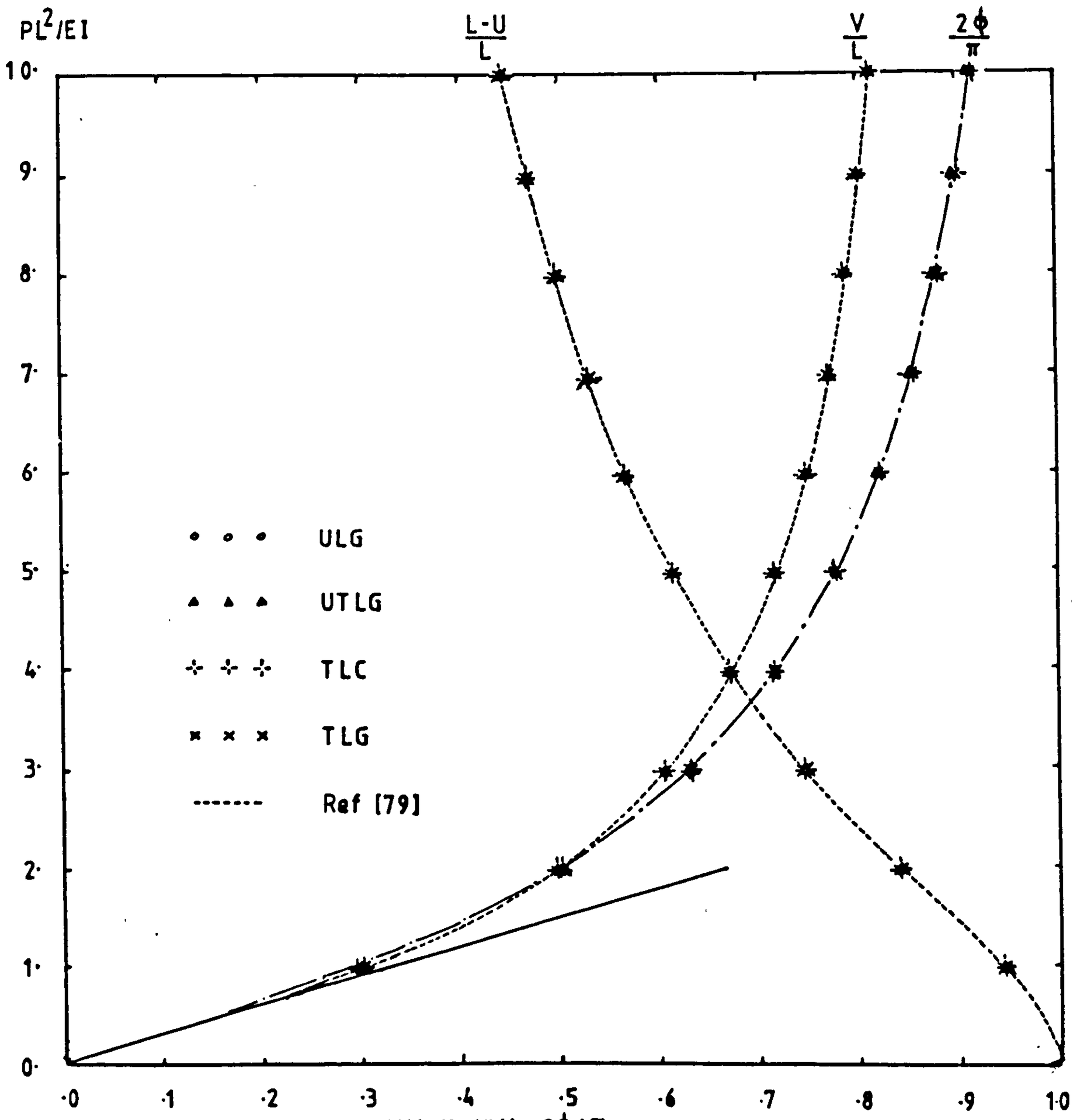

FIGURE 4.17 - Cantilever under Vertical Load at Free Eng - SUBBEAM Results

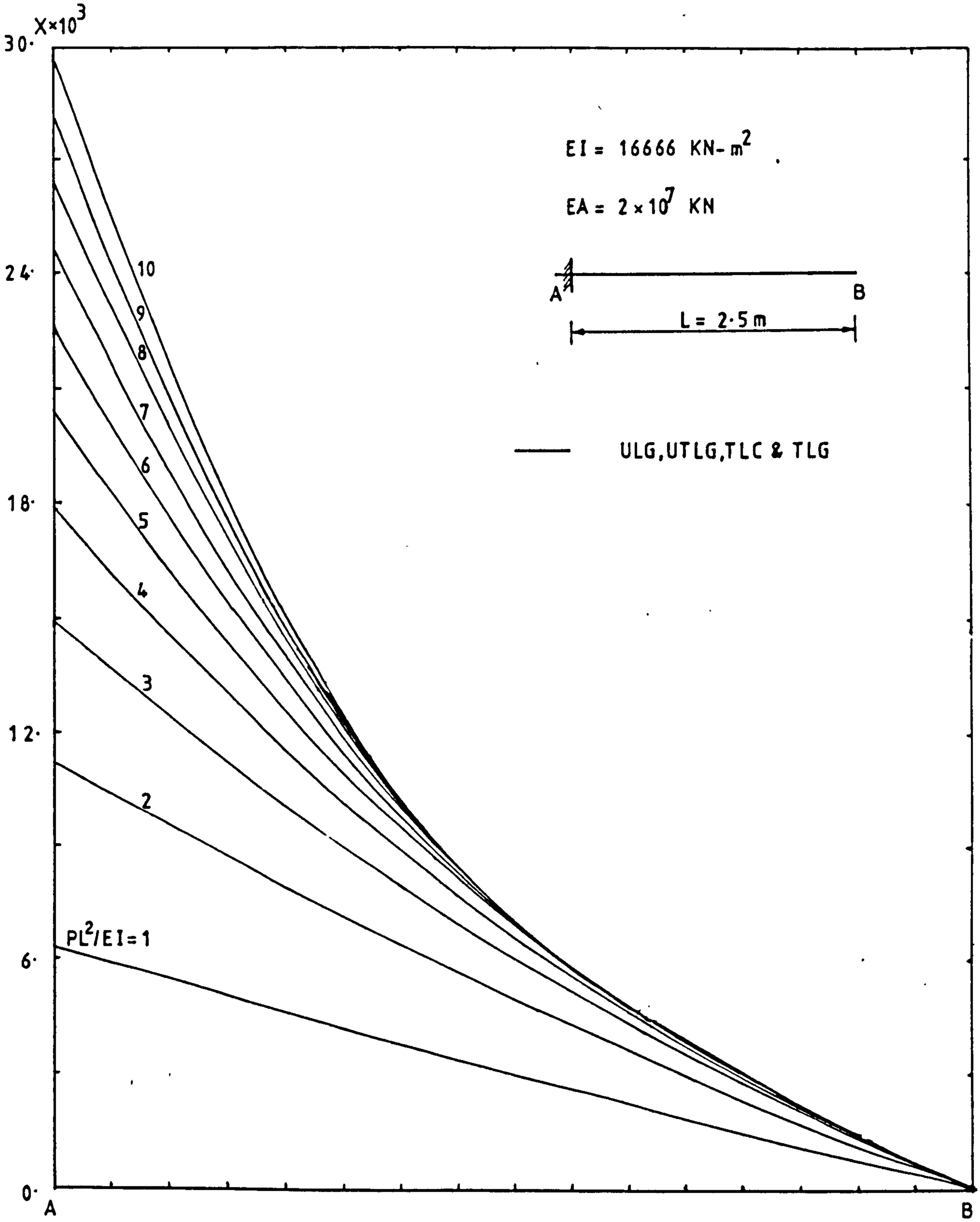

FIGURE 4.18a - Cantilever under Vertical Load at Free End - Variation of Bending Moment along Length - ISOBEM 2 (SUBBEAM) Results

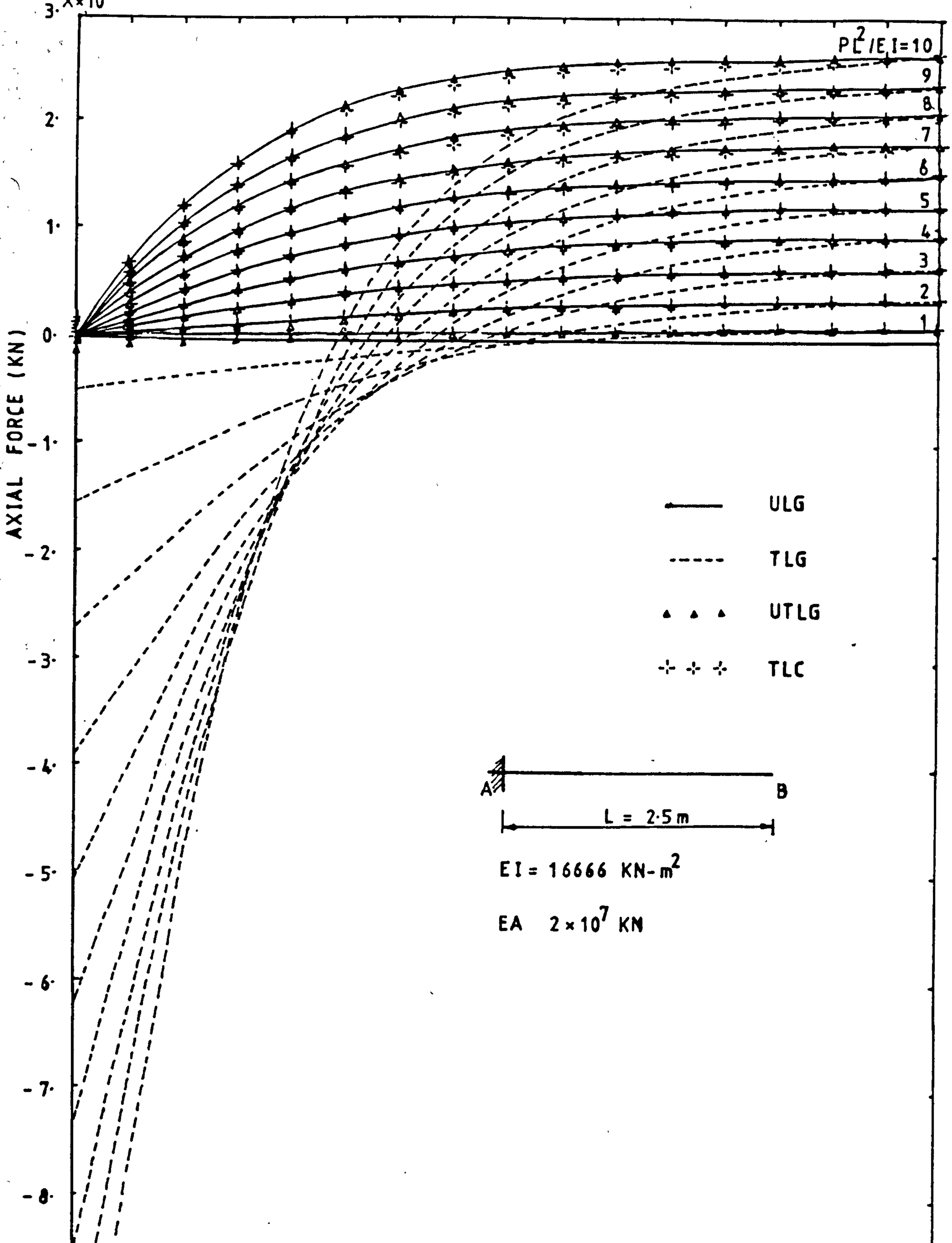

FIGURE 4.18b - Cantilever under Vertical Load at Free End - Variation of Axial Force along Length - ISOBEM 2 (SUBBEAM) Results

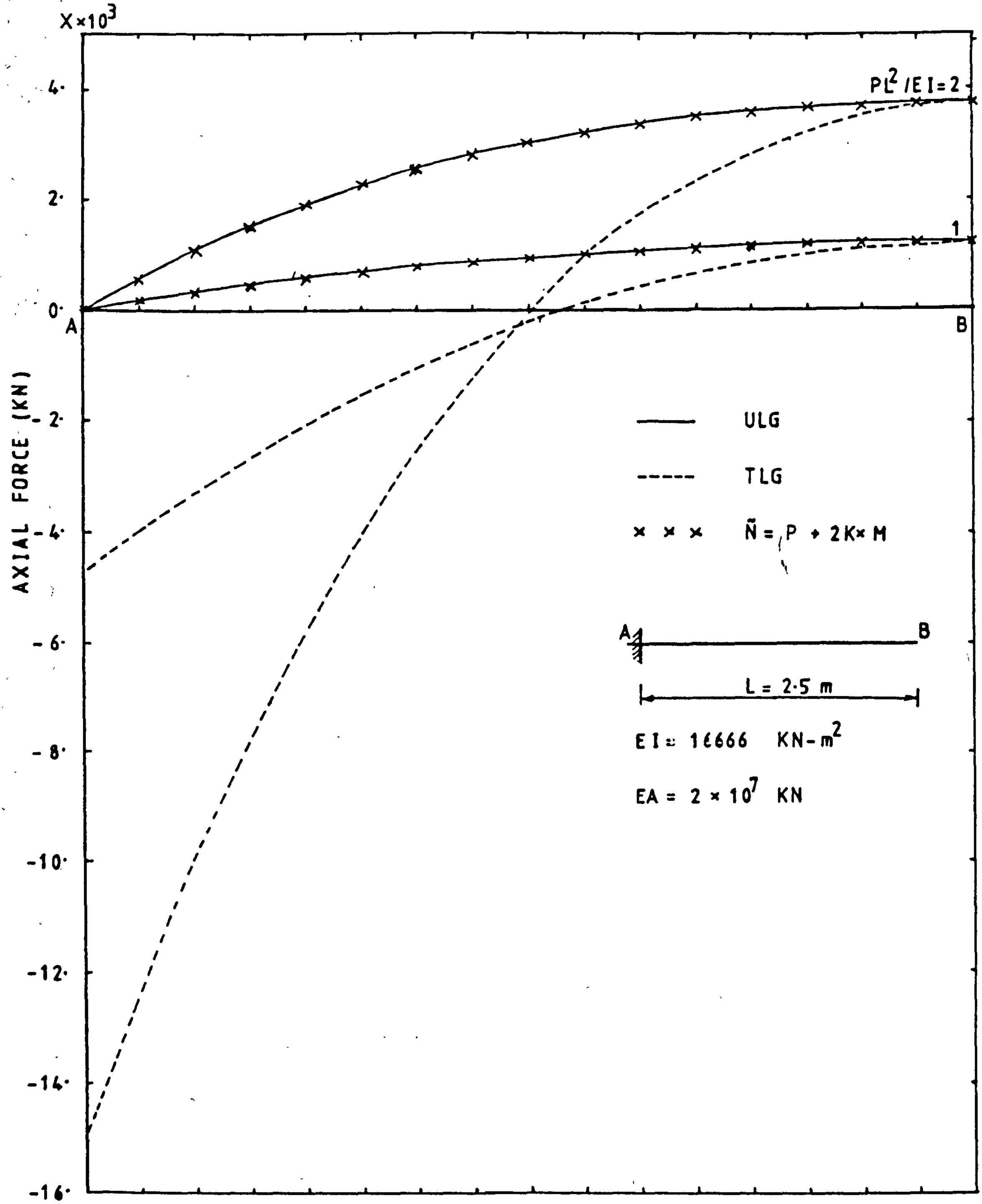

FIGURE 4.19 - Cantilever under Vertical Load at Free End - Variation of Axial Force along Length - Comparison with Calculated $\tilde{N}$ (Equation (2.26))

$EI = 16666 \quad KN\text{-}m^2$

$EA = 2 \times 10^7 \quad KN$

16 elements

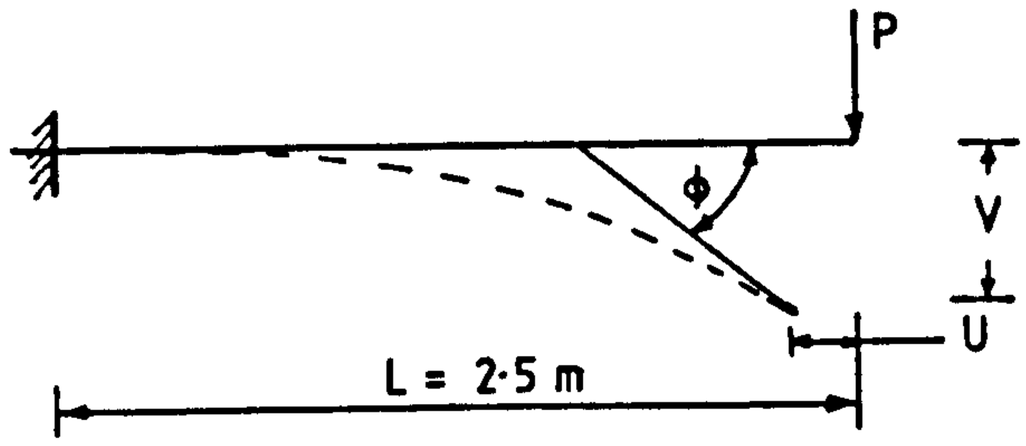

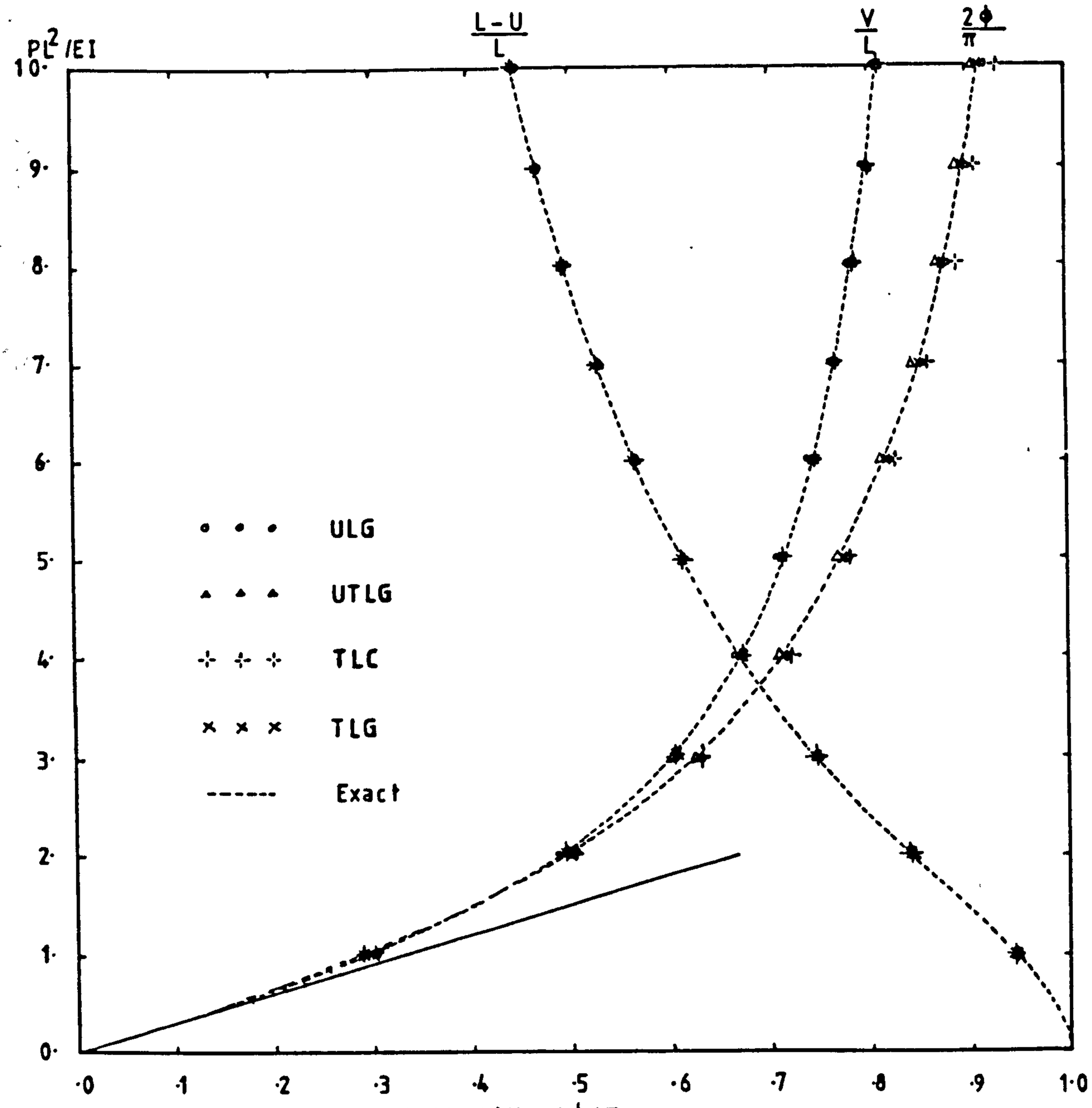

FIGURE 4.20 - Cantilever under Vertical Load at Free End - 20 Load Increments

$EI = 16666 \quad KN\text{-}m^2$

$EA = 2 \times 10^7 \quad KN$

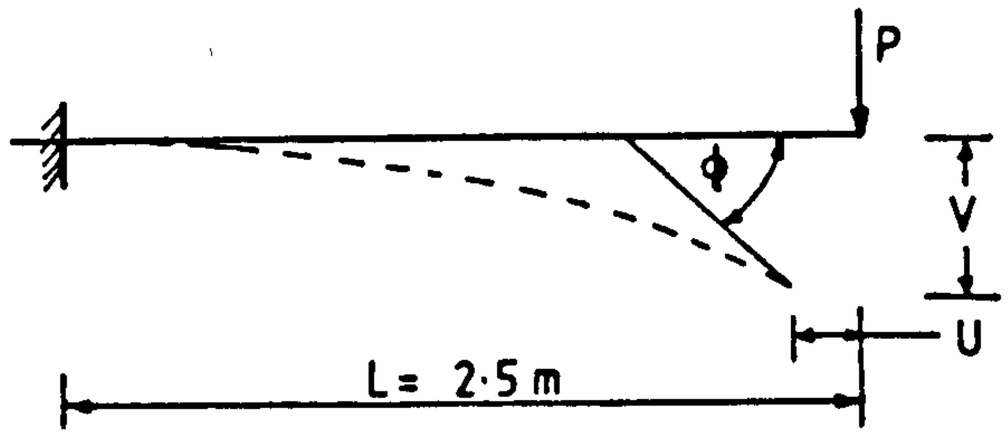

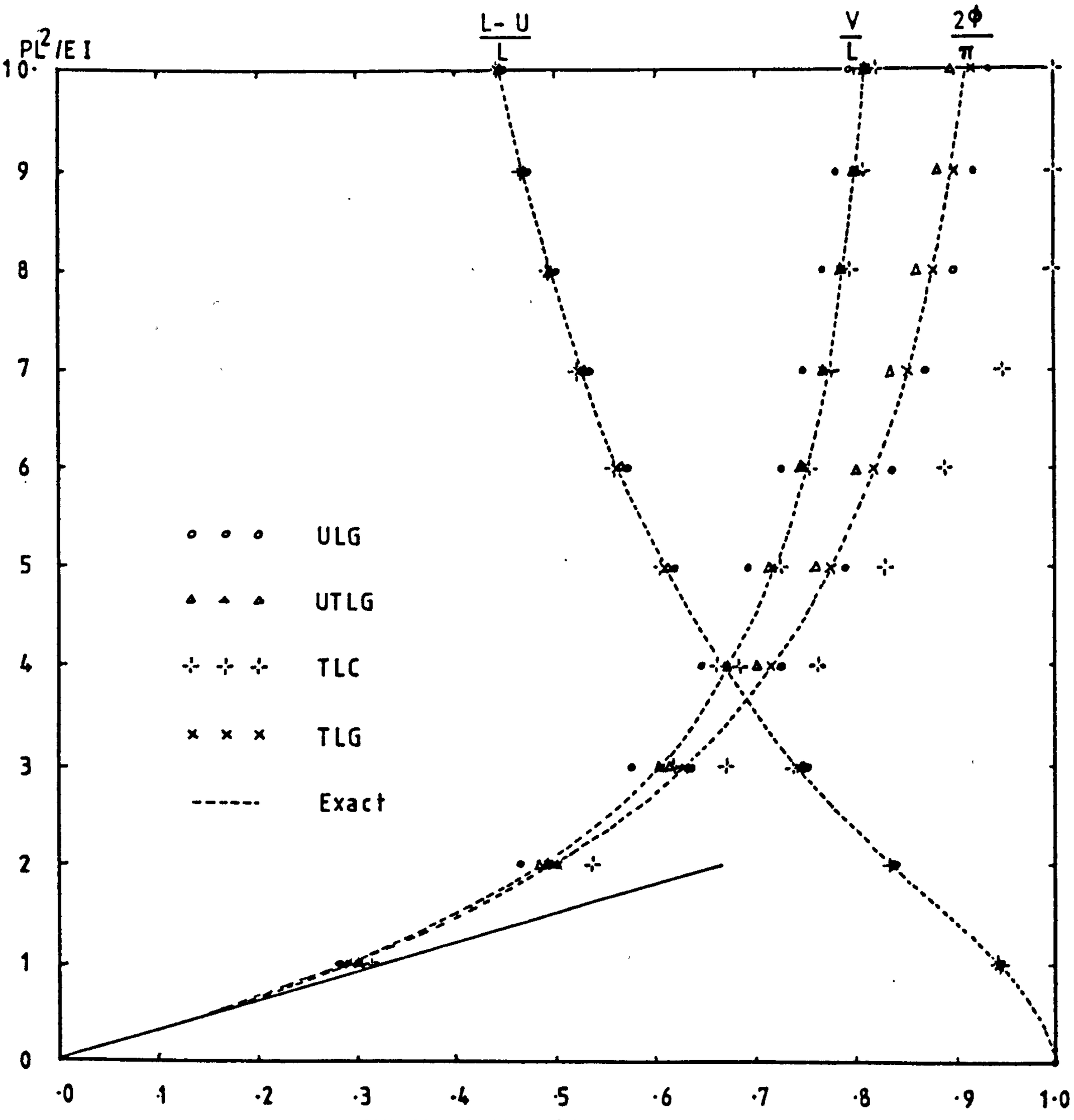

FIGURE 4.21 - Cantilever under Vertical Load at Free Eng - 10 Load Increments

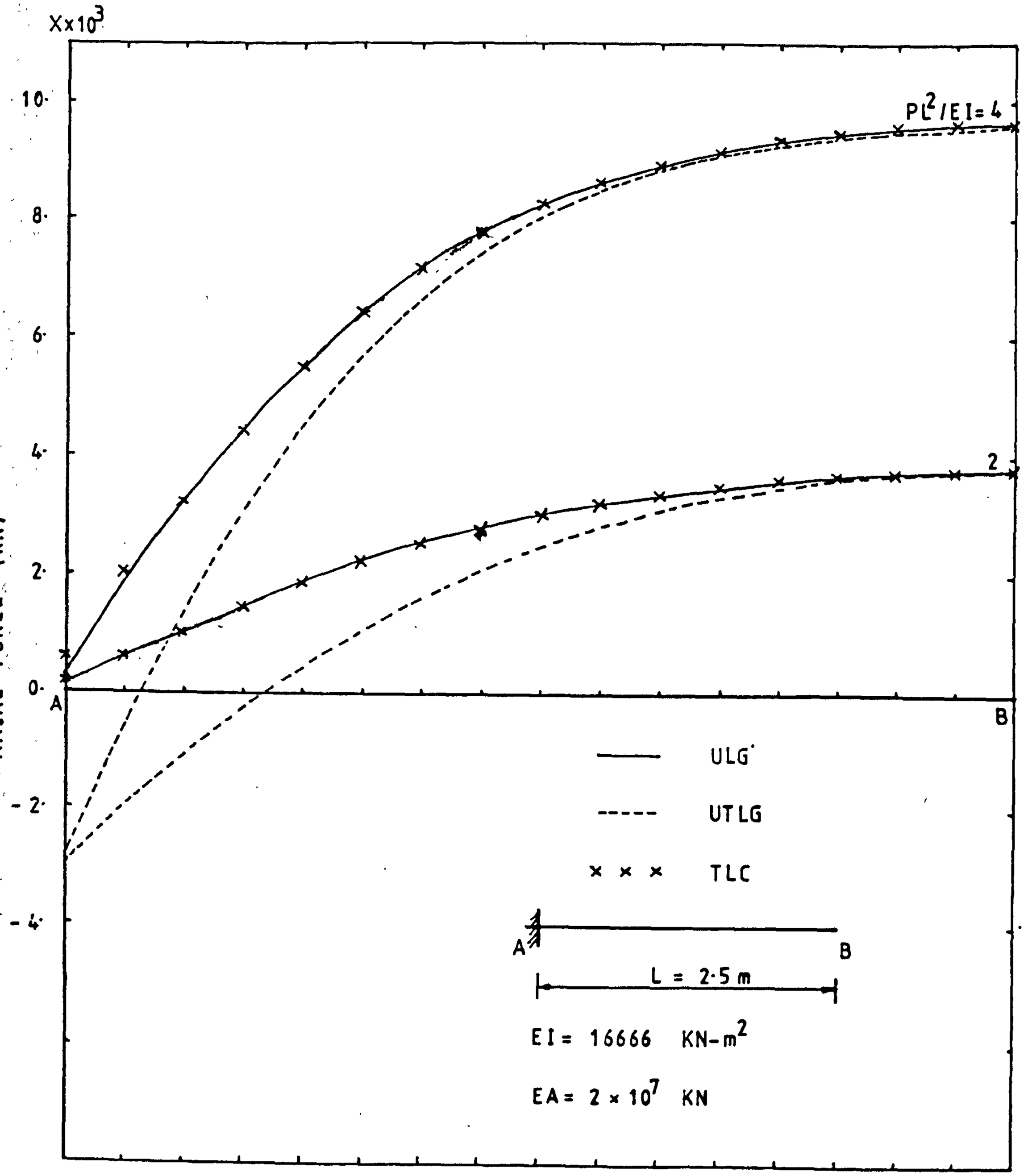

FIGURE 4.22 - Cantilever under Vertical Load at Free End - 20 Load Increments - Variation of Axial Force along Length

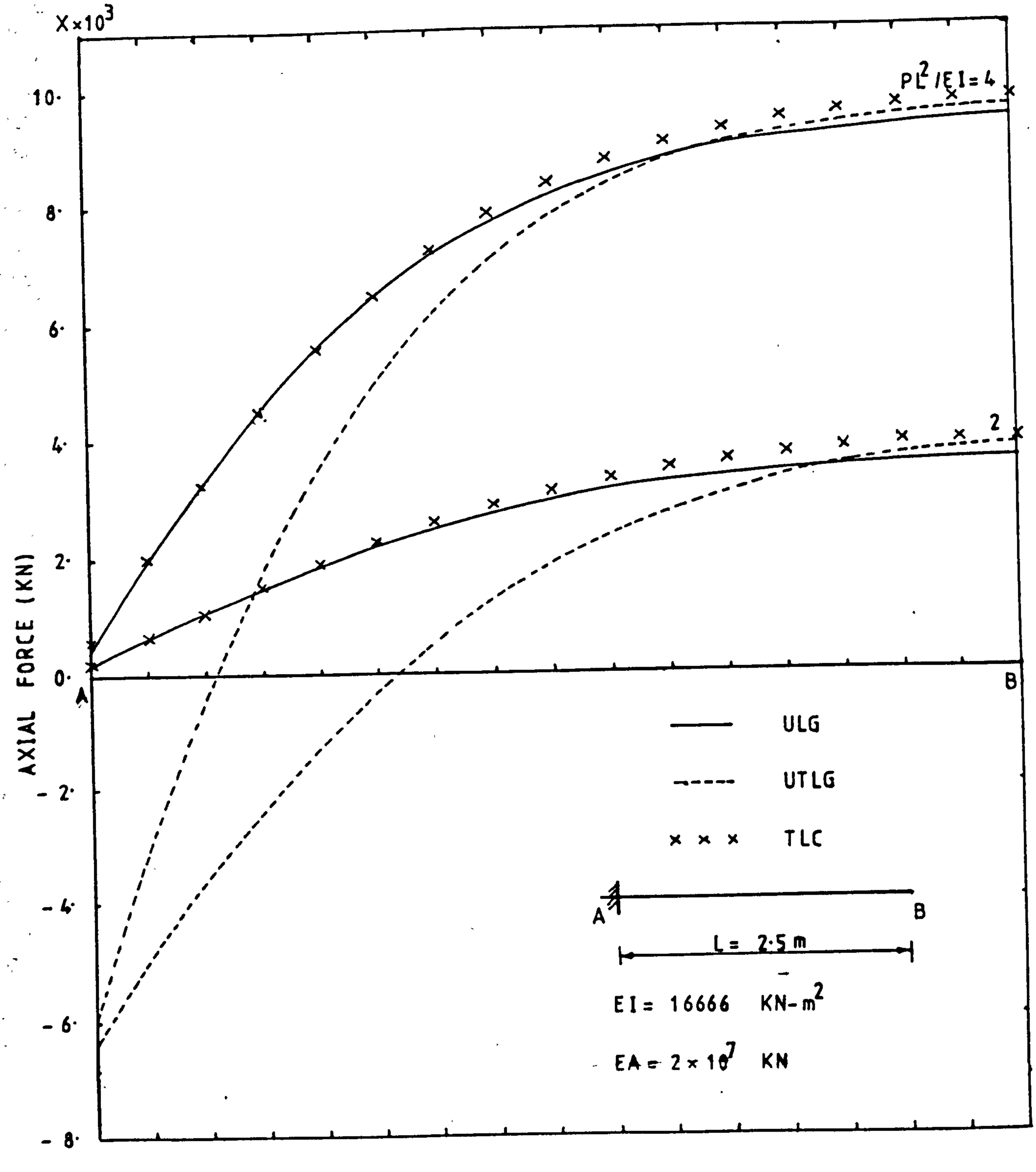

FIGURE 4.23 - Cantilever under vertical Load at Free End - 10 Load Increments - Variation of Axial Force along Length

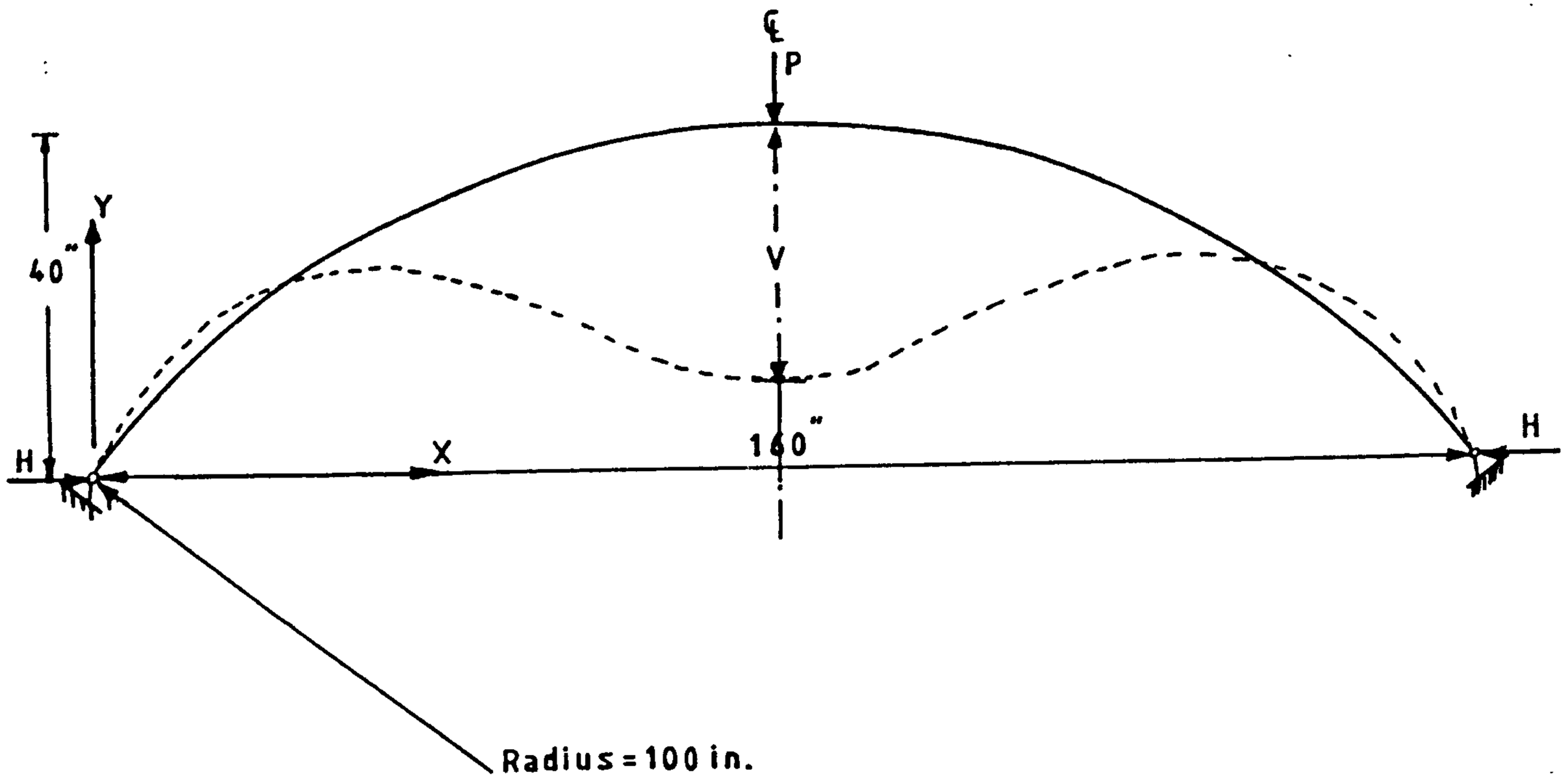

FIGURE 4.24 – Two-hinged Deep Arch Geometry

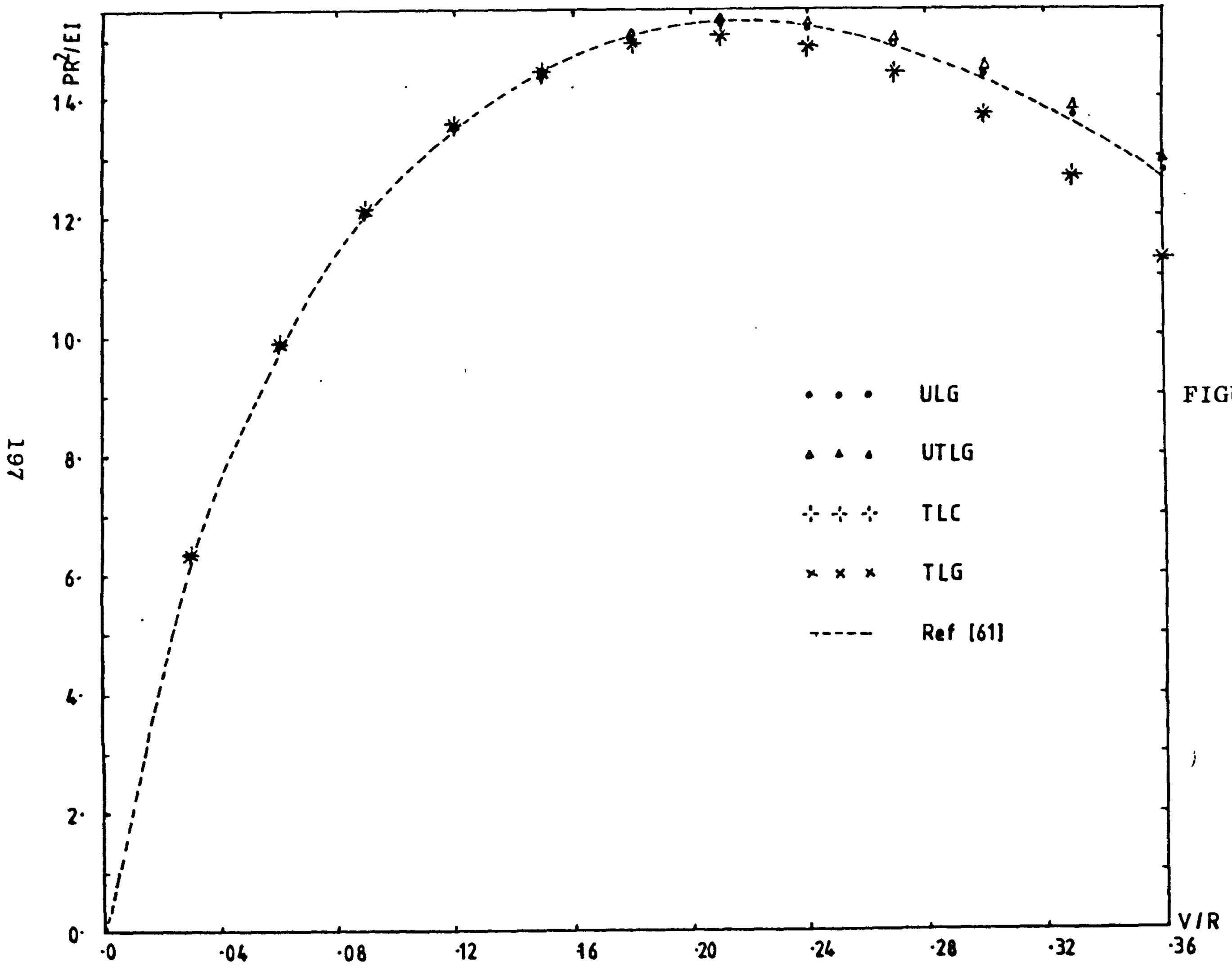

FIGURE 4.25a - Two-hinged Deep Arch - Central Load vs Deflection - ISOBEM 1 Results

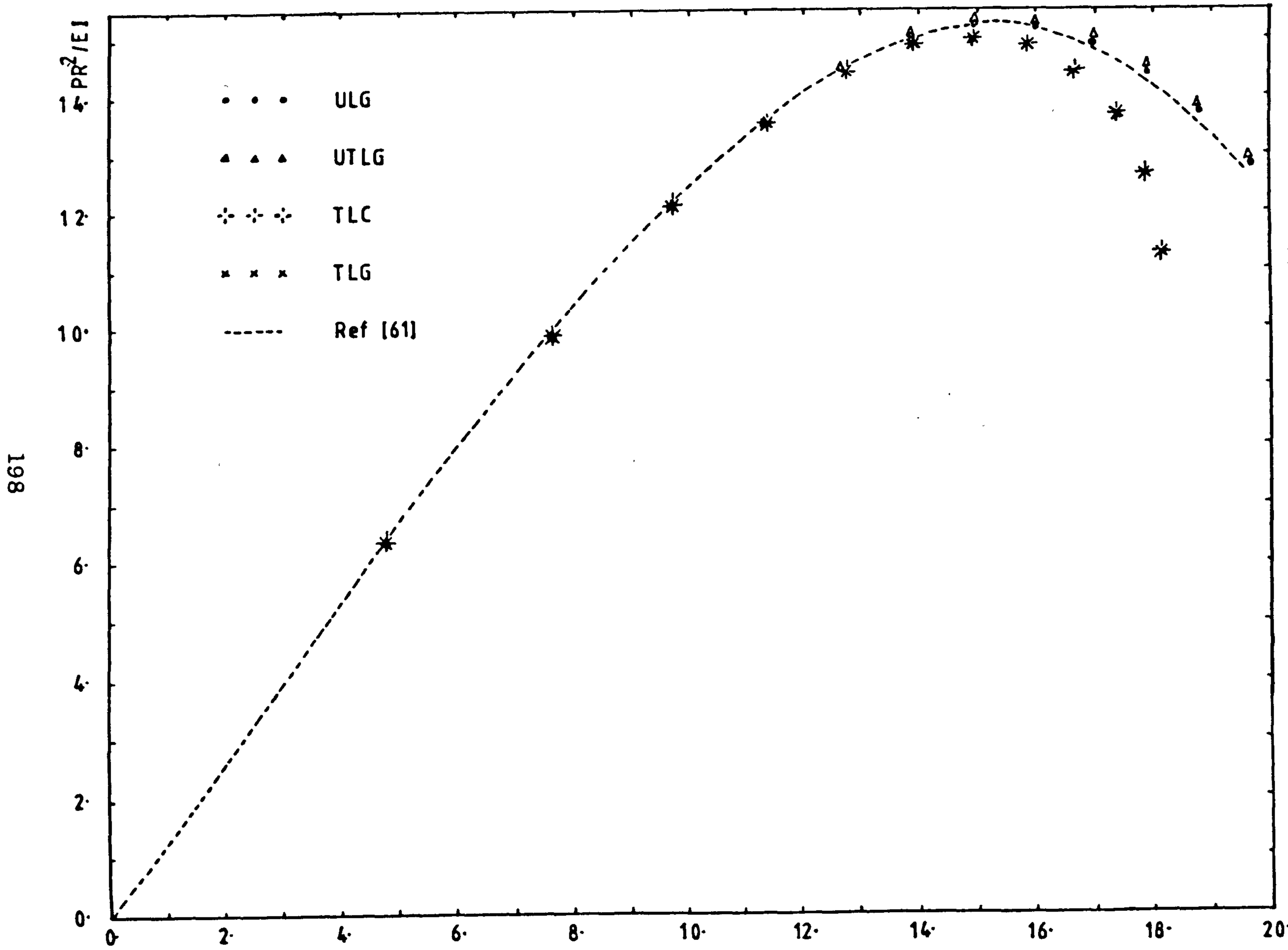

FIGURE 4.25b - Two-hinged Deep Arch - Central Load vs Horizontal Reaction - ISOBEM 1 Results

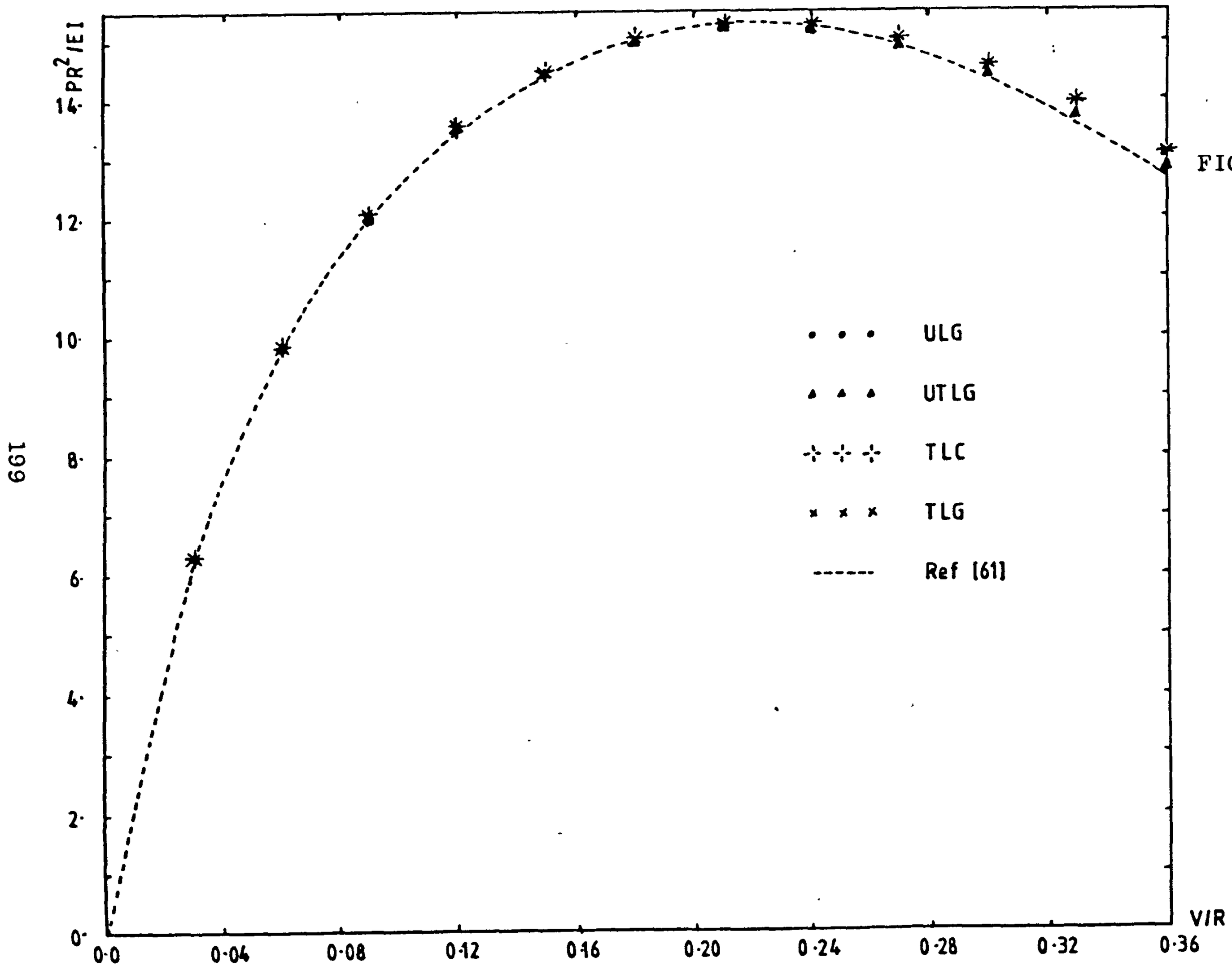

FIGURE 4.26a - Two-hinged Deep Arch - Central Load vs Deflection - ISOBEM 2 Results

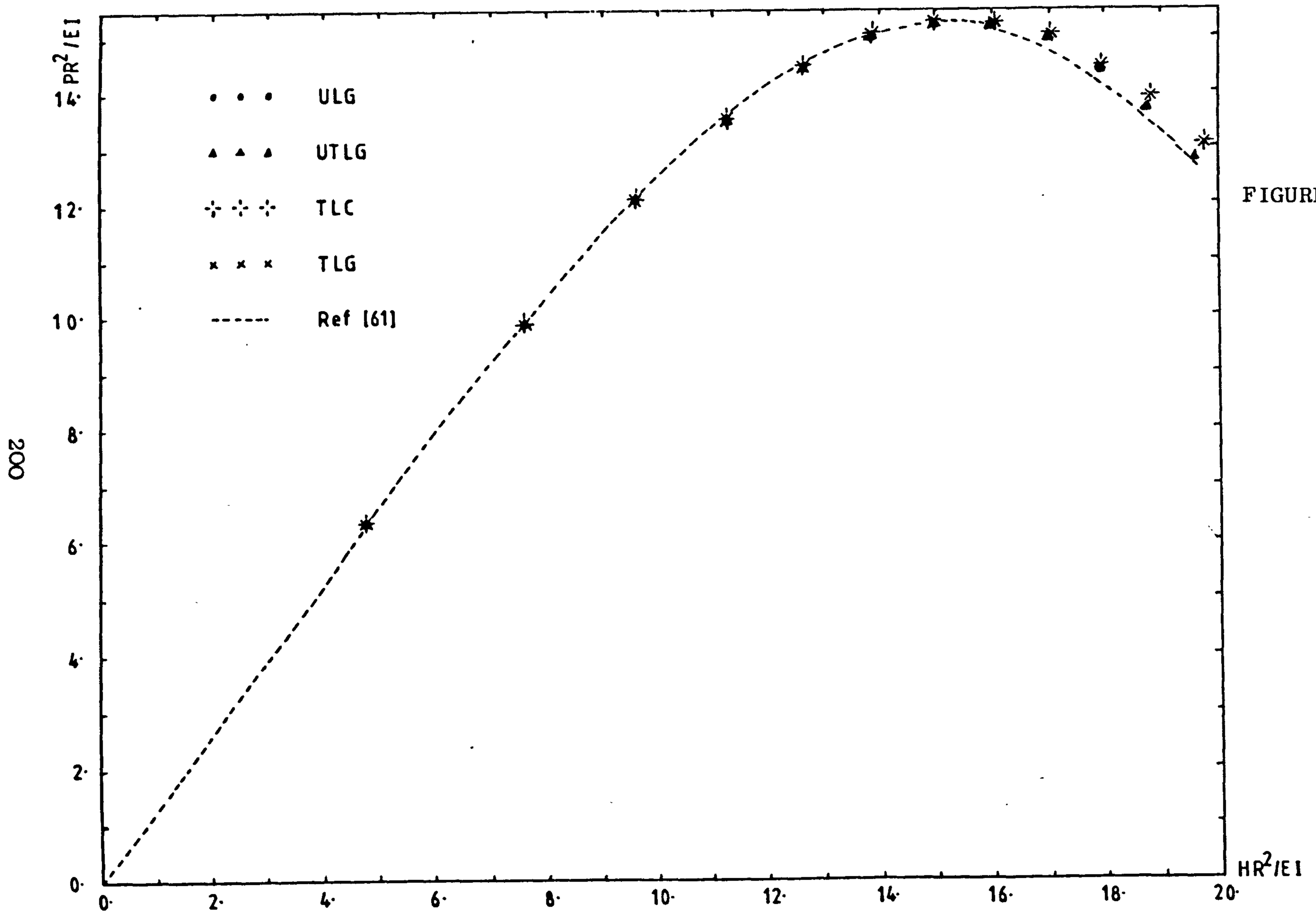

FIGURE 4.26b - Two-hinged Deep Arch - Central Load vs Horizontal Reaction - ISOBEM 2 Results

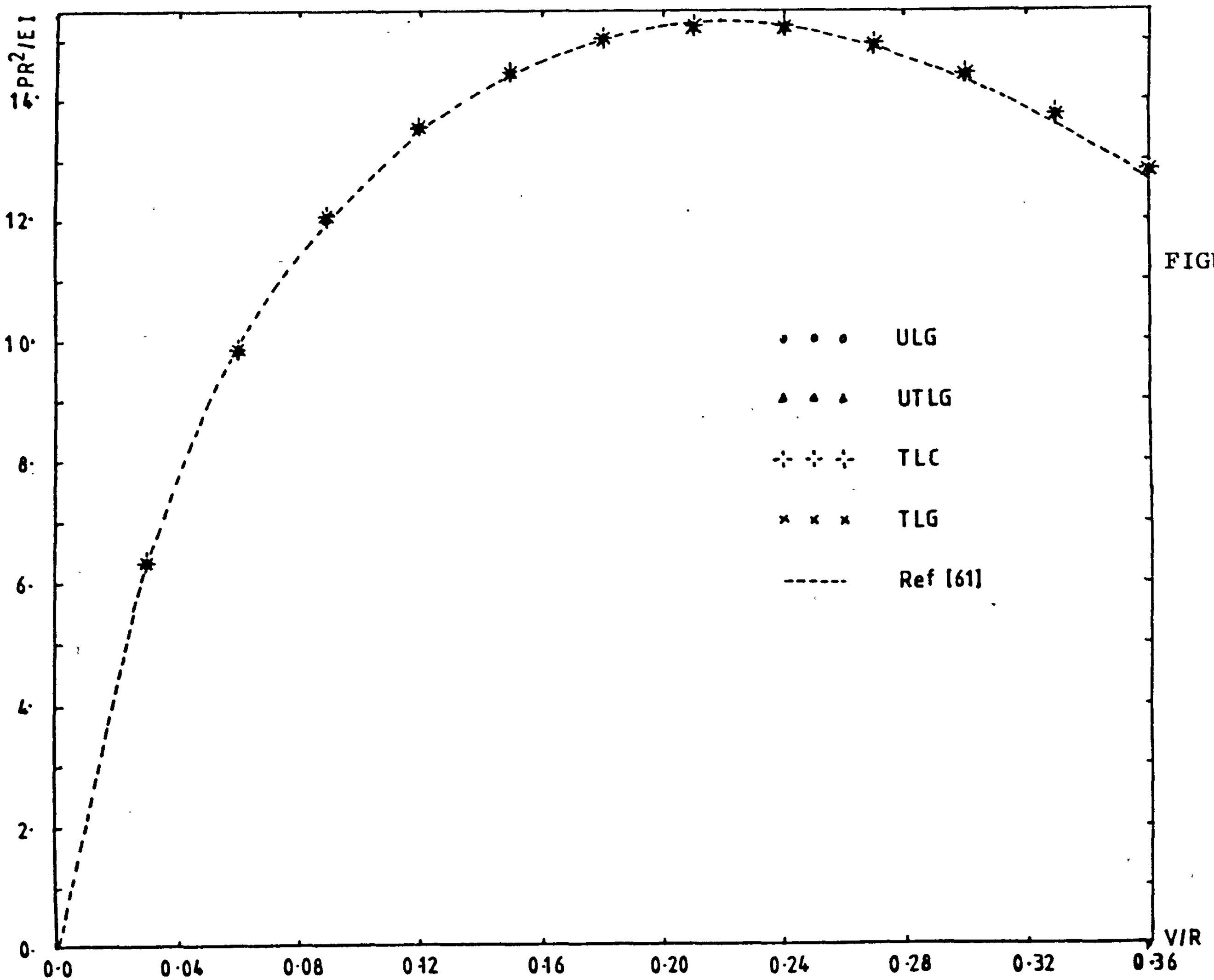

FIGURE 4.27a - Two-hinged Deep Arch - Central Load vs Deflection - SUBBEAM Results

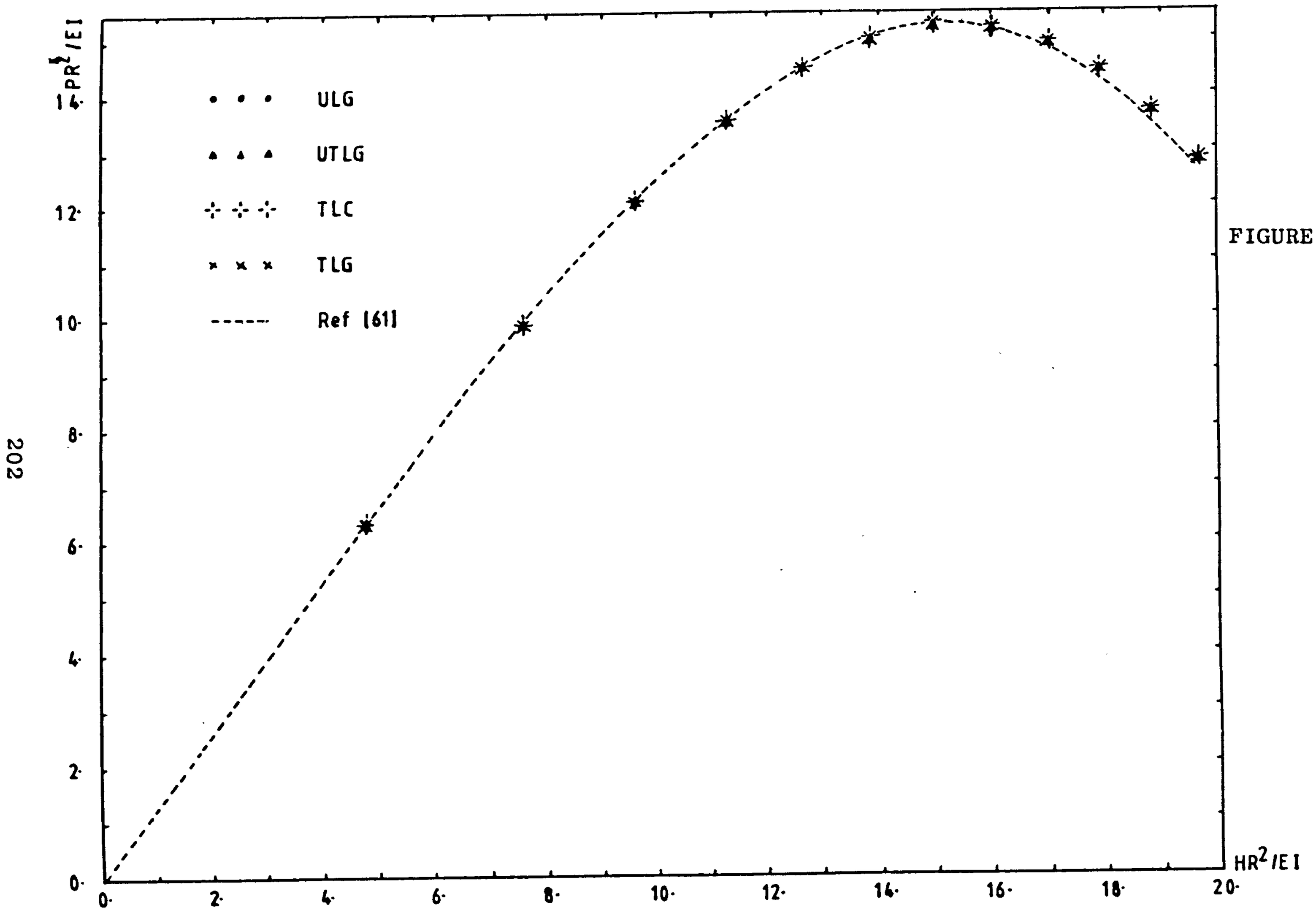

FIGURE 4.27b - Two-hinged Deep Arch - Central Load vs Horizontal Reaction - SUBBEAM Results

$\frac{V}{R}$	PR^2/EI				HR^2/EI			
	TLG	TLC	UTLG	ULG	TLG	TLC	UTLG	ULG
0.03	6.3293	6.3305	6.3288	6.3294	4.7596	4.7605	4.7593	4.7598
0.06	9.8582	9.8617	9.8538	9.8546	7.6058	7.6084	7.6030	7.6037
0.09	12.0816	12.0874	12.0702	12.0711	9.6444	9.6489	9.6375	9.6382
0.12	13.5419	13.5499	13.5206	13.5215	11.2656	11.2719	11.2528	11.2536
0.15	14.4870	14.4969	14.4527	14.4535	12.6436	12.6517	12.6231	12.6239
0.18	15.0462	15.0579	14.9962	14.9970	13.8675	13.8776	13.8375	13.8384
0.21	15.2943	15.3076	15.2255	15.2263	14.9861	14.9982	14.9461	14.9470
0.24	15.2792	15.2938	15.1857	15.1865	16.0275	16.0416	15.9780	15.9789
0.27	15.0336	15.0490	14.9060	14.9067	17.0101	17.0263	16.9508	16.9518
0.30	14.5789	14.5949	14.4058	14.4065	17.9488	17.9669	17.8747	17.8757
0.33	13.9259	13.9423	13.6991	13.6997	18.8567	18.8766	18.7554	18.7564
0.36	13.0764	13.0931	12.7965	12.7970	19.7431	19.7646	19.5953	19.5963

TABLE 4.7 Symmetrical Buckling of Arch - ISOBEM 2 Results.

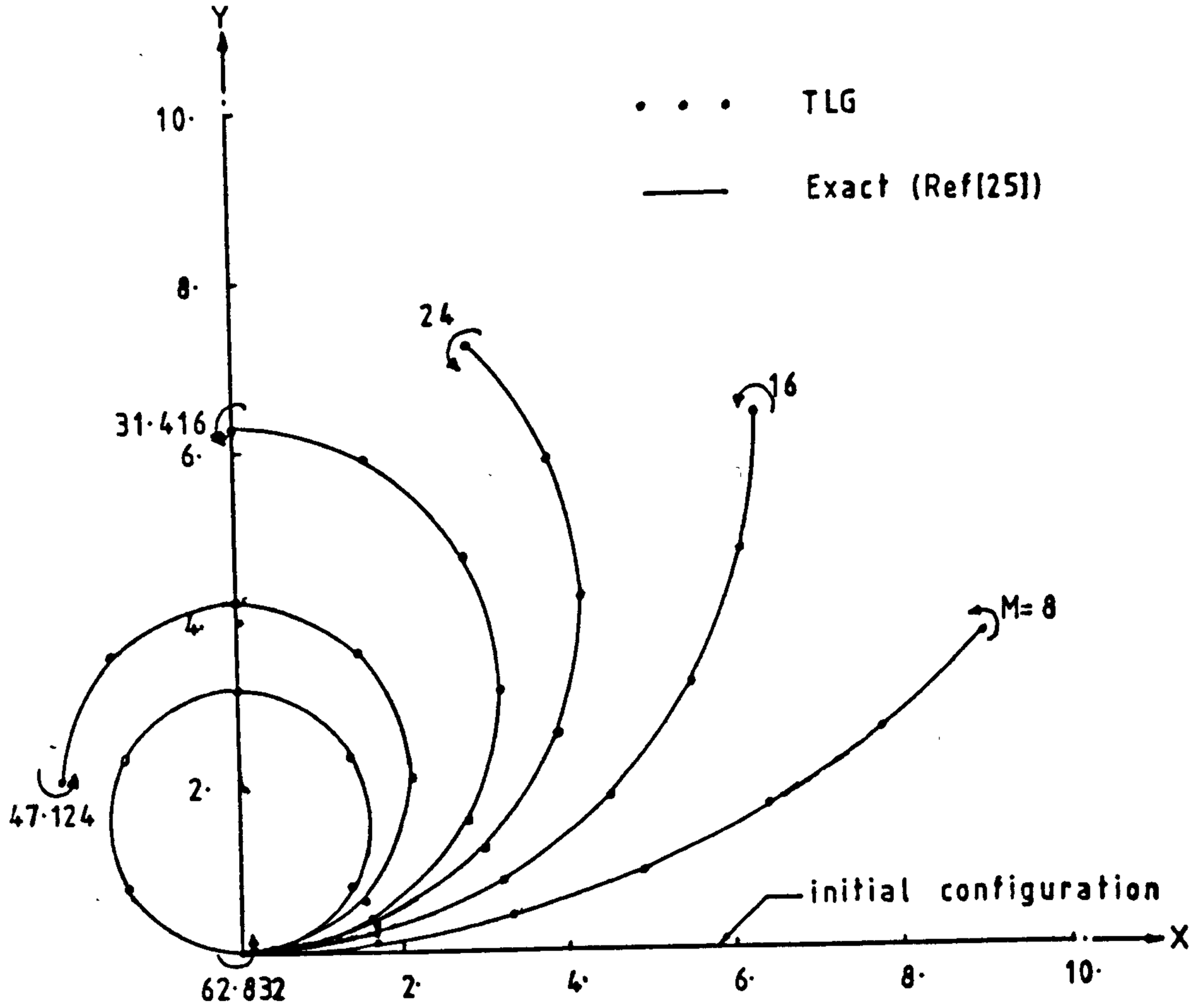

$E = 10^{6}$

$A = 1$

$I = 10^{-4}$

FIGURE 4.28 - Cantilever under Pure Moment - Sample Configurations - SUBBEAM Results

M	V		U		dv/dx		du/dx	
	F.E.	Exact*	F.E.	Exact*	F.E.	Exact*	F.E.	Exact*
1.0	.4996	.4996	-.01666	-.0166	.0998	.0988	-.005	-.005
2.0	.9967	.9967	-.0665	-.0665	.1987	.1987	-.0199	-.0199
4.0	1.9735	1.9735	-.2645	-.2645	.3894	.3894	-.0789	-.0789
8.0	3.7912	3.7912	-1.0331	-1.0330	.7174	.7174	-.3033	-.3033
10.0	4.5970	4.5970	-1.5853	-1.5853	.8415	.8415	-.4597	-.4597
12.0	5.3137	5.3137	-2.2331	-2.2331	.9320	.9320	-.6376	-.6376
14.0	5.9289	5.9289	-2.9612	-2.9611	.9855	.9854	-.8300	-.8299
16.0	6.4326	6.4325	-3.7528	-3.7527	.9996	.9996	-1.0292	-1.0292
18.0	6.8179	6.8178	-4.5899	-4.5897	.9739	.9738	-1.2273	-1.2272
20.0	7.0809	7.0807	-5.4538	-5.4535	.9093	.9093	-1.4162	-1.4161
22.0	7.2206	7.2204	-6.3255	-6.3250	.8085	.8085	-1.5886	-1.5885
24.0	7.2393	7.2391	-7.1863	-7.1856	.6754	.6755	-1.7376	-1.7374
26.0	7.1419	7.1419	-8.0183	-8.0173	.5153	.5155	-1.8571	-1.8569
27.0	7.0521	7.0521	-8.4183	-8.4171	.4271	.4271	-1.9043	-1.9041
28.0	6.9364	6.9365	-8.8049	-8.8035	.3347	.3350	-1.9425	-1.9422
29.0	6.7961	6.7964	-9.1765	-9.1750	.2389	.2392	-1.9712	-1.9709
30.0	6.6329	6.6333	-9.5313	-9.5296	.1407	.1411	-1.9902	-1.9899
31.416	6.3655	6.3678	-10.002	-10.000	-.0006	.000	-2.0002	-2.000
34.0	5.7832	5.7847	-10.754	-10.752	-.2565	-.2555	-1.9669	-1.9668
37.0	4.9920	4.9949	-11.4347	-11.432	-.5312	-.5298	-1.8478	-1.848
40.0	4.1295	4.1341	-11.8947	-11.892	-.7585	-.7568	-1.6526	-1.6536
43.0	3.2509	3.2577	-12.1324	-12.131	-.9179	-.9162	-1.3986	-1.4008
47.124	2.112	2.1226	-12.1211	-12.123	-1.0011	-1.000	-.9958	-1.000
50.0	1.4212	1.4327	-11.9136	-11.918	-.9586	-.9589	-.7106	-.7163
53.0	.8286	.8408	-11.5615	-11.570	-.8296	-.8323	-.4385	-.4456
56.0	.3896	.4008	-11.1129	-11.127	-.6251	-.6313	-.2167	-.2244
59.0	.1150	.1229	-10.6133	-10.634	-.3632	-.3739	-.0655	-.0725
62.832	.0002	.000	-9.9729	-10.000	.0171	.000	.0032	0.000

TABLE 4.8 Comparative Results for Cantilever under Pure Moment - Values at the Free End -
- 6 SUBBEAM Elements - TLG.
* Ref(25).

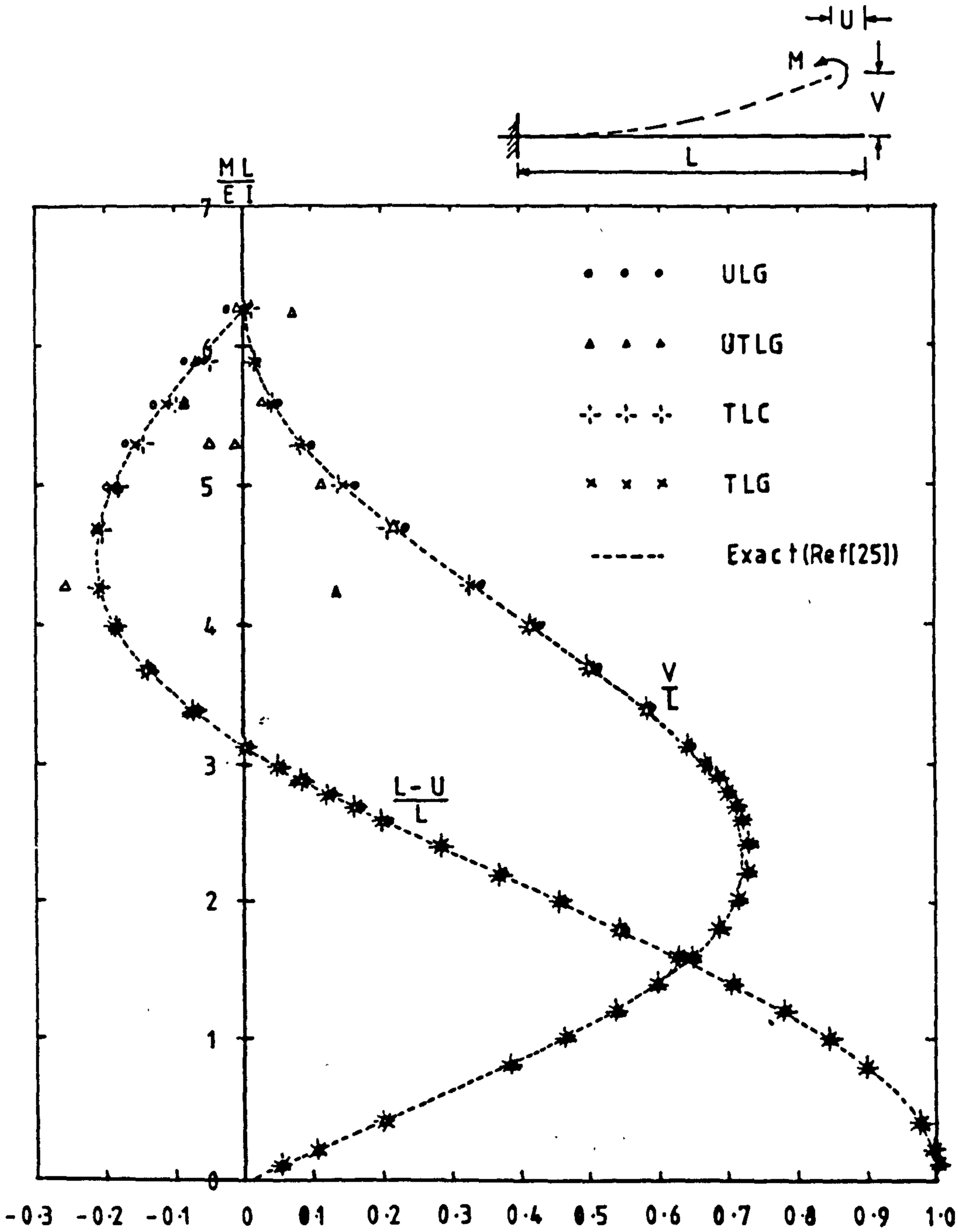

FIGURE 4.29a - Cantilever under Pure Moment -
Displacements at Free End -
6 SUBBEAM Elements

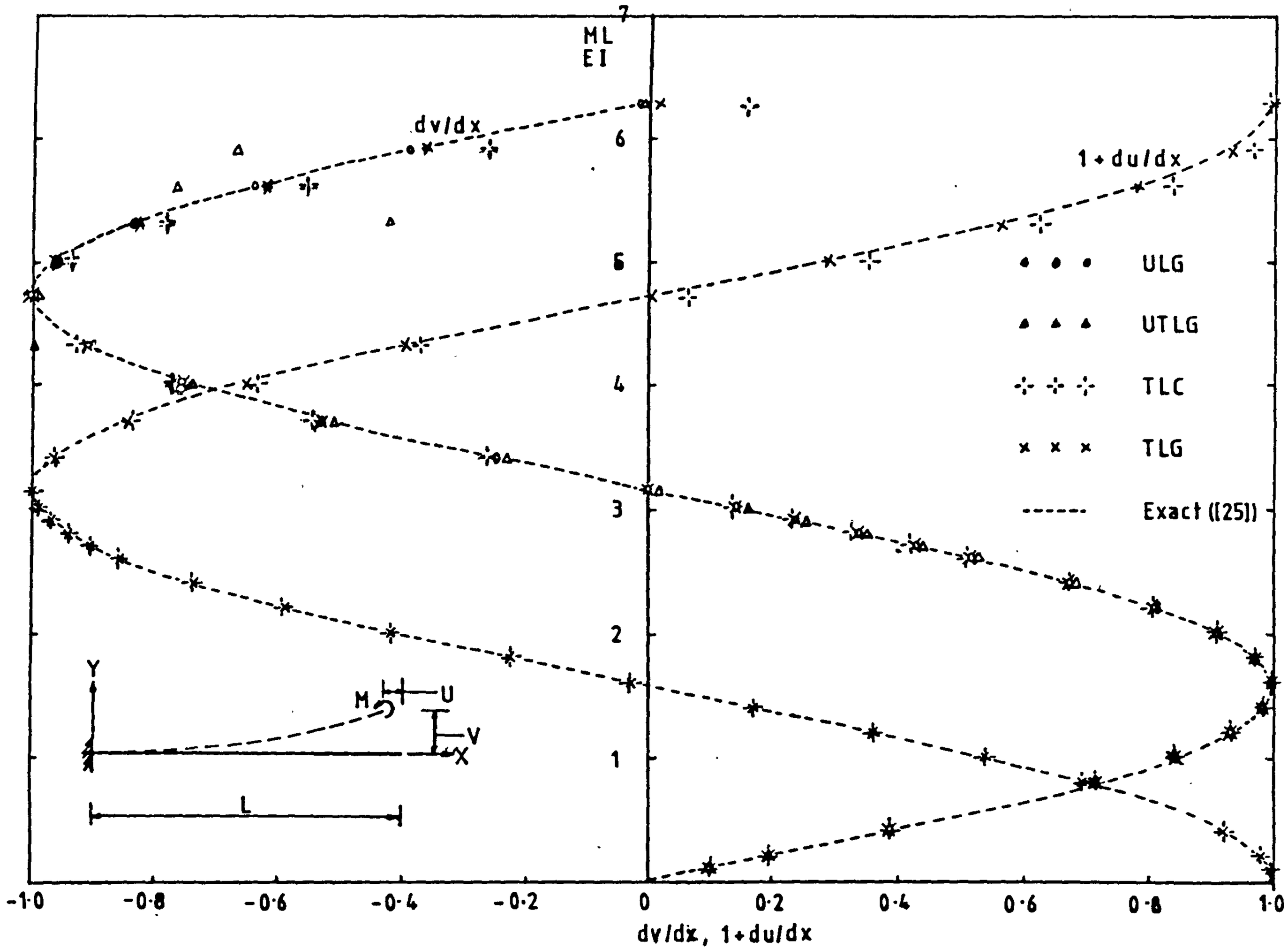

FIGURE 4.29b - Cantilever under Pure Moment - Displacement Derivatives at Free End - 6 SUBBEAM Elements.

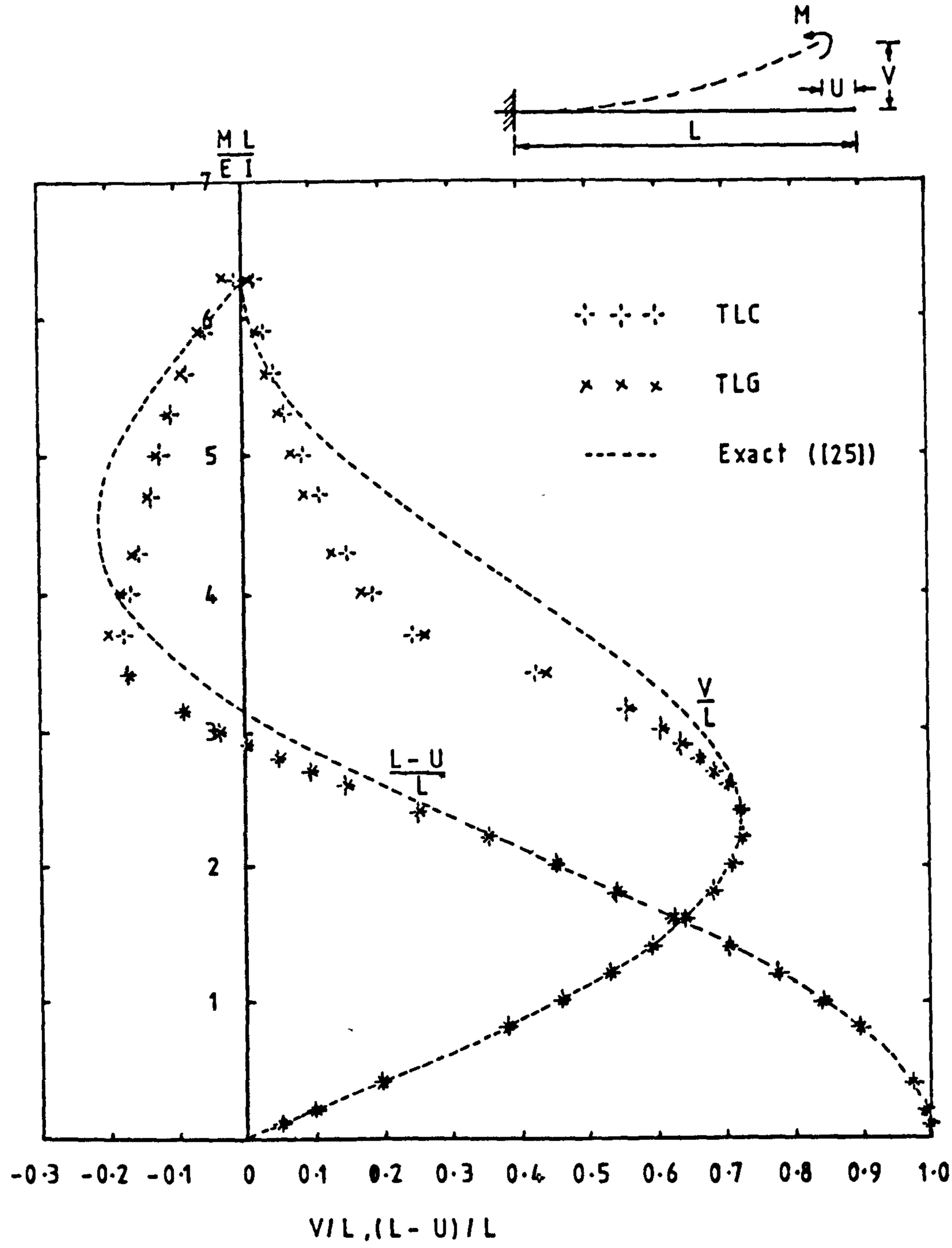

FIGURE 4.30a - Cantilever under Pure Moment - Displacements at Free End - 6 ISOBEM 2 Elements

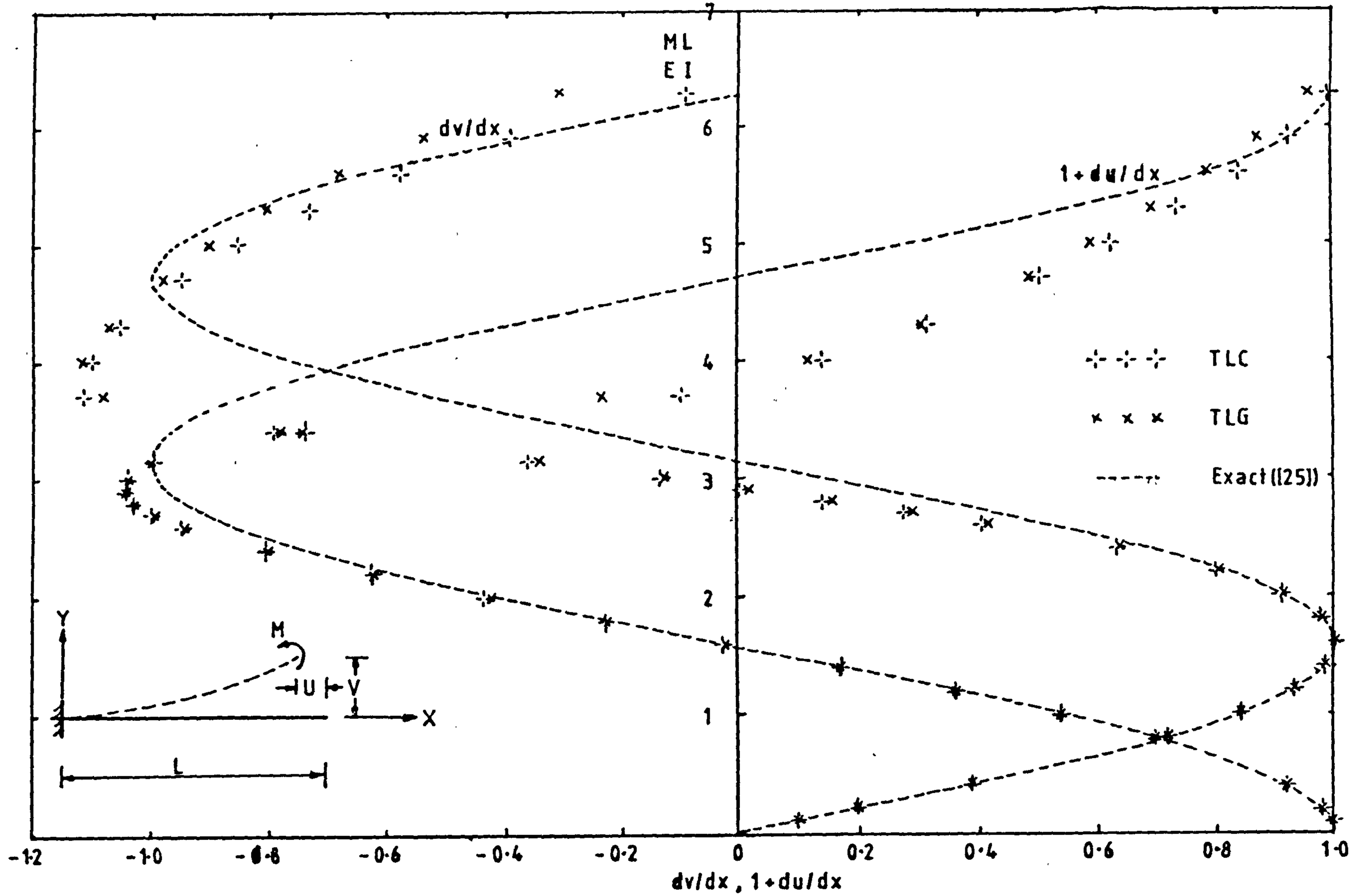

FIGURE 4.30b - Cantilever under Pure Moment - Displacement Derivatives at Free End - 6 ISOBEM 2 Elements

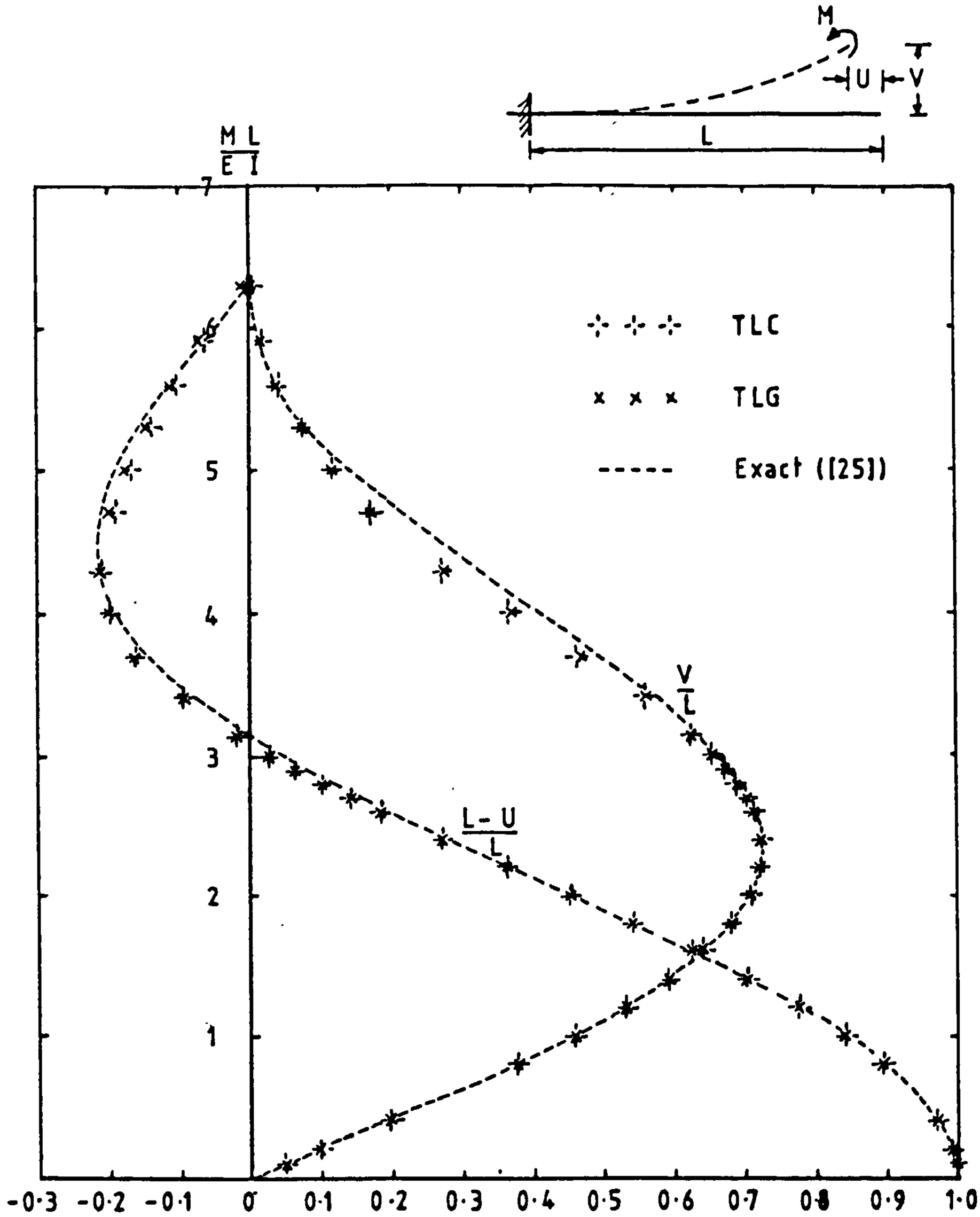

FIGURE 4.31a - Cantilever under Pure Moment - Displacements at Free End - 12 ISOBEM 2 Elements

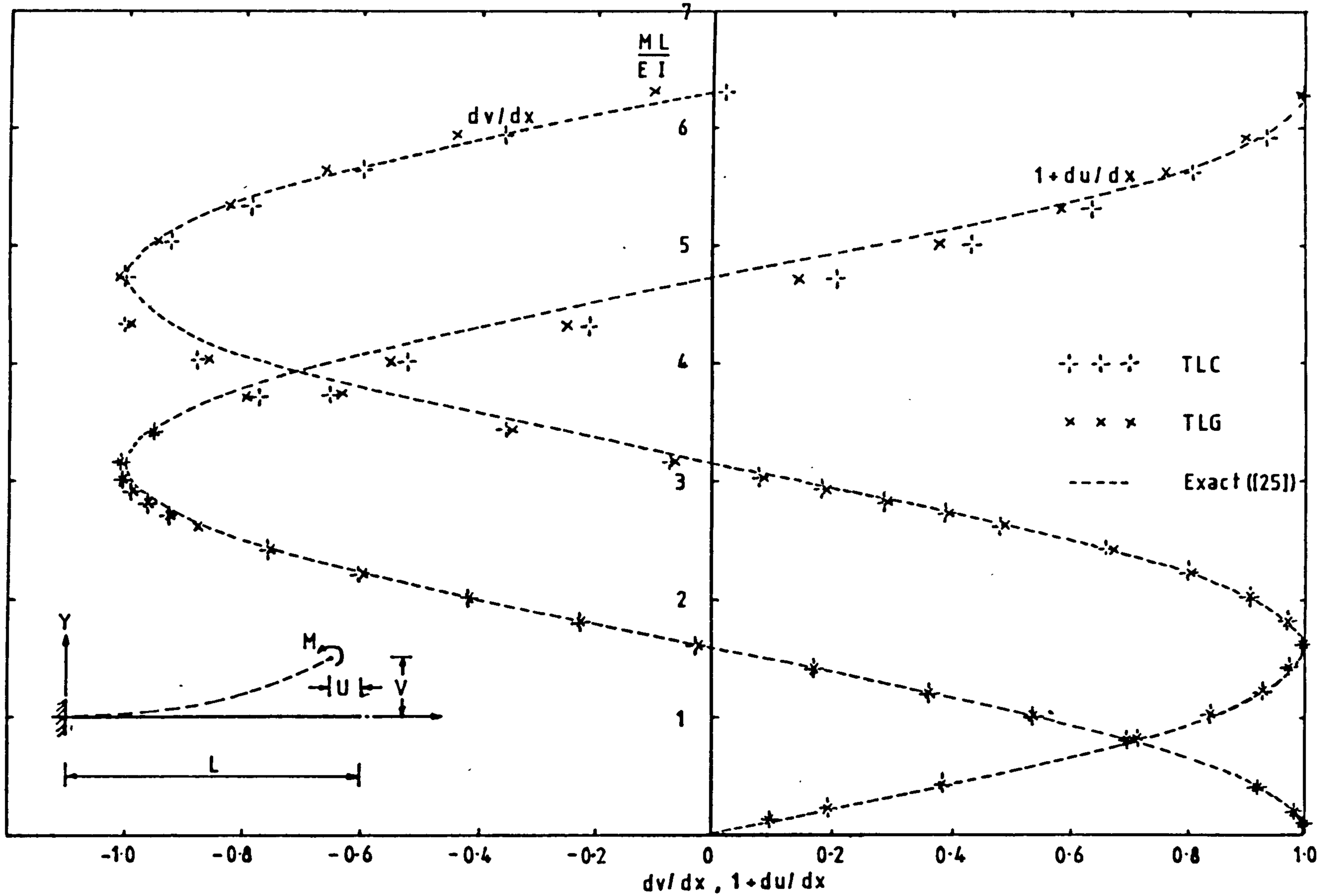

FIGURE 4.31b - Cantilever under Pure Momoment - Displacement Derivatives at Free End - 12 ISOBEM 2 Elements

Example	Element Type	Time/ULG Time			
		ULG	UTLG	TLC	TLG
Cantilever under vertical load 20 increments 16 elements	ISOBEM 1	1.00	0.2923	-	-
	ISOBEM 2	1.00	0.4781	0.3998	0.5200
	SUBBEAM	1.00	0.3502	0.2590	0.3298
Cantilever under vertical load 10 increments 16 elements	ISOBEM 1	1.00	0.3185	-	-
	ISOBEM 2	1.00	0.5225	0.4821	0.4373
	SUBBEAM	1.00	0.3534	0.2773	0.2446
Symmetrical buckling of Arch 60 increments 8 elements	ISOBEM 1	1.00	0.5714	0.6278	0.4672
	ISOBEM 2	1.00	0.5688	0.5038	0.4614
	SUBBEAM	1.00	0.3987	0.3196	0.2608
Cantileter under pure moment 30 increments 6 elements	SUBBEAM	1.00	1.0723	0.4412	0.5176

TABLE 4.9 Relative Computer Times

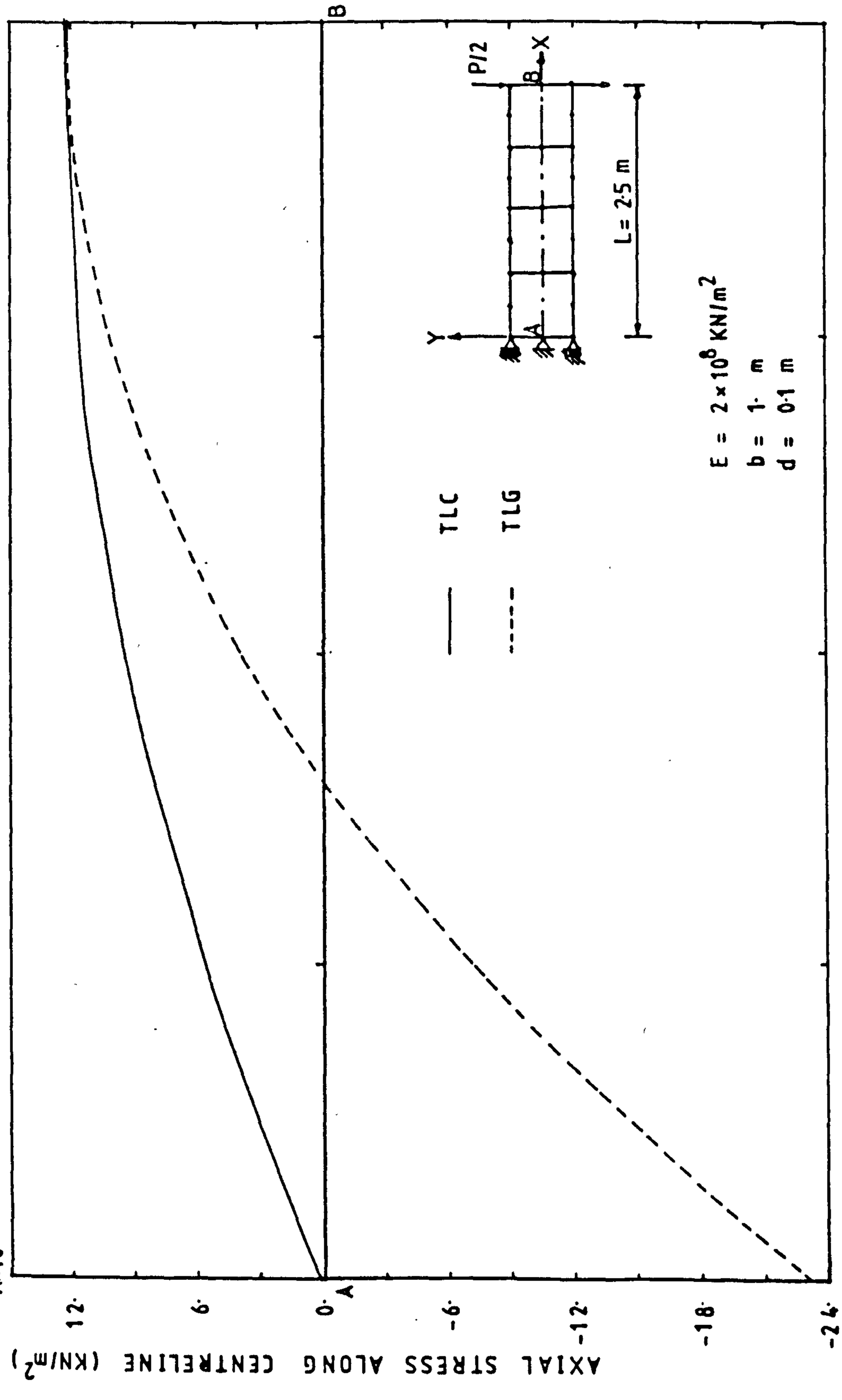

FIGURE 4.32 - Cantilever under Vertical Load at Free End - 4 ISOPARAMETRIC Elements - Variation of Axial Stress along Centreline

$\frac{wL^3}{EI}$	V/L		$\frac{L-U}{L}$		$2\phi^*/\pi$	
	TLG	TLC	TLG	TLC	TLG	TLC
1	.1235	.1243	.9912	.9912	.1052	.1061
2	.2385	.2400	.9669	.9666	.2047	.2065
3	.3397	.3416	.9315	.9309	.2950	.2974
4.	.4252	.4272	.8901	.8892	.3745	.3772
5	.4959	.4977	.8466	8456	.4432	4459
6	.5540	.5557	.8035	.8025	.5023	.5051
7	.6016	.6031	.7625	.7614	.5528	.5556
8	.6408	.6422	.7240	.7229	.5960	.5988
9	.6733	.6762	.6884	.6852	.6330	.6382
10	.7006	.7030	.6555	.6526	.6646	.6696

$$\phi^* = \sin^{-1} \frac{dv}{dx}$$

TABLE 4.10 Cantilever under Uniformly distributed Load

ISOBEM 2 Results.

$EI = 833{\cdot}4 \ KN\text{-}m^2$

$EA = 10^6 \ KN$

8 elements

10 load increments

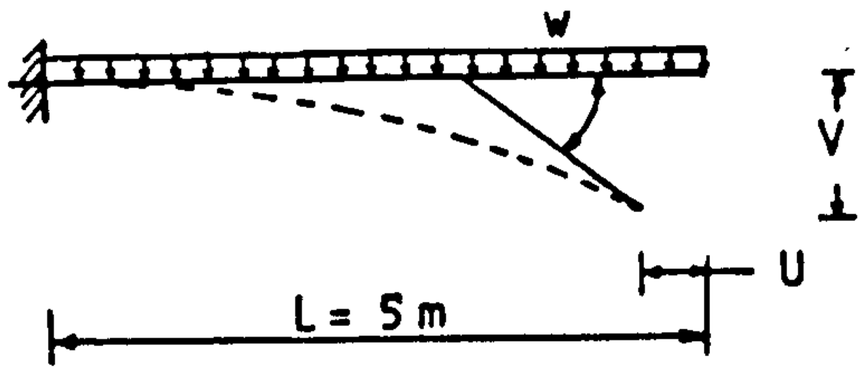

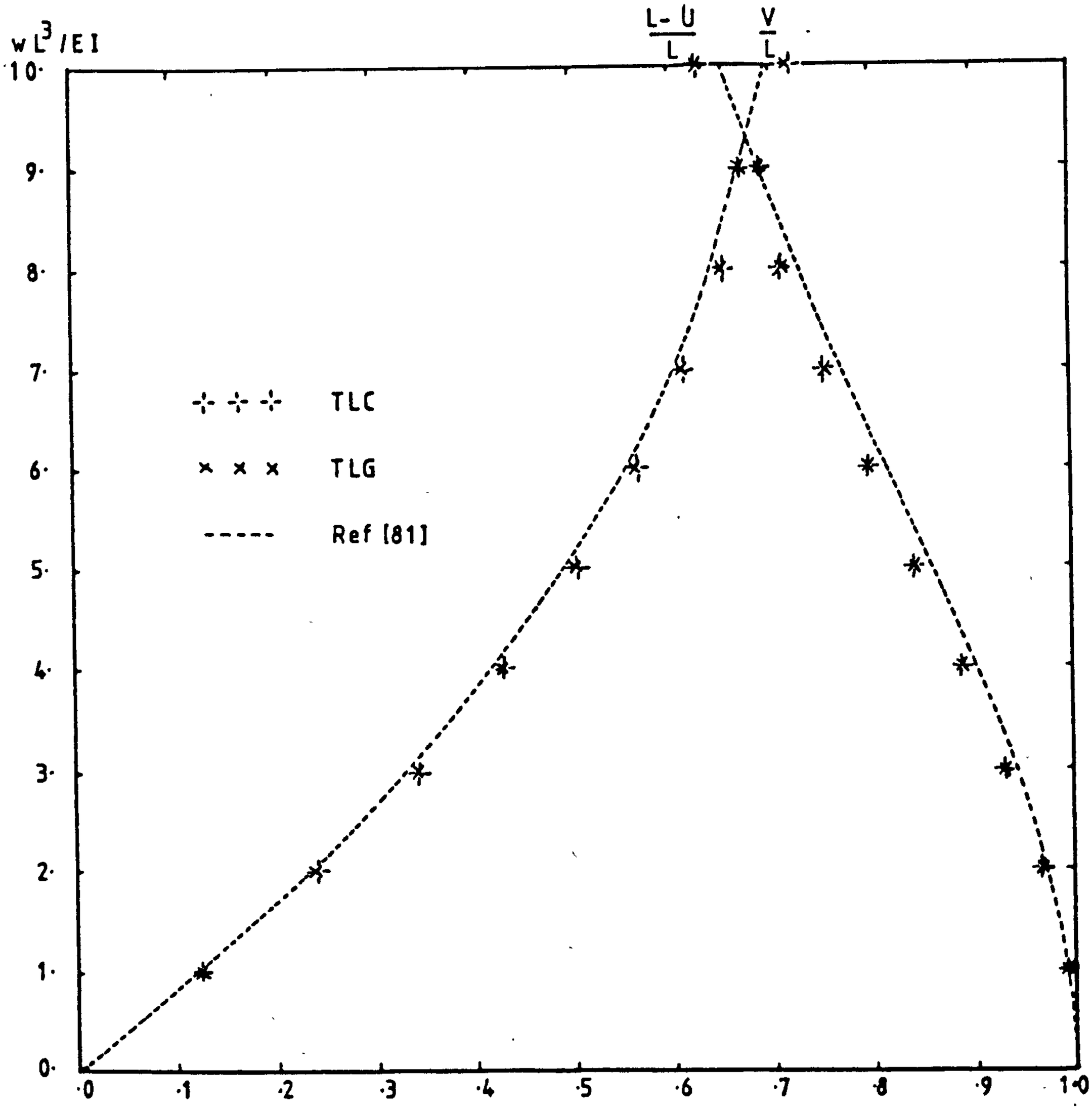

FIGURE 4.33 - Cantilever under Uniformly Distributed Load
ISOBEM 1 Results

$EI = 833 \cdot 4 \quad KN\text{-}m^2$

$EA = 10^6 \quad KN$

8 elements

10 load increments

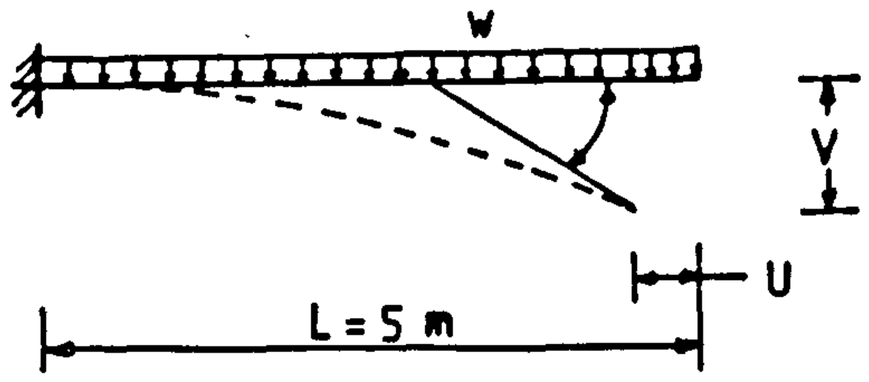

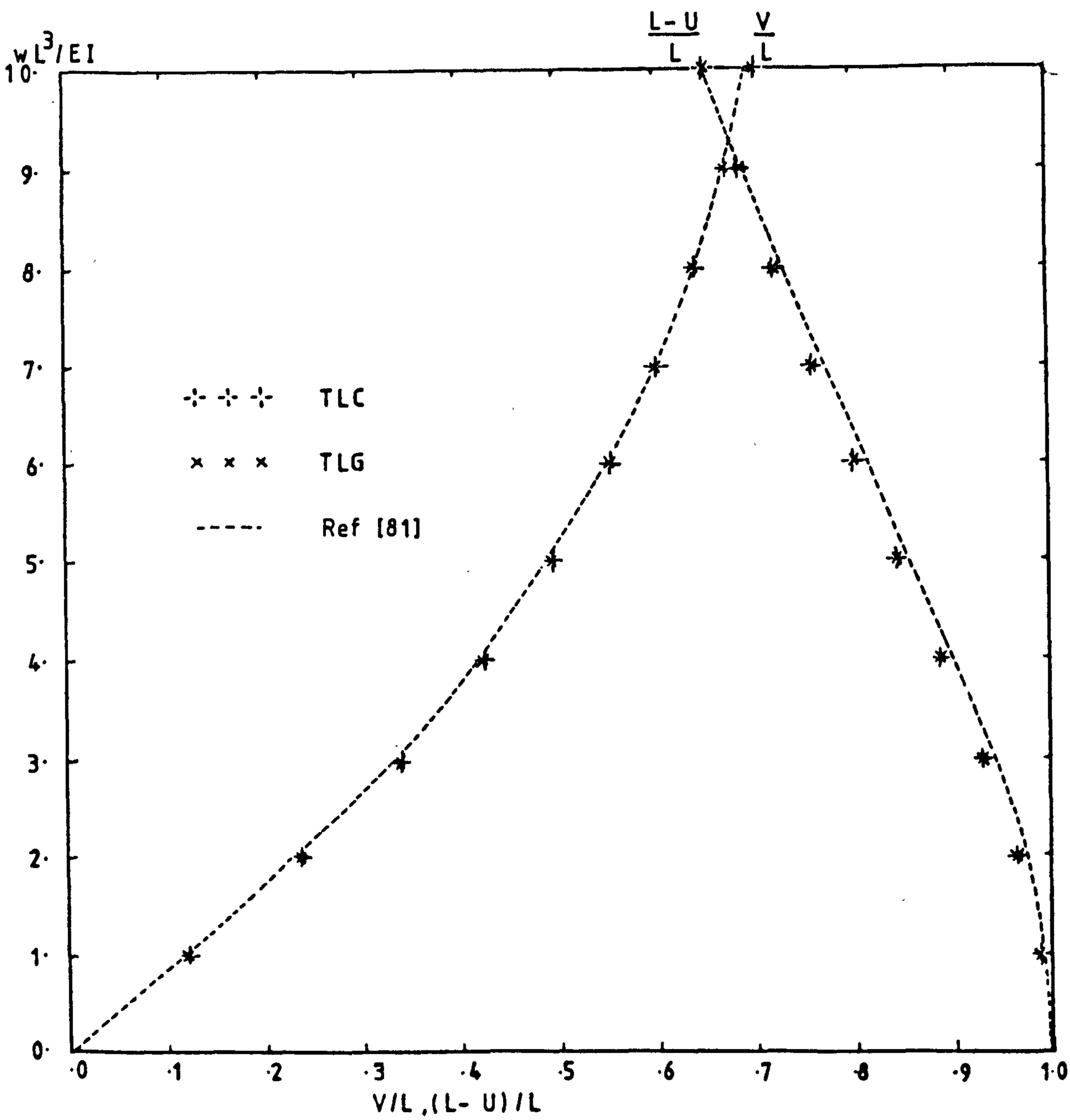

FIGURE 4.34 - Cantilever under Uniformly Distributed Load - ISOBEM 2 Results

$EI = 833{\cdot}4 \quad KN\text{-}m^2$

$EA = 10^6 \quad KN$

8 elements

10 load increments

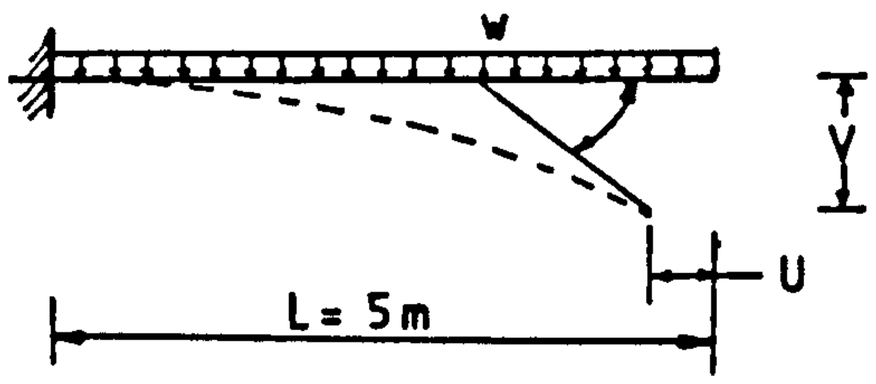

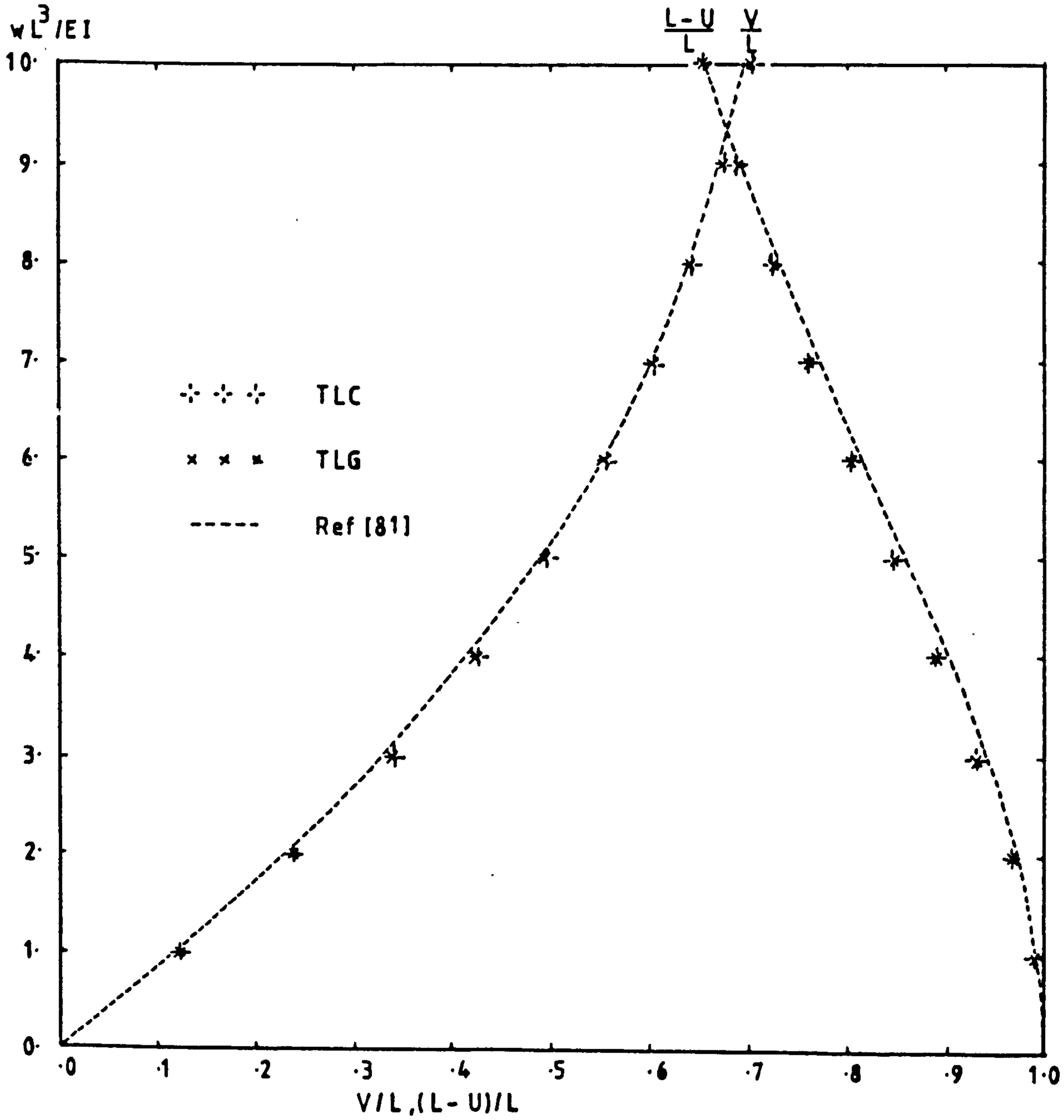

FIGURE 4.35 - Cantilever under Uniformly Distributed Load - SUBBEAM Results

$\frac{wL^2}{EI}$	V/L		$\frac{L-U}{L}$		$2\phi/\pi$	
	ULG	TLG	ULG	TLG	ULG	TLG*
1	.1235	.1244	.9911	.9911	.1060	.1060
2	.2436	.2456	.9650	.9648	.2114	.2116
3	.3573	.3604	.9230	.9221	.3157	.3163
4.	.4619	.4662	.8668	.8649	.4187	.4196
5	.5555	.5607	.7986	.7952	.5198	.5212
6	.6365	.6423	.7209	.7157	.6187	.6207
7	.7040	.7102	.6365	.6291	.7151	.7179
8	.7578	.7639	.5478	.5381	.8088	.8125
9	.7981	.8038	.4574	.4451	.8994	.9038
10	.8256	.8304	.3676	.3525	.9869	.9919

* $\phi = \sin^{-1} \frac{dv}{dx}$

TABLE 4.11 Cantilever under Follower Pressure Loading

SUBBEAM Result.

$EI = 833{\cdot}4 \quad KN\text{-}m^2$

$EA = 10^6 \quad KN$

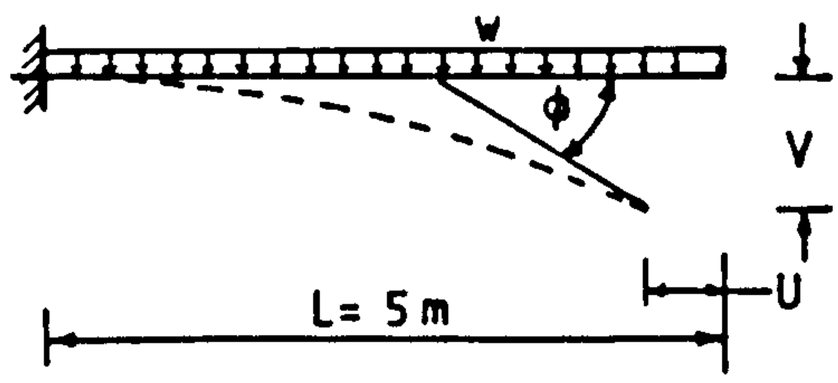

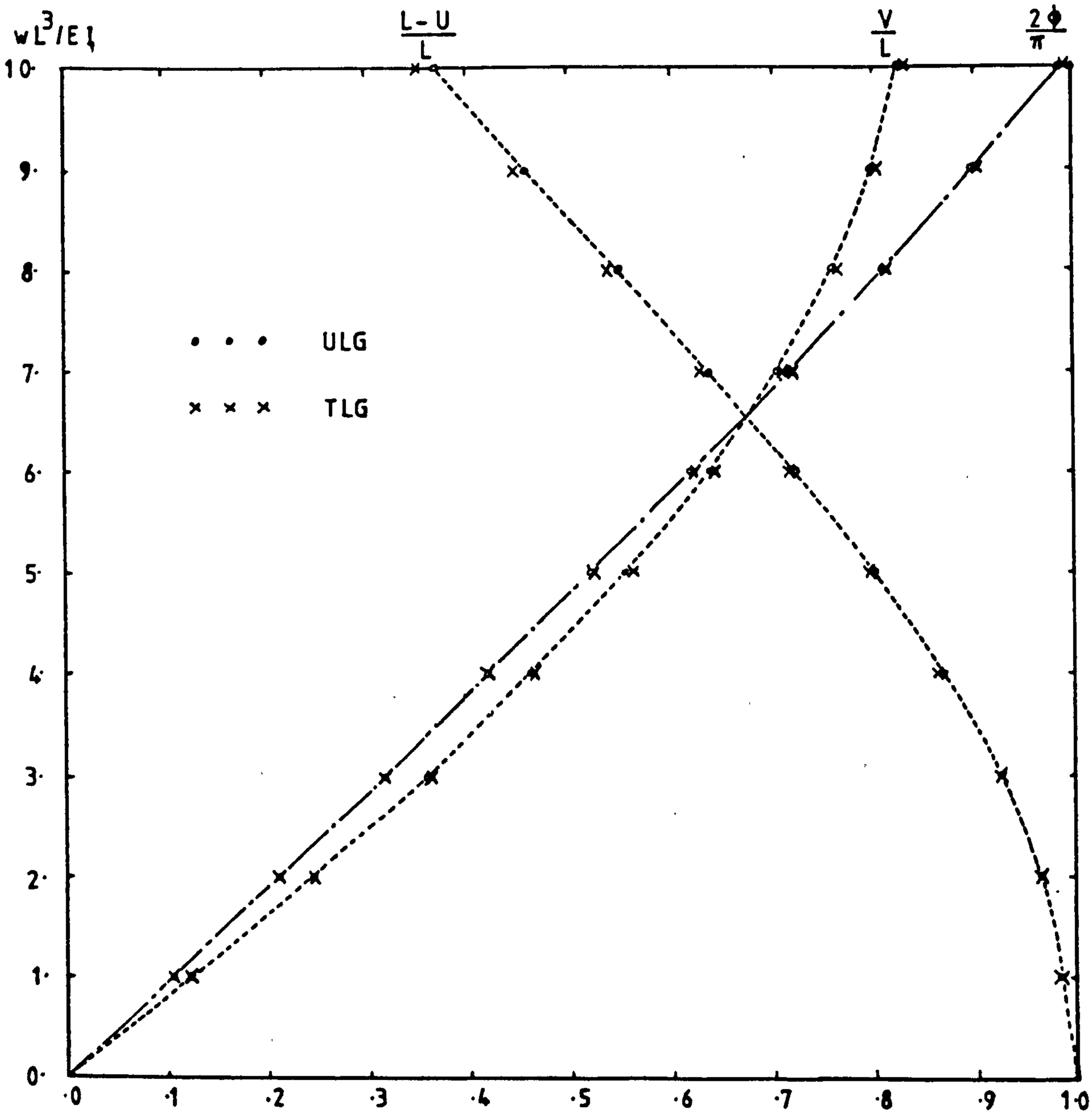

FIGURE 4.36 - Cantilever under Follower Pressure Loading - SUBBEAM Elements

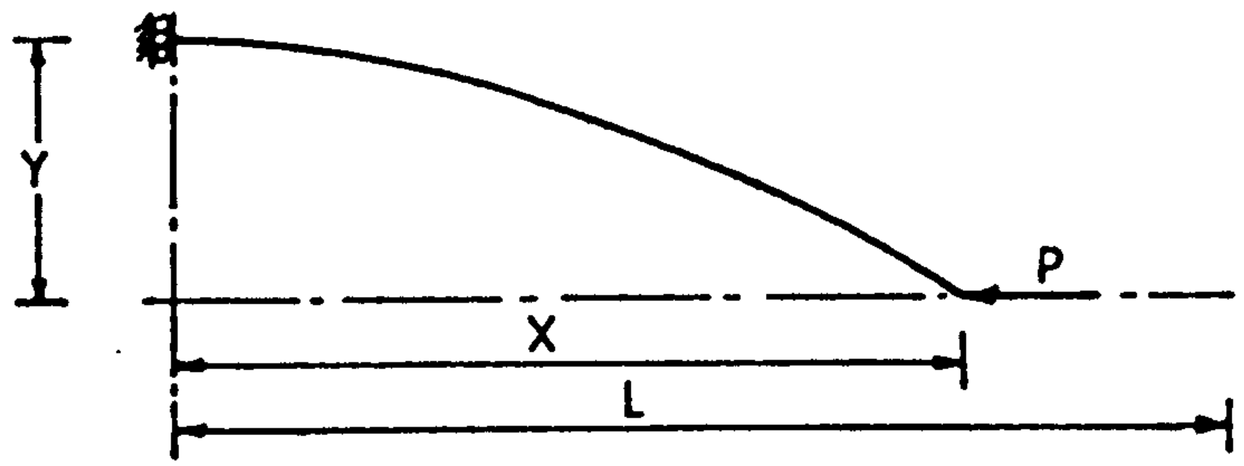

Deformed Configrations

$L = 1000$ ft. $\qquad P_{cr} = \dfrac{\pi^2 EI}{4L^2}$

$EI = 1.195 \times 10^7$ lb-ft^2

$EA = 9.46 \times 10^7$ lb

FIGURE 4.37 - Simply Supported Beam

X/L	Initial Imperfection $y_o = 2L/1000$			Initial Imperfection $y_o = L/1000$			Eccentric Modulus Matrix $e_{max} = L/1000$		
	Y/L	P/P_{cr}	Number of Iterations	Y/L	P/P_{cr}	Number of Iterations	Y/L	P/P_{cr}	Number of Iterations
1.0	0.002	1.0		0.001	1.0		0.0	1.0	
0.8	0.5326	1.1102	30	0.5326	1.1121	32	0.5326	1.1133	29
0.6	0.6973	1.25577	16	0.6973	1.2592	16	0.6972	1.2595	16
0.4	0.7797	1.4561	10	0.7797	1.4595	10	0.7796	1.4570	10
0.2	0.8059	1.7407	9	0.8059	1.7420	9	0.8059	1.7507	9
0.0	0.7826	2.1865	11	0.7826	2.1879	11	0.7826	2.1851	11
-0.2	0.7084	2.9861	13	0.7084	2.9876	13	0.7086	2.9818	14
-0.4	0.5778	4.7699	16	0.5779	4.7716	16	0.5780	4.7573	21
-0.6	0.3957	10.3558	25	0.3958	10.3574	25	0.3960	10.3054	22
-0.8	0.1951	43.5517	14	0.1951	43.5534	14	0.1952	43.1043	14

TABLE 4.12 Simply-Supported Beam Results (TLG Formulation)
10 SUBBEAM Elements.

L = 1000 ft

L/R = 2.81×10^3

EI = 1.195×10^7 lb - ft^2

EA = 9.46×10^7 lb

$$P_{cr} = \frac{\pi^2 EI}{4L^2}$$

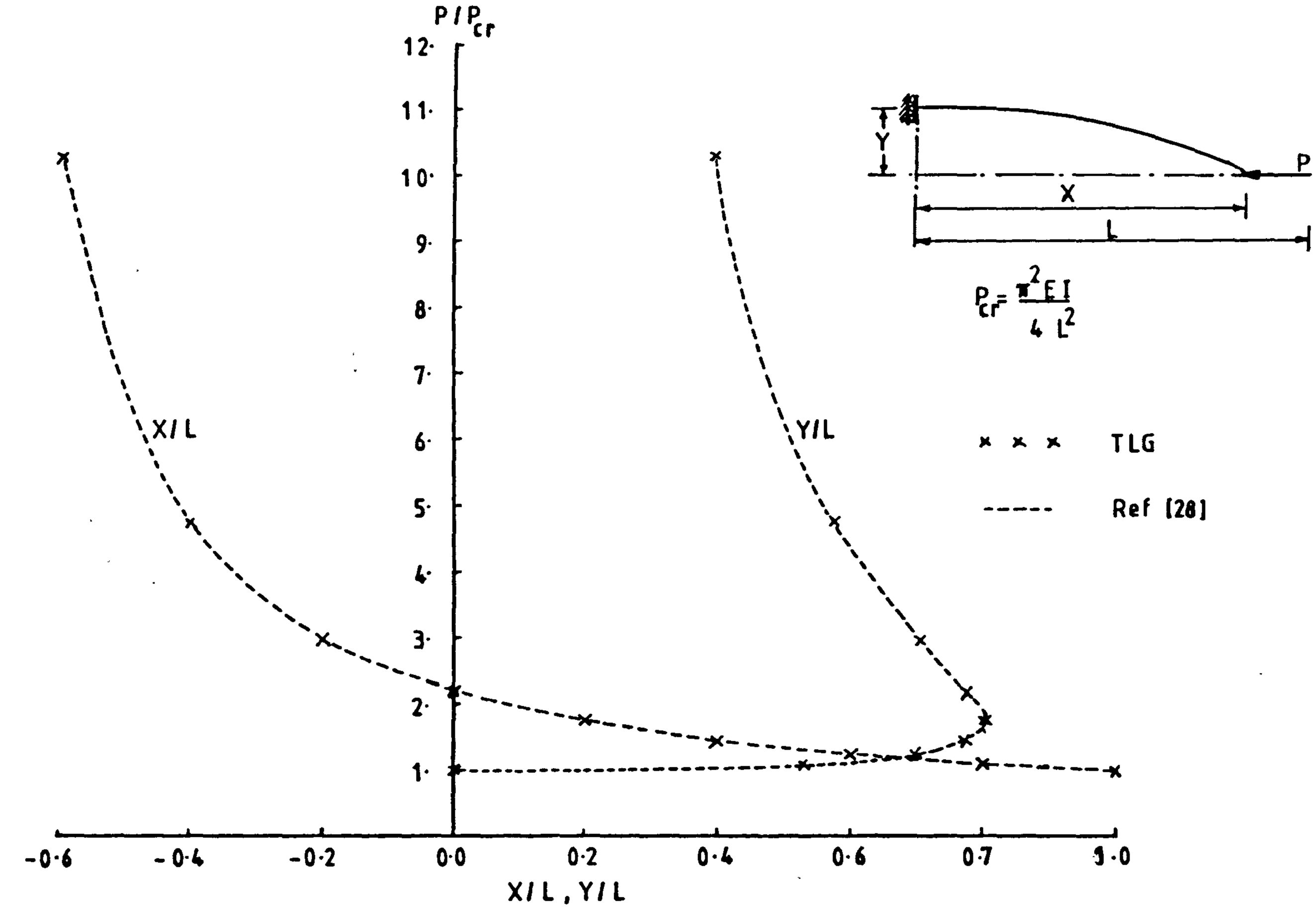

FIGURE 4.38 - Simply Supported Beam - End Position vs Load - 10 SUBBEAM Elements

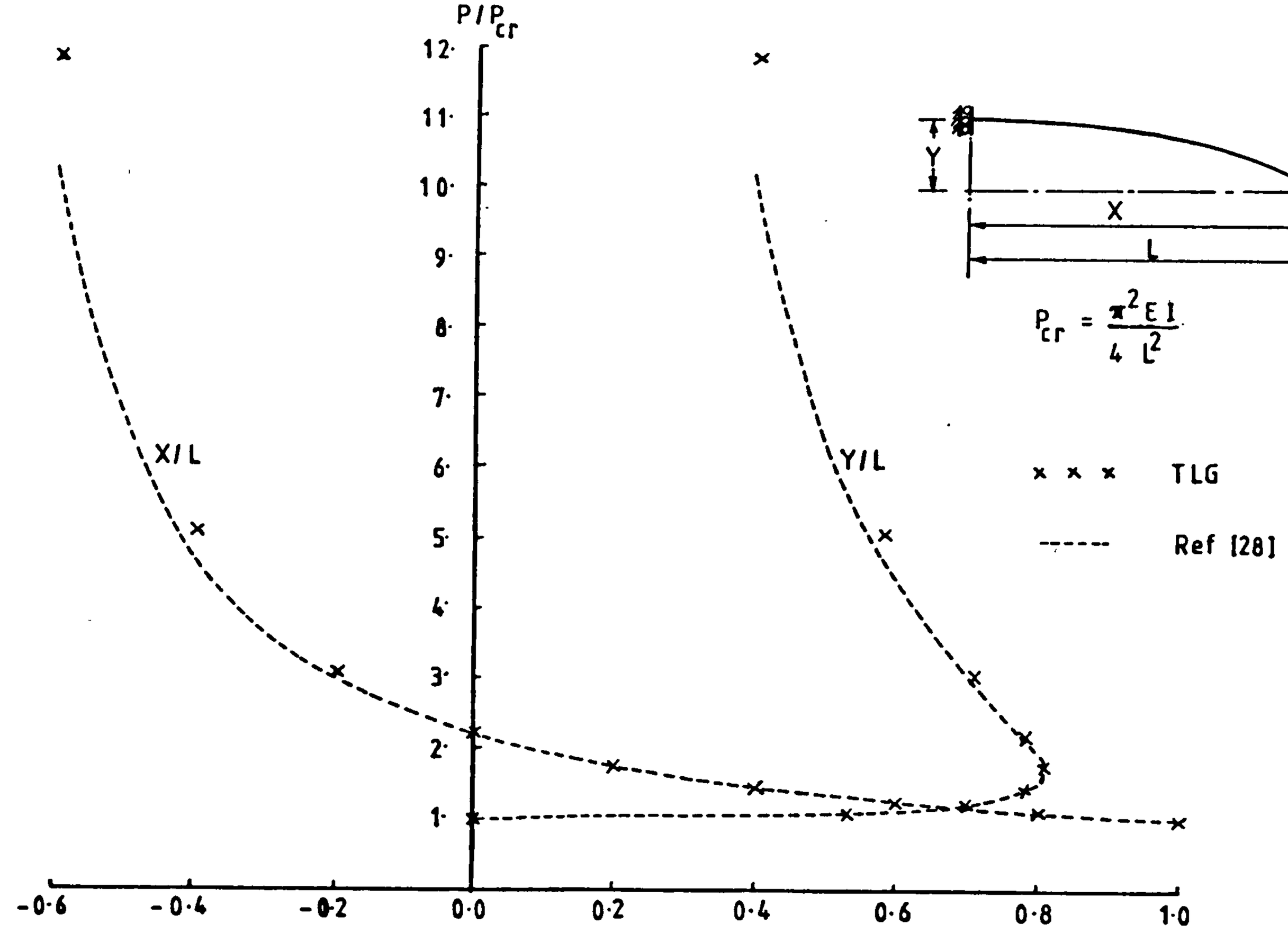

FIGURE 4.39 - Simply Supported Beam - End Position vs Load - 10 ISOBEM'2 Elements

CHAPTER 5

THREE-DIMENSIONAL LARGE ROTATION ELASTO-PLASTIC THEORY FOR THIN CURVED ECCENTRIC BEAM ELEMENTS

5.1 INTRODUCTION

A geometrically nonlinear theory for three-dimensional thin curved displacement beam finite elements, which is based on the Total Lagrangian formulation, that admits large rotations is not yet available. This is mainly due to the difficulty arising from the fact that finite rotations referred to fixed axes in space are not vector quantities and hence not commutative. This difficulty has lead to the conclusion that for three-dimensional beam elements the Updated Lagrangian formulation is numerically more effective than the Total Lagrangian formulation [20]. It has been shown, however, in Chapter 4 that the disadvantage of the Updated Lagrangian formulation is the excessive amount of computer time required compared to a Total Lagrangian solution time.

For small displacement formulations it is reasonable to assume that the rotations are small and so equal to the relevant displacement gradients for thin beams.

It is possible to obtain good results using this assumption for linear beam finite element solutions. For nonlinear solutions, once the theory is correctly formulated taking into account the assumption that displacement gradients are used as measures of rotation, the performance of the element can be expected to be of the same accuracy as that of the linear element. This is a consequence of the same convergence criteria applying for both linear and geometrically nonlinear finite element solutions[41].

It has been shown in Chapter 2 that, taking into consideration beam assumptions, exact small strain Total Lagrangian formulations, based on either the Green-Lagrange strains or the conventional strains, can be obtained for thin curved two-dimensional beams. This Chapter extends that theory to three-dimensional thin curved beam formulations. The theory presented here is based on linear elements wherein the assumption that rotations are small is used. Thus the displacement gradients, which are vectors, are used as measures of rotation. The large rotation effects are contained in the definition of the nonlinear strain-diesplacement relations. This is achieved by using a convective coordinate system within the element.

The theory is based on the assumption that plane sections remain plane and normal to the beam reference line after deformation. Distortional warping is, therefore, not permitted. The cross-section of the element is assumed to be solid rectangular for which warping can be neglected [71, 73, 74]. The cross-section can vary with length and can be eccentric (Figure 5.1). Cross-sections other than solid rectangles are considered as combinations of eccentric beam elements with a common nodal line. This presents an approximate approach for the analysis of thin walled beams. An additional assumption that longitudinal warping of the reference line is small and hence negligible is used. This amounts to assuming that the torsional curvature is small. The effects of large rotations on the torsional moments, however, are taken into consideration.

5.2 GEOMETRIC DEFINITION OF ELEMENT REFERENCE LINE

The assumptions stated above are used to define the geometric shape of the reference line before and after deformation. The nonlinear strain-displacement relations are obtained from the definition of geometry after deformation using convected coordinates.

The geometry of the reference line before deformation is defined by four nodes, three along the reference nodal line and the fourth is positioned to define the local axes (Figure 5.1). The fourth node is introduced to fix the direction of the binormal thus avoiding the difficulty that arises when using the general definition of the principal normal and the binormal (Figure 5.2), especially for straight elements. This gives the user a control on the directions of the local axes. On considering the geometry of deformation and taking variations, however, both normals are assumed to deform as principal normals.

The local x axis is tangential to the reference line from nodes 1 to 3 (Figure 5.1). The variation of the reference line geometry before deformation is defined by the three nodes and is therefore parabolic. The local z is defined to be normal to the plane formed by the two end nodes and the fourth node. The second node is assumed to lie on this plane. Local y is normal to both x and z and is defined so that x, y and z form a right-handed system. This definition of axes assumes that the four element nodes lie on one plane. Hence, for a generally curved beam the second and fourth nodes must coincide.

Referring to Figure 5.3, the local axes are defined as follows:

a) The position vector of any point on the reference line is

$$\vec{r} = X\hat{i} + Y\hat{j} + Z\hat{k} \quad \ldots \quad \ldots \quad \ldots \quad \ldots \quad \ldots \quad (5.1)$$

where the global coordinates X, Y and Z are functions of the natural coordinate ξ.

b) The unit vector (defining the local x axis) tangential to the reference line is given by the following definition

$$\hat{x} = \frac{dX/d\xi\ \hat{i} + dY/d\xi\ \hat{j} + dZ/d\xi\ \hat{k}}{((dX/d\xi)^2 + (dY/d\xi)^2 + (dZ/d\xi)^2)^{1/2}} \quad \ldots \quad (5.2)$$

c) From Figure 5.1 a vector normal to the plane 1 - 3 - 4 is

$$\vec{Z} = \vec{V}_{13} \times \vec{V}_{14} \quad \ldots \quad \ldots \quad \ldots \quad \ldots \quad \ldots \quad (5.3)$$

from which the unit vector defining the local z is obtained as

$$\hat{z} = \frac{\vec{V}_{13} \times \vec{V}_{14}}{|\vec{V}_{13} \times \vec{V}_{14}|} \quad \ldots \quad \ldots \quad \ldots \quad \ldots \quad (5.4)$$

The vector normal to plane plane 1-2-4 is

$$\vec{Z}_2 = \vec{V}_{12} \times \vec{V}_{14} \quad \ldots \quad \ldots \quad \ldots \quad \ldots \quad (5.5)$$

For node 2 to lie on plane 1-3-4, $\vec{Z}_2$ must be parallel to $\vec{Z}$ i.e.

$$\vec{Z} \times \vec{Z}_2 = 0 \quad \ldots \quad \ldots \quad \ldots \quad \ldots \quad \ldots \quad (5.5a)$$

This is used as a check for the condition that the four element nodes lie on the same plane.

d) The local y is normal to both x and z. It is defined so that x, y and z form a right-handed system. Therefore,

$$\hat{y} = \hat{z} \times \hat{x} \quad \ldots \quad \ldots \quad \ldots \quad \ldots \quad \ldots \quad (5.6)$$

5.3 DEFORMATION GEOMETRY

The position vector of a point on the beam reference line after deformation (Figure 5.3) is

$$\bar{r} = \vec{r} + \vec{V} \quad \ldots \quad \ldots \quad \ldots \quad \ldots \quad \ldots \quad \ldots \quad (5.7)$$

where $\vec{V}$ is the displacement vector and is obtained in terms of the components u, v, w in the local axes directions as

$$\vec{V} = u\,\hat{x} + v\,\hat{y} + w\,\hat{z} \qquad \ldots \quad \ldots \quad \ldots \quad \ldots \qquad (5.8)$$

Using convected coordinates and the Kirchhoff hypothesis for beams, the displacement gradient vectors for the reference line are defined from (5.7) and (5.8) as follows

$$g_x = (1 + \frac{du}{dx})\hat{x} + \frac{dv}{dx}\,\hat{y} + \frac{dw}{dx}\,\hat{z}$$

$$g_y = -\frac{dv}{dx}\,\hat{x} + \hat{y} + \frac{dw}{dy}\,\hat{z}$$

$$g_z = -\frac{dw}{dx}\,\hat{x} - \frac{dw}{dy}\,\hat{y} + \hat{z} \qquad \ldots \quad \ldots \quad \ldots \quad \ldots \qquad (5.9)$$

Referring to Figure 5.3 , the position vector of a point (y, z) before deformation is

$$\vec{R} = \vec{r} + y\hat{y} + z\hat{z} \qquad \ldots \quad \ldots \quad \ldots \quad \ldots \quad \ldots \qquad (5.10)$$

From the assumption that plane sections remain plane and normal to the reference line after deformation and using convective coordinates, the position vector of point (y, z) after deformation is given by

$$\bar{R} = \bar{r}(x) + y\,\hat{n}_y + z\,\hat{n}_z \quad \ldots \quad \ldots \quad \ldots \quad \ldots \quad (5.11)$$

in which $\hat{n}_y$ and $\hat{n}_z$ are unit vectors normal to the tangent to the reference line after deformation. These unit vectors are evaluated as follows

$$\hat{n}_y = \frac{g^y}{|g^y|}$$

$$\hat{n}_z = \frac{g^z}{|g^z|} \quad \ldots \quad \ldots \quad \ldots \quad \ldots \quad \ldots \quad \ldots \quad (5.12)$$

where g^y and g^z are vectors which are normal to the convected x coordinate surface in the deformed configuration. These vectors are reciprocals of the tangent vectors g_y and g_z respectively. The three reciprocal vectors are given in terms of the displacement gradient vectors by the following definition [12]

$$g^i = \frac{1}{2\sqrt{G}}\,\varepsilon^{ijk}\,g_j \times g_k \quad \ldots \quad \ldots \quad \ldots \quad \ldots \quad (5.13)$$

$\varepsilon^{ijk} = \varepsilon_{ijk}$ being the permutation symbol given by

$$\varepsilon_{123} = \varepsilon_{231} = \varepsilon_{312} = +1$$

$$\varepsilon_{213} = \varepsilon_{132} = \varepsilon_{321} = -1$$

$$\varepsilon_{ijk} = 0 \quad \text{if } i = j,\ j = k \text{ or } k = i \quad \ldots \quad (5.14)$$

and

$$\sqrt{G} = |g_1 \cdot (g_2 \times g_3)| = |g_x \cdot (g_y \times g_z)| \quad \ldots \quad (5.15)$$

Thus, in terms of the displacement gradient vectors (Equation (5.9)), relations (5.12) become

$$\hat{n}_y = \frac{g_z \times g_x}{|g_z \times g_x|}$$

$$\hat{n}_z = \frac{g_x \times g_y}{|g_x \times g_y|} \quad \ldots \quad \ldots \quad \ldots \quad \ldots \quad \ldots \quad (5.16)$$

Using the hypothesis that the strains normal to the reference line and the shear strains are zero, (5.16) can be written in the following form

$$\hat{n}_y = \vec{N}_y/(1 + 2e)^{1/2}$$

$$\hat{n}_z = \vec{N}_z/(1 + 2e)^{1/2} \quad \ldots \quad \ldots \quad \ldots \quad \ldots \quad (5.17)$$

where e is the Green strain measure of the reference line defined by

$$e = \frac{1}{2}(g_x \cdot g_x - 1) = \frac{du}{dx} + \frac{1}{2}(\frac{du}{dx})^2 + \frac{1}{2}(\frac{dv}{dx})^2 + \frac{1}{2}(\frac{dw}{dx})^2$$

$$\ldots \quad \ldots \quad \ldots \quad \ldots \quad (5.18)$$

The definitions of the unit vectors in (5.17) are similar to the definition of the vector $\hat{n}$ after deformation of the two-dimensional beam theory (Equation (2.10)). An approach similar to that used for the two-dimensional formulation is followed here to obtain the strain-displacement relations.

Referring to Figure 5.2, since plane sections are assumed to remain plane, the derivatives of the vectors in (5.16) with respect to the convected x coordinate are

$$\frac{d\hat{n}_y}{dx} = \tau_z \hat{n}_z - K_{xz} g_x$$

$$\frac{d\hat{n}_z}{dx} = \tau_y \hat{n}_y - K_{xy} g_x \quad \ldots \quad \ldots \quad \ldots \quad \ldots \quad (5.19)$$

where K_{xy} and K_{xz} are measures of the bending curvatures about the local y and z axes respectively, and τ_y, τ_z are the torsions about the local x of the y and z normals respectively.

From (5.11) and (5.19), the derivatives of the position vector after deformation with respect to the convected coordinate axes are given by

$$\frac{\partial \bar{R}}{\partial x} = g_x + y \frac{d\hat{n}_y}{dx} + z \frac{d\hat{n}_z}{dx}$$

$$= (1 - y K_{xz} - z K_{xy}) g_x + y \tau_z \hat{n}_z + z \tau_y \hat{n}_z$$

$$\frac{\partial \bar{R}}{\partial y} = \hat{n}_y$$

$$\frac{\partial \bar{R}}{\partial z} = \hat{n}_z \quad \ldots \quad \ldots \quad \ldots \quad \ldots \quad \ldots \quad \ldots \quad \ldots \qquad (5.20)$$

Assuming that second order terms in torsion are negligible i.e. neglecting longitudinal warping of the reference line, the components of the deformation tensor are obtained from (5.20) and (5.18) as

$$\frac{\partial \bar{R}}{\partial x} \cdot \frac{\partial \bar{R}}{\partial x} \simeq (1 + 2e)(1 - y K_{xz} - z K_{xy})^2$$

$$\frac{\partial \bar{R}}{\partial x} \cdot \frac{\partial \bar{R}}{\partial y} = z \hat{n}_y \cdot \frac{d\hat{n}_z}{dx} = z \tau_y$$

$$\frac{\partial \bar{R}}{\partial x} \cdot \frac{\partial \bar{R}}{\partial z} = y \hat{n}_z \cdot \frac{d\hat{n}_y}{dx} = y \tau_z$$

$$\frac{\partial \bar{R}}{\partial y} \cdot \frac{\partial \bar{R}}{\partial y} = \hat{n}_y \cdot \hat{n}_y = 1$$

$$\frac{\partial \bar{R}}{\partial z} \cdot \frac{\partial \bar{R}}{\partial z} = \hat{n}_z \cdot \hat{n}_z = 1$$

$$\frac{\partial \bar{R}}{\partial y} \cdot \frac{\partial \bar{R}}{\partial z} = \hat{n}_y \cdot \hat{n}_z \quad \ldots \quad \ldots \quad \ldots \quad \ldots \quad \ldots \qquad (5.21)$$

5.4 THE INTERNAL VIRTUAL WORK EXPRESSION AND NONLINEAR STRAIN-DISPLACEMENT RELATIONS

5.4.1 Conventional Strains at a General Point

Using the conventional definition of strains, the only non-zero direct strain term is ε'_{xx} in the local x axis direction. Thus, from (5.21)

$$\varepsilon'_{xx} = \left(\frac{\partial \bar{R}}{\partial x} \cdot \frac{\partial \bar{R}}{\partial x}\right)^{1/2} - 1$$

$$= (1 + 2e)^{1/2} (1 - y\, K_{xz} - z\, K_{xy}) - 1 \qquad (5.22)$$

and the shear strains are obtained from the relations

$$\frac{\partial \bar{R}}{\partial x} \cdot \frac{\partial \bar{R}}{\partial y} = z\, \tau_y = (1 + 2e)^{1/2}\, \gamma'_{xy}$$

$$\frac{\partial \bar{R}}{\partial x} \cdot \frac{\partial \bar{R}}{\partial z} = y\ _z = (1\ z\ 2e)^{1/2}\, \gamma'_{xz}$$

$$\frac{\partial \bar{R}}{\partial y} \cdot \frac{\partial \bar{R}}{\partial z} = \hat{n}_y \cdot \hat{n}_z = \gamma_{yz} \qquad \ldots \quad \ldots \quad \ldots \qquad (5.23)$$

OR

$$\gamma'_{xy} = z\, \tau_y / (1 + 2e)^{1/2}$$

$$\gamma'_{xz} = y\, \tau_z / (1 + 2e)^{1/2}$$

$$\gamma_{yz} = \hat{n}_y \cdot \hat{n}_z \qquad \ldots \quad \ldots \quad \ldots \quad \ldots \quad \ldots \qquad (5.24)$$

Therefore, from (5.22) and (5.24), the strain vector ϵ' of a general point within an element is defined as follows

$$\epsilon' = \begin{Bmatrix} (1+2e)^{1/2} - 1 - y(1+2e)^{1/2} K_{xz} - z(1+2e)^{1/2} K_{xy} \\ z\,\tau_y/(1+2e)^{1/2} \\ y\,\tau_z/(1+2e)^{1/2} \\ \gamma_{yz} \end{Bmatrix}$$

$$= H\,\epsilon^* \quad \ldots \quad \ldots \quad \ldots \quad \ldots \quad \ldots \quad \ldots \quad (5.25)$$

in which

$$H = \begin{bmatrix} 1 & z & y & 0 & 0 & 0 \\ 0 & 0 & 0 & z & 0 & 0 \\ 0 & 0 & 0 & 0 & -y & 0 \\ 0 & 0 & 0 & 0 & 0 & 1 \end{bmatrix} \quad \ldots \quad \ldots \quad (5.26)$$

and

$$\varepsilon^* = \begin{Bmatrix} e^* \\ \chi^*_{xy} \\ \chi^*_{xz} \\ \tau^*_y \\ \tau^*_z \\ \gamma_{yz} \end{Bmatrix} = \begin{Bmatrix} (1+2e)^{1/2} - 1 \\ -(1+2e)^{1/2}\, K_{xy} \\ -(1+2e)^{1/2}\, K_{xz} \\ \tau_y/(1+2e)^{1/2} \\ -\tau_z/(1+2e)^{1/2} \\ \gamma_{yz} \end{Bmatrix} \quad \ldots \quad \ldots \quad (5.27)$$

From (5.25) the variation in strain $\delta\varepsilon'$ is

$$\delta\varepsilon' = H\, \delta\, \varepsilon^* \quad \ldots \quad \ldots \quad \ldots \quad \ldots \quad \ldots \quad \ldots \quad (5.28)$$

The measures of curvature in (5.27) are now defined in terms of measures which are explicit functions of the displacement gradients, so that

$$\begin{Bmatrix} \chi^*_{xy} \\ \chi^*_{xz} \\ \tau^*_y \\ \tau^*_z \end{Bmatrix} = \frac{1}{1+2e} \begin{Bmatrix} \chi_{xy} \\ \chi_{xz} \\ \chi_y \\ \chi_z \end{Bmatrix} \quad \ldots \quad \ldots \quad \ldots \quad \ldots \quad (5.29)$$

The variations in strain $\delta\varepsilon^*$ in (5.28) are obtained from (5.27) and (5.29) as

$$\delta\,\boldsymbol{\varepsilon}^* = \mathbf{H}^*\,\delta\,\boldsymbol{\varepsilon} \quad \ldots \quad \ldots \quad \ldots \quad \ldots \quad \ldots \quad \ldots \qquad (5.30)$$

where

$$\delta\boldsymbol{\varepsilon} = \{\delta e,\ \delta\chi_{xy}\ ,\delta\chi_{xz}\ ,\delta\chi_{y}\ ,\delta\chi_{z}\ ,\ \delta\gamma_{yz}\}^{T} \quad \ldots \qquad (5.31)$$

and

$$\mathbf{H}^* = \begin{bmatrix} \frac{1}{(1+2e)^{1/2}} & 0 & 0 & 0 & 0 & 0 \\ \frac{-2\,\chi_{xy}}{(1+2e)^{2}} & \frac{1}{1+2e} & 0 & 0 & 0 & 0 \\ \frac{-2\,\chi_{xz}}{(1+2e)^{2}} & 0 & \frac{1}{1+2e} & 0 & 0 & 0 \\ \frac{-2\,\chi_{y}}{(1+2e)^{2}} & 0 & 0 & \frac{1}{1+2e} & 0 & 0 \\ \frac{-2\,\chi_{z}}{(1+2e)^{2}} & 0 & 0 & 0 & \frac{1}{1+2e} & 0 \\ 0 & 0 & 0 & 0 & 0 & 1 \end{bmatrix} \qquad (5.32)$$

From (5.28) and (5.30), the internal virtual work expression in a Lagrangian frame of reference at time t (Equation (1.2)) takes the following form:

$$\delta W_{int} = \int_{V_t} \delta \varepsilon_t'^{T} S_t \, dV_t$$

$$= \int_{V_t} \delta \varepsilon_t^{T} H^{*T} \int_{A_t} H^{T} S_t \, dA_t \, dL_t \ldots \qquad (5.33)$$

5.4.2 Green-Lagrange Strains at a General Point

The Green-Lagrange strain tensor in three dimensions is

$$[\varepsilon'] = \frac{1}{2}\left(\begin{bmatrix} \frac{\partial \bar{R}}{\partial x} \cdot \frac{\partial \bar{R}}{\partial x} & \frac{\partial \bar{R}}{\partial x} \cdot \frac{\partial \bar{R}}{\partial y} & \frac{\partial \bar{R}}{\partial x} \cdot \frac{\partial \bar{R}}{\partial z} \\ \frac{\partial \bar{R}}{\partial y} \cdot \frac{\partial \bar{R}}{\partial x} & \frac{\partial \bar{R}}{\partial y} \cdot \frac{\partial \bar{R}}{\partial y} & \frac{\partial \bar{R}}{\partial y} \cdot \frac{\partial \bar{R}}{\partial z} \\ \frac{\partial \bar{R}}{\partial z} \cdot \frac{\partial \bar{R}}{\partial x} & \frac{\partial \bar{R}}{\partial z} \cdot \frac{\partial \bar{R}}{\partial y} & \frac{\partial \bar{R}}{\partial z} \cdot \frac{\partial \bar{R}}{\partial z} \end{bmatrix} - \begin{bmatrix} 1 & 0 & 0 \\ 0 & 1 & 0 \\ 0 & 0 & 1 \end{bmatrix} \right)$$

$$\ldots \quad \ldots \quad \ldots \quad \ldots \quad \ldots \qquad (5.34)$$

The Green-Lagrange strain vector is given from (5.21) and (5.34) by

$$\varepsilon' = \begin{Bmatrix} \varepsilon_{xx} \\ \gamma_{xy} \\ \gamma_{xz} \\ \gamma_{yz} \end{Bmatrix} = \begin{Bmatrix} (1 - y\, K_{xz} - z\, K_{xy})^2 (\frac{1}{2} + e) - \frac{1}{2} \\ z\, \tau_y \\ y\, \tau_z \\ \hat{n}_y \cdot \hat{n}_z \end{Bmatrix} \qquad (5.35)$$

Assuming proportionality between the 2nd Piola-Kirchhoff stresses and the Green-Lagrange strains in the virtual work equation, thus neglecting the coupling between the strain resultant measures the Green-Lagrange strain vector ϵ' and its variation $\delta\epsilon'$ are written as

$$\epsilon' = \mathbf{H}\,\epsilon$$

$$\delta\epsilon' = \mathbf{H}\,\delta\epsilon \quad \ldots \quad \ldots \quad \ldots \quad \ldots \quad \ldots \quad \ldots \qquad (5.36)$$

wherein H is given by (5.26)

The strain resultants ϵ are defined by

$$\epsilon = \{e,\ \chi_{xy}\ ,\ \chi_{xz}\ ,\ \chi_{y}\ ,\ \chi_{z}\ ,\ \gamma_{yz}\}^{T} \quad \ldots \qquad (5.37)$$

The internal virtual work expression (Equation (1.2)) now takes the following form

$$\delta W_{int} = \int_{V_t} \delta\epsilon_t'^{T}\ S_t\ dV_t$$

$$= \int_{L_t} \delta\epsilon_t^{T} \int_{A_t} H^{T}\ S_t\ dL_t \quad \ldots \quad \ldots \qquad (5.38)$$

5.4.3 Strain Resultants in Terms of Displacement Gradients

From (5.29), (5.27), (5.19) and (5.18), the generalised Strain resultant measures $\boldsymbol{\varepsilon}$ are

$$\boldsymbol{\varepsilon} = \begin{Bmatrix} e \\ \chi_{xy} \\ \chi_{xz} \\ \chi_{y} \\ \chi_{z} \\ \gamma_{yz} \end{Bmatrix} = \begin{Bmatrix} \frac{1}{2}(\mathbf{g}_x \cdot \mathbf{g}_x - 1) \\ ((1+2e)^{3/2}\, \frac{d\hat{\mathbf{n}}_z}{dx} \cdot \mathbf{g}_x)/(\mathbf{g}_x \cdot \mathbf{g}_x) \\ ((1+2e)^{3/2}\, \frac{d\hat{\mathbf{n}}_y}{dx} \cdot \mathbf{g}_x)/(\mathbf{g}_x \cdot \mathbf{g}_x) \\ (1+2e)^{1/2}\, \frac{d\hat{\mathbf{n}}_z}{dx} \cdot \hat{\mathbf{n}}_y \\ -(1+2e)^{1/2}\, \frac{d\hat{\mathbf{n}}_y}{dx} \cdot \hat{\mathbf{n}}_z \\ \hat{\mathbf{n}}_y \cdot \hat{\mathbf{n}}_z \end{Bmatrix} \qquad (5.39)$$

The explicit form of the relations in (5.39) are obtained as follows:

a) For the unit vectors in (5.15) a binomial series expansion, neglecting third and higher order terms in displacement derivatives, gives

$$\hat{n}_y \approx (-\frac{dw}{dx}\ \frac{dw}{dy} - \frac{dv}{dx}(1 - \frac{du}{dx}))\hat{x} + (1 - \frac{1}{2}(\frac{dv}{dx})^2 - \frac{1}{2}(\frac{dw}{dy})^2)\hat{y}$$

$$+ (\frac{dw}{dy} - \frac{dv}{dx}\ \frac{dw}{dx})\hat{z}$$

$$\hat{n}_z \approx (\frac{dv}{dx}\ \frac{dw}{dy} - \frac{dw}{dx}(1 - \frac{du}{dx}))\hat{x} + (-\frac{dw}{dy} - \frac{dv}{dx}\ \frac{dw}{dx})\hat{y}$$

$$+ (1 - \frac{1}{2}(\frac{dv}{dx})^2 - \frac{1}{2}(\frac{dw}{dy})^2)\hat{z} \qquad \ldots \quad \ldots \quad \ldots \qquad (5.40)$$

The derivatives $\frac{d\hat{n}_y}{dx}$ and $\frac{d\hat{n}_z}{dx}$ are then obtained from (5.40) as

$$\frac{d\hat{n}_y}{dx} = (-\frac{d^2w}{dx^2}\ \frac{dw}{dy} - \frac{dw}{dx}\ \frac{d^2w}{dxdy} - \frac{d^2v}{dx^2}(1 - \frac{du}{dx}) + \frac{dv}{dx}\ \frac{d^2u}{dx^2})\hat{x}$$

$$+ (-\frac{dv}{dx}\ \frac{d^2v}{dx^2} - \frac{dw}{dy}\ \frac{d^2w}{dxdy})\hat{y} + (\frac{d^2w}{dxdy} - \frac{dw}{dx}\ \frac{d^2v}{dx^2} - \frac{dv}{dx}\ \frac{d^2w}{dx^2})\hat{z}$$

$$\frac{d\hat{n}_z}{dx} = (\frac{d^2v}{dx^2}\ \frac{dw}{dy} + \frac{dv}{dx}\ \frac{d^2w}{dxdy} - \frac{d^2w}{dx^2}(1 - \frac{du}{dx}) + \frac{dw}{dx}\ \frac{d^2u}{dx^2})\hat{x}$$

$$+(-\frac{d^2w}{dxdy} - \frac{dw}{dx}\ \frac{d^2v}{dx^2} - \frac{dv}{dx}\ \frac{d^2w}{dx^2})\hat{y} + (-\frac{dw}{dx}\ \frac{d^2w}{dx^2} - \frac{dw}{dy}\ \frac{d^2w}{dxdy})\hat{z}$$

$$\ldots \quad \ldots \quad \ldots \quad \ldots \quad \ldots \quad \ldots \qquad (5.41)$$

b) The deformation measures are, therefore, given from (5.9), (5.40) and (5.41), neglecting third and higher order terms in displacement derivatives, by

$$g_x \cdot g_x = 1 + 2\frac{du}{dx} + \left(\frac{du}{dx}\right)^2 + \left(\frac{dv}{dx}\right)^2 + \left(\frac{dw}{dx}\right)^2$$

$$\frac{d\hat{n}_y}{dx} \cdot g_x \simeq -\frac{d^2v}{dx^2} + \frac{dv}{dx}\frac{d^2u}{dx^2} - \frac{dw}{dy}\frac{d^2w}{dx^2}$$

$$\frac{d\hat{n}_z}{dx} \cdot g_x \simeq -\frac{d^2w}{dx^2} + \frac{dw}{dx}\frac{d^2u}{dx^2} + \frac{dw}{dy}\frac{d^2v}{dx^2}$$

$$\frac{d\hat{n}_z}{dx} \cdot \hat{n}_y = -\frac{d^2w}{dxdy} - \frac{dw}{dx}\frac{d^2v}{dx^2}$$

$$\frac{d\hat{n}_y}{dx} \cdot \hat{n}_z = -\frac{d^2w}{dxdy} - \frac{dv}{dx}\frac{d^2w}{dx^2}$$

$$\hat{n}_y \cdot \hat{n}_z = -\frac{dv}{dx}\frac{dw}{dx} \quad \ldots \quad \ldots \quad \ldots \quad \ldots \quad \ldots \quad (5.42)$$

c) Substituting from (5.42) and (5.18) into (5.39) using the binomial series expansion and neglecting third and higher order terms in displacement derivatives, the following relations for the strain resultants ϵ in terms of the displacement gradients are obtained

$$\varepsilon = \begin{Bmatrix} \frac{du}{dx} + \frac{1}{2}\left(\frac{du}{dx}\right)^2 + \frac{1}{2}\left(\frac{dv}{dx}\right)^2 + \frac{1}{2}\left(\frac{dw}{dx}\right)^2 \\ -\frac{d^2w}{dx^2}\left(1 + \frac{du}{dx}\right) + \frac{dw}{dx}\frac{d^2u}{dx^2} + \frac{dw}{dy}\frac{d^2v}{dx^2} \\ -\frac{d^2v}{dx^2}\left(1 + \frac{du}{dx}\right) + \frac{dv}{dx}\frac{d^2u}{dx^2} - \frac{dw}{dy}\frac{d^2w}{dx^2} \\ -\frac{d^2w}{dxdy}\left(1 + \frac{du}{dx}\right) - \frac{dw}{dx}\frac{d^2v}{dx^2} \\ -\frac{d^2w}{dxdy}\left(1 + \frac{du}{dx}\right) + \frac{dv}{dx}\frac{d^2w}{dx^2} \\ -\frac{dv}{dx}\frac{dw}{dx} \end{Bmatrix} \quad \ldots \quad (5.43)$$

C^1 continuity in all three displacement components is a necessary requirement for relations (5.43). It has been shown in Chapter 4 that the equations become indefinite if strain-displacement relations similar to (5.43) are used with elements which are only C^o continuous in the in-plane displacement in a Total Lagrangian solution of large rotation and curvature problems. Approximate strain-displacement relations based on the conventional strains can be used in these elements. Using the binomial series expansion and neglecting third and higher order terms in displacement derivatives, the following relationship is obtained from Equations (5.19), (5.25) and (5.42)

$$\varepsilon' \simeq H\begin{Bmatrix} \frac{du}{dx} + \frac{1}{2}(\frac{dv}{dx})^2 + \frac{1}{2}(\frac{dw}{dx})^2 \\ -\frac{d^2w}{dx^2}(1 - \frac{du}{dx}) + \frac{dw}{dx}\frac{d^2u}{dx^2} + \frac{dw}{dy}\frac{d^2v}{dx^2} \\ -\frac{d^2v}{dx^2}(1 - \frac{du}{dx}) + \frac{dv}{dx}\frac{d^2u}{dx^2} - \frac{dw}{dy}\frac{d^2w}{dx^2} \\ -\frac{d^2w}{dxdy}(1 - \frac{du}{dx}) - \frac{dw}{dx}\frac{d^2v}{dx^2} \\ -\frac{d^2w}{dxdy}(1 - \frac{du}{dx}) + \frac{dv}{dx}\frac{d^2w}{dx^2} \\ -\frac{dv}{dx}\frac{dw}{dx} \end{Bmatrix} \quad \ldots \quad (5.43a)$$

5.5 STRESS-STRAIN RELATIONS

Since the strains are assumed to be small the stress-strain relations are considered to be the same as the constitutive relations employed in small displacement elasto-plastic formulations.

5.5.1 Elastic Material

For an elastic material, the stresses at a general point (y, z) are given in terms of the strains by

$$\mathbf{S} = \begin{Bmatrix} S_{xx} \\ \tau_{xy} \\ \tau_{xz} \\ \tau_{yz} \end{Bmatrix} = \begin{bmatrix} E & 0 & 0 & 0 \\ 0 & G/k_s & 0 & 0 \\ 0 & 0 & G/k_s & 0 \\ 0 & 0 & 0 & G/k_s \end{bmatrix} \begin{Bmatrix} \varepsilon_{xx} \\ \gamma_{xy} \\ \gamma_{xz} \\ \gamma_{yz} \end{Bmatrix}$$

OR

$$\mathbf{S} = \mathbf{D}^e \boldsymbol{\varepsilon}' \quad \ldots \quad \ldots \quad \ldots \quad \ldots \quad \ldots \quad \ldots \quad (5.44)$$

where E is Young's modulus and G is the shear modulus. The factor k_s included in the shear terms to improve the shear displacement approximation is taken as 1.2 [10].

From (5.38) (or (5.33)), (5.44) and (5.36) (or (5.28)), the stress resultants are

$$\bar{\mathbf{S}} = \int_A \mathbf{H}^T \mathbf{S} \, dA = \int_y \int_z \mathbf{H}^T \mathbf{D}^e \mathbf{H} \, dy \, dz \, \boldsymbol{\varepsilon}$$

$$= \bar{\mathbf{D}}^e \boldsymbol{\varepsilon} \quad \ldots \quad \ldots \quad \ldots \quad \ldots \quad (5.45)$$

in which $\bar{\mathbf{D}}^e$ is the modulus matrix given from (5.45) and (5.26) by

$$\bar{D}^e = \int_y \int_z \begin{bmatrix} E & Ez & Ey & 0 & 0 & 0 \\ & Ez^2 & Eyz & 0 & 0 & 0 \\ & & Ey^2 & 0 & 0 & 0 \\ & & & \frac{Gz^2}{k_s} & 0 & 0 \\ & & & & \frac{Gy^2}{k_s} & 0 \\ & & & & & \frac{G}{k_s} \end{bmatrix} dy\ dx \quad \ldots \quad (5.46)$$

For an eccentric rectangular cross-section carrying out the integration in (5.46) explicitly gives

$$\bar{D}^e = \begin{bmatrix} EA & EA\ e_z & EA\ e_y & 0 & 0 & 0 \\ & E(I_{zz}+Ae_z^2) & EA\ e_y e_z & 0 & 0 & 0 \\ & & E(I_{yy}+Ae_y^2) & 0 & 0 & 0 \\ & & & \frac{G}{k_s}(I_{zz}+Ae_z^2) & 0 & 0 \\ & & & & \frac{G}{k_s}(I_{yy}+Ae_y^2) & 0 \\ & & & & & \frac{GA}{k_s} \end{bmatrix} \quad \ldots \quad \ldots \quad \ldots \quad \ldots \quad (5.47)$$

where A is the area of the cross-section, e_y , e_z are the eccentricities along the local y, z axes respectively, and I_{yy} , I_{zz} are the second moments of area about the centroidal axes of the cross-section.

The relations for torsion in (5.47) are strictly true for a circular cross-section only. These relations are modified to represent exactly the torsion of a rectangular cross-section, so that

$$\bar{D}^e = \begin{bmatrix} EA & EA\,e_y & 0 & 0 & 0 \\ & E(I_{zz}+Ae_z^2) & EA\,e_y\,e_z & 0 & 0 & 0 \\ & & E(I_{yy}+Ee_y^2) & 0 & 0 & 0 \\ & & & Gk_1\,I_{zz} & 0 & 0 \\ & & & & Gk_2\,I_{yy} & 0 \\ & \text{Symm} & & & & \frac{GA}{k_s} \end{bmatrix} \quad \ldots \quad \ldots \quad \ldots \quad \ldots \qquad (5.47a)$$

The factors k_1 and k_2 are defined in terms of the cross-section dimensions d and b (Figure 5.1) as follows [8]

$$k_1 = 2\left[1 - 0.63\,\frac{d}{b} + 0.052\left(\frac{d}{b}\right)^2\right] \qquad d \leq b$$

$$k_2 = k_1 \times \left(\frac{d}{b}\right)^2$$

$$k_2 = 2\left[1 - 0.63\,\frac{b}{d} + 0.052\left(\frac{b}{d}\right)^2\right] \qquad d > b$$

$$k_1 = k_2 \times \left(\frac{b}{d}\right)^2$$

... ... (5.47b)

Alternatively, the integration in (5.46) can be carried out numerically. Referring to Figure 5.1, the local coordinates (y, z) of the corner nodes of the cross-section at any point ξ along the element are interpolated from the coordinates of the cross-sections at the three nodes to give

$$y_i = \sum_{i=1}^{3} \bar{N}_i\, y_n \qquad n = j + 4(i-1),\ j=1,\ 4$$

$$z_j = \sum_{i=1}^{3} \bar{N}_i\, z_n \qquad \text{... ... ...} \qquad (5.48)$$

in which $\bar{N}_i$ are the parabolic interpolation functions.

The modulus matrix (Equation (5.46))at any point along the beam is then obtained by using the coordinates (5.48), the shape functions of the 4-node isoparametric

element and a 2 x 2 numerical integration rule. The modification of the torsional rigidity presented in (5.47a) and (5.47b), however, is not included in this case. Thus, the shear stresses are correctly evaluated only for a concentric square cross-section.

5.5.2 Elasto-Plastic Material

For elasto-plastic materials, the stress increments at a general point are related to the strain increments by

$$\Delta \mathbf{S} = \mathbf{D}(S, k)\Delta \boldsymbol{\epsilon}' \quad \ldots \quad \ldots \quad \ldots \quad \ldots \quad \ldots \quad \ldots \quad (5.49)$$

in which **D** is the elasto-plastic modulus matrix (Equation (1.28)),

S is the current stress level, and

k is a strain hardening factor.

Using the von-Mises yield criterion (Equation (1.27)), for beams the following inequality must hold for any stress state

$$f = \frac{1}{\sigma_y^2}\left(S_{xx}^2 + 3\,\tau_{xy}^2 + 3\,\tau_{xz}^2 + 3\,\tau_{ys}^2\right) = \frac{\bar{\sigma}^2}{\sigma_y^2} \leqslant 1$$

$$\ldots \quad \ldots \quad \ldots \quad \ldots \quad (5.50)$$

where σ_y is the uniaxial yield stress and

$\bar{\sigma}$ is the effective stress.

Therefore, from (5.50)

$$\frac{\partial f}{\partial \mathbf{s}} = \frac{1}{\sigma y^2} \{2\, S_{xx} ,\ 6\, \tau_{xy} ,\ 6\, \tau_{xz} ,\ 6\, \tau_{yz}\}^T \quad \ldots \qquad (5.51)$$

From (1.28), (5.44) and (5.51), the elasto-plastic modulus matrix is defined as follows

$$\mathbf{D}(\mathbf{s},\ k) = \mathbf{D}^e - \mathbf{D}^e \{\frac{\partial f}{\partial \mathbf{s}}\}\ \{\frac{\partial f}{\partial \mathbf{s}}\}^T\ \mathbf{D}^e / r \quad \ldots \ \ldots \qquad (5.52)$$

The factor r is given for isotropic hardening by

$$r = \{\frac{\partial f}{\partial \mathbf{s}}\}^T\ \mathbf{D}^e\ \{\frac{\partial f}{\partial \mathbf{s}}\} + \frac{4\ E\ k\ \bar{\sigma}^2}{\sigma_y^4} \quad \ldots \ \ldots \ \ldots \qquad (5.53)$$

in which k is the hardening parameter given by

$$k = E_p/(E - E_p)$$

E_p being the post yield uniaxial modulus for a bilinear strain hardening material.

The plastic strain rate multiplier λ (Equation (1.30)) is obtained from (5.51) and (5.53) as follows

$$\lambda = \frac{1}{r}\ \{\frac{\partial f}{\partial \mathbf{s}}\}^T\ \mathbf{D}^e\ \Delta\boldsymbol{\varepsilon}' \quad \ldots \ \ldots \ \ldots \ \ldots \ \ldots \qquad (5.55)$$

From (5.49) and (5.36) (or (5.28)), the relation between the increments in stress resultants (5.45) and the generalised strain increments now takes the form

$$\Delta \bar{\mathbf{S}} = \int_A \mathbf{H}^T \Delta \mathbf{S} \, dA$$

$$= \int_z \int_y \mathbf{H}^T \mathbf{D}(\mathbf{s}, k)\mathbf{H} \, dy \, dz \, \Delta\boldsymbol{\epsilon}$$

$$= \bar{\mathbf{D}}(\mathbf{s}, k)\Delta\boldsymbol{\epsilon} \quad \ldots \quad \ldots \quad \ldots \quad \ldots \quad \ldots \quad (5.56)$$

Thus, $\bar{\mathbf{D}}(\mathbf{s}, k)$ is the tangential elasto-plastic rigidity matrix that relates the stress resultant increments to the generalised strain resultant increments $\Delta\boldsymbol{\epsilon}$ of the beam beam reference line.

The integral in (5.56) for $\bar{\mathbf{D}}(\mathbf{s}, k)$ is evaluated numerically using the local y, z coordinates of the cross-section (Equation (5.48)), the shape functions of the four node isoparametric element and a 5 x 5 Gauss point rule. For beams under torsion, however, the tangential elasto-plastic rigidity matrix evaluated in this manner is correct only for a concentric square cross-section.

The state of stress at a general point within the element is evaluated by employing the sub-incremental technique [33] because of the complex non-linear nature of the elasto-plastic modulus matrix (Equation (5.49)). In

this technique the strain increment $\Delta\varepsilon'$ is divided into n sub-increments $\Delta^j \Delta\varepsilon'$, j = 1, n. The stress sub-increments are then determined from the linearised version of Equation (5.49) as

$$\Delta S^j = D(s^j, k)\Delta^j\Delta\varepsilon' \quad \ldots \quad \ldots \quad \ldots \quad \ldots \quad (5.57)$$

from which the new total stresses are given by

$$S^{j+1} = S^j + \Delta S^j \quad \ldots \quad \ldots \quad \ldots \quad \ldots \quad \ldots \quad (5.58)$$

This procedure is repeated for the n strain sub-increments. Thus, the total stresses are evaluated following the stress-strain curve more accurately. The advantage of the sub-incremental technique is that fewer load increments can be used for a given accuracy.

5.6 THE INCREMENTAL EQUILIBRIUM EQUATIONS

In formulating the incremental equilibrium equations the applied load vector is assumed to be conservative. Thus, the load correction stiffness matrix which is unsymmetrical is neglected. In Section 5.6.3 the effect of follower pressure loads and applied concentrated moments is introduced to the equilibrium equations as a modification of the applied load vector.

5.6.1 Total Lagrangian Formulation Based on Green Strains (TLG)

The strains at a general point are written from (5.36) and (5.43) in terms of the displacement gradients in the following form

$$\varepsilon' = H\{\varepsilon_o^o + \varepsilon_o^L\} \quad \ldots \quad \ldots \quad \ldots \quad \ldots \quad \ldots \quad (5.59)$$

where ε_o^o , the infinitesimal strain, is given in a finite element representation by

$$\varepsilon_o^o = \{\frac{du_o}{dx} , -\frac{d^2w_o}{dx^2} , -\frac{d^2v_o}{dx^2} , -\frac{d^2w_o}{dxdy} , -\frac{d^2w_o}{dxdy} , 0\}^T$$

$$= \bar{B}_o a_o \quad \ldots \quad \ldots \quad \ldots \quad \ldots \quad \ldots \quad \ldots \quad \ldots \quad (5.60)$$

a_o being the vector of nodal variables.

The nonlinear strain ε_o^L is written in terms of the displacement gradients as

$$\varepsilon_o^L = \frac{1}{2} A_\theta \theta_o = \frac{1}{2} \bar{B}_L(a_o) a_o \quad \ldots \quad \ldots \quad \ldots \quad (5.61)$$

in which

$$
\mathbf{A}_\theta = \begin{bmatrix}
\frac{du}{dx} & \frac{dv}{dx} & \frac{dw}{dx} & 0 & 0 & 0 & 0 & 0 \\
-\frac{d^2w}{dx^2} & 0 & -\frac{d^2u}{dx^2} & \frac{dw}{dx} & -\frac{dw}{dy} & \frac{du}{dx} & \frac{d^2v}{dx^2} & 0 \\
-\frac{d^2v}{dx^2} & \frac{d^2u}{dx^2} & 0 & \frac{dv}{dx} & \frac{du}{dx} & \frac{dw}{dy} & -\frac{d^2w}{dx^2} & 0 \\
-\frac{d^2w}{dxdy} & 0 & -\frac{d^2v}{dx^2} & 0 & \frac{dw}{dx} & 0 & 0 & \frac{du}{dx} \\
-\frac{d^2w}{dxdy} & \frac{d^2w}{dx^2} & 0 & 0 & 0 & -\frac{dv}{dx} & 0 & \frac{du}{dx} \\
0 & -\frac{dw}{dx} & -\frac{dv}{dx} & 0 & 0 & 0 & 0 & 0
\end{bmatrix}
$$

... ... (5.62)

and

$$
\theta_o = \{\frac{du_o}{dx}, \frac{dv_o}{dx}, \frac{dw_o}{dx}, \frac{d^2u_o}{dx^2}, -\frac{d^2v_o}{dx^2}, -\frac{d^2w_o}{dx^2}, \frac{dw_o}{dy}, -\frac{d^2w_o}{dxdy}\}^T
$$

$$
= G_o\, a_o \qquad \ldots \quad \ldots \quad \ldots \quad \ldots \quad \ldots \quad \ldots \qquad (5.63)
$$

Taking variations of (5.59) with respect to the nodal variables, the strain-displacement matrix B is given by

$$
B = B_o + B_L(u_o) = H[\bar{B}_o + \bar{B}_L(a_o)]
$$

$$
= H\,\bar{B} \qquad \ldots \quad \ldots \quad \ldots \quad \ldots \qquad (5.64)
$$

From (5.38), the nonlinear equilibrium equations now become

$$\psi = \int_{L_o} \bar{B}^T \int_{A_o} H^T S_o \, dA_o \, dL_o - R$$

$$= \int_{L_o} \bar{B}^T S_o \, dL_o - R = 0 \quad \ldots \quad \ldots \quad \ldots \quad (5.65)$$

The vector of stress resultants $\bar{S}_o$ is given

by

$$\bar{S}_o = \int_{A_o} H^T S_o \, dA$$

$$= \{P, M_{xy}, M_{xz}, T_y, T_z, F_{yz}\}^T \quad .. \quad (5.66)$$

where P is the axial force,

M_{xy} , M_{xz} are the bending moments about the y, z axes respectively,

T_y , T_z are the moments due to the torsions about the x axis of the y, z axes respectively (Total torque T $= T_y + T_z$), and

F_{yz} is the shear force. (See Figure 5.4).

From (5.65), (5.64) and (5.56), the tangent stiffness matrix (Equation (1.14)) now takes the following form

$$K_T = \frac{\partial \Psi}{\partial a} = \int_{L_o} \bar{B}^T \bar{D}\, \bar{B}\, dL_o + \int_{L_o} \frac{\partial \bar{B}^T}{\partial a} \bar{S}_o\, dL_o$$

$$= \int_{L_o} \bar{B}^T \bar{D}\, \bar{B}\, dL_o + \int_{L_o} G_o^T\, \bar{P}_{oi}\, G_o\, dL_o$$

$$= (K_o + K_L(a_o)) + K_\sigma \quad \ldots \quad \ldots \quad \ldots \quad \ldots \quad (5.67)$$

in which $\bar{P}_{oi}$ is the initial stress matrix which is defined in terms of the initial stress resultants (Equation (5.66)) by

$$\bar{P}_{oi} = \begin{bmatrix} [P_i] & [M_1] & [T_1] \\ & 0 & [M_2] \\ \text{Symm} & & 0 \end{bmatrix} \quad \ldots \quad \ldots \quad \ldots \quad \ldots \quad (5.68)$$

where

$$[P_i]_{3x3} = \begin{bmatrix} P & 0 & 0 \\ 0 & P & -F_{yz} \\ 0 & -F_{yz} & P \end{bmatrix}$$

$$[M_1]_{3x3} = \begin{bmatrix} 0 & M_{xz} & M_{xy} \\ M_{xz} & 0 & -T_z \\ M_{xy} & T_y & 0 \end{bmatrix}$$

$$[T_1]_{3x2} = \begin{bmatrix} 0 & (T_y + T_z) \\ 0 & 0 \\ 0 & 0 \end{bmatrix}$$

$$[M_2]_{3x2} = \begin{bmatrix} 0 & 0 \\ -M_{xy} & 0 \\ M_{xz} & 0 \end{bmatrix} \quad \ldots \quad \ldots \quad \ldots \quad \ldots \quad \ldots \quad (5.69)$$

5.6.2 Total Lagrangian Formulation Based on Conventional Strains (TLC)

The variation in the conventional strain is written from (5.28), (5.30) and (5.64) in a finite element representation as follows.

$$\delta\varepsilon'_o = H H^* \delta\varepsilon_o = H H^* \bar{B} \delta a_o$$
$$= H B^* \delta a_o \quad \ldots \quad \ldots \quad \ldots \quad (5.70)$$

From (5.70), (5.56) and (5.38), the nonlinear equilibrium equations then become

$$\psi = \int_{L_o} B^{*T} \bar{S}_o \, dL_o - R = O \quad \ldots \quad \ldots \quad \ldots \qquad (5.71)$$

$\bar{S}_o$ being the stress resultant vector defined in (5.66).

The tangent stiffness matrix is obtained by differentiating (5.71) with respect to the nodal variables. Thus,

$$K_T = \frac{\partial \psi}{\partial a} = \int_{L_o} B^{*T} \bar{D} B^* \, dL_o + \int_{L_o} \frac{\partial \bar{B}^T}{\partial a} H^{*T} \bar{S}_o \, dL_o$$

$$+ \int_{L_o} \bar{B}^T \frac{\partial H^{*T}}{\partial a} \bar{S}_o \, dL_o$$

$$= (K_o^* + K_L^*(a_o)) + K_\sigma + K_\sigma^* \quad \ldots \quad \ldots \quad \ldots \qquad (5.72)$$

The initial stress stiffness matrix K_σ is evaluated as follows

$$K_\sigma = \int_{L_o} \frac{\partial \bar{B}^T}{\partial a} H^{*T} \bar{S}_o \, dL_o$$

$$= \int_{L_o} G_o^T \bar{P}_{oi} G_o \, dL_o \quad \ldots \quad \ldots \quad \ldots \quad \ldots \qquad (5.73)$$

in which the initial stress matrix $\bar{P}_{oi}$ is given by

$$\bar{P}_{oi} = \begin{bmatrix} [P_i]^* & [M_1]^* & [T_1]^* \\ & 0 & [M_2]^* \\ \text{Symm} & & 0 \end{bmatrix} \quad \ldots \quad \ldots \quad \ldots \quad (5.74)$$

and its components are the same as (5.69), but are functions of the initial stress vector

$$\bar{S}^* = H^{*T} \bar{S}_o \quad \ldots \quad \ldots \quad \ldots \quad \ldots \quad \ldots \quad \ldots \quad (5.75)$$

The additional geometric stiffness matrix K^*_σ is defined from (5.72), (5.70), (5.66) and (5.32) as

$$K^*_\sigma = \int_{L_o} \bar{B}^T \frac{\partial H^*}{\partial a} \bar{S}_o \, dL_o$$

$$= \int_{L_o} \bar{B}^T \bar{P}^*_{oi} \bar{B} \, dL_o \quad \ldots \quad \ldots \quad \ldots \quad \ldots \quad (5.76)$$

where the additional initial stress matrix $\bar{P}^*_{oi}$ is given in terms of the initial stress and strain resultants by

$$\bar{P}_{oi}^{*} = \begin{bmatrix} P^{**} - \frac{2\,M_{xy}}{(1+2e)^2} & - \frac{2\,M_{xz}}{(1+2e)^2} & - \frac{2\,T_y}{(1+2e)^2} & - \frac{2\,T_z}{(1+2e)^2} & 0 \\ 0 & 0 & 0 & 0 & 0 \\ & 0 & 0 & 0 & 0 \\ & & 0 & 0 & 0 \\ \text{Symm} & & & 0 & 0 \\ & & & & 0 \end{bmatrix}$$

... ... (5.77)

$$P^{**} = - \frac{P}{(1+2e)^{3/2}} + \frac{8\,\chi_{xy}\,M_{xy}}{(1+2e)^3} + \frac{8\,\chi_{xz}\,M_{xz}}{(1+2e)^3}$$

$$+ \frac{8\,\chi_y\,T_y}{(1+2e)^3} + \frac{8\,\chi_z\,T_z}{(1+2e)^3}$$

For small strains, e can be assumed to be small compared to unity and hence neglected in (5.77), (5.75) and (5.32).

On using the approximate relations for the conventional strains in terms of displacement derivatives (Equation (4.43a)), the tangent stiffness matrix becomes

$$K_T = \frac{\partial \psi}{\partial a} = \int_{L_o} B'^{T}\,\bar{D}\,B'\,dL_o$$

$$+ \int G_o^T\,P'_{oi}\,G_o\,dL_o \qquad \ldots \quad \ldots \quad \ldots \quad \ldots \qquad (5.72a)$$

and its component matrices are defined by the following relations:

$$B' = \bar{B}_o + B'_L(a_o) = \bar{B}_o + A'_\theta \, G_o \quad \ldots \quad \ldots \quad \ldots \quad (5.72b)$$

$$A'_\theta = \begin{bmatrix} 0 & \frac{dv}{dx} & \frac{dw}{dx} & 0 & 0 & 0 & 0 & 0 \\ \frac{d^2w}{dx^2} & 0 & \frac{d^2u}{dx^2} & \frac{dw}{dx} & -\frac{dw}{dy} & -\frac{du}{dx} & \frac{d^2v}{dx^2} & 0 \\ \frac{d^2v}{dx^2} & \frac{d^2u}{dx^2} & 0 & \frac{dv}{dx} & -\frac{du}{dx} & \frac{dw}{dy} & -\frac{d^2w}{dx^2} & 0 \\ \frac{d^2w}{dxdy} & 0 & -\frac{d^2v}{dx^2} & 0 & \frac{dw}{dx} & 0 & 0 & -\frac{du}{dx} \\ \frac{d^2w}{dxdy} & \frac{d^2w}{dx^2} & 0 & 0 & 0 & -\frac{dv}{dx} & 0 & -\frac{du}{dx} \\ 0 & -\frac{dw}{dx} & -\frac{dv}{dx} & 0 & 0 & 0 & 0 & 0 \end{bmatrix}$$

$$\ldots \quad \ldots \quad \ldots \quad \ldots \quad (5.72c)$$

$$P'_{oi} = \begin{bmatrix} [P_i]' & [M_1]' & [T_1]' \\ & 0 & [M_2]' \\ \text{Symm} & & 0 \end{bmatrix} \quad \ldots \quad \ldots \quad \ldots \quad (5.72d)$$

$$[P_i]'_{3x3} = \begin{bmatrix} 0 & 0 & 0 \\ 0 & P & -F_{yz} \\ 0 & -F_{yz} & P \end{bmatrix} \quad [T_1]'_{3x2} = \begin{bmatrix} 0 & -(T_y + T_z) \\ 0 & 0 \\ 0 & 0 \end{bmatrix}$$

$$[M_1]'_{3x3} = \begin{bmatrix} 0 & -M_{xz} & -M_{xy} \\ M_{xz} & 0 & -T_z \\ M_{xy} & T_y & 0 \end{bmatrix} \quad [M_2]'_{3x2} = \begin{bmatrix} 0 & 0 \\ -M_{xy} & 0 \\ M_{xz} & 0 \end{bmatrix}$$

... ... (5.72e)

5.6.3 Follower Pressure Loads and Applied Concentrated Moments

To take into account the effect of follower pressure loads and applied concentrated flexural moments, it becomes necessary to modify the equivalent nodal forces when using the Total Lagrangian formulation.

Consider follower pressure loads acting normally to the reference line after deformation and defined as

$$\vec{p} = p_y \hat{n}_y + p_z \hat{n}_z \quad \ldots \ldots \ldots \ldots \quad (5.78)$$

per unit deformed length of the reference line.

For small strains, neglecting second and higher order terms in displacement gradients and substituting from (5.40) into (5.78) we obtain

$$\vec{p} = (\frac{dw}{dx} p_z - \frac{dv}{dx} p_y)\hat{x} + ((1 + \frac{du}{dx})p_y + \frac{dw}{dy} p_z)\hat{y}$$

$$+ ((1 + \frac{du}{dx})p_z - \frac{dw}{dy})p_y)\hat{z} \quad \ldots \quad \ldots \quad \ldots \quad \ldots \qquad (5.79)$$

per unit undeformed length of the reference line.

The external virtual work due to this load is

$$\delta W_p = \int_{L_o} \delta\vec{V}.\vec{p}\, dL_o = \delta a_o^T \int_{L_o} N_o^T \begin{Bmatrix} \frac{dw}{dx} p_z - \frac{dv}{dx} p_y \\ (1 + \frac{du}{dx} p_y + \frac{dw}{dy} p_z \\ (1 + \frac{du}{dx})p_z - \frac{dw}{dy} p_y \end{Bmatrix} dL_o$$

$$\ldots \quad \ldots \quad \ldots \quad \ldots \quad \ldots \qquad (5.80)$$

where the shape functions N_o are given by

$$N_o = \frac{\partial}{\partial a} \begin{Bmatrix} u \\ v \\ w \end{Bmatrix} \quad \ldots \quad \ldots \quad \ldots \quad \ldots \quad \ldots \quad \ldots \qquad (5.81)$$

Consider that concentrated moments M^j_{xy} and M^j_{xz} are applied at node point j. The external virtual work due to these moments is

$$\delta W_m = \delta\phi^j_y \, M^j_{xz} + \delta\phi^j_z \, M^j_{xy} \quad \ldots \quad \ldots \quad \ldots \quad \ldots \quad (5.82)$$

The angles of rotation ϕ_y and ϕ_z are obtained from the following relations

$$\begin{aligned} \cos \phi_y &= \hat{y}.\hat{n}_y \\ \sin \phi_y &= |\hat{y} \times \hat{n}_y| \\ \cos \phi_z &= \hat{z}.\hat{n}_z \\ \sin \phi_z &= |\hat{z} \times \hat{n}_z| \end{aligned} \quad \ldots \quad \ldots \quad \ldots \quad \ldots \quad \ldots \quad (5.83)$$

Assuming that the strain e and the torsional rotation measure $\frac{dw}{dy}$ are small, the rotation angles are given from (5.83), (5.17) and (5.16) by

$$\begin{aligned} \phi_y &= \arctan \frac{dv/dx}{1 + du/dx} \\ \phi_z &= \arctan \frac{dw/dx}{1 + du/dx} \end{aligned} \quad \ldots \quad \ldots \quad \ldots \quad \ldots \quad (5.84)$$

and their variations are

$$\delta\phi_y = \delta\frac{dv}{dx}\left(1 + \frac{du}{dx}\right) - \frac{dv}{dx}\ \delta\frac{du}{dx}$$

$$\delta\phi_z = \delta\frac{dw}{dx}\left(1 + \frac{du}{dx}\right) - \frac{dw}{dx}\ \delta\frac{du}{dx} \quad \ldots \quad \ldots \quad \ldots \quad (5.85)$$

Substituting from (5.85) into (5.82) gives

$$\delta W_m = \delta a_o^T N_j^T \begin{Bmatrix} -\frac{dv}{dx} M_{xz} - \frac{dw}{dx} M_{xy} \\ \left(1 + \frac{du}{dx}\right) M_{xz} \\ \left(1 + \frac{du}{dx}\right) M_{xy} \end{Bmatrix}_j \quad \ldots \quad \ldots \quad (5.86)$$

The shape functions N_j are given by

$$N_j = \frac{\partial}{\partial a_o} \begin{Bmatrix} \frac{du}{dx} \\ \frac{dv}{dx} \\ \frac{dw}{dx} \end{Bmatrix} \quad \ldots \quad \ldots \quad \ldots \quad \ldots \quad (5.87)$$

The total external virtual work is then obtained as

$$\delta W = \delta a_o^T (R + R_d) \quad \ldots \quad \ldots \quad \ldots \quad \ldots \quad \ldots \quad (5.88)$$

in which R is the conservative vector of equivalent nodal forces and R_d is the deformation dependent vector of nodal forces. Thus, from (5.80) and (5.86)

$$R_d = \int_{L_o} N_o^T \left\{ \begin{bmatrix} \frac{dw}{dx} p_z - \frac{dv}{dx} p_y \\ \frac{du}{dx} p_y + \frac{dw}{dy} p_z \\ \frac{du}{dx} p_z - \frac{dw}{dy} p_y \end{bmatrix} dL_o + N_j^T \left\{ \begin{bmatrix} -\frac{dv}{dx} M_{xz} - \frac{dw}{dx} M_{xy} \\ \frac{du}{dx} M_{xz} \\ \frac{du}{dx} M_{xy} \end{bmatrix} \right\}_j \right\}$$

... ... (5.89)

5.7 CONCLUSIONS

1. A theory and Total Lagrangian formulations of the theory, which are based on the Green strains and the conventional strains, have been presented for geometrically nonlinear, elasto-plastic, thin, curved, eccentric three-dimensional beam elements. The theory has been developed assuming that the strains are small, but the rotations may be large. An intrinsic coordinate system has been used. The theory is an extension of the exact two-dimensional theory which has been presented in Chapter 2, the only additional feature being the effect of torsion.

2. Plane sections have been assumed to remain plane and normal to the beam reference line after deformation. So the cross-section has been considered to be solid rectangular and hence does not distort. Cross-sections other than solid rectangles have been considered as combinations of eccentric beam elements with a common reference line. This presents an approximate method for the analysis of thin walled beams.

3. The torsional curvature has been assumed to be small so that second order terms in torsion are negligible. Thus, longitudinal warping of the reference line has been neglected. The nonlinear effect of large bending rotations on torsion has been taken into account by considering the torsional deformation of the local x-y and x-z planes separately.

4. The torsional rigidities have been modified for elastic materials to represent correctly the torsion of a rectangular cross-section. The development of the elasto-plastic modulus matrix has been based on the von-Mises yield criterion, the Prandtl-Reuss flow rule and isotropic hardening. Such a formulation is suitable for metal structures. For beams under torsion the elasto-plastic formulation is correct only for concentric square cross-sections.

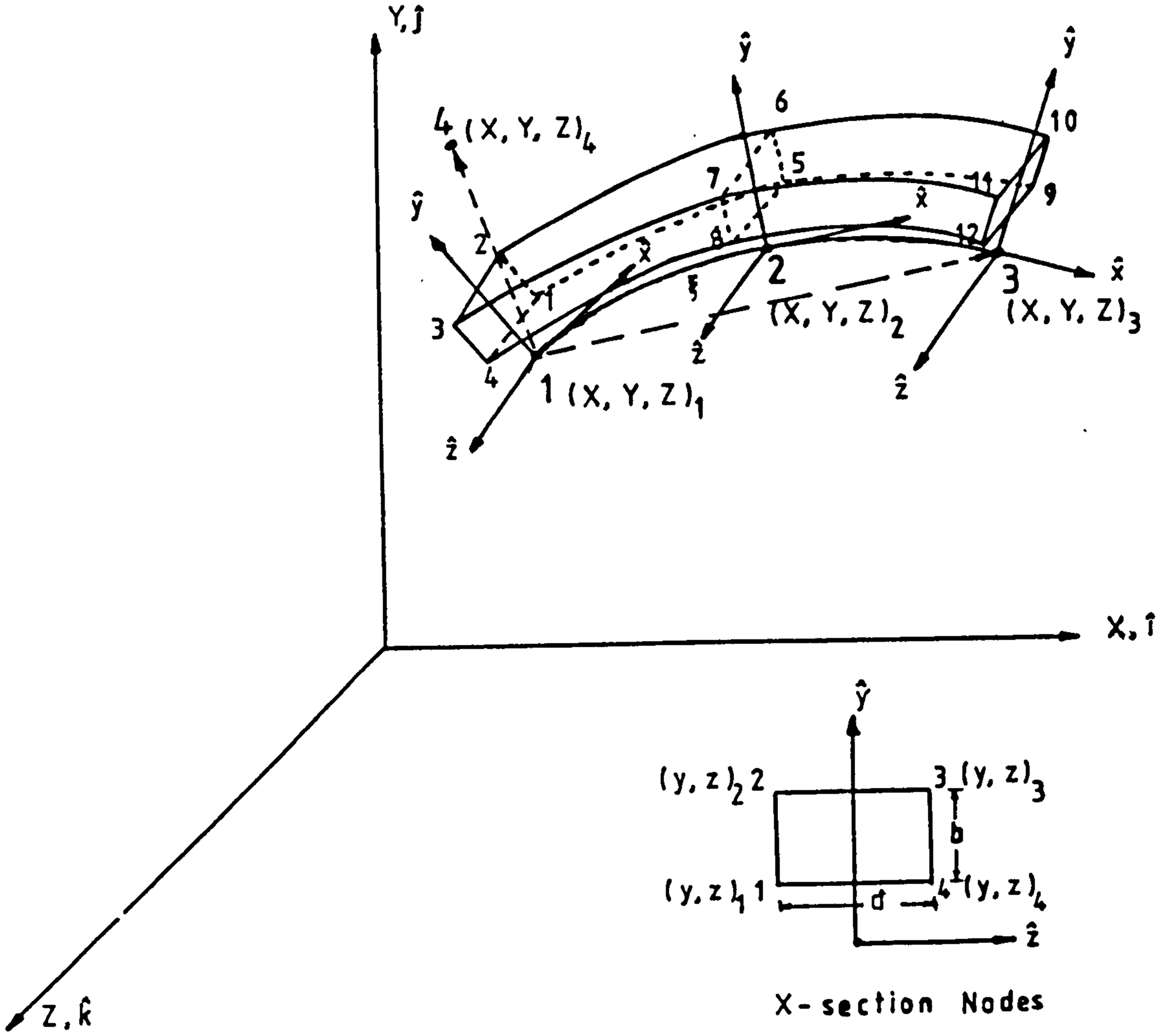

Local Axes :

$$\hat{z} = \frac{\vec{V}_{13} \times \vec{V}_{14}}{|\vec{V}_{13} \times \vec{V}_{14}|}$$

$$\hat{x} = (dX/d\xi\,\hat{i} + dY/d\xi\,\hat{j} + dZ/d\xi\,\hat{k}) / \left(\left(\frac{dX}{d\xi}\right)^2 + \left(\frac{dY}{d\xi}\right)^2 + \left(\frac{dZ}{d\xi}\right)^2\right)^{1/2}$$

$$\hat{y} = \hat{z} \times \hat{x}$$

$$[\ \hat{z} \times (\vec{V}_{12} \times \vec{V}_{14}) = 0\ ]$$

FIGURE 5.1 - 3-D Beam Element Geometry

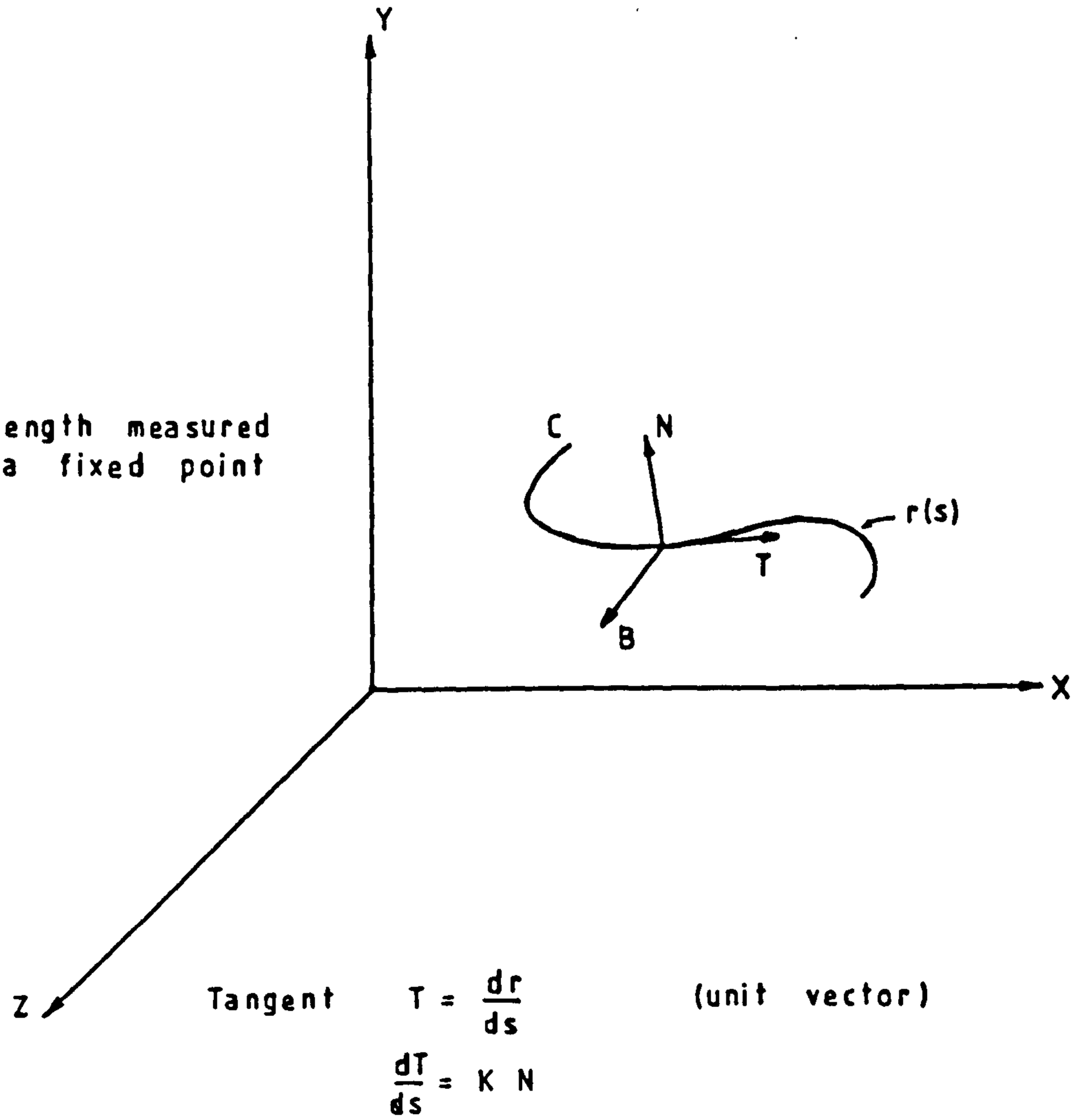

s = arc length measured from a fixed point on C

Tangent $T = \frac{dr}{ds}$ (unit vector)

$\frac{dT}{ds} = K\ N$

N = Principal normal
K = curvature

Binormal $B = T \times N$

T, N, B form a localised right-handed rectangular coordinate system

$\frac{dN}{ds} = \tau B - K N$ $\qquad$ $\frac{dB}{ds} = -\tau N$ $\qquad$ τ = torsion

FIGURE 5.2 - Differential Geometry Relations for a Space Curve (Ref [82])

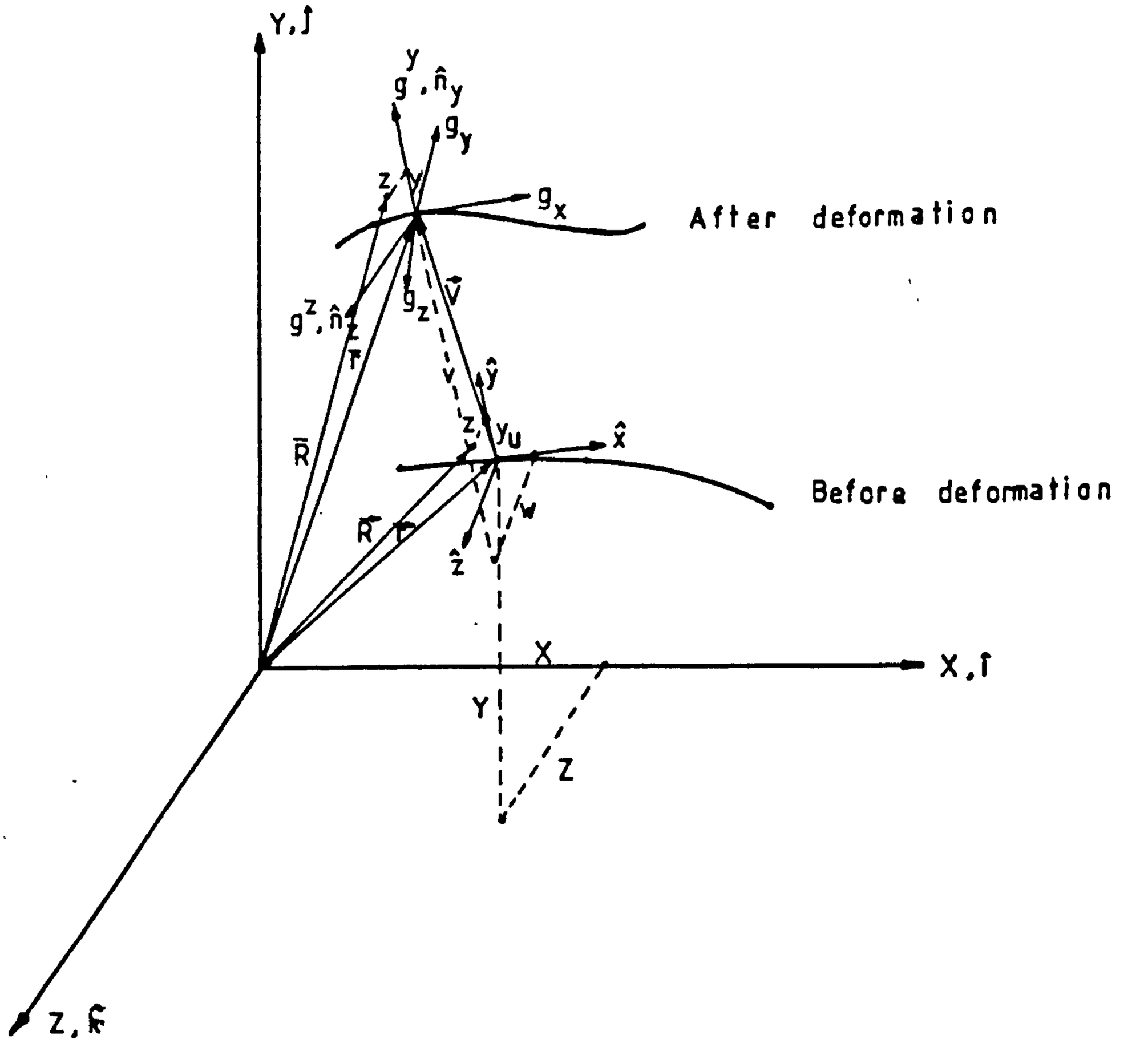

$$\vec{r} = X\hat{I} + Y\hat{J} + Z\hat{K}$$
$$\vec{R} = r + y\hat{y} + z\hat{z}$$
$$\vec{V} = u\hat{x} + v\hat{y} + w\hat{z}$$
$$\vec{r} = \vec{r} + \vec{V}$$
$$\vec{R} = \vec{r} + y\hat{n}_y + z\hat{n}_y$$

FIGURE 5.3 - 3-D Beam Deformation Geometry

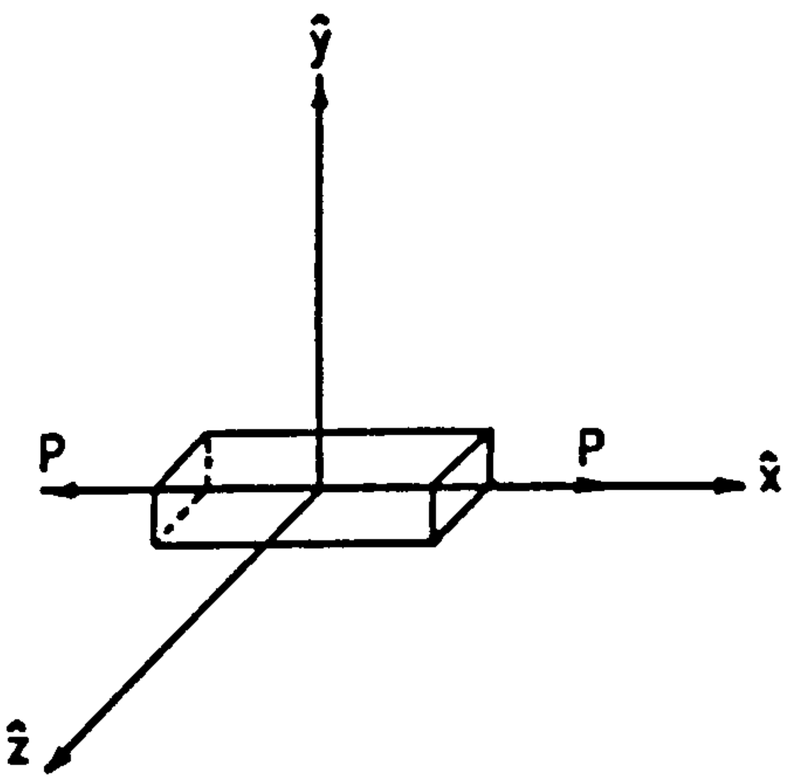

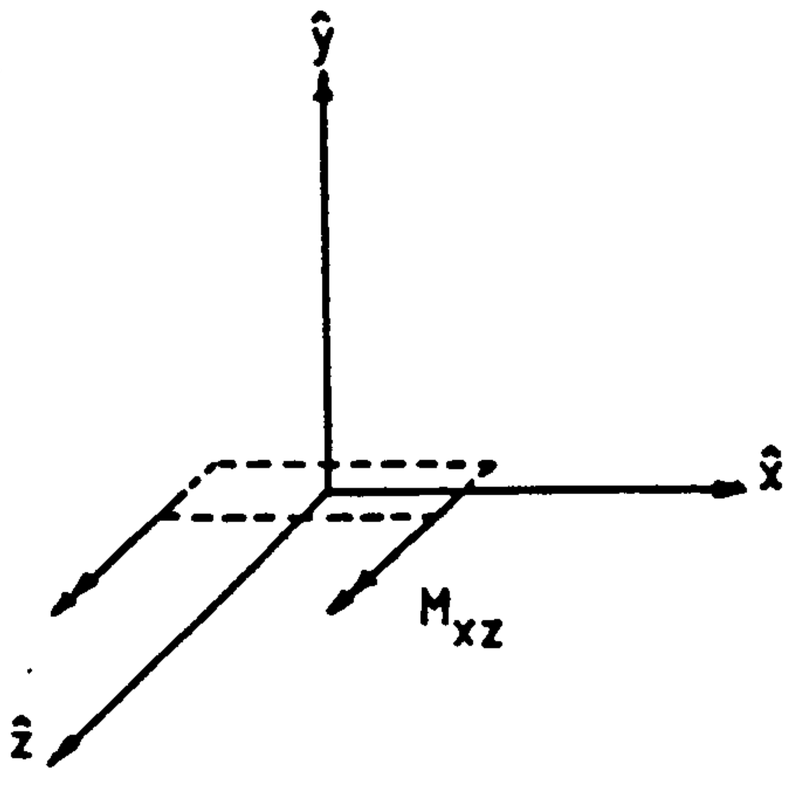

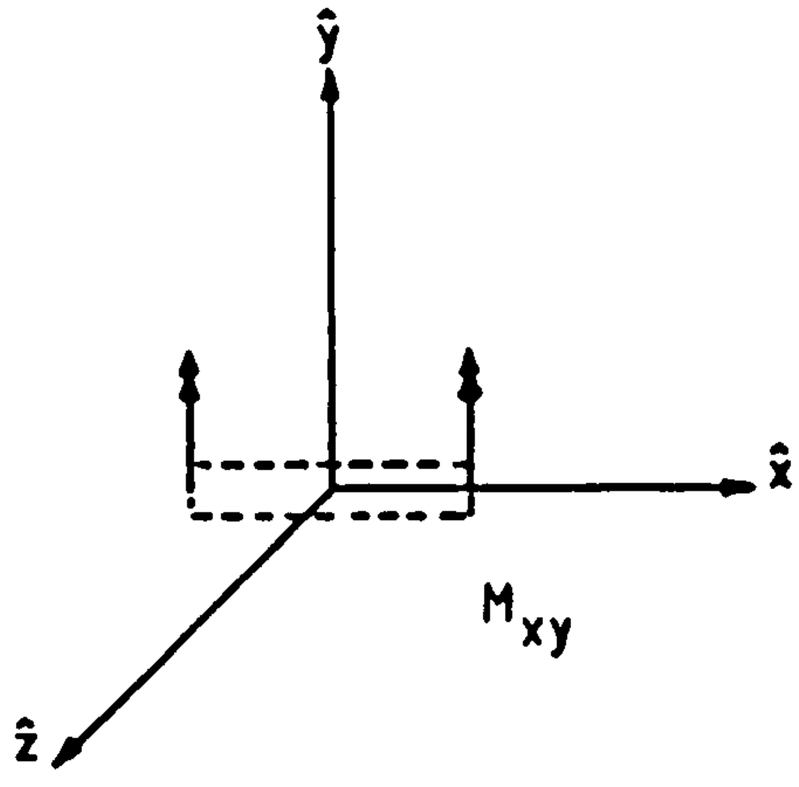

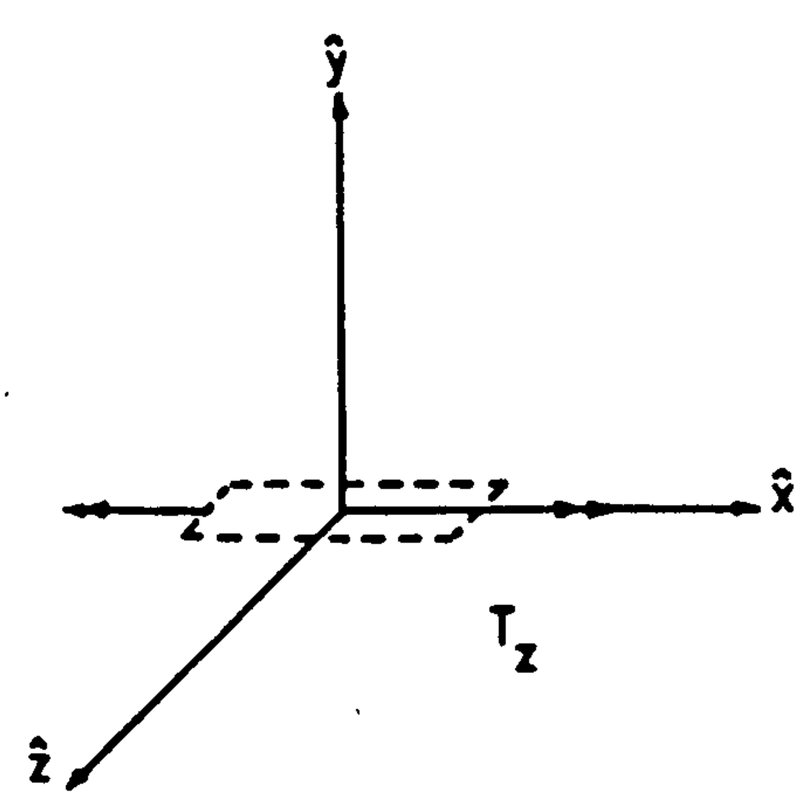

$T = T_y + T_z$

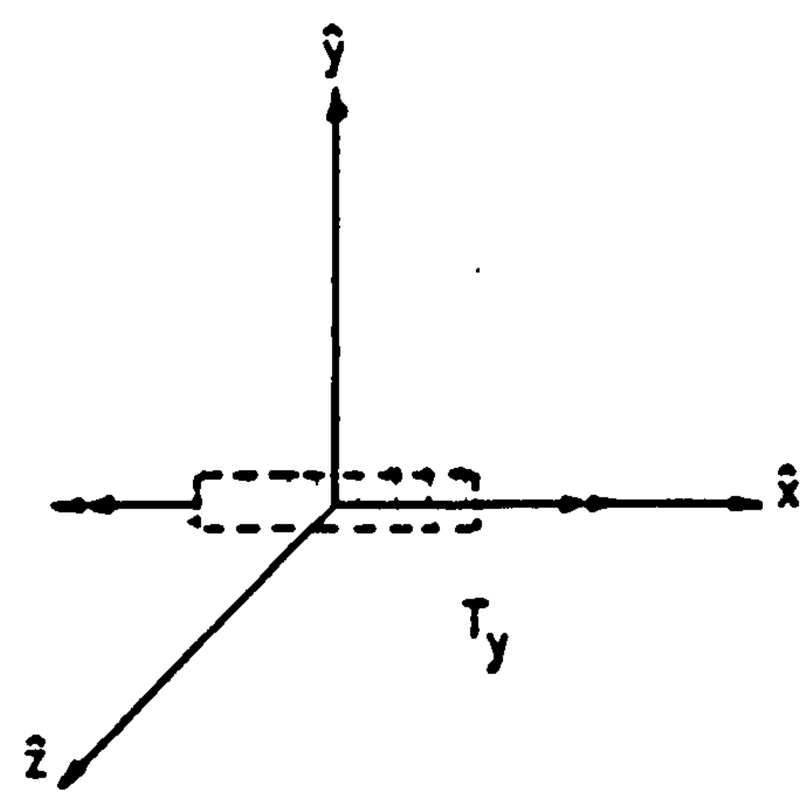

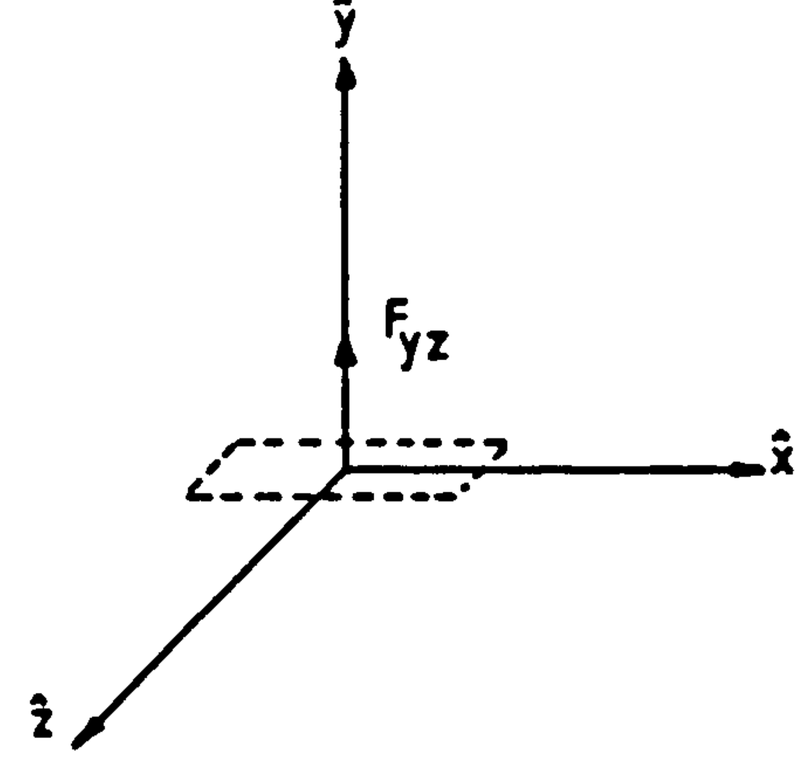

FIGURE 5.4 - 3-D Beam Stress Resultants

CHAPTER 6

THREE-DIMENSIONAL ECCENTRIC CURVED THIN BEAM ELEMENTS-FORMULATION AND APPLICATIONS

6.1 INTRODUCTION

The formulation of the elements is based on the large rotation theory which has been presented in Chapter 5. The theory has been developed by using an intrinsic coordinate system definition. The constraint technique, which has been discussed in Chapter 2, has been used to formulate the elements to include discretely such a coordinate system. While it is possible to obtain completely conforming elements by the constraint technique, the non-conforming elements are preferred since they show improved performance in linear analyses. (See Chapter 4). The non-conformity in the elements seriously affects the results only in large rotation problems in which the applied loads are not conservative. It has been demonstrated in Chapter 4, however, that this effect can be reduced by increasing the number of elements. Therefore, only the non-conforming elements ISOBEM 3 and ISOBEM 4, which are the three-dimensional versions of the ISOBEM 1 and ISOBEM 2 elements respectively, are presented in this chapter. The SEMILOOF thin beam element [64, 65, 83], which is compatible with the SEMILOOF shell element is also presented.

The main objectives of the linear applications which were carried out are:

(i) to assess the performance of the three elements under in-plane, bending and torsional deformations

(ii) to test the eccentric element formulation.

The three-dimensional large rotation theory (Chapter 5) is an extension of the two-dimensional theory. The three-dimensional theory therefore possesses all the excellent capabilities of the two-dimensional theory which have been demonstrated in Chapter 4. C^1 continuity of the three displacement components is a requirement of the theory when a Total Lagrangian formulation is employed. Thus, only the ISOBEM 4 element (Figure 6.3) can be correctly used with this theory in the analysis of large rotation and curvature problems. Idealisations by any one of the three elements are expected to give satisfactory results for small curvature and rotation problems. The large rotation Total Lagrangian formulations (TLG, TLC) are, therefore, tested by using ISOBEM 4 elements. The solution of a three-dimensional 45^{o} bend is presented to demonstrate the excellent capability of the element and the formulations. The other two elements can be used by employing the approximate theory which is based on the conventional strains, when C^1 continuity of the in-plane

displacement component is undesirable. The example of the straight cantilever under vertical load is used to assess the approximation.

This thesis has been primarily concerned with the study of geometric nonlinearity. Therefore, existing nonlinear material routines in the LUSAS system were used without carrying out an in depth study of material nonlinearity. The formulation that combines geometric and material nonlinearity has been tested using the SEMILOOF beam element. The aim of the applications which were carried out is to test the combined formulation and to demonstrate that the elements are suitable for use as stiffeners.

6.2 FORMULATION OF ELEMENTS

The geometry of the reference line of the elements is defined by four nodes (Figure 5.1). The local coordinate system ($\hat{x}$, $\hat{y}$, $\hat{z}$) is defined by Equations (5.2) to (5.6).

A minimum of six degrees of freedom which are the three translations and the three rotations are required at the end nodes to ensure a definite path for the bending and torsional moments and to avoid hinging.

Referring to Figure 6.1, for infinitesimal strains and small displacements, the normals to the centreline after deformation are given from Equations (5.16) and (5.9) by the following relations

$$\hat{n}_y \simeq g_y = -\frac{dv}{dx}\hat{x} + \hat{y} + \frac{dw}{dy}\hat{z}$$

$$\hat{n}_z \simeq g_z = -\frac{dw}{dx}\hat{x} - \frac{dw}{dy}\hat{y} + \hat{z} \quad \ldots \quad \ldots \quad \ldots \quad (6.1)$$

The rotations are defined in this case, from the Kirchhoff hypothesis that the shear strains are zero, as

$$\theta_x = -\frac{dv}{dx} = \frac{dw}{dy}$$

$$\theta_y = \frac{du}{dz} = -\frac{dw}{dx}$$

$$\theta_z = -\frac{du}{dy} = \frac{dv}{dx} \quad \ldots \quad \ldots \quad \ldots \quad \ldots \quad \ldots \quad \ldots \quad (6.2)$$

The position vector of a point P(y, z) after deformation can be written in terms of the displacement vector $\vec{d}$ of point P(y, z) and the position vector before deformation $\vec{R}$, so that

$$\bar{R} = \vec{R} + \vec{d} \quad \ldots \quad \ldots \quad \ldots \quad \ldots \quad \ldots \quad \ldots \quad \ldots \quad (6.3)$$

Substituting from (6.1), (6.2) and (5.7) into (5.11) gives

$$\bar{R} = \vec{r} + \vec{V} + y(-\theta_z\hat{x} + \hat{y} + \theta_x\hat{z}) + z(\theta_y\hat{x} - \theta_x\hat{y} + \hat{z}) \quad \ldots \quad \ldots \quad \ldots \quad \ldots \quad (6.4)$$

Therefore, from (6.4), (6.3) and (5.10) the displacement vector $\vec{d}$ is given by

$$\vec{d} = \bar{R} - \vec{R}$$

$$\simeq \vec{V} + y(-\theta_z\hat{x} + \theta_x\hat{z}) + z(\theta_y\hat{x} - \theta_x\hat{y}) \quad \ldots \quad (6.5)$$

from which the components of the displacement in the local axes directions are obtained as follows

$$\begin{Bmatrix} u \\ v \\ w \end{Bmatrix}_P = \begin{Bmatrix} \vec{d}.\hat{x} \\ \vec{d}.\hat{y} \\ \vec{d}.\hat{z} \end{Bmatrix} \simeq \begin{Bmatrix} \vec{V}.\hat{x} - y\,\theta_z + z\,\theta_y \\ \vec{V}.\hat{y} - z\,\theta_x \\ \vec{V}.\hat{z} + y\,\theta_x \end{Bmatrix}$$

$$= \begin{Bmatrix} u - y\,\theta_z + z\,\theta_y \\ v - z\,\theta_x \\ w + y\,\theta_x \end{Bmatrix} \quad \ldots \quad \ldots \quad (6.6)$$

The shear strains to be used to obtain the constraint equations are

$$\gamma_{xy} = -\theta_z + \frac{dv}{dx} = 0$$

$$\gamma_{xz} = \theta_y + \frac{dw}{dx} = 0 \quad \ldots \quad \ldots \quad \ldots \quad \ldots \quad (6.7)$$

The displacement vector $\vec{V}$ of a point on the beam reference line is given in terms of the displacement components in the global axes directions by

$$\vec{V} = U\,\hat{i} + V\,\hat{j} + W\,\hat{k} \quad \ldots \quad \ldots \quad \ldots \quad \ldots \quad (6.8)$$

A rotation vector $\vec{\Omega}$ can be defined in terms of rotations about the global axes for small rotations. Therefore,

$$\vec{\Omega} = \alpha\,\hat{i} + \beta\,\hat{j} + \theta\,\hat{k} \quad \ldots \quad \ldots \quad \ldots \quad \ldots \quad (6.9)$$

The displacement components in the local axes directions are now defined from (6.8) by the relations

$$\begin{Bmatrix} u \\ v \\ w \end{Bmatrix} = \begin{Bmatrix} \vec{V}.\hat{x} \\ \vec{V}.\hat{y} \\ \vec{V}.\hat{z} \end{Bmatrix} = \begin{bmatrix} \hat{i}.\hat{x} & \hat{j}.\hat{x} & \hat{k}.\hat{x} \\ \hat{i}.\hat{y} & \hat{j}.\hat{y} & \hat{k}.\hat{y} \\ \hat{i}.\hat{z} & \hat{j}.\hat{z} & \hat{k}.\hat{z} \end{bmatrix} \begin{Bmatrix} u \\ v \\ w \end{Bmatrix} \quad \ldots \quad (6.10)$$

Similarly the local rotation components are approximated from (6.9) as follows

$$\begin{Bmatrix}\theta_x\\ \theta_y\\ \theta_z\end{Bmatrix} = \begin{Bmatrix}\vec{\Omega}.\hat{x}\\ \vec{\Omega}.\hat{y}\\ \vec{\Omega}.\hat{z}\end{Bmatrix} = \begin{bmatrix}\hat{i}.\hat{x} & \hat{j}.\hat{x} & \hat{k}.\hat{x}\\ \hat{i}.\hat{y} & \hat{j}.\hat{y} & \hat{k}.\hat{y}\\ \hat{i}.\hat{z} & \hat{j}.\hat{z} & \hat{k}.\hat{z}\end{bmatrix}\begin{Bmatrix}\alpha\\ \beta\\ \theta\end{Bmatrix}\ldots \quad \ldots \qquad (6.11)$$

By assuming a parabolic variation of the initial geometry of the elements, the global coordinates of any point on the reference line are obtained by interpolation from the nodal coordinates, so that

$$\begin{Bmatrix}X\\ Y\\ Z\end{Bmatrix} = \sum_{i=1}^{3} N_i \begin{Bmatrix}X\\ Y\\ Z\end{Bmatrix}_i \quad \ldots \quad \ldots \quad \ldots \quad \ldots \quad \ldots \qquad (6.12)$$

where N_i are the hierarchial shape functions (Equation (3.7)). The local coordinate system is then defined explicitly at any point on the reference line by Equations (6.12) and (5.2) to (5.6).

6.2.1 ISOBEM 3 Element

The element (Figure 6.2) is a thin non-conforming beam element with C^o continuity of the in-plane displacement and C^1 continuity of the out-of-plane displacements. Two Gauss integration points are used to evaluate the element characteristics.

The initial variation of the global displacements and rotations is assumed to be parabolic. Thus, the total number of variables is eighteen. Four constraint equations are obtained by applying the two shear constraints (Equation (6.7)) at the two Gauss points ($\xi = \pm 1/\sqrt{3}$). These are used to eliminate the two transverse displacements and the two bending rotations at the middle node.

The global displacements and rotations are defined in terms of the nodal values as

$$\begin{Bmatrix} U \\ V \\ W \\ \alpha \\ \beta \\ \theta \end{Bmatrix} = \sum_{i=1}^{3} N_i \begin{Bmatrix} U \\ V \\ W \\ \alpha \\ \beta \\ \theta \end{Bmatrix}_i \quad \ldots \quad \ldots \quad \ldots \quad \ldots \qquad (6.13)$$

By applying the zero shear strain constraints (6.7) at the two Guass points (I, II)

$$\begin{Bmatrix} \gamma_{xy} \\ \\ \gamma_{xz} \end{Bmatrix}_{I,II} = \sum_{i=1}^{3} \begin{bmatrix} \frac{dN_i}{dx}\hat{i}.\hat{y}, & \frac{dN_i}{dx}\hat{j}.\hat{y}, & \frac{dN_i}{dx}\hat{k}.\hat{y}, & -N_i\hat{i}.\hat{z}, & -N_i\hat{j}.\hat{z}, & -N_i\hat{k}.\hat{z} \\ \\ \frac{dN_i}{dx}\hat{i}.\hat{z}, & \frac{dN_i}{dx}\hat{j}.\hat{z}, & \frac{dN_i}{dx}\hat{k}.\hat{z}, & N_i\hat{i}.\hat{y}, & N_i\hat{j}.\hat{y}, & N_i\hat{k}.\hat{y} \end{bmatrix}_{I,II} \begin{Bmatrix} U \\ V \\ W \\ \alpha \\ \beta \\ \theta \end{Bmatrix}_i = 0$$

OR

$$M\,\delta = O \qquad \ldots \quad \ldots \quad \ldots \quad \ldots \quad \ldots \quad \ldots \qquad (6.14)$$

The middle node (2) displacements and rotations are transformed into the local axes directions so that

$$\delta = T\,\delta^* \qquad \ldots \quad \ldots \quad \ldots \quad \ldots \quad \ldots \quad \ldots \qquad (6.15)$$

where the transformation matrix T is given by

$$T = \begin{bmatrix} [I] & & & & & \\ & [I] & & O & & \\ & & [CS]_2 & & & \\ & & & [CS]_2 & & \\ & O & & & [I] & \\ & & & & & [I] \end{bmatrix} \qquad \ldots \qquad (6.16)$$

in which

$$[I] = \begin{bmatrix} 1 & 0 & 0 \\ 0 & 1 & 0 \\ 0 & 0 & 1 \end{bmatrix} \quad \text{and} \quad [CS] = \begin{bmatrix} \hat{i}.\hat{x} & \hat{i}.\hat{y} & \hat{i}.\hat{z} \\ \hat{j}.\hat{x} & \hat{j}.\hat{y} & \hat{j}.\hat{z} \\ \hat{k}.\hat{x} & \hat{k}.\hat{y} & \hat{k}.\hat{z} \end{bmatrix} \quad \ldots \quad \ldots \quad \ldots \quad \ldots \qquad (6.17)$$

Substituting from (6.15) into (6.14) gives constraint equations of the form

$$\mathbf{M} \times \mathbf{T}\ \delta^* = \mathbf{M}^*\ \delta^* = 0 \qquad \ldots \quad \ldots \quad \ldots \quad \ldots \qquad (6.18)$$

which are written in terms of the wanted variables **a** and the variables to be eliminated **b**, as

$$\mathbf{M}^*\ \delta^* = [M_A \vdots M_B] \left\{ \begin{matrix} \mathbf{a} \\ \cdots \\ \mathbf{b} \end{matrix} \right\} = 0 \qquad \ldots \quad \ldots \qquad (6.19)$$

in which

$$\mathbf{a} = \{U_1, V_1, W_1, \alpha_1, \beta_1, \theta_1, \Delta u_2, \Delta\theta_{x2}, U_3, V_3, W_3, \alpha_3, \beta_3, \theta_3\}^T$$

$$\mathbf{b} = \{\Delta v_2,\ \Delta w_2,\ \Delta\theta_{y2},\ \Delta\theta_{z2}\}^T \qquad \ldots \quad \ldots \quad \ldots \qquad (6.20)$$

Solving (6.19) for the unwanted variables in terms of the wanted variables we have

$$\mathbf{b} = -\ M_B^{-1}\ M_A\ \mathbf{a} \qquad \ldots \quad \ldots \quad \ldots \quad \ldots \quad \ldots \quad \ldots \qquad (6.21)$$

The shape function array defines the local displacements and their derivatives at any point $\underline{\xi}$ on the beam reference line in terms of the nodal variables. From (6.10), (6.11) and (6.13) the unconstrained shape function array is

$$
\begin{Bmatrix}
u \\ v \\ w \\ du/dx \\ dv/dx \\ dw/dx \\ \theta_x \\ \theta_y \\ \theta_z \\ d\theta_x/dx \\ d\theta_y/dx \\ d\theta_z/dx \\ d^2u/dx^2
\end{Bmatrix}
= \sum_{i=1}^{3}
\begin{bmatrix}
N_i[CS] & 0 & 0 \\
\frac{dN_i}{dx}[CS] & 0 & 0 \\
0 & N_i[CS] & 0 \\
0 & 0 & \frac{dN_i}{dx}[CS] \\
\frac{d^2N_i}{dx^2}\hat{i}.\hat{x}, & \frac{d^2N_i}{dx^2}\hat{j}.\hat{x}, & \frac{d^2N_i}{dx^2}\hat{k}.\hat{x}, \quad 0, \quad 0, \quad 0
\end{bmatrix}
\begin{Bmatrix} U \\ V \\ W \\ \alpha \\ \beta \\ \theta \end{Bmatrix}_i
$$

OR

$$\gamma = WN\delta \quad \ldots \quad \ldots \quad \ldots \quad \ldots \quad \ldots \quad \ldots \quad (6.22)$$

The unconstrained array is modified by transforming the middle node displacements into the local axes directions. The array is then partitioned to be in terms of the wanted and unwanted variables, so that

$$\gamma \quad = \quad WN \quad x \quad T\,\delta^{*} = \left[W_A \;\vdots\; W_B\right] \left\{\begin{matrix} a \\ --- \\ b \end{matrix}\right\} \quad \ldots \quad \ldots \quad (6.23)$$

The shape function array is constrained by substituting for the unwanted variables from (6.21) into (6.23) to give

$$\gamma \quad = \quad \left[W_A \;-\; W_B\, M_B^{-1}\, M_A\right] \quad a$$

$$= \quad W \; a \quad \ldots \quad \ldots \quad \ldots \quad \ldots \quad \ldots \quad \ldots \quad (6.24)$$

6.2.2 ISOBEM 4 Element

The three displacement components are C^1 continuous for the ISOBEM 4 element (Figure 6.3). The global displacements and their derivatives are independently interpolated. A set of constraint equations is formed by equating the independently interpolated displacement gradients to the derivatives of the local displacements with respect to the local x coordinate at the two Gauss points ($\xi = \pm 1/\sqrt{3}$). These are used to eliminate appropriate degrees of freedom.

The axial strain is defined by the independently interpolated in-plane strain term to avoid the developemnt of spurious mechanisms. Three integration points are used to evaluate the element characteristics. The resulting element is non-conforming with two sets of variations for the displacement derivatives - one parabolic and the other linear (or smoothed). The use of the smoothed derivatives for the nonlinear strain terms in geometric nonlinearity computations improves the element results.

The constraint equations are given for this element by the following relations

$$\frac{dv}{dx} - \theta_z = 0$$

$$\frac{dw}{dx} + \theta_y = 0$$

$$\frac{du}{dx} - \varepsilon = 0 \quad \ldots \quad \ldots \quad \ldots \quad \ldots \quad \ldots \quad \ldots \qquad (6.25)$$

A parabolic variation of variables is assumed initially and the element has twenty-one degrees of freedom (Figure 6.3). Six constraint equations are obtained by evaluating Equation (6.25) at the two Gauss points ($\xi = \pm 1/\sqrt{3}$). These are used to eliminate the three

local translations, the two bending rotations and the in-plane strain variable at the middle node.

The global displacements and their derivatives are independently interpolated as follows

$$\begin{Bmatrix} U \\ V \\ W \\ \alpha \\ \beta \\ \theta \\ \varepsilon \end{Bmatrix} = \sum_{i=1}^{3} N_i \begin{Bmatrix} U \\ V \\ W \\ \alpha \\ \beta \\ \theta \\ \varepsilon \end{Bmatrix}_i \quad \ldots \quad \ldots \quad \ldots \qquad (6.26)$$

in which N_i are the hierarchical shape functions.

The constraint equations are obtained by evaluating (6.25) at the two Gauss points (I, II). Therefore, from (6.26), (6.10) and (6.11) we have

$$\sum_{i=1}^{3} \begin{bmatrix} \frac{dN_i}{dx}\hat{i}.\hat{y}, & \frac{dN_i}{dx}\hat{j}.\hat{y}, & \frac{dN_i}{dx}\hat{k}.\hat{y}, & -N_i\hat{i}.\hat{z}, & -N_i\hat{j}.\hat{z}, & -N_i\hat{k}.\hat{z}, & O \\ \frac{dN_i}{dx}\hat{i}.\hat{z}, & \frac{dN_i}{dx}\hat{j}.\hat{z}, & \frac{dN_i}{dx}\hat{k}.\hat{z}, & N_i\hat{i}.\hat{y}, & N_i\hat{j}.\hat{y}, & N_i\hat{k}.\hat{y}, & O \\ \frac{dN_i}{dx}\hat{i}.\hat{x}, & \frac{dN_i}{dx}\hat{j}.\hat{x}, & \frac{dN_i}{dx}\hat{k}.\hat{x}, & O, & O, & O, & -N_i \end{bmatrix}_{I,II} \begin{Bmatrix} U \\ V \\ W \\ \alpha \\ \beta \\ \theta \\ \varepsilon \end{Bmatrix}_i$$

$$= M\,\delta = O \quad \ldots\ \ldots\ \ldots \quad \ldots\ \ldots\ \ldots\ \ldots \quad (6.27)$$

which is modified and written in terms of the wanted and unwanted variables to give

$$M\,\delta = M^*\,\delta^* = [M_A \,\vdots\, M_B] \left\{\begin{array}{c} a \\ \hline b \end{array}\right\} = O \quad \ldots\ \ldots \quad (6.28)$$

The wanted variables **a** are now given by

$$a = \{U_1, V_1, W_1, \alpha_1, \beta_1, \theta_1, \varepsilon_1, \Delta\theta_{x2}, U_3, V_3, W_3, \alpha_3, \beta_3, \theta_3, \varepsilon_3\}^T$$

$$\ldots\ \ldots\ \ldots\ \ldots\ \ldots \quad (6.29a)$$

The variables to be eliminated are

$$b = \{\Delta u_2, \Delta v_2, \Delta w_2, \Delta\theta_{y2}, \Delta\theta_{z2}, \Delta\varepsilon_2\}^T \quad \ldots\ \ldots\ \ldots \quad (6.29b)$$

The unwanted variables are obtained in terms of the wanted variables from Equation (6.28).

The unconstrained shape function array is

$$\begin{Bmatrix} u \\ v \\ w \\ \frac{du}{dx} \\ \frac{dv}{dx} \\ \frac{dw}{dx} \\ \theta_x \\ \theta_y \\ \theta_z \\ \frac{d\theta_x}{dx} \\ \frac{d\theta_y}{dx} \\ \frac{d\theta_z}{dx} \\ \varepsilon \\ \frac{d\varepsilon}{dx} \end{Bmatrix} = \sum_{i=1}^{3} \begin{bmatrix} N_i[CS] & O \\ \frac{dN_i}{dx}[CS] & O \\ O & N_i[CS] \\ O & \frac{dN_i}{dx}[CS] \\ O, O, O, O, O, O, N_i \\ O, O, O, O, O, O, \frac{dN_i}{dx} \end{bmatrix} \begin{Bmatrix} U \\ V \\ W \\ \alpha \\ \beta \\ \theta \\ \varepsilon \end{Bmatrix}_i$$

OR

$$\gamma = WN\,\delta$$

$$= WN^*\ \delta^* = \begin{bmatrix} W_A \vdots W_B \end{bmatrix} \begin{Bmatrix} a \\ --- \\ b \end{Bmatrix} \quad \ldots \quad \ldots \quad (6.30)$$

The constrained shape function array is then obtained from (6.30) and (6.28) as

$$\gamma = \left[W_A - W_B M_B^{-1} M_A \right] \quad a$$

$$= \quad W \; a \qquad \ldots \quad \ldots \quad \ldots \quad \ldots \quad \ldots \quad \ldots \qquad (6.31)$$

6.2.3 The SEMILOOF Beam Element

The nodal configuration of the SEMILOOF BEAM (Figure 6.4) is closely linked with that of the SEMILOOF shell element. The global displacements at the three nodes and the normal rotations at the two Gauss points (LOOF nodes) ensure C^o continuity between the shell and the beam elements. Three additional rotational degrees of freedom are introduced at each of the end nodes for the beam to avoid hinging. The bending rotations are not not necessarily equal between the shell and the beam elements at all points [64, 65, 83].

The original thin beam element shape functions [65] have been modified to introduce the four node definition of geometry and include the second derivative of the in-plane displacement. All the element characteristics are evaluated by using the three point integration rule since the shear strains are assumed to be equal to zero.

The displacements and rotations are independently interpolated initially. A parabolic variation is assumed for the global displacements. The variation of the rotations is assumed to be cubic. Thus, the element originally has twenty-one degrees of freedom (Figure 6.5).

The global displacements of any point on the reference line are interpolated from the nodal variables, so that

$$\begin{Bmatrix} U \\ V \\ W \end{Bmatrix} = \sum_{i=1}^{3} \bar{N}_i \begin{Bmatrix} U \\ V \\ W \end{Bmatrix}_i \quad \ldots \quad \ldots \quad \ldots \quad \ldots \quad \ldots \quad (6.32)$$

where $\bar{N}_i$ are the quadratic interpolation functions given by

$$\bar{N}_1 = \frac{\xi(\xi - 1)}{2}$$

$$\bar{N}_2 = 1 - \xi^2$$

$$\bar{N}_3 = \frac{\xi(\xi + 1)}{2} \quad \ldots \quad \ldots \quad \ldots \quad \ldots \quad \ldots \quad (6.33)$$

These shape functions are also used to define the geometry of the reference line (Equation (6.12).

The rotations about the global axes are defined in terms of the nodal values as

$$\begin{Bmatrix} \alpha \\ \beta \\ \theta \end{Bmatrix} = \sum_{i=1}^{4} \bar{\bar{N}}_i \begin{Bmatrix} \alpha \\ \beta \\ \theta \end{Bmatrix}_i \quad \ldots \quad \ldots \quad \ldots \quad \ldots \quad (6.34)$$

in which $\bar{\bar{N}}_i$ are cubic interpolation functions given by

$$\bar{\bar{N}}_1 = \frac{(\xi^2 - g^2)\ (\xi - 1)}{(1 - g^2)\ (-2)}$$

$$\bar{\bar{N}}_2 = \frac{(1 - \xi^2)\ (\xi - g)}{(1 - g^2)\ (-2g)}$$

$$\bar{\bar{N}}_3 = \frac{(1 - \xi^2)\ (\xi + g)}{(1 - g^2)\ (2g)}$$

$$\bar{\bar{N}}_4 = \frac{(\xi^2 - g^2)\ (\xi + 1)}{(1 - g^2)\ (2)}$$

$$g = 1/\sqrt{3} \quad \ldots \quad \ldots \quad \ldots \quad \ldots \quad \ldots \quad (6.35)$$

The four internal bending rotations are eliminated by introducing the constraints of zero shear strain (Equation (6.7)) at the two Gauss points (I, II). The constraint equations can be written as

$$\sum_{i=1}^{3} \begin{bmatrix} \frac{d\bar{N}_i}{dx}\hat{i}.\hat{y}, & \frac{d\bar{N}_i}{dx}\hat{j}.\hat{y}, & \frac{d\bar{N}_i}{dx}\hat{k}.\hat{y} \\ \\ \frac{d\bar{N}_i}{dx}\hat{i}.\hat{z}, & \frac{d\bar{N}_i}{dx}\hat{j}.\hat{z}, & \frac{d\bar{N}_i}{dx}\hat{k}.\hat{z} \end{bmatrix}_{I,II} \begin{Bmatrix} U \\ V \\ \\ W \end{Bmatrix}_i$$

$$\sum_{i=1}^{4} \begin{bmatrix} -\bar{\bar{N}}_i\,\hat{i}.\hat{z}, & -\bar{\bar{N}}_i\,\hat{j}.\hat{z}, & -\bar{\bar{N}}_i\,\hat{k}.\hat{z} \\ \\ \bar{\bar{N}}_i\,\hat{i}.\hat{y}, & \bar{\bar{N}}_i\,\hat{j}.\hat{y}, & \bar{\bar{N}}_i\,\hat{k}.\hat{y} \end{bmatrix}_{I,II} \begin{Bmatrix} \alpha \\ \beta \\ \theta \end{Bmatrix}_i = 0$$

OR

$$\mathbf{M}\ \delta = 0 \quad \ldots \quad \ldots \quad \ldots \quad \ldots \quad \ldots \quad \ldots \quad (6.36)$$

where

$$\delta = \{U_1, V_1, W_1, U_2, V_2, W_2, U_3, V_3, W_3, \alpha_i, \beta_1, \theta_1, \alpha_2, \beta_2, \theta_2, \alpha_3, \beta_3, \theta_3, \alpha_4, \beta_4, \theta_4\}^T$$

The internal rotations are then transformed into the local axes directions and substituted into the constraint equations (5.36) to give

$$\mathbf{M}\ \delta = \mathbf{M} \times \mathbf{T}\ \delta^* = [M_A \,\vdots\, M_B] \begin{Bmatrix} a \\ --- \\ b \end{Bmatrix} \quad \ldots \quad \ldots \quad (6.37)$$

in which the transformation matrix T is given by

$$T = \begin{bmatrix} [I] & & & & & & \\ & [I] & & & & & \\ & & [I] & & 0 & & \\ & & & [I] & & & \\ & & & & [CS]_I & & \\ & 0 & & & & [CS]_{II} & \\ & & & & & & [I] \end{bmatrix} \quad \ldots \quad \ldots \quad (6.38)$$

where [I] and [CS] are given by (6.17).

The wanted and unwanted variables (Figure 6.5) are

$$a = \{U_1, V_1, W_1, U_2, V_2, W_2, T_I, T_{II}, U_3, V_3, W_3, \alpha_1, \beta_1, \theta_1, \alpha_4, \beta_4, \theta_4\}^T$$

$$b = \{B_I, \Delta_I, B_{II}, \Delta_{II}\}^T$$

The unconstrained shape function array is of the following form

$$
\begin{Bmatrix} U \\ V \\ W \\ \frac{du}{dx} \\ \theta_x \\ \theta_y \\ \theta_z \\ \frac{d\theta_z}{dx} \\ \frac{d\theta_y}{dx} \\ \frac{d\theta_x}{dx} \\ \gamma_{xy} \\ \gamma_{xz} \\ \frac{d^2u}{dx^2} \end{Bmatrix}
=
\sum_{i=1}^{3}
\begin{bmatrix}
\bar{N}_i , & 0 , & 0 \\
0 , & \bar{N}_i , & 0 \\
0 , & 0 , & \bar{N}_i \\
\frac{d\bar{N}_i}{dx}\hat{i}.\hat{x}, & \frac{d\bar{N}_i}{dx}\hat{j}.\hat{x}, & \frac{d\bar{N}_i}{dx}\hat{k}.\hat{x} \\
0 , & 0 , & 0 \\
0 , & 0 , & 0 \\
0 , & 0 , & 0 \\
0 , & 0 , & 0 \\
0 , & 0 , & 0 \\
\frac{d\bar{N}_i}{dx}\hat{i}.\hat{y}, & \frac{d\bar{N}_i}{dx}\hat{j}.\hat{y}, & \frac{d\bar{N}_i}{dx}\hat{k}.\hat{y} \\
\frac{d\bar{N}_i}{dx}\hat{i}.\hat{z}, & \frac{d\bar{N}_i}{dx}\hat{j}.\hat{z}, & \frac{d\bar{N}_i}{dx}\hat{k}.\hat{z} \\
\frac{d^2\bar{N}_i}{dx^2}\hat{i}.\hat{x}, & \frac{d^2\bar{N}_i}{dx^2}\hat{j}.\hat{x}, & \frac{d^2\bar{N}_i}{dx^2}\hat{k}.\hat{x}
\end{bmatrix}
\begin{Bmatrix} U \\ V \\ W \end{Bmatrix}_i
+
\sum_{i=1}^{4}
\begin{bmatrix}
0 , & 0 , & 0 \\
0 , & 0 , & 0 \\
0 , & 0 , & 0 \\
0 , & 0 , & 0 \\
\bar{\bar{N}}_i\hat{i}.\hat{x}, & \bar{\bar{N}}_i\hat{j}.\hat{x}, & \bar{\bar{N}}_i\hat{k}.\hat{x} \\
\bar{\bar{N}}_i\hat{i}.\hat{y}, & \bar{\bar{N}}_i\hat{j}.\hat{y}, & \bar{\bar{N}}_i\hat{k}.\hat{y} \\
\bar{\bar{N}}_i\hat{i}.\hat{z}, & \bar{\bar{N}}_i\hat{j}.\hat{z}, & \bar{\bar{N}}_i\hat{k}.\hat{z} \\
\frac{d\bar{\bar{N}}_i}{dx}\hat{i}.\hat{z}, & \frac{d\bar{\bar{N}}_i}{dx}\hat{j}.\hat{z}, & \frac{d\bar{\bar{N}}_i}{dx}\hat{k}.\hat{z} \\
\frac{d\bar{\bar{N}}_i}{dx}\hat{i}.\hat{y}, & \frac{d\bar{\bar{N}}_i}{dx}\hat{j}.\hat{y}, & \frac{d\bar{\bar{N}}_i}{dx}\hat{k}.\hat{y} \\
\frac{d\bar{\bar{N}}_i}{dx}\hat{i}.\hat{x}, & \frac{d\bar{\bar{N}}_i}{dx}\hat{j}.\hat{x}, & \frac{d\bar{\bar{N}}_i}{dx}\hat{k}.\hat{x} \\
-\bar{\bar{N}}_i\hat{i}.\hat{z}, & -\bar{\bar{N}}_i\hat{j}.\hat{z}, & -\bar{\bar{N}}_i\hat{k}.\hat{z} \\
\bar{\bar{N}}_i\hat{i}.\hat{y}, & \bar{\bar{N}}_i\hat{j}.\hat{y}, & \bar{\bar{N}}_i\hat{k}.\hat{y} \\
0 , & 0 , & 0
\end{bmatrix}
\begin{Bmatrix} \alpha \\ \beta \\ \theta \end{Bmatrix}_i
$$

OR

$$\gamma = WN\delta$$

$$= WN \times T\,\delta^* = [W_A \,\vdots\, W_B] \left\{\begin{array}{c} a \\ \hline b \end{array}\right\} \quad \ldots \qquad (6.40)$$

The constrained shape function array is obtained from (6.40) and (6.37) as follows

$$\gamma = \left[W_A - W_B M_B^{-1} M_A\right] a$$

$$= W a \qquad \ldots \quad \ldots \quad \ldots \quad \ldots \quad \ldots \qquad (6.41)$$

The three elements presented above in which the theory presented in Chapter 5 was incorporated, were implemented in the LUSAS finite element system. Figures (6.6), (6.7) and (6.8) give flow diagrams of the computational procedure for the element shape functions, the pre-solution calculations and the post-solution calculations respectively.

The following applications were carried out to test the elements and the theory.

6.3 LINEAR ELASTIC SOLUTIONS

The linear elastic applications were carried out to assess the performance of the three elements in bending and torsion. The torsions of the x-y and x-z planes have been considered to be independent as a requirement of the large rotation theory. The total torque is equal to the summ of the torsional moments T_y and T_z which are equal in all the examples considered.

6.3.1 Straight Cantilever Beam

The cantilever beam (Figure 6.9) was modelled by one element. A square cross-section and a rectangular cross-section were considered. Solutions were obtained by using each of the three elements for the six

concentrated load cases at the free end. The results are presented in Tables 6.1 and 6.2 for the square and rectangular cross-sections respectively. These are in exact agreement with values obtained from the beam theory.

A channel-section cantilever beam (Figure 6.10) was idealised by three eccentric rectangular elements to test the eccentric formulation of the elements. The six concentrated load cases were applied at the free end. Solutions were obtained by each of the three elements. Table 6.3 gives the results compared with the beam theory. These show excellent agreement.

6.3.2 L-Type Cantilever Frame

The cantilever frame (Figure 6.11) was idealised by four elements. The frame was subjected to a concentrated transverse load at the free end. Idealisations by each of the three elements were used to obtain solutions.

A plot of the displacement, bending moment and torsion is given in Figure 6.13. These demonstrate that the bending moments have been accurately transferred into torsion from one beam to the other. The results from idealisations by each of the three elements are in

exact agreement. The use of the ISOBEM 4 element in such a problem, however, is not desirable unless careful attention is given to the arrangement of the degrees of freedom at the joint. It is necessary in this case to realise that the in-plane strain degree of freedom is in the local in-plane direction.

6.3.3 Semi-circular Beam

The semi-circular cantilever beam (Figure 6.12) was analysed by the employment of a three-element idealisation to assess the performance of the elements as curved beam elements. The beam was subjected to a concentrated transverse load at the free end. Solutions were obtained by each of the three elements. For comparison a nine SEMILOOF beam elements idealisation was also used to solve the semi-circular beam.

The results are presented in Figure 6.14. These clearly show that the elements can accurately accommodate very large curvatures.

6.4 GEOMETRICALLY NON-LINEAR SOLUTIONS

It has been shown in Chapter 4 that elements which are not C^1 continuous in all displacement components will give satisfactory results for small curvature problems only. The use of the correct large rotation theory

with such elements in the analysis of large rotation and curvature problems results in the equations becoming indefinite. The approximate theory based on the conventional strains (Equations (5.43a) and (5.72a) to (5.72d), which is commonly used in plate and shell problems, can be employed in cases where the use of such elements is essential. It is important to note, however, that only approximate answers are obtained by this theory. Therefore, the accuracy of the Total Lagrangian large rotation formulations is tested by using ISOBEM 4 elements only.

6.4.1 Straight Cantilever Under Point Load at Free End

The cantilever beam (Figure 6.9a), subjected to a point load at the free end in the global Y direction, was modelled by eight ISOBEM 4 elements. Twenty load increments, with Newton-Raphson equilibrium iterations within each increment, were applied up to a total load of $10 \frac{EI}{L^2}$. Solutions were obtained by the TLG and TLC formulations.

An average of four iterations per increment was required for convergence to a relative error of 10^{-3} by both formulations. The results are presented in Table 6.4

and Figure 6.15. These are in very good agreement with values from reference [79].

The eight element cantilever model was also solved using the SEMILOOF and ISOBEM 4 beam elements in which the approximate theory based on the geometric strains was employed. The results are shown in Figure 6.16. The ISOBEM 4 elements solution was carried out to show the effect of the approximation introduced in the theory. It can be seen from Figures 6.15 and 6.16 that the approximation results in errors of up to 27% in the displacement components. This is a confirmation of the importance of the correct large rotation theory which has been developed.

6.4.3 Three-dimensional 45-degree Bend

Bathe and Bolourchi [20] have presented the solution to the problem of a cantilever 45-degree bend (Figure 6.17) by the Updated Lagrangian formulation. They modelled the bend by eight beam elements and sixteen 16-node three-dimensional solid elements for comparison. The solution was obtained by applying the load in sixty equal steps.

The bend is used here to test the accuracy of the Total Lagrangian formulations of the three-dimensional large rotation theory which has been developed. This example is the only one, for which a solution is available, that can clearly demonstrate the excellent capabilities of the Total Lagrangian formulations.

The circular bend was idealised by eight ISOBEM 4 elements. The load was applied in thirty increments with Newton-Raphson equilibrium iterations within each increment. Solutions were obtained by the TLG and TLC formulations. An average of four iterations was required for convergence to a relative error of 10^{-3} for both solutions.

The results for the tip displacements are presented in Table 6.5. These show very close agreement between the two Total Lagrangian formulations. Figure 6.18 gives a plot of the results compared with those from reference [20] and can be seen to be in good agreement. A plot of sample deformed configurations of the bend at various load levels is presented in Figure 6.19. The results clearly demonstrate the accuracy of the Total Lagrangian formulations in predicting displacements.

The stress resultants from the two formulations are compared in Figures 6.20a-e for the fifteenth load increment ($\frac{PR^2}{EI} = 3.6$). All six stress resultants (Figure 5.4) are equally important for the convergence of the solution to the correct answers.

Identical results are obtained from the two formulations for the two bending moments M_{xz} (Figure 6.20a) and M_{xy} (Figure 6.20b).

In the development of the large rotation theory (Chapter 5) the torsion of the local y and z normals has been considered independently. The results for the two torsional moments T_y and T_z have been found to be almost identical in this example. The requirement that the two torsions should be considered independently has arisen, however, from the definition of the local axes and the nonlinear strain-displacement relations. Figure 6.20c gives the variation of the total torsional moment ($T = T_y + T_z$) along the length. This shows excellent agreement been the two formulations.

The values of the shear force F_{yz} show slight oscillations in both formulations. The average nodal values from the two formulations (Figure 6.20d) are in very good agreement.

The axial force results, however, demonstrate clearly the difference between the two formulations. This can be seen from Figure 6.20e. The TLG results are obviously wrong since the axial force is expected to be zero at the support (Point A, Figure 6.20e). The error reduces with the reduction in curvature along the beam. The values from the two formulations agree at the free end where the curvature is zero. The error is, therefore, due to neglecting the effect of curvature change on the axial force when using the Green strains. The axial force values from the TLC formulation represent the true axial forces. The slight error at the support in these values, compared to the TLG results, and the slight variations between elements in the shear force F_{yz} values can be considered to be an indication that more elements are required in order to obtain the exact answers.

6.5 COMBINED GEOMETRIC AND MATERIAL NON-LINEARITY SOLUTIONS

The following combined geometric and material nonlinearity solutions were carried out in the earlier stages of the research by using the SEMILOOF beam element. A geometric nonlinearity theory in which the curvatures were assumed to be small was used [33]. Such an approximation will have no effect on the results since the curvatures

are small in the three examples considered. An elastic perfectly plastic stress-strain relationship was used in all solutions.

6.5.1 Fully-Encastre Beam Under Central Point Load

This problem has been studied by Crisfield [6] using finite elements and experimentally by Campbell and Charlton [84] using a mild steel beam. The properties of the beam are given in Table 6.6.

Half the beam was modelled by six equal length SEMILOOF beam elements. The load was applied incrementally with five Newton-Raphson equilibrium iterations within each increment. The results are presented in Table 6.6.

The relationship between the central load and central deflection is compared with results from references [6] and [84] in Figure 6.21. The relationship between the axial force and central deflection is shown in Figure 6.22. The values obtained closely agree with Crisfield's finite element solution in which an allowance is made for fibre yield. The results also agree with the experimental values.

6.5.2 Simply Supported Rectangular Strut

The complete load-central deflection relationship for a simply supported strut (Figure 6.23) has been obtained by Crisfield using finite elements [6] and a Ritz procedure [85].

Half the span of the strut was idealised by six equal length SEMILOOF beam elements. The solution was obtained incrementally applying displacements with a residual correction within each increment. An initial imperfection in the form of a sine wave was assumed with a maximum value at mid-span of $\frac{L}{1000}$, where L is the span of the strut.

The results are presented in Table 6.7. Figure 6.23 shows the relationship between the axial load and central deflection compared with values from references [6] and [85]. The SEMILOOF beam solution is in excellent agreement with the Ritz method solution.

6.5.3 Continuous T-Beam Strut

A single span of the continuous T-beam strut (Figure 6.24) was modelled by two sets of eight eccentric SEMILOOF beam elements along the length. The solution was carried out by applying displacement increments with a residual correction within each increment. The initial

deflected shape was defined by a sine wave with a maximum value of $\frac{L}{750}$ at mid-span.

The results are given in Table 6.8. Figure 6.24 shows the relationship between the axial load and maximum deflection. These are compared with finite element solutions which have been obtained by Crisfield and Moan and Soreide [6]. This indicates close agreement between the solutions.

6.6 CONCLUSIONS

1. The formulation of the three eccentric thin curved three-dimensional beam elements ISOBEM 3, ISOBEM 4 and SEMILOOF has been presented. The elements have been developed by using the constraint technique. The elements are suitable for use as stiffeners.

2. The elements are of rectangular cross-section. It has been demonstrated that the linear elastic solutions by the elements are in excellent agreement with the beam theory results.

3. It has been shown that the ISOBEM 4 element, in which all three displacement components are C^1 continuous, can exactly accommodate the Total

Lagrangian large rotation formulations which have been developed. The capability of the formulations, when used with this element, to correctly predict the large rotation response of curved beam structures in a three-dimensional space has been demonstrated.

4. The superiority of the Total Lagrangian formulation which is based on the conventional strains (TLC) compared to the Total Lagrangian formulation which is based on the Green strains (TLG) in predicting true axial forces in large rotation and curvature problems has been reaffirmed.

5. The SEMILOOF and ISOBEM 3 beam elements, which are only C^o continuous in the in-plane displacements, are not suitable for use in the Total Lagrangian solution of thin structures in which both the rotation and curvature are large. It has been shown, however, that these elements can be used when the approximate theory based on the geometric strains is employed. This gives an approximate method for the analysis of large rotation and curvature problems in which the continuity of the linear axial strain measure is objectionable.

6. Combined geometric and material nonlinearity solutions agree with published experimental and finite element results. The solutions having been obtained using the SEMILOOF beam element which has been presented in this chapter.

$$\vec{r} = X\hat{\imath} + Y\hat{\jmath} + Z\hat{k}$$

$$\vec{R} = \vec{r} + y\hat{y} + z\hat{z}$$

$$\vec{V} = u\hat{x} + v\hat{y} + w\hat{z}$$

$$= U\hat{\imath} + V\hat{\jmath} + W\hat{k}$$

$$\bar{r} = \vec{r} + \vec{V}$$

$$\bar{R} \simeq \bar{r} + y g_y + z g_z$$

$$\vec{\Omega} \simeq \theta_x \hat{x} + \theta_y \hat{y} + \theta_z \hat{z}$$

$$\simeq \alpha\hat{\imath} + \beta\hat{\jmath} + \theta\hat{k}$$

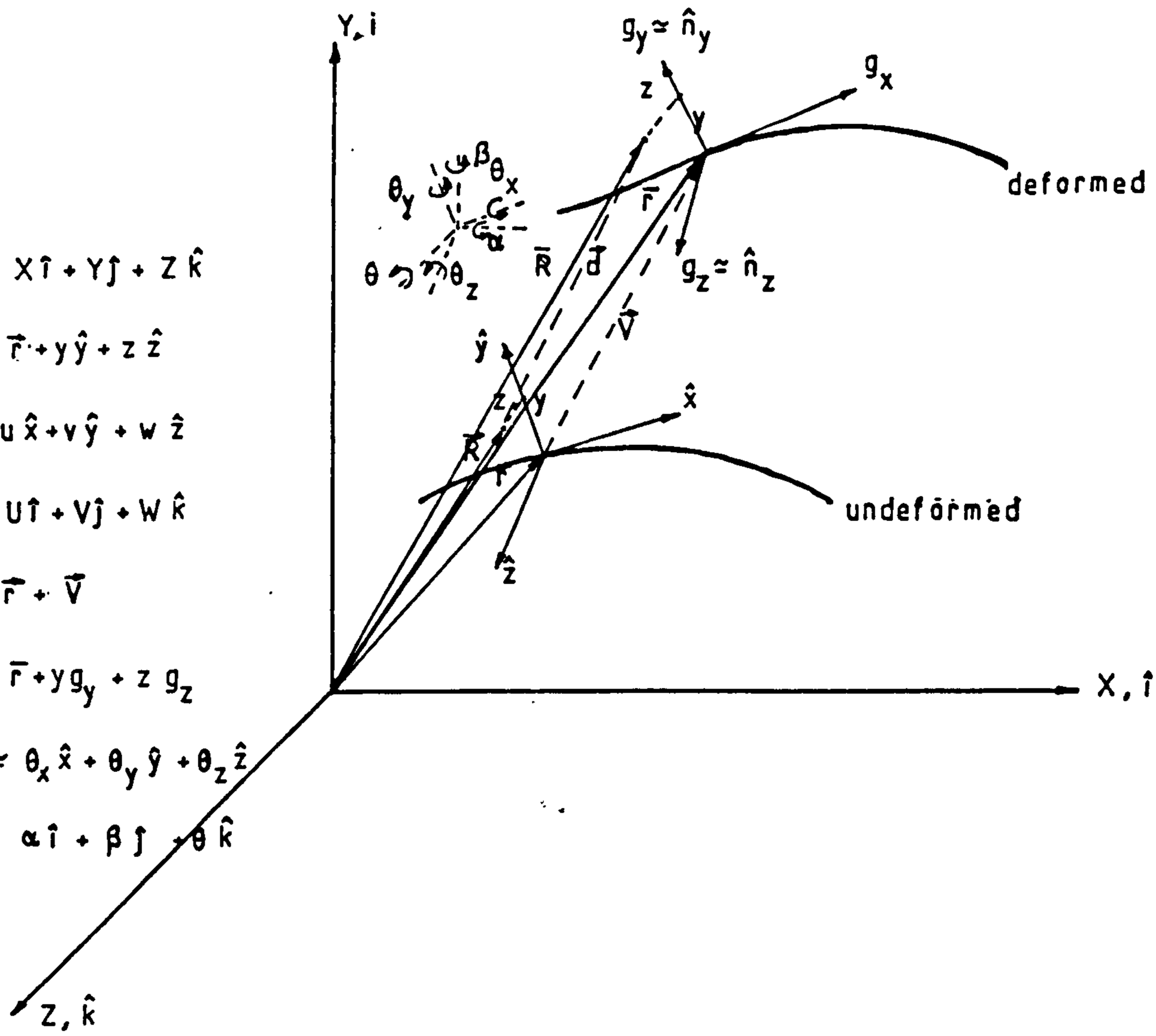

FIGURE 6.1 - 3-D Beam Deformation Geometry (Small Displacements)

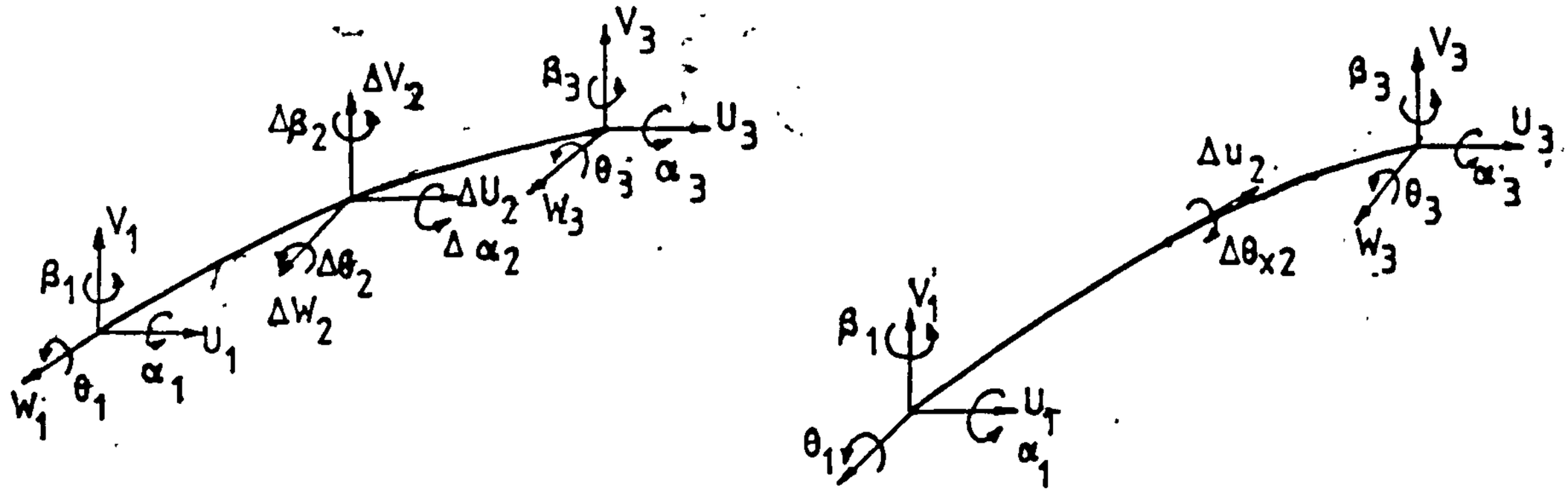

FIGURE 3.2 - ISOBEM 3 Nodal Variables

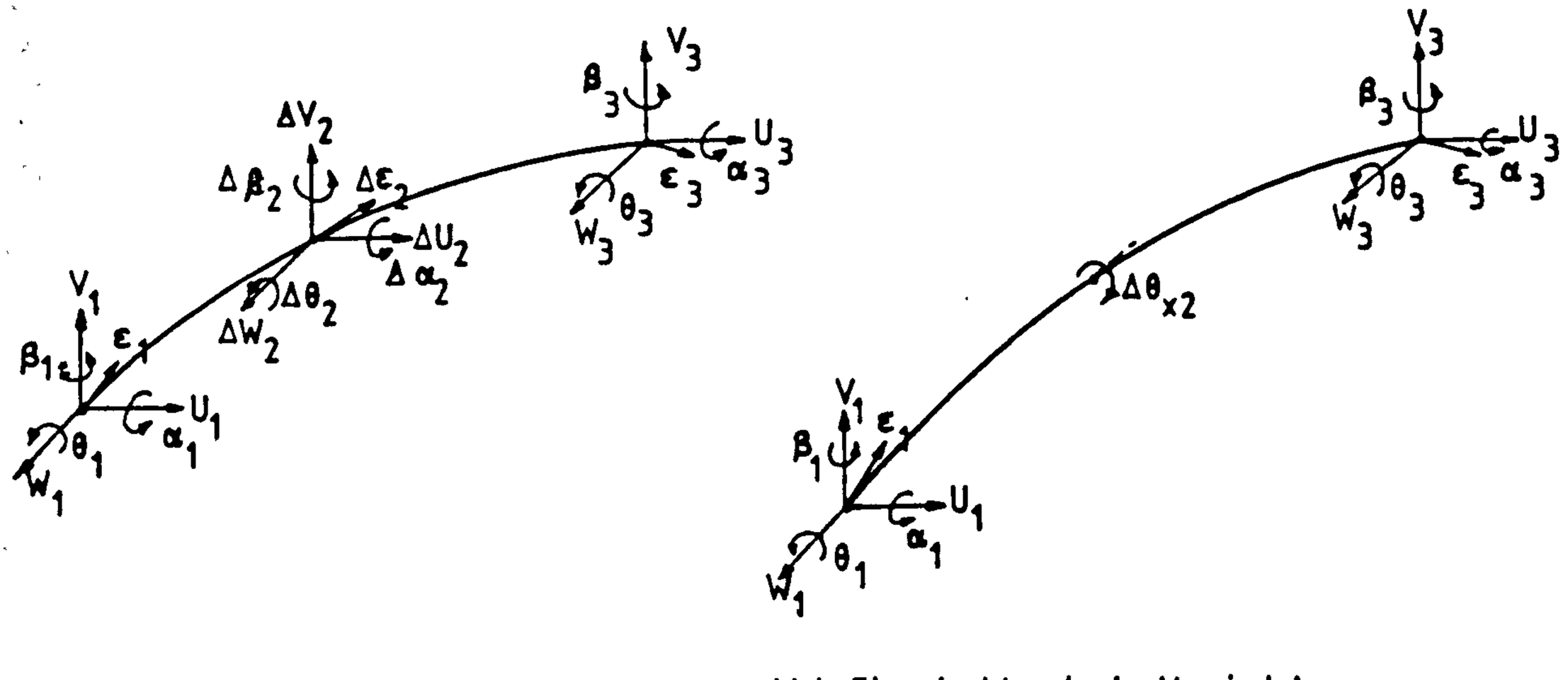

(a) Initial Variables a+b (21 D.O.F.)

(b) Final Wanted Variables a (15 D.O.F.)

FIGURE 6.3 - ISOBEM 4 Nodal Variables

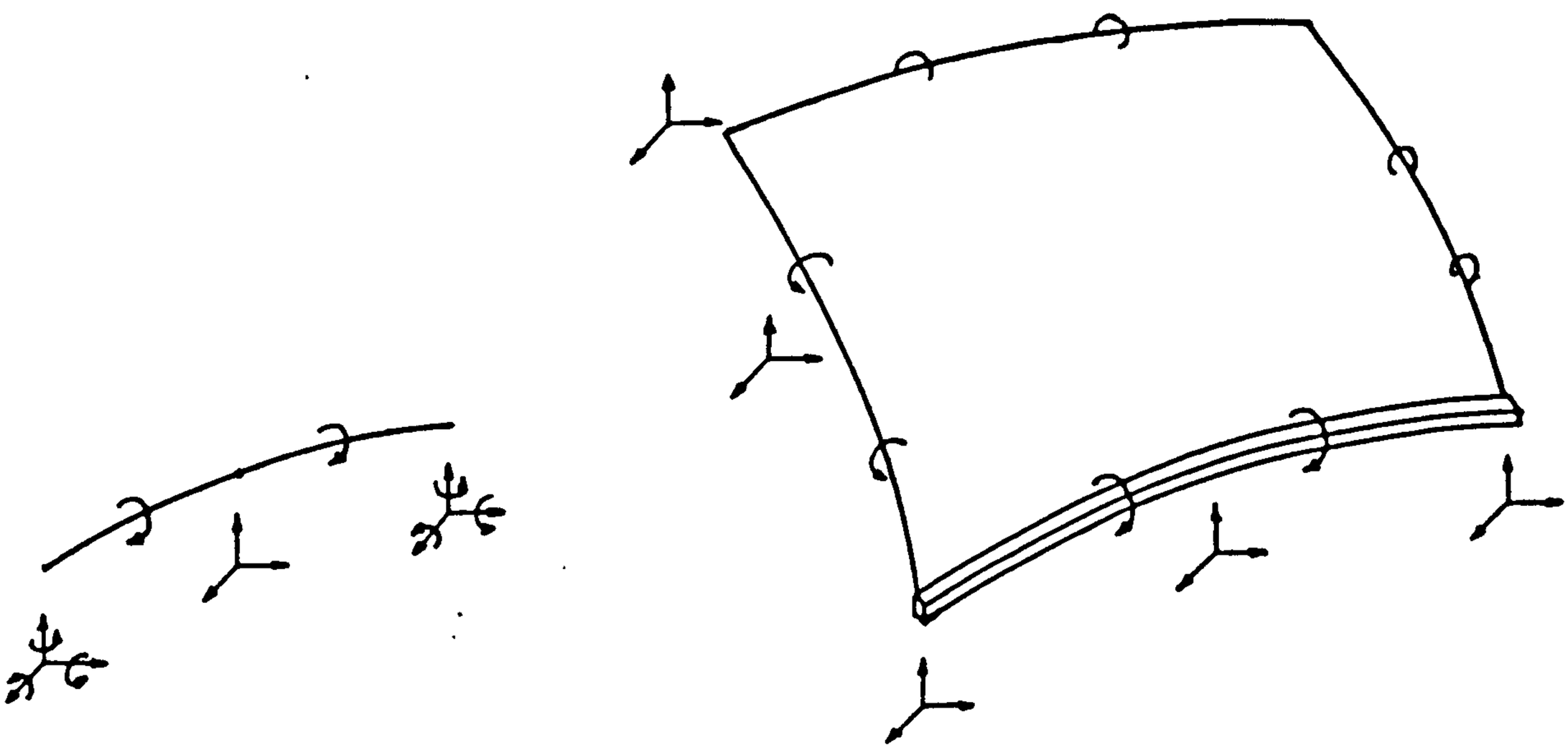

(a) Nodal variables of thin element

(b) Variables shared with shell element

FIGURE 6.4 – Nodal Configuration of the SEMILOOF Thin Beam Element

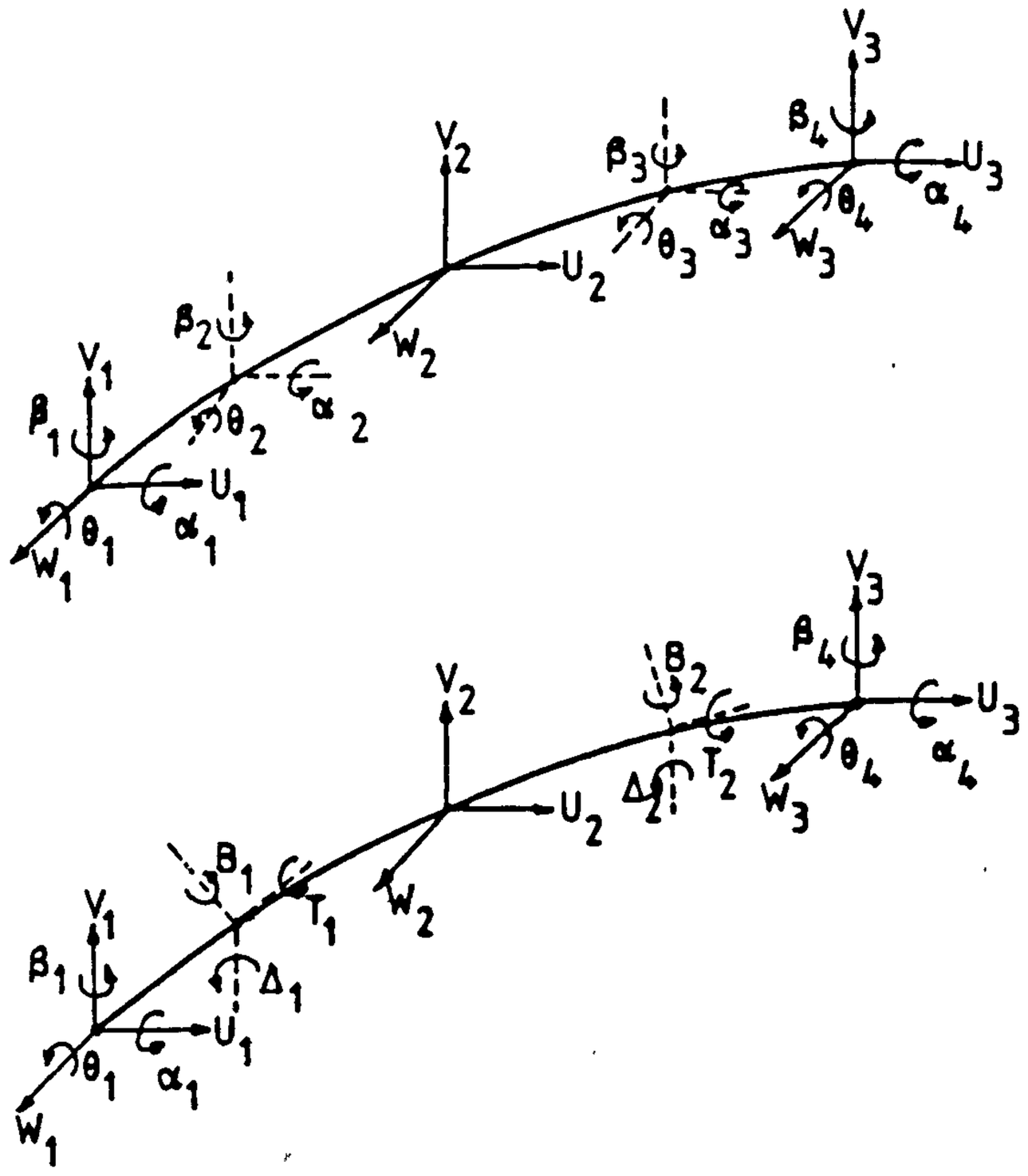

(a) Initial Variables (21 D.O.F.)

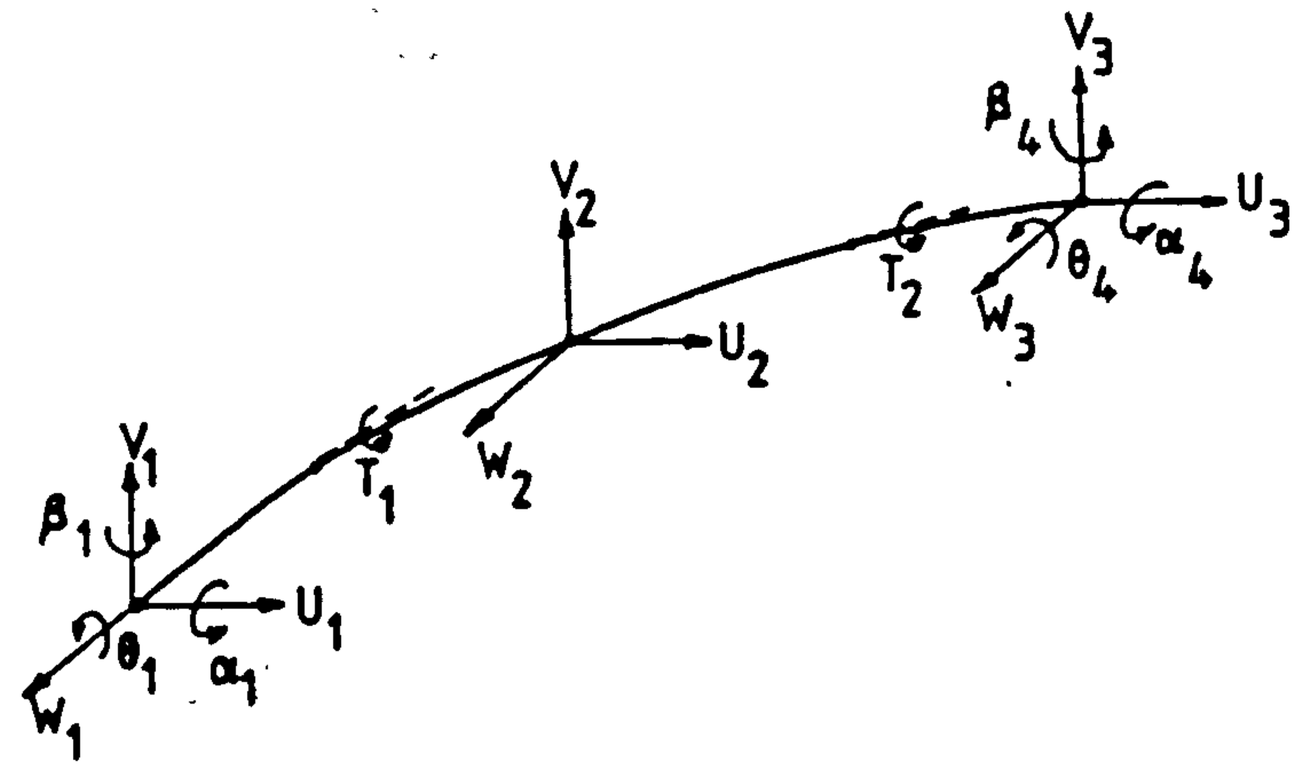

(b) Final Wanted Variables (17 D.O.F.)

FIGURE 6.5 - SEMILOOF Beam Nodal Variables

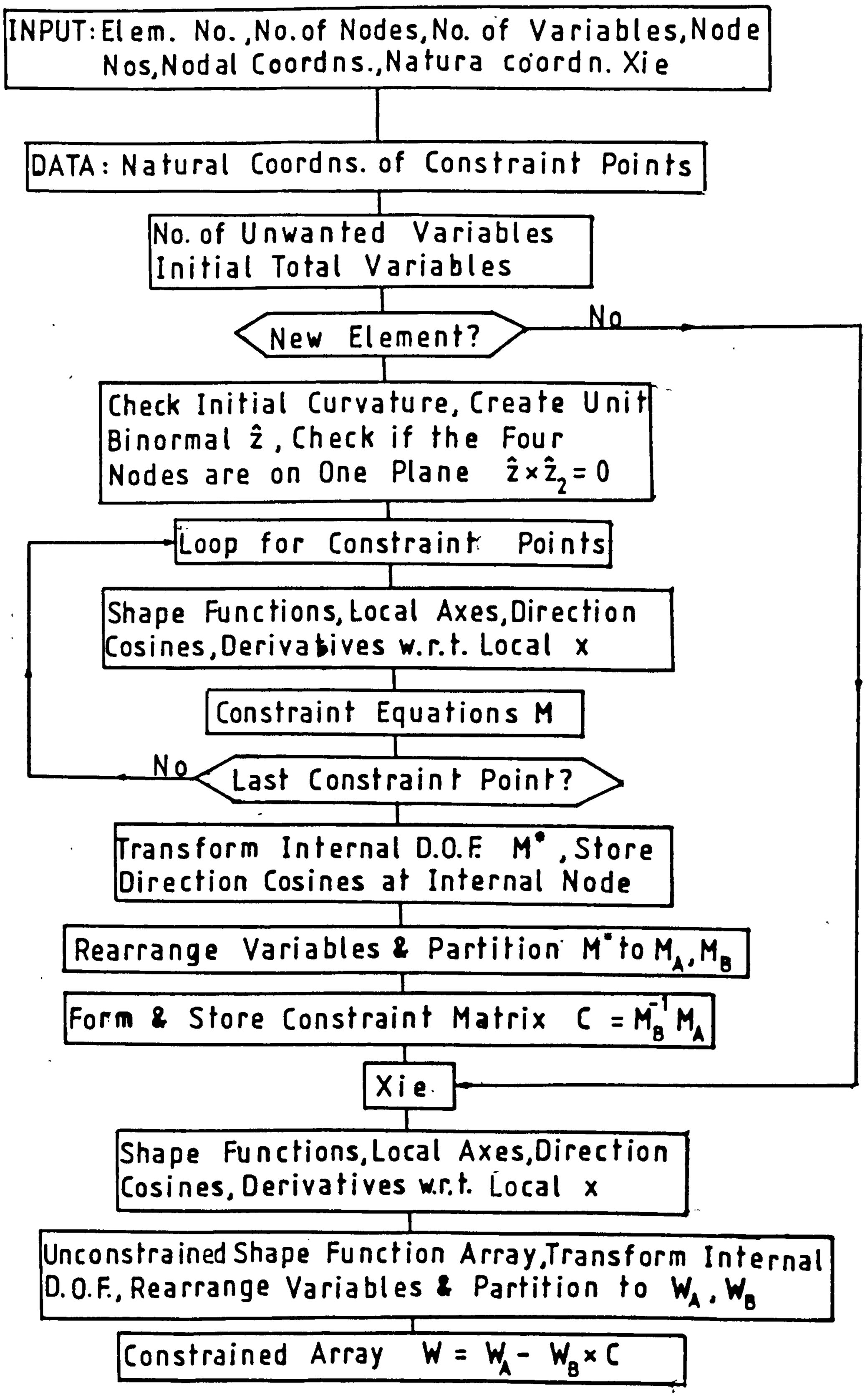

FIGURE 6.6 - 3-D Beam Element Computations - The Constrained Shape Function Array

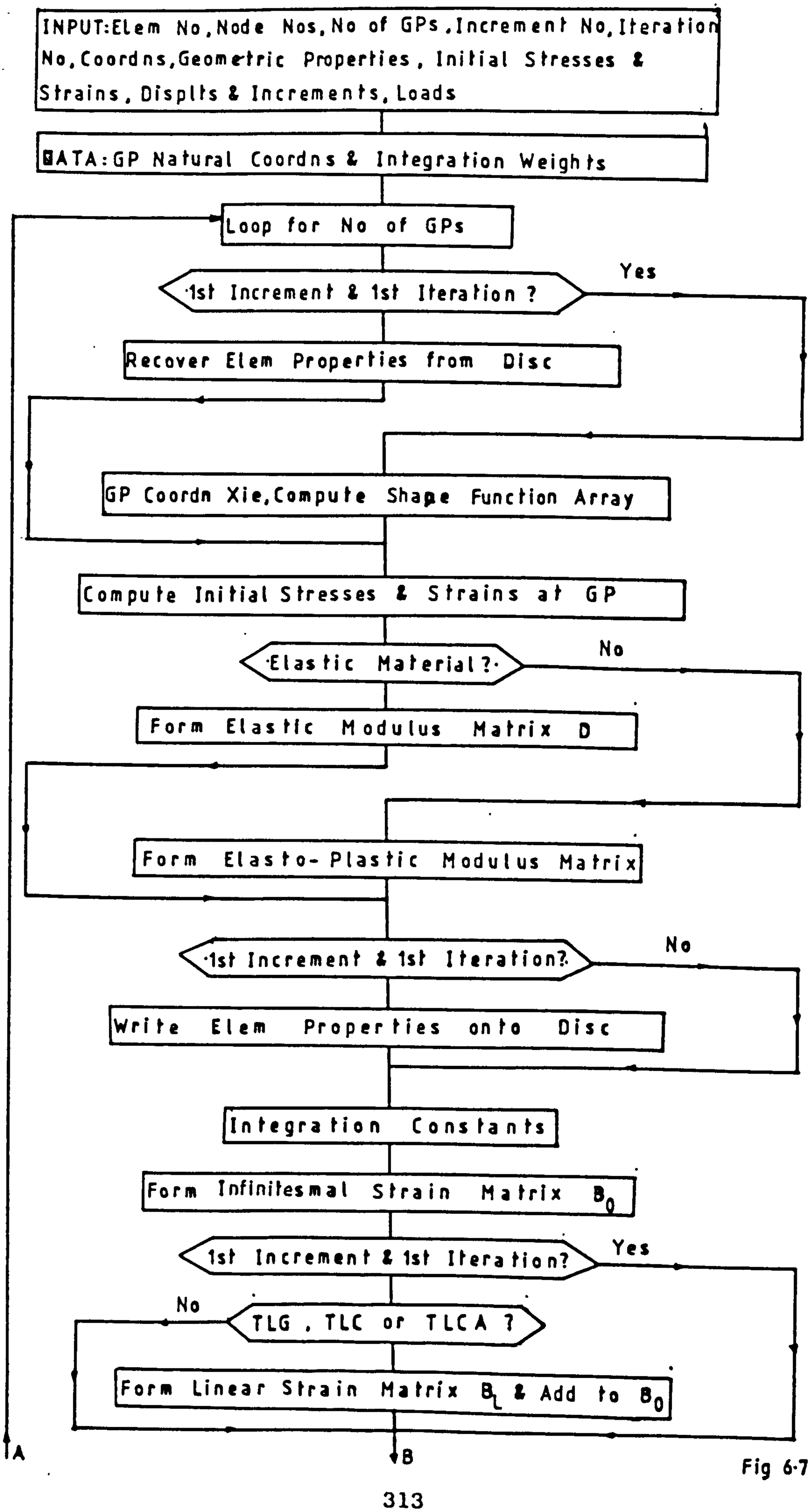
INPUT:Elem No,Node Nos,No of GPs,Increment No,Iteration No,Coordns,Geometric Properties, Initial Stresses & Strains, Displts & Increments, Loads
DATA:GP Natural Coordns & Integration Weights
Loop for No of GPs
1st Increment & 1st Iteration ?
Yes
Recover Elem Properties from Disc
GP Coordn Xie,Compute Shape Function Array
Compute Initial Stresses & Strains at GP
Elastic Material?
No
Form Elastic Modulus Matrix D
Form Elasto-Plastic Modulus Matrix
1st Increment & 1st Iteration?
No
Write Elem Properties onto Disc
Integration Constants
Form Infinitesmal Strain Matrix B_0
1st Increment & 1st Iteration?
Yes
No
TLG , TLC or TLCA ?
Form Linear Strain Matrix B_L & Add to B_0
A
B

Fig 6·7

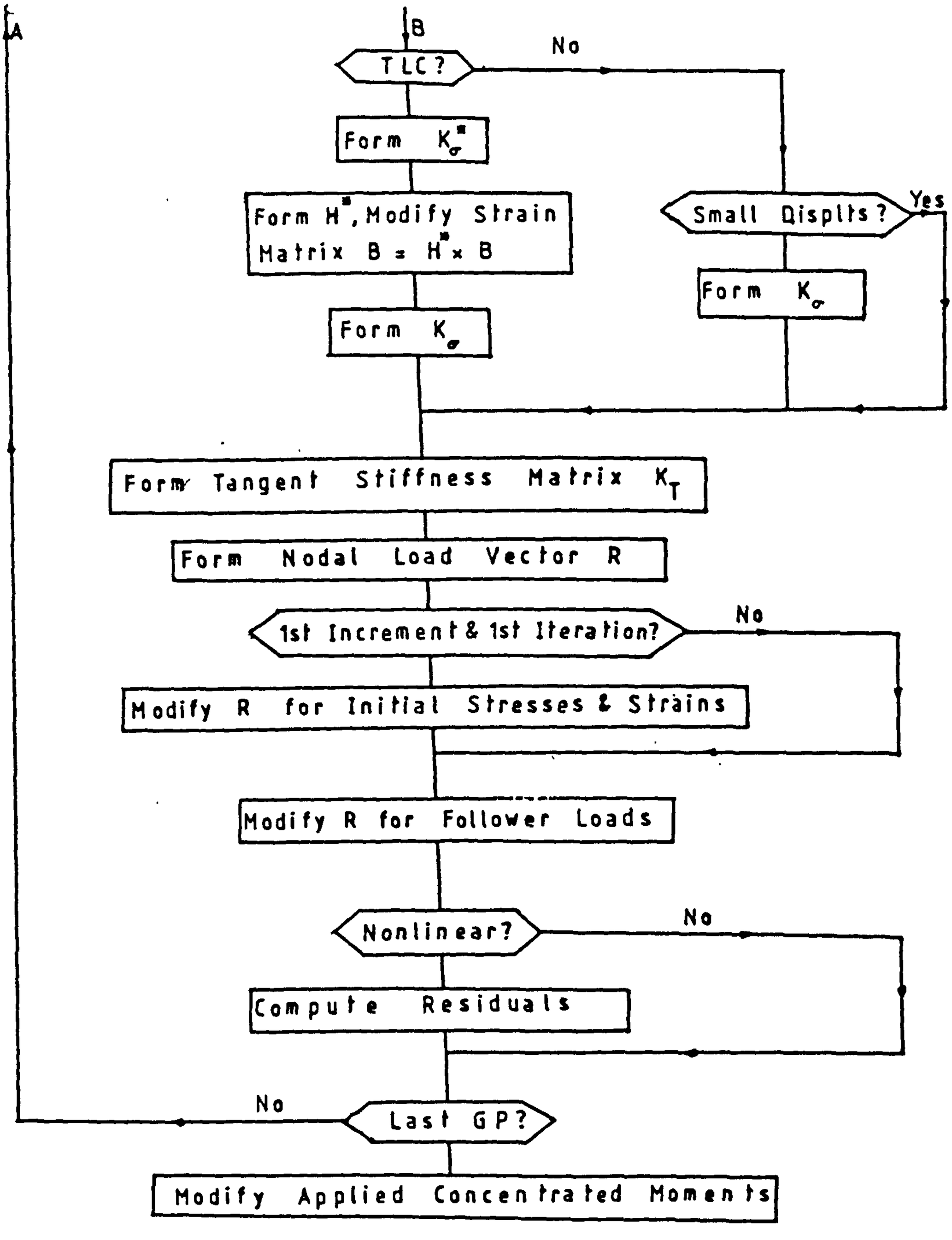

FIGURE 6.7 - 3-D Beam Element Pre-solution Computations - The Tangent Stiffness Matrix and The Nodal Residuals

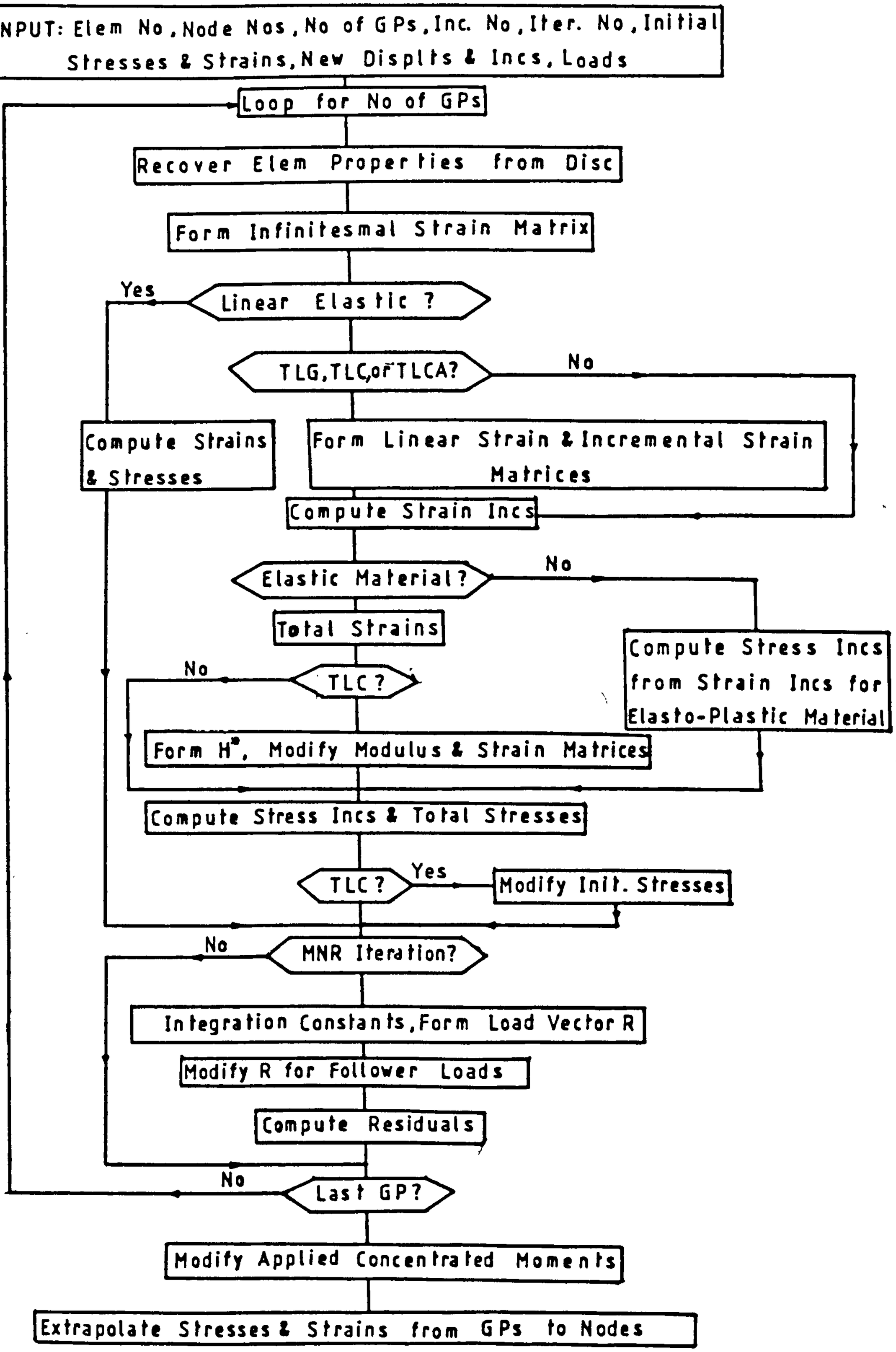

FIGURE 6.8 - 3-D Beam Element Post-solution Computations - Calculation of Strains and Stresses

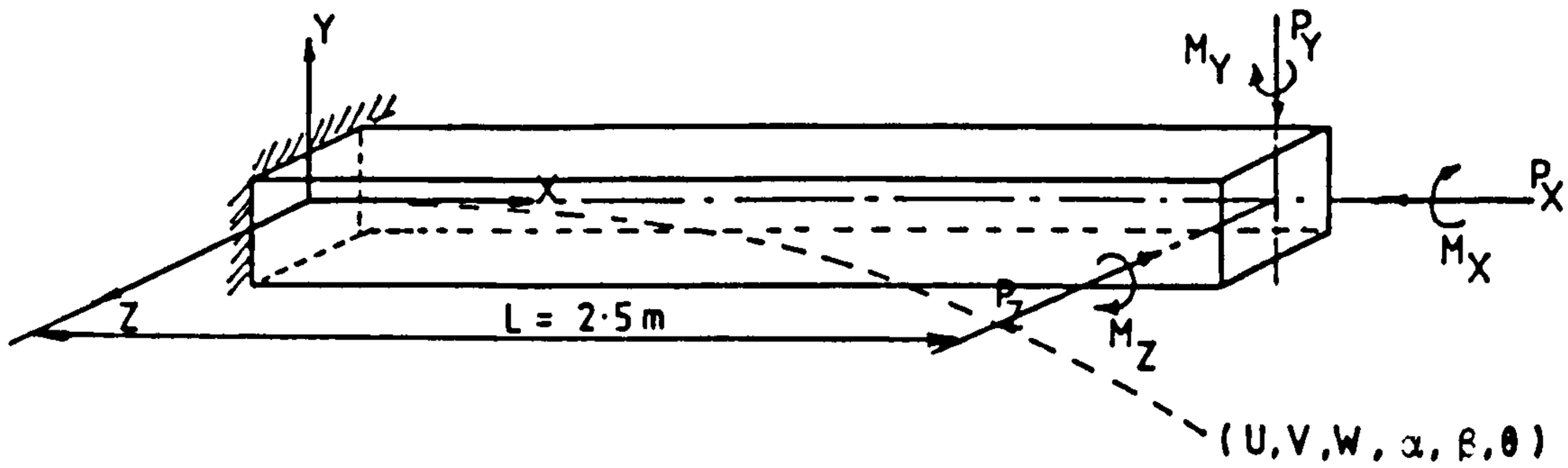

$E = 0{\cdot}2 \times 10^9 \quad KN/m^2$ $\qquad \nu = 0{\cdot}3$

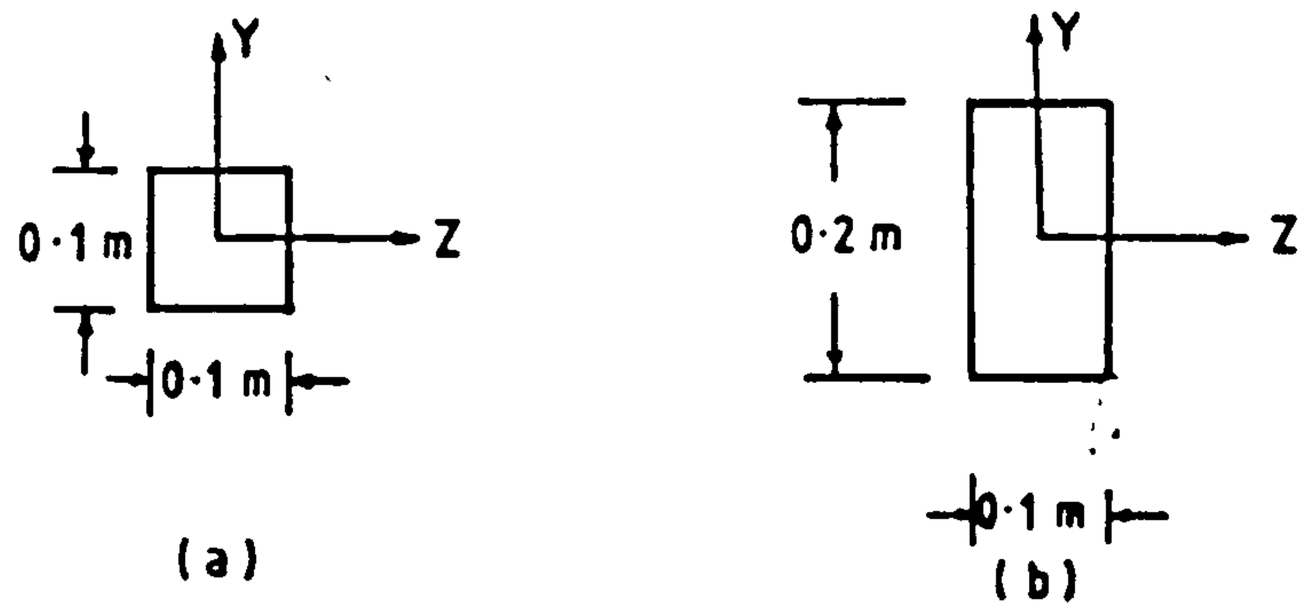

FIGURE 6.9 - Straight Cantilever Beam Properties

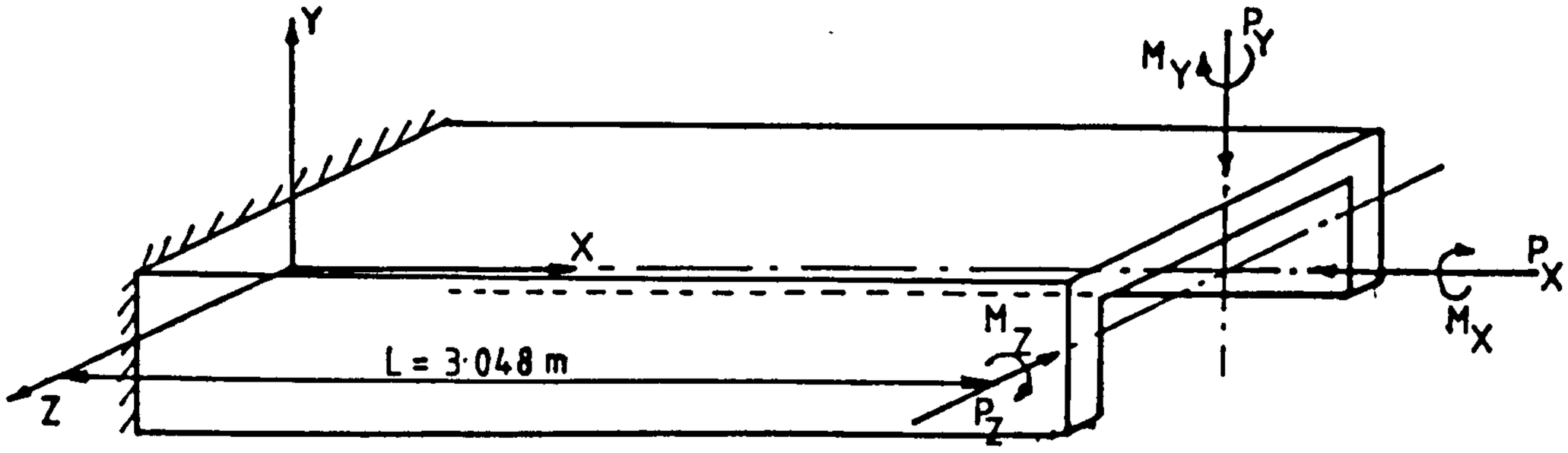

$E = 2{\cdot}07 \times 10^8 \quad KN/m^2$

$\nu = 0{\cdot}3$

$A = 3{\cdot}354832 \times 10^{-2} \; m^2$

$I_{YY} = 4{\cdot}11958 \times 10^{-3} \; m^4$

$I_{ZZ} = 6{\cdot}34379 \times 10^{-5} \; m^4$

$J = 6{\cdot}955036 \times 10^{-6} \; m^4$

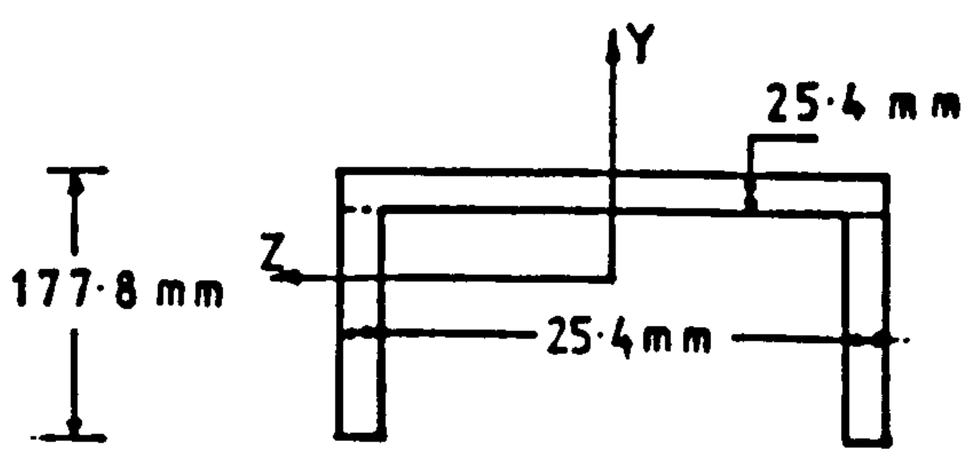

FIGURE 6.10 - Channel-section Straight Cantilever Beam Properties

Load Case (at Free End)	Description of Value	Finite Element Solution			Beam Theory
		ISOBEM 3	ISOBEM 4	SEMILOOF	
Axial compressive load $P_x = -1$	$U \times 10^5$ P_A	- .125 -1.0	- .125 -1.0	- .125 -1.0	$\frac{P_x L}{AE} = -.125$ $P_x = -1.0$
Point load in y-direction $P_y = -1$	$V \times 10^2$ $\theta \times 10^2$ $M_{xy(A)}$	- .3125 - .1875 2.5	- .3125 - .1875 2.5	- .3125 - .1875 2.5	$\frac{P_y L^3}{3EI_{zz}} = -.3125$ $\frac{P_y L^2}{2EI_{zz}} = -.1875$ $-P_y L = 2.5$
Point load in z-direction $P_z = -1$	$W \times 10^2$ $\beta \times 10^2$ $M_{xz(A)}$	- .3125 .1875 2.5	- .3125 .1875 2.5	- .3125 .1875 2.5	$\frac{P_z L^3}{3EI_{yy}} = -.3125$ $\frac{-P_z L^2}{2EI_{yy}} = .1875$ $-P_z L = 2.5$
Torque $M_x = -1$	$\alpha \times 10^2$ T_A	-.231043 1.0	-.231043 1.0	-.231043 1.0	$\frac{M_x L}{GJ} = -.231043$ $-M_x = 1.0$
Concentrated moment $M_y = -1$	$W \times 10^2$ $\beta \times 10^2$ $M_{xz(A)}$	.1875 - .15 -1.0	.1875 - .15 -1.0	.1875 - .15 -1.0	$\frac{-M_y L^2}{2EI_{yy}} = .1875$ $\frac{M_y L}{EI_{yy}} = -.15$ $M_y = -1.0$
Concentrated moment $M_z = -1$	$V \times 10^2$ $\theta \times 10^2$ $M_{xy(A)}$	- .1875 - .15 1.0	- .1875 - .15 1.0	- .1875 - .15 1.0	$\frac{M_z L^2}{2EI_{zz}} = -.1875$ $\frac{M_z L}{EI_{zz}} = -.15$ $-M_z = 1.0$

TABLE 6.1 Straight Cantilever Beam Results (square x - section).

Load Case (at Free End)	Description of Value	Finite Element Solution			Beam Theory
		ISOBEM 3	ISOBEM 4	SEMILOOF	
Axial compressive Load $P_x = -1$	$U \times 10^6$	-.625	-. 625	-.625	$\frac{P_x L}{AE} = -.625$
	P_A	-1.0	-1.0	-1.0	$P_x = -1.0$
Point load in Y-direction $P_y = -1$	$V \times 10^3$	-.390625	-.390625	-.390625	$\frac{P_y L^3}{3EI_{zz}} = -.390625$
	$\theta \times 10^3$	-.234375	-234375	-.234375	$\frac{P_y L^2}{2EI_{zz}} = -.234375$
	$M_{xy(A)}$	2.5	2.5	2.5	$-P_y L = 2.5$
Point load in Z-direction $P_z = -1$	$W \times 10^2$	-.15625	-.15625	-.15625	$\frac{P_z L^3}{3EI_{yy}} = -.15625$
	$\beta \times 10^3$	.9375	.9375	.9375	$\frac{-P_z L^2}{2EI_{yy}} = .9375$
	$M_{xz(A)}$	2.5	2.5	2.5	$-P_z L = 2.5$
Torque $M_x = -1$	$\alpha \times 10^3$	-.698424	-.698424	-.698424	$\frac{M_x L}{GJ} = -.698424$
	T_A	1.0	1.0	1.0	$-M_x = 1.0$
Concentrated moment $M_y = -$	$W \times 10^3$	.9375	.9375	.9375	$\frac{-M_y L^2}{2EI_{yy}} = .9375$
	$\beta \times 10^3$	-.75	-.75	-.75	$\frac{M_y L}{EI_{yy}} = -.75$
	$M_{xz(A)}$	-1.0	-1.0	-1.0	$M_y = -1.0$
Concentrated moment $M_z = -1$	$V \times 10^3$	-.234375	-.234375	-.234375	$\frac{M_z L^2}{2EI_{zz}} = -.234375$
	$\theta \times 10^3$	-.1875	-.1875	-.1875	$\frac{M_z L}{EI_{zz}} = -.1875$
	$M_{xy(A)}$	1.0	1.0	1.0	$-M_z = 1.0$

TABLE 6.2 Straight Cantilever Beam Results (Rectangular x-Section).

Load Case (at Free End)	Description of Value	Finite Element Solution			Beam Theory
		ISOBEM 3	ISOBEM 4	SEMILOOF	
Axial compressive load	$U \times 10^6$	-.438908	-.438908	-.438908	$\frac{P_x L}{AE} = -.438908$
$P_x = -1$	P_{xA}	-1.00	-1.00	-1.00	$P_x = -1$
Point load in Y-direction	$V \times 10^3$	-.718794	-.718794	-.718794	$\frac{P_y L^3}{3EI_{zz}} = -.718794$
$P_y = -1$	$\theta \times 10^3$	-.353737	-.353737	-.353737	$\frac{P_y L^2}{2EI_{zz}} = -.353737$
	$M_{xy(A)}$	3.0480	3.0480	3.0480	$-P_y L = 3.048$
Point load in Z-direction	$W \times 10^4$	-.110688	-.110688	-.110688	$\frac{P_z L^3}{3EI_{yy}} = -.110688$
	$\beta \times 10^5$	.544724	.544724	.544724	$-\frac{P_z L^2}{2EI_{yy}} = .544724$
$P_z = -1$	$M_{xz(A)}$	3.0480	3.0480	3.0480	$-P_z L = 3.048$
Torque	$\alpha \times 10^2$	-.550451	-.550451	-.550451	$\frac{M_x L}{GJ} = -.550451$
$M_x = -1$	T_A	1.00	1.00	1.00	$-M_x = 1.0$
Concentrated moment	$W \times 10^5$	.544724	.544724	.544724	$-\frac{M_y L^2}{2EI_{yy}} = .544724$
	$\beta \times 10^5$	-.357430	-.357430	-.357430	$\frac{M_y L}{EI_{yy}} = -.357430$
$M_y = -1$	$M_{xz(A)}$	-1.00	-1.00	-1.00	$M_y = -1.0$
Concentrated moment	$V \times 10^3$	-.353737	-.353737	-.353737	$\frac{M_z L^2}{2EI_{zz}} = -.353737$
	$\theta \times 10^3$	-.232111	-.232111	-.232111	$\frac{M_z L}{EI_{zz}} = -.232111$
$M_z = -1$	$M_{xy(A)}$	1.00	1.00	1.00	$-M_z = 1.00$

TABLE 6.3 - Straight Cantilever Beam Results (Channel Section).

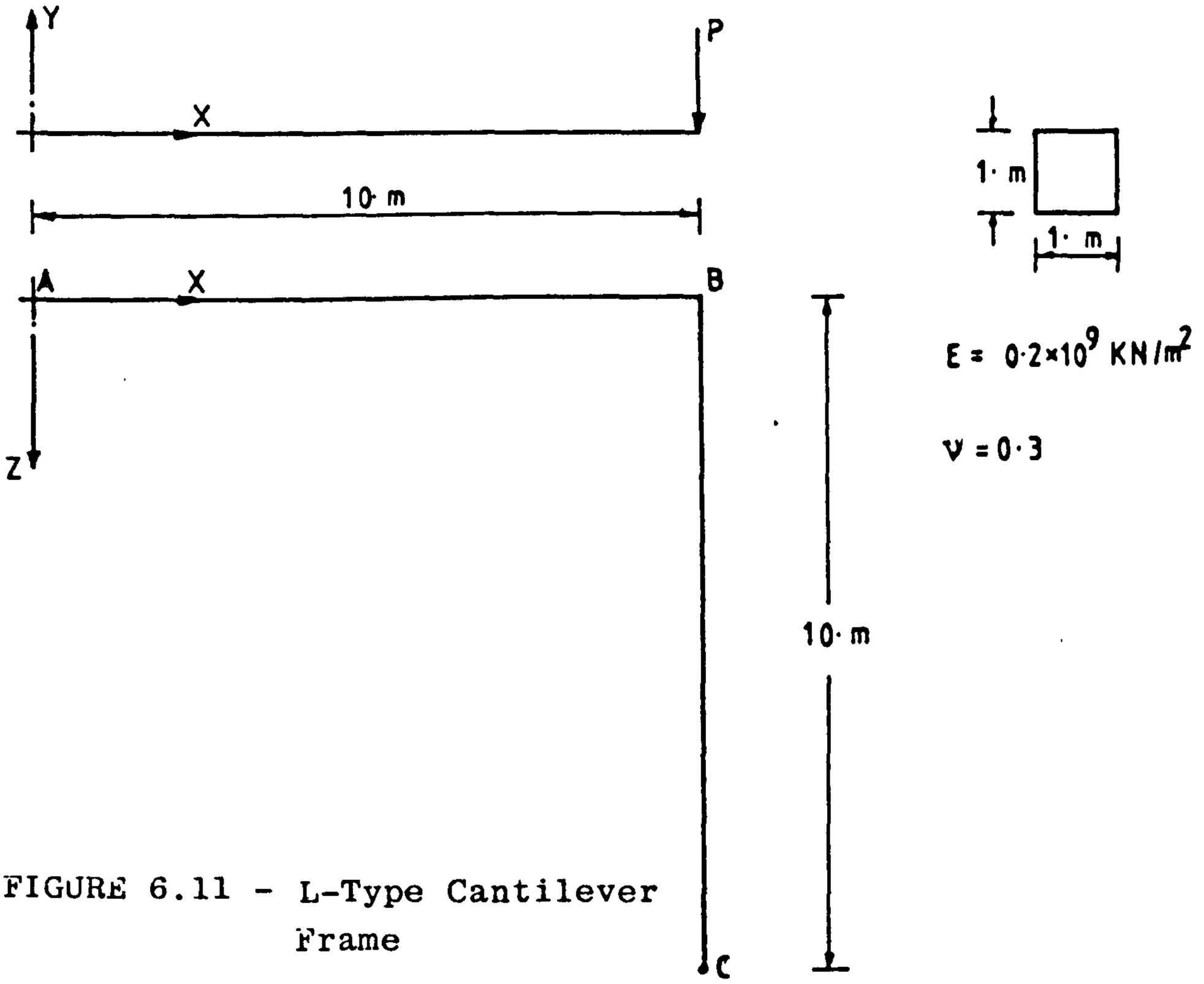

FIGURE 6.11 - L-Type Cantilever Frame

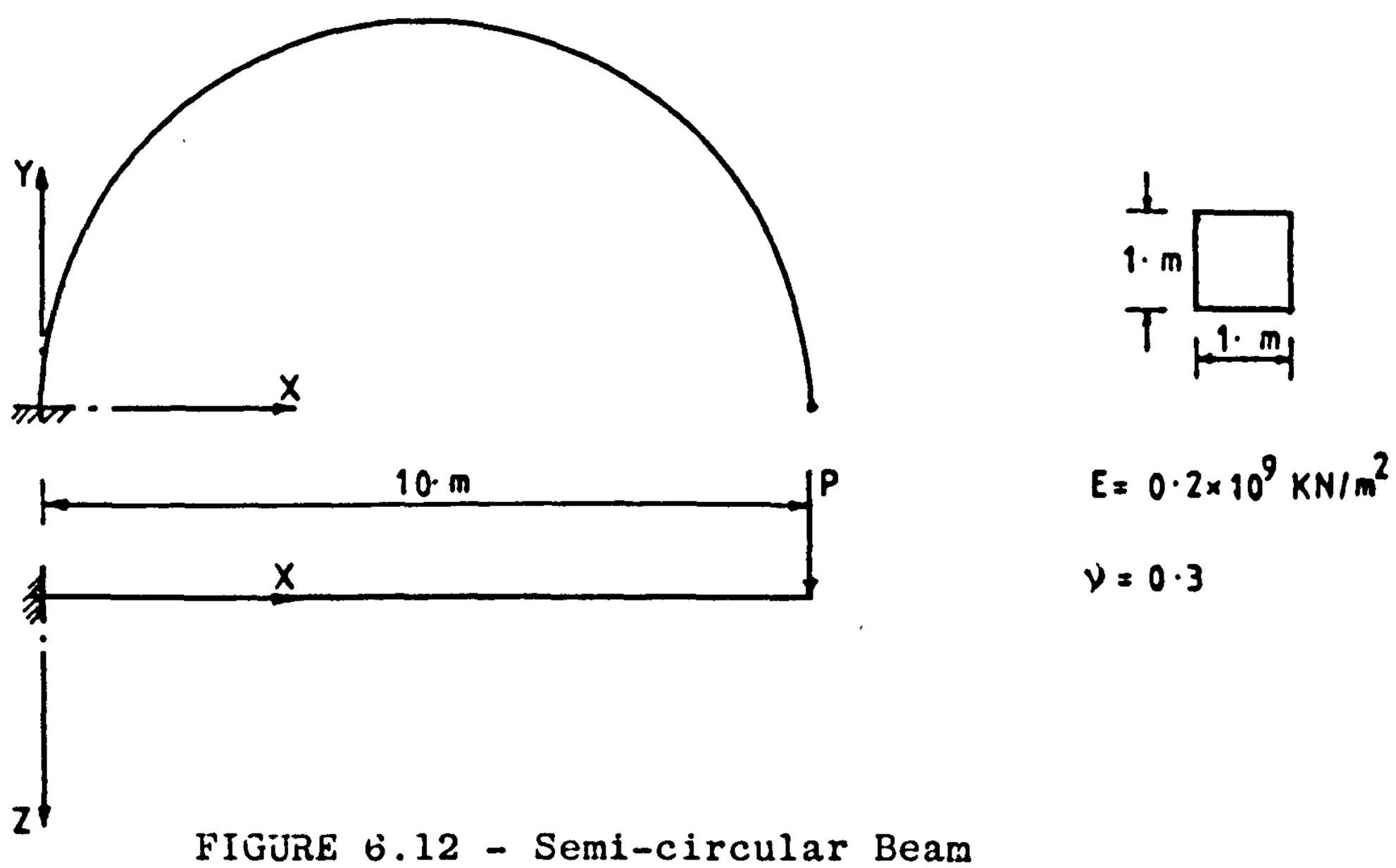

FIGURE 6.12 - Semi-circular Beam

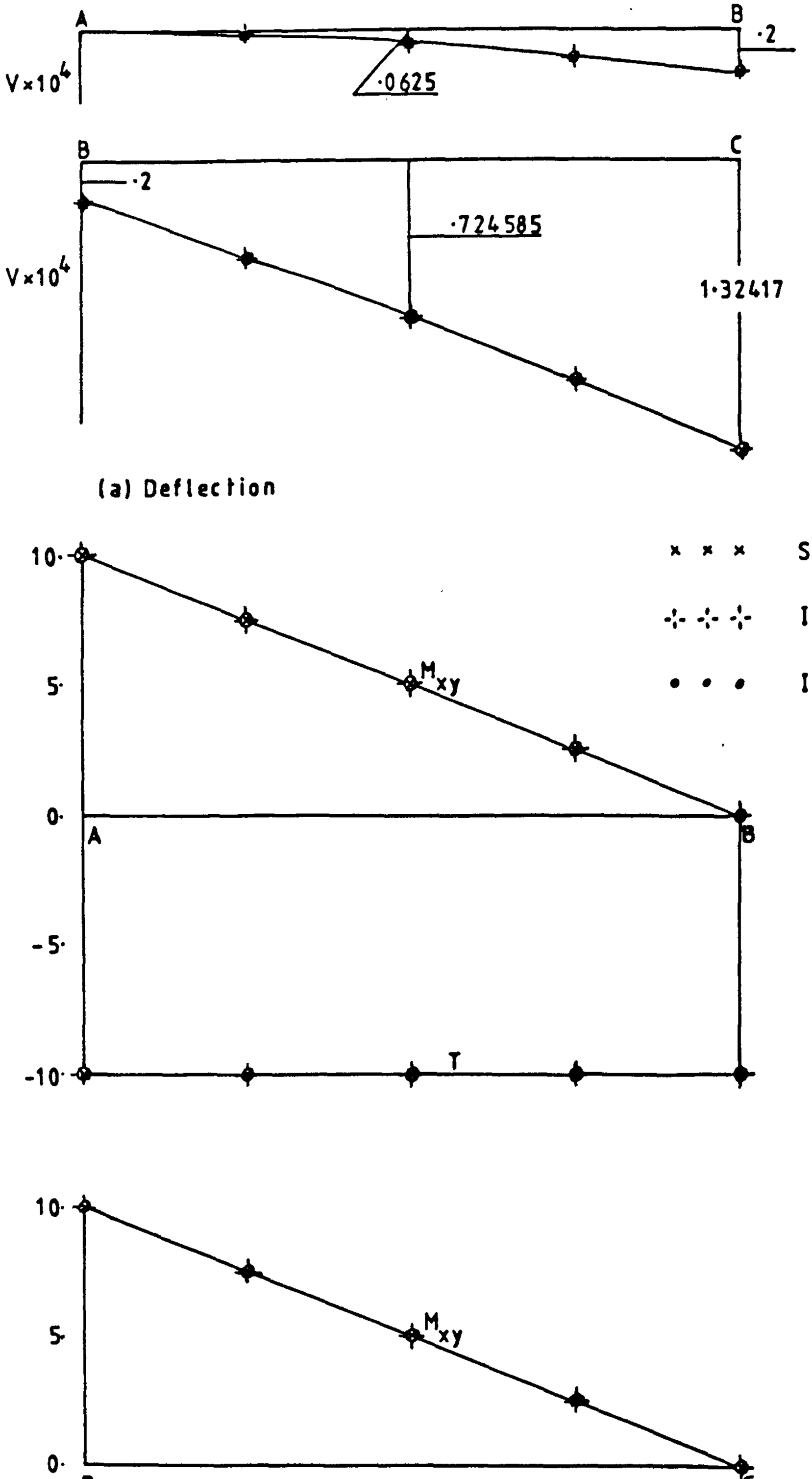

FIGURE 6.13 - L-Type Cantilever Beam Results

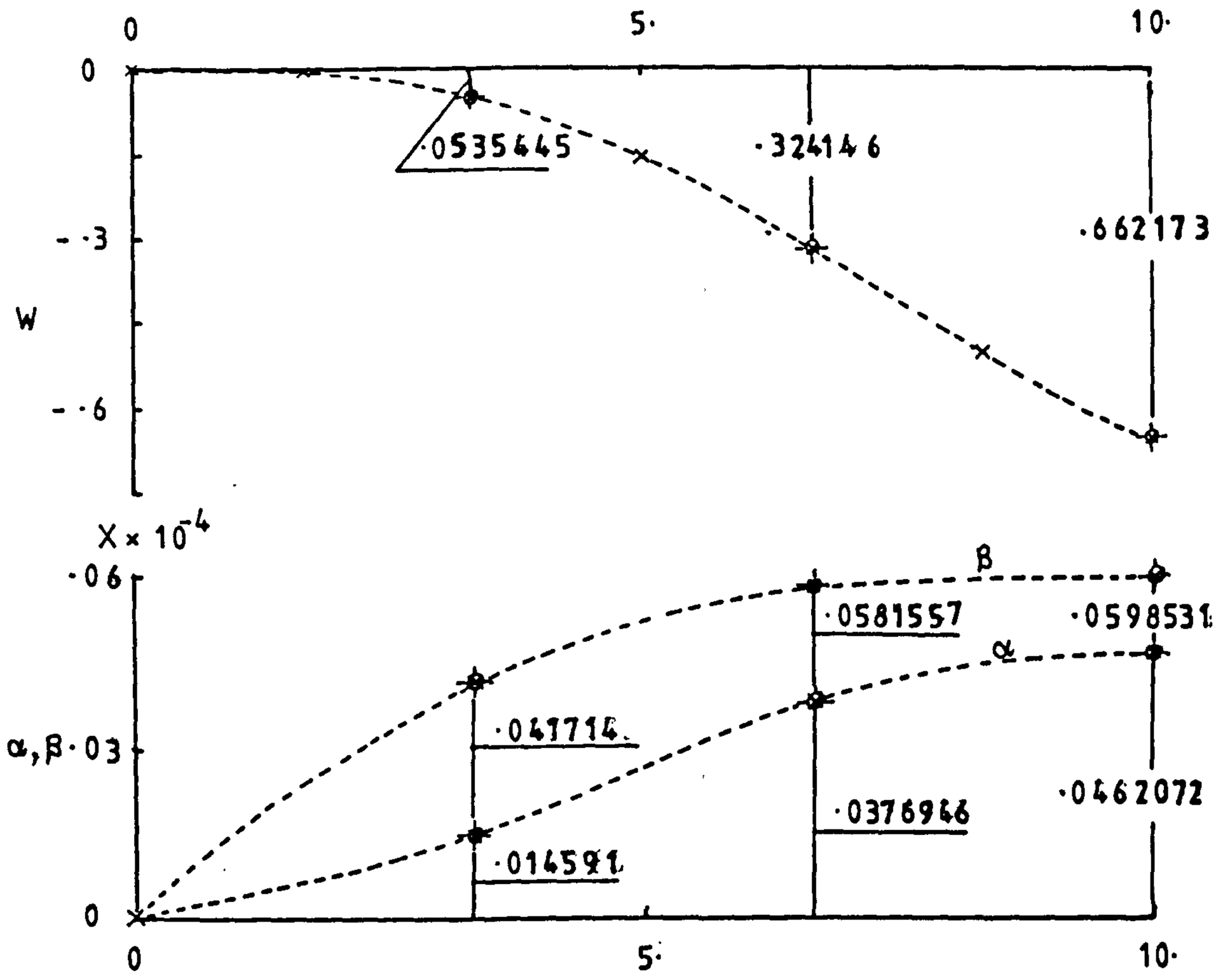

(a) Deflection

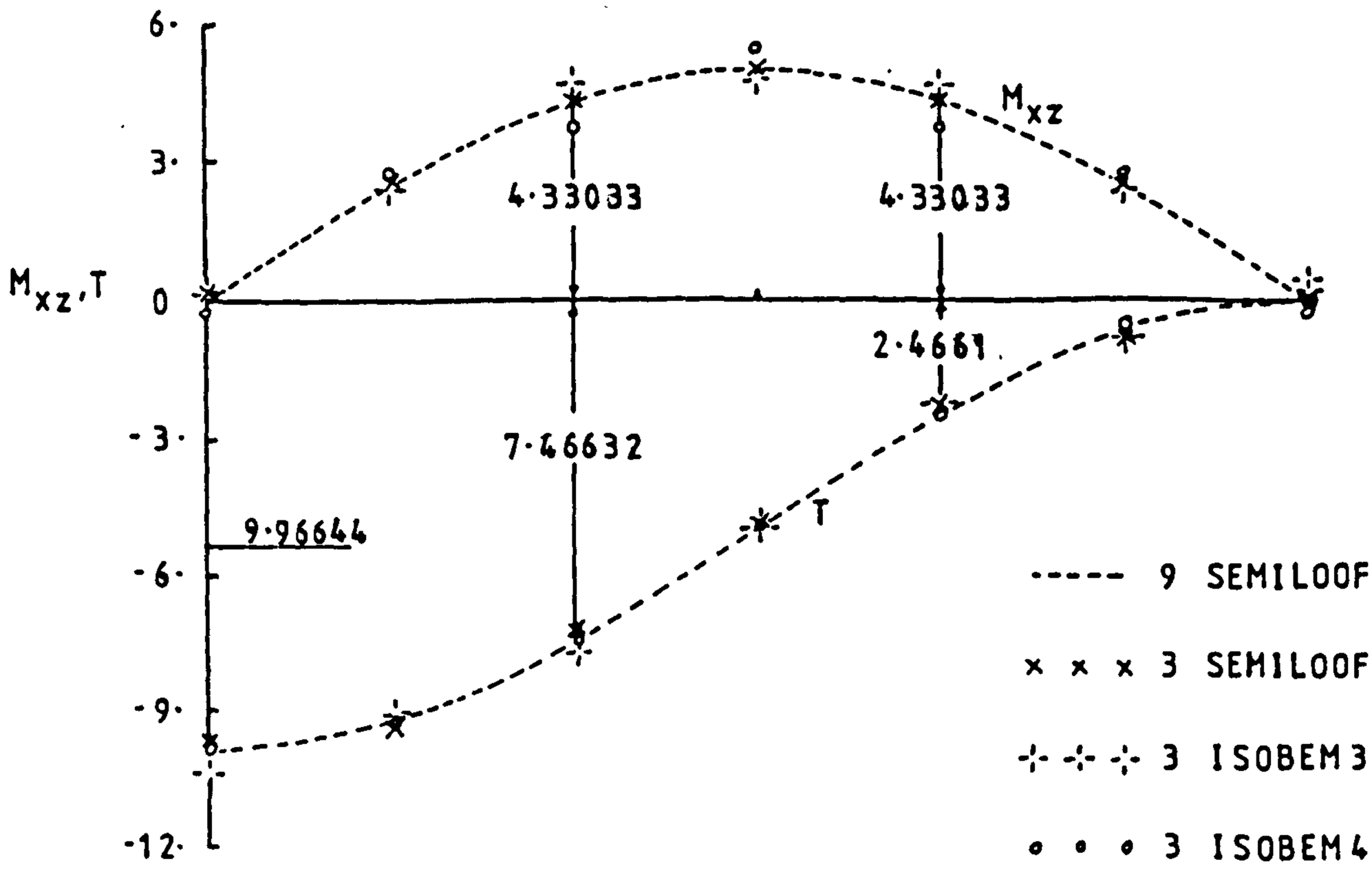

(b) Bending moment & Torsion

FIGURE 6.14 - Semi-circular Beam Results

$\frac{PL^2}{EI}$	V/L			$\frac{L-U}{L}$			$\frac{2\phi_z^*}{\pi}$	
	TLG	TLC	Ref(79)	TLG	TLC	Ref(79)	TLG	TLC
1	.3019	.3054	.302	.9435	.9427	.944	.2936	.2993
2	.4939	.4972	.494	.8390	.8374	.840	.4969	.5040
3.	.6040	.6062	.603	.7448	.7435	.745	.6249	.6319
4	.6709	.6724	.670	.6700	.6692	.671	.7071	.7141
5.	.7149	.7159	.714	.6111	.6107	.612	.7610	.7682
6.	.7458	.7465	.744	.6539	.5640	.566	.7964	.8039
7.	.7688	.7692	.676	.5254	.5259	.528	.8192	.8271
8	.7866	.7868	.785	.4934	.4942	.496	.8332	.8415
9	.8008	.8009	.799	.4663	.4674	.469	.8413	.8498
10	.8125	.8125	.811	.4430	.4444	.445	.8452	.8538

* $\phi_z = \sin^{-1}\theta$

TABLE 6.4 Cantilever under Point Load at Feee End

ISOBEM 4 Results.

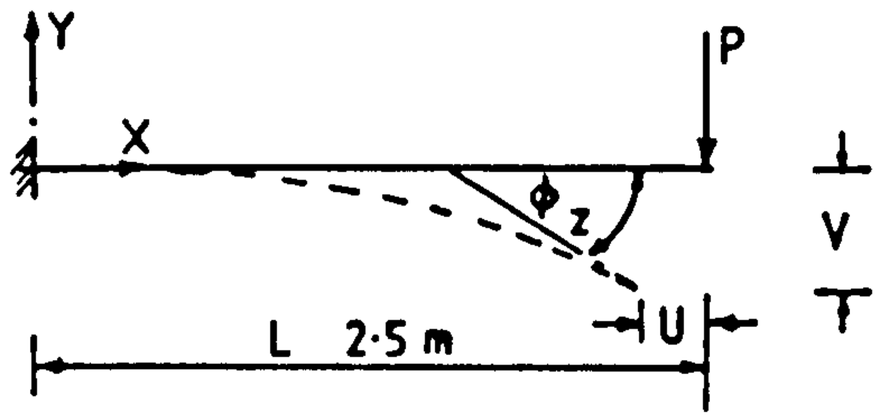

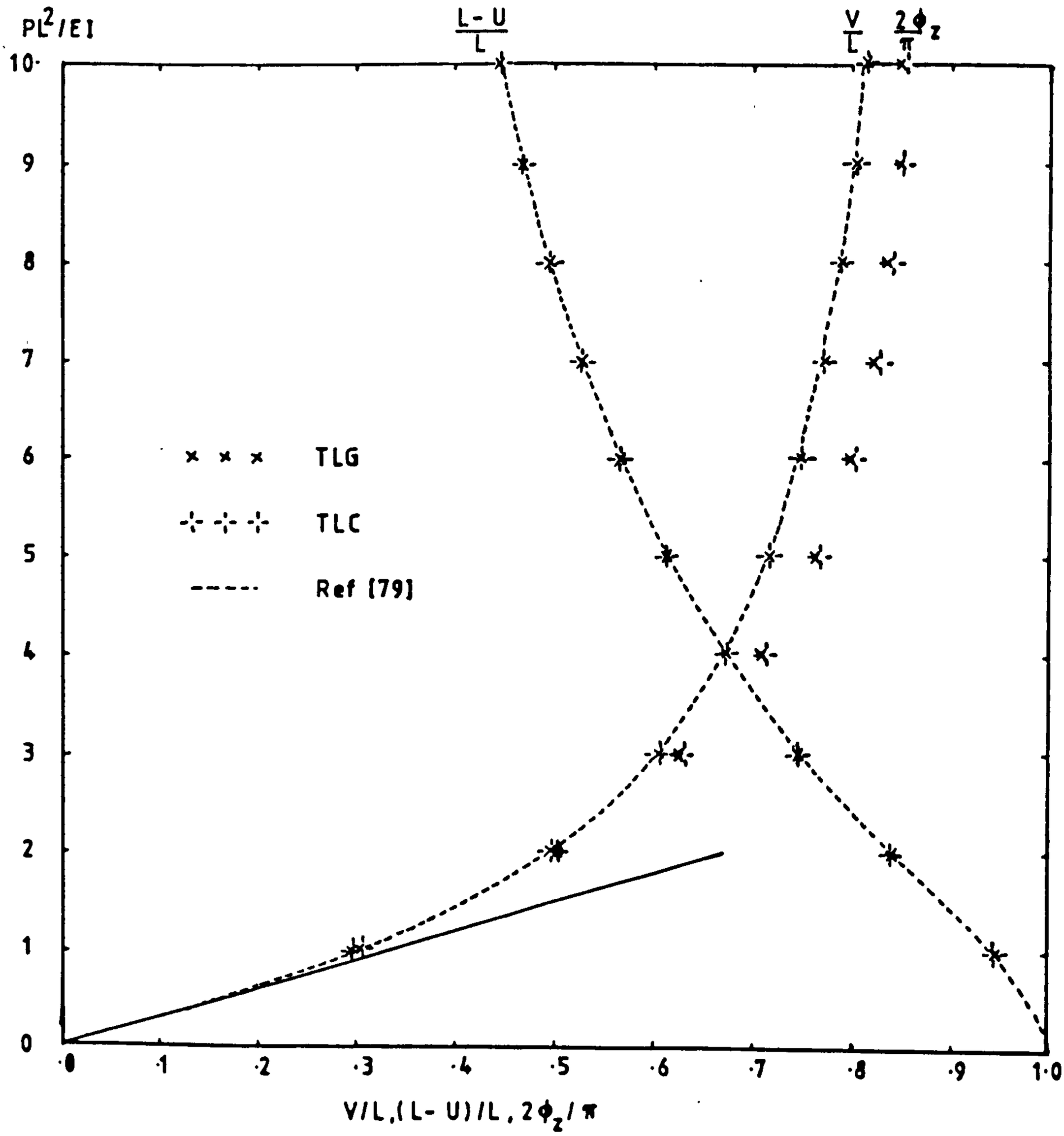

FIGURE 6.15 - Cantilever under Vertical Load at Free End - ISOBEM 4 Results

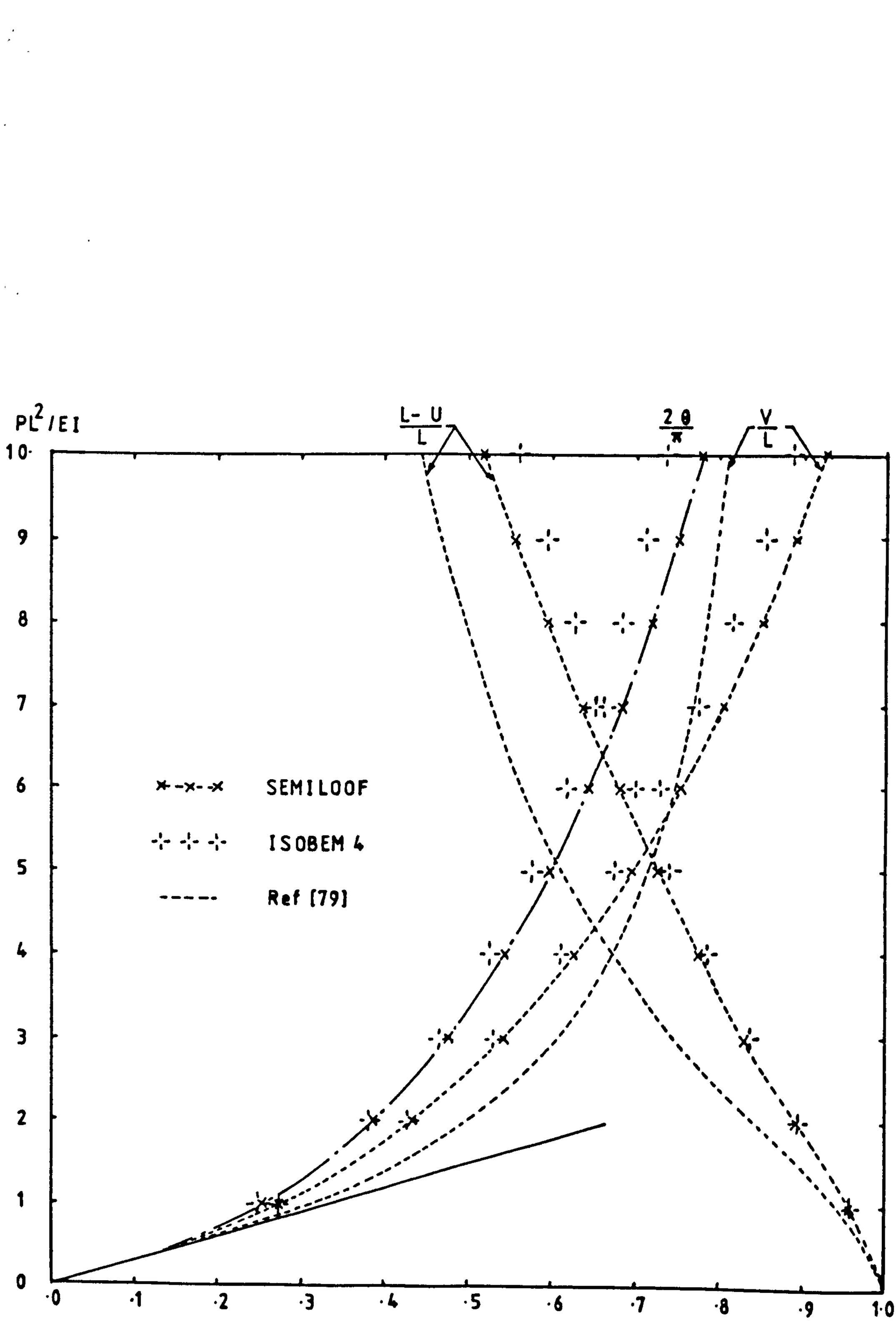

FIGURE 6.16 - Cantilever under Vertical Load at Free End
- Approximate Theory (TLCA)

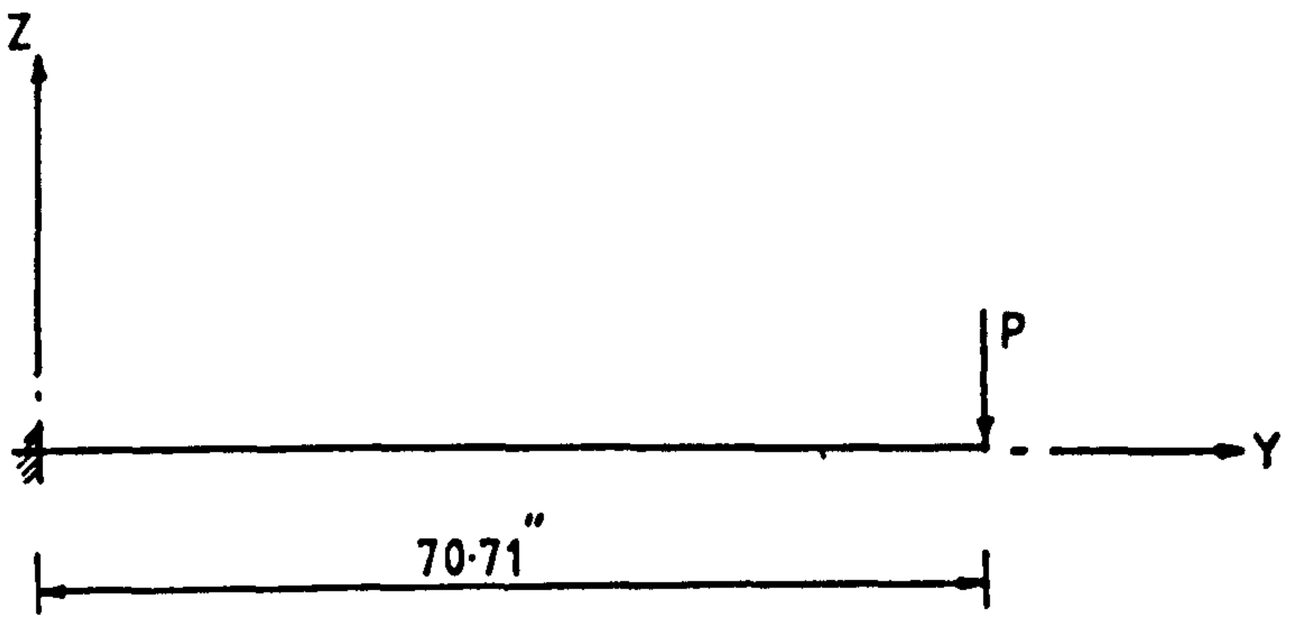

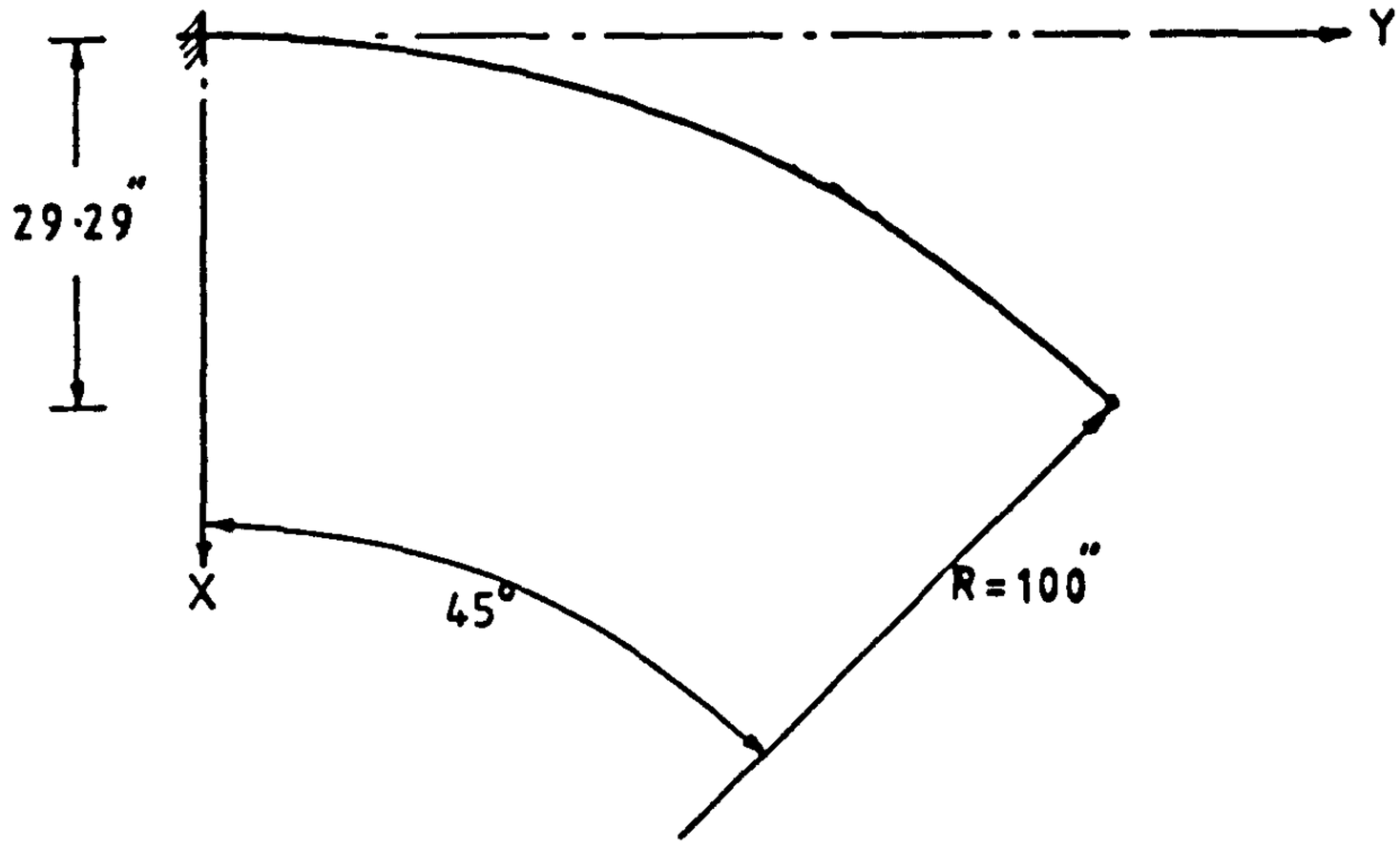

$E = 10^7$ psi

$\nu = 0$

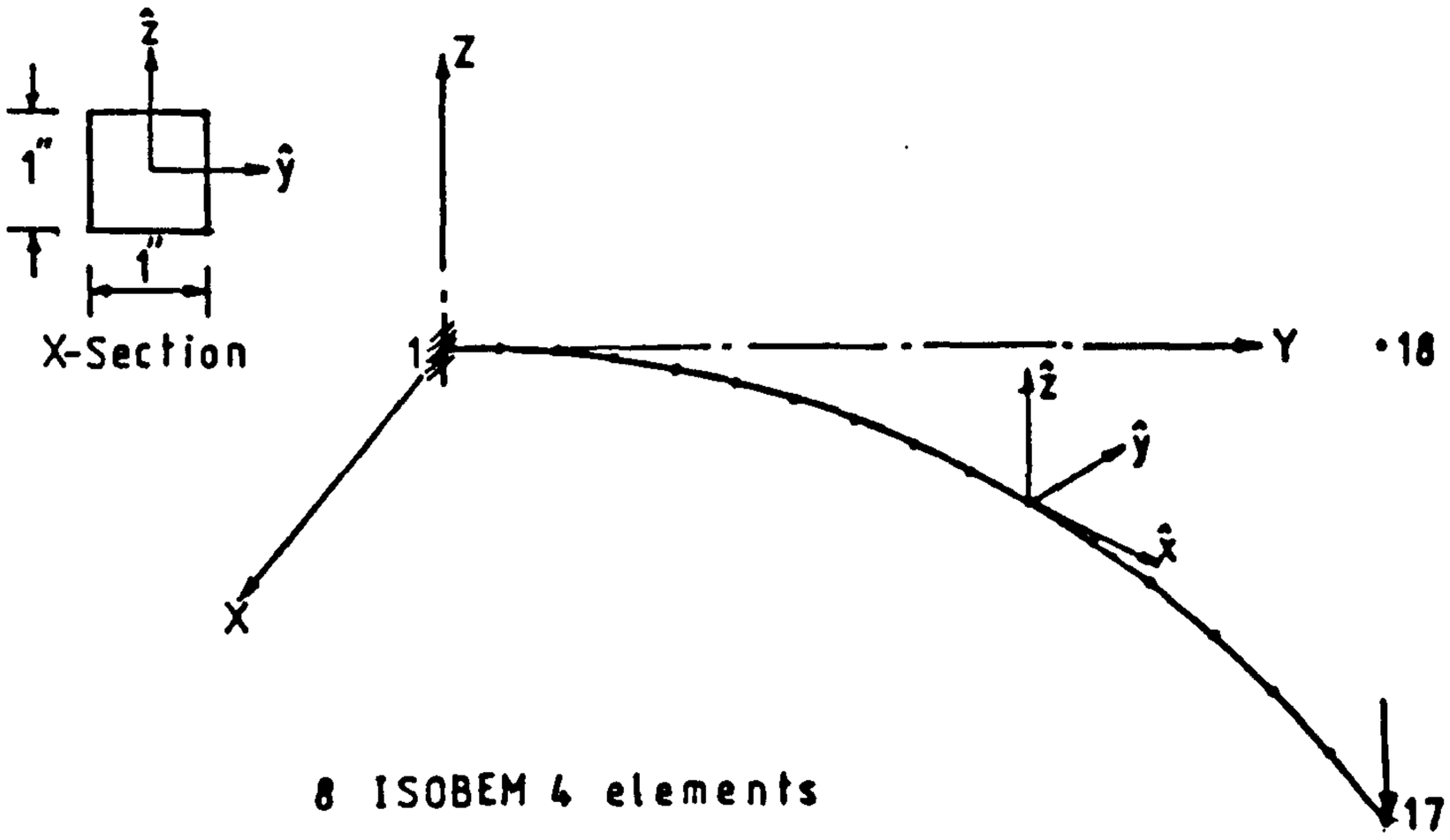

FIGURE 6.17 - Properties and Idealisation of 45° Circular Bend

$\frac{PR^2}{EI}$	TLC					TLG				
	$\frac{U}{R}$	$\frac{V}{R}$	$\frac{W}{R}$	α	β	$\frac{U}{R}$	$\frac{V}{R}$	$\frac{W}{R}$	α	β
.72	-.004933	-.008264	.1123	.1829	-.1163	-.004923	-.008250	.1122	.1826	-.1161
1.44	-.01794	-.03002	.2120	.3434	-.2161	-.01790	-.02997	.2118	.3430	-.2158
2.16	-.03519	-.05908	.2936	.4718	-.2931	-.03513	-.05901	.2934	.4713	-.2927
2.88	-.05354	-.09031	.3579	.5696	-.3495	-.05347	-.09022	.3577	.5691	-.3492
3.60	-.07124	-.1207	.4081	.6426	-.3901	-.07117	-.1206	.4079	.6422	-.3898
4.32	-.08753	-.1490	.4474	.6970	-.4194	-.08746	-.1490	.4473	.6967	-.4192
5.04	-.1022	-.1748	.4787	.7378	-.4408	-.1021	-.1748	.4786	.7375	-.4406
5.76	-.1153	-.1981	.5039	.7685	-.4566	-.1152	-.1981	.5039	.7683	-.4564
6.48	-.1269	-.2191	.5245	.7918	-.4685	-.1269	-.2191	.5245	.7916	-.4683
7.2	-.1373	-.2380	.5417	.8096	-.4777	-.13725	-.2380	.5417	.8095	-.4775

TABLE 6.5 3-D 45^{o} - Circular Bend Results

(8 - ISOBEM 4 Elements).

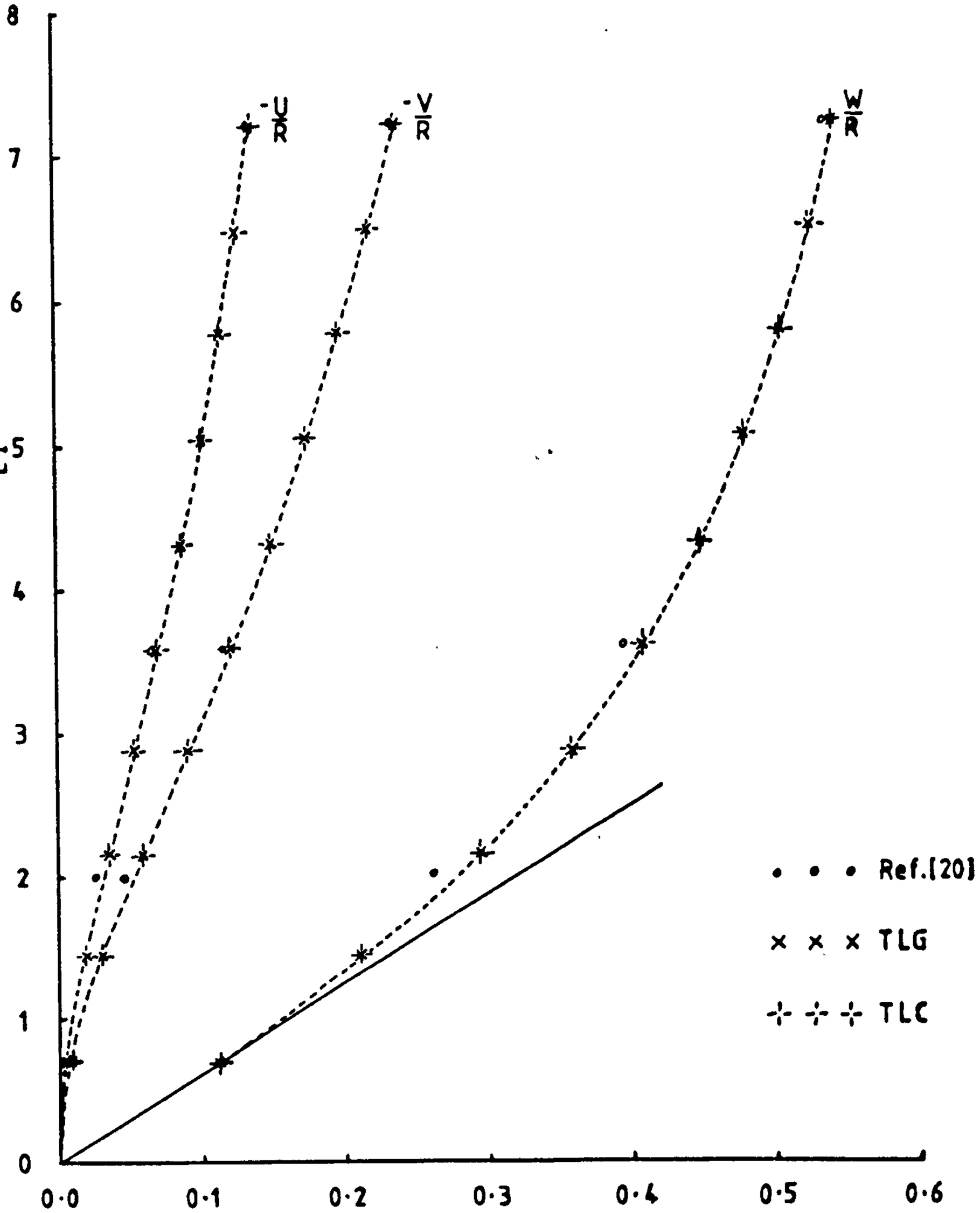

FIGURE 6.18 - 3-D Large Deflection Analysis of a 45° Circular Bend 8 ISOBEM 4 Elements

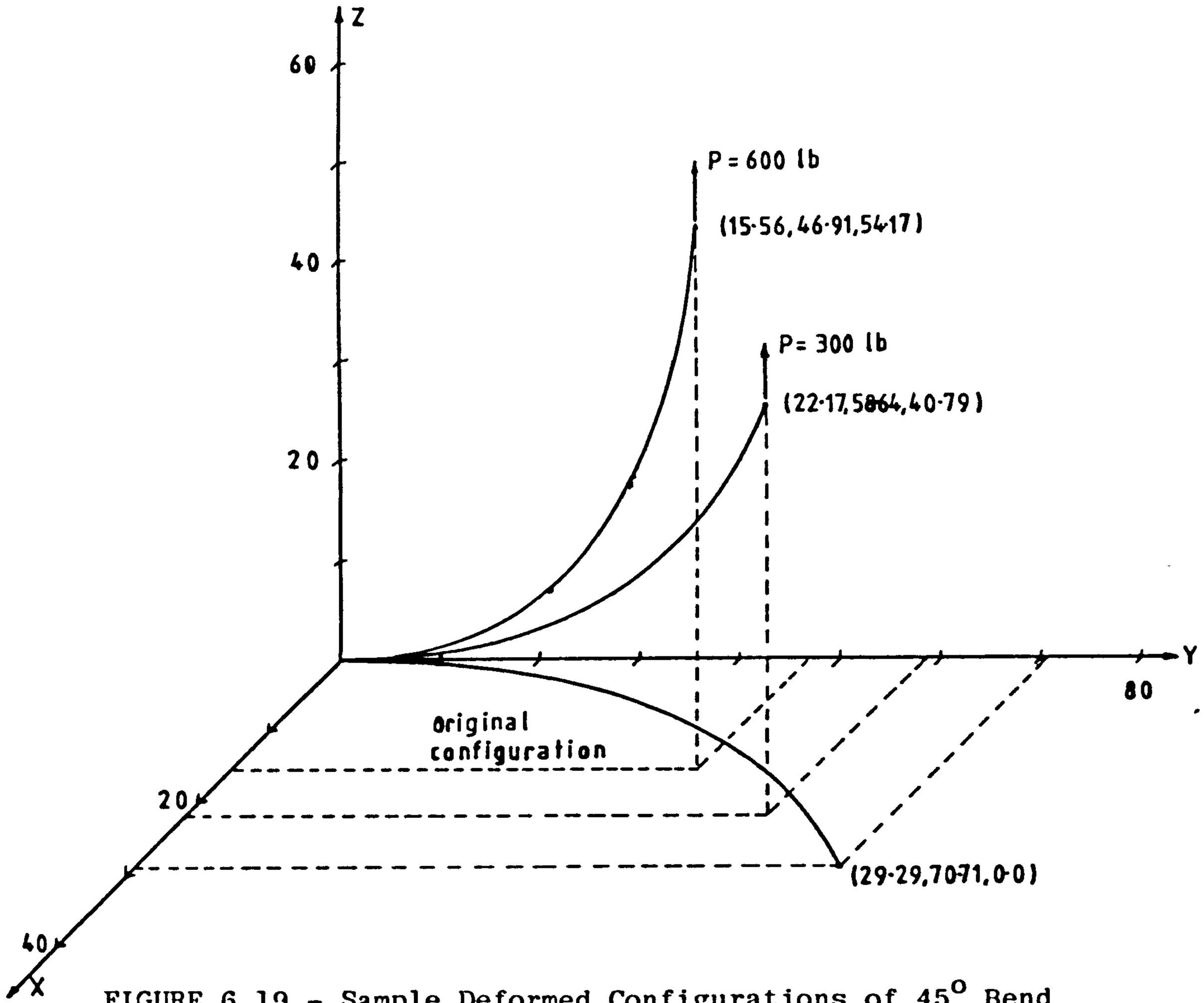

FIGURE 6.19 - Sample Deformed Configurations of 45^{o} Bend

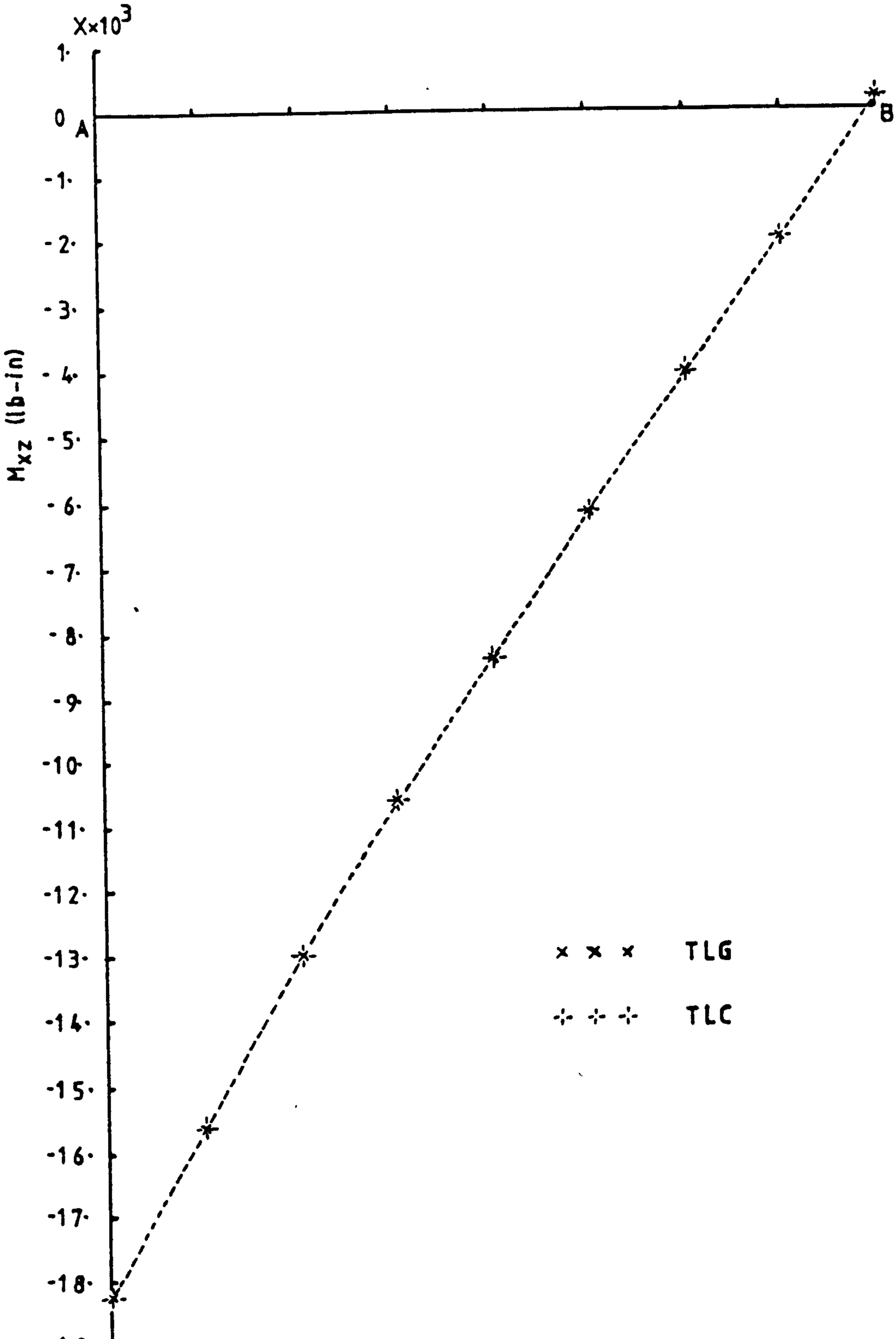

FIGURE 6.20a-45° Bend - Variation of Bending Moment M_{xz} along Lengty ($\frac{PL^2}{EI} = 3.6$)

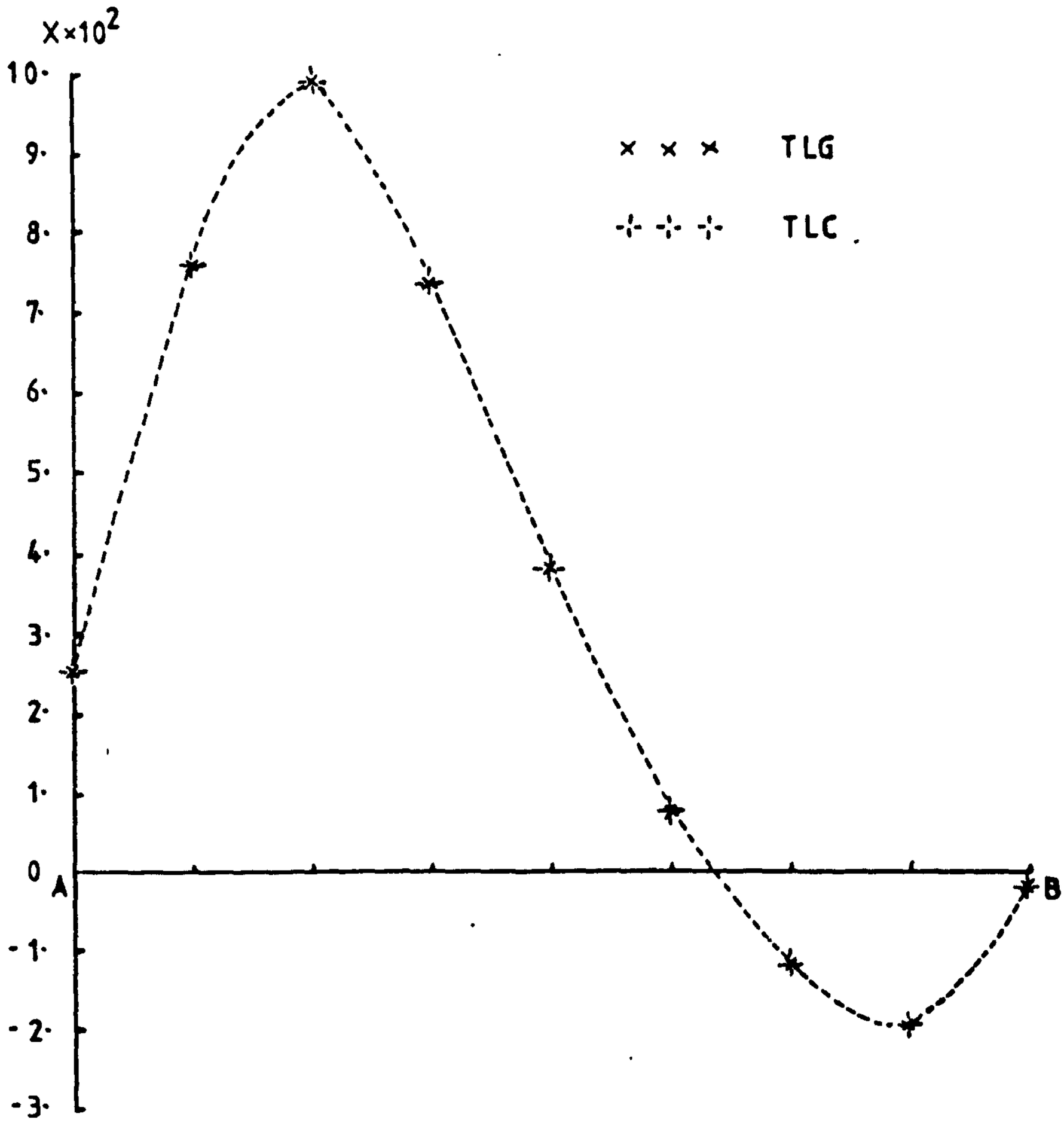

FIGURE 6.20b - 3-D 45^{o} Bend - Variation of Bending Moment M_{xy} along Length

$(\frac{PL^2}{EI} = 3.6)$

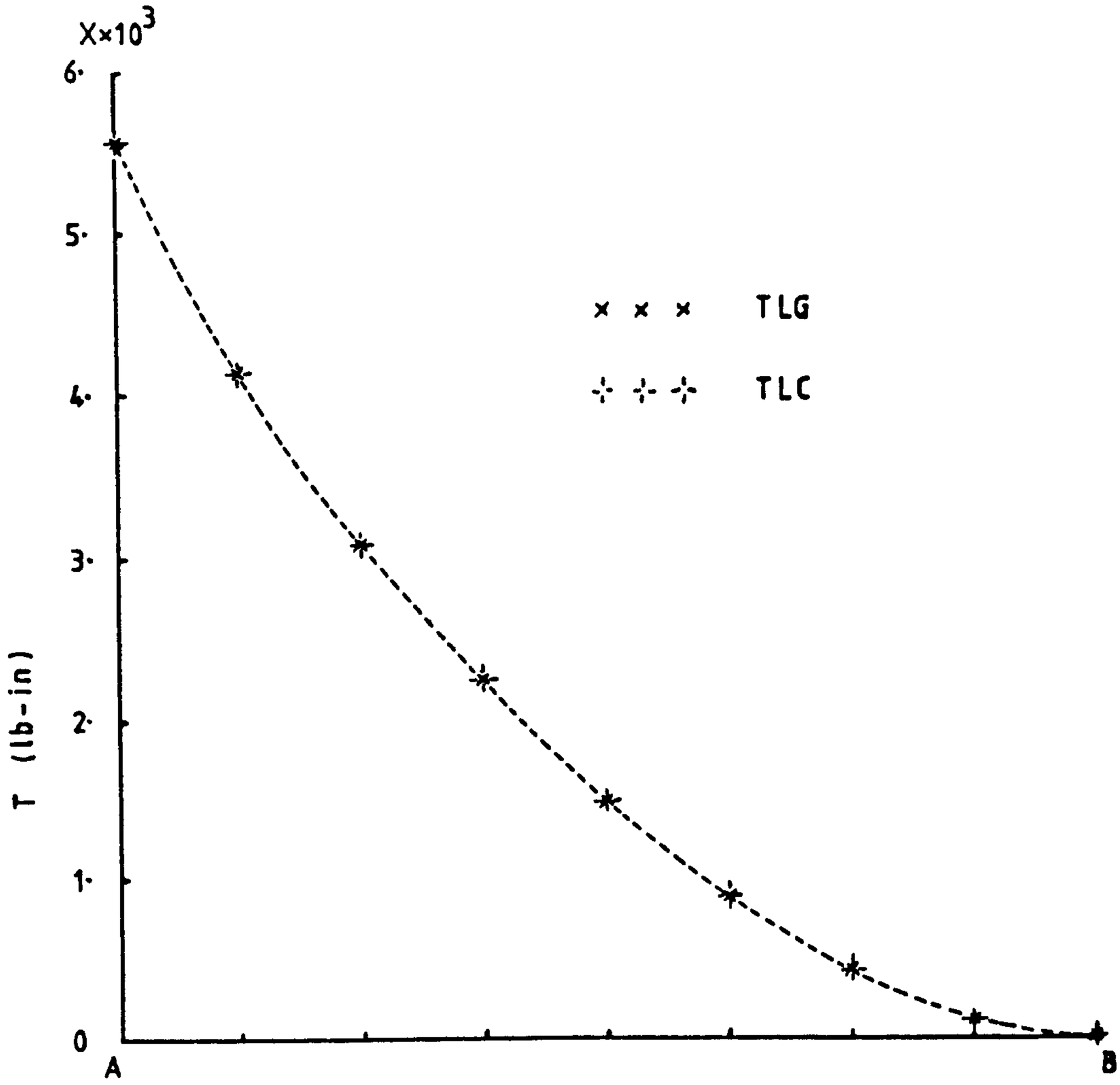

FIGURE 6.20C - 3-D 45^{O} Bend - Variation of Torsional Moment $T = T_y + T_z$ along Length
$(\frac{PL^2}{EI} = 3.6)$

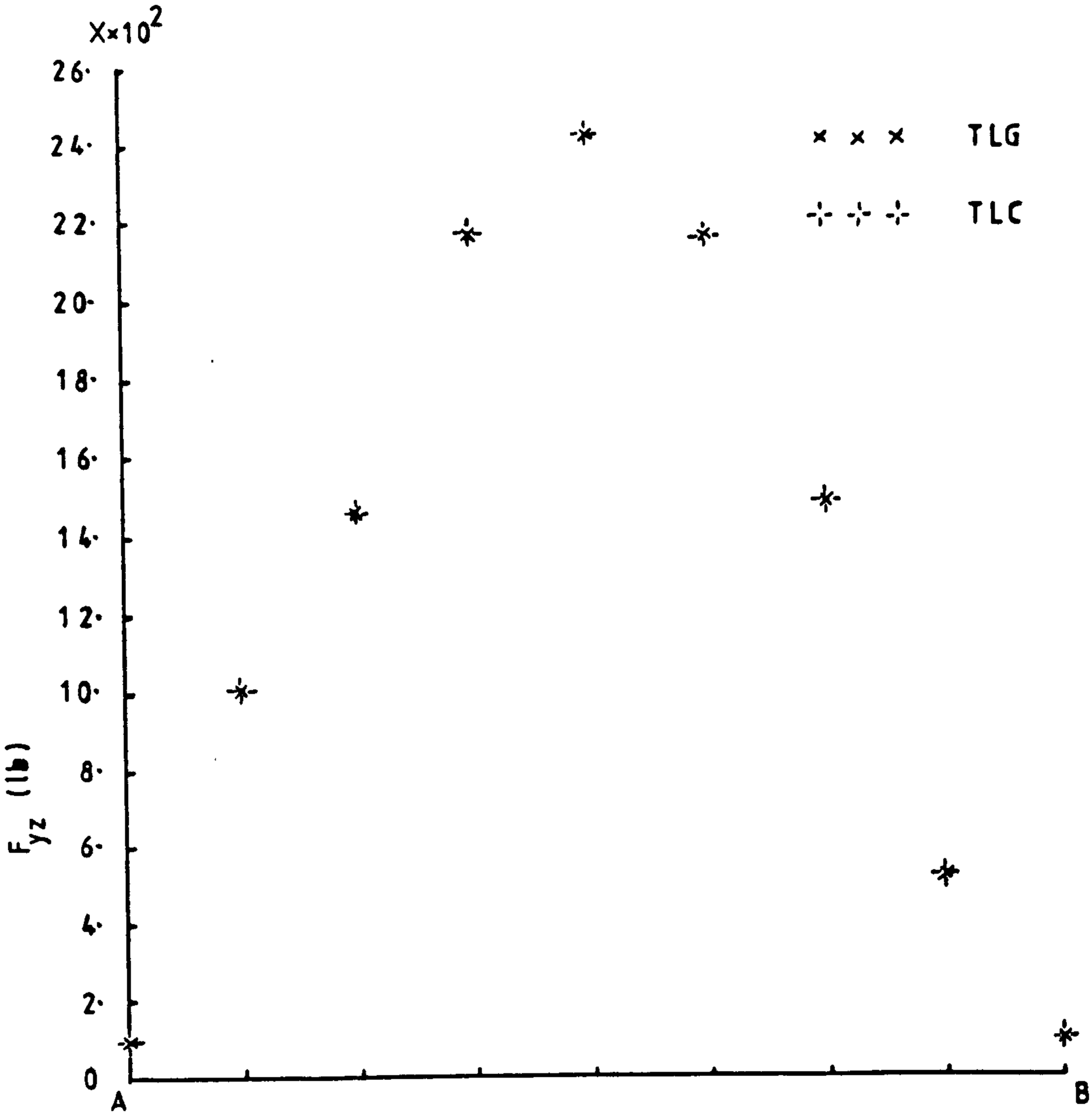

FIGURE 6.20d - 3-D 45° Bend - Variation of Shear Force F_{yz} along Length

($\frac{PL^2}{EI}$ = 3.6) (average nodal values)

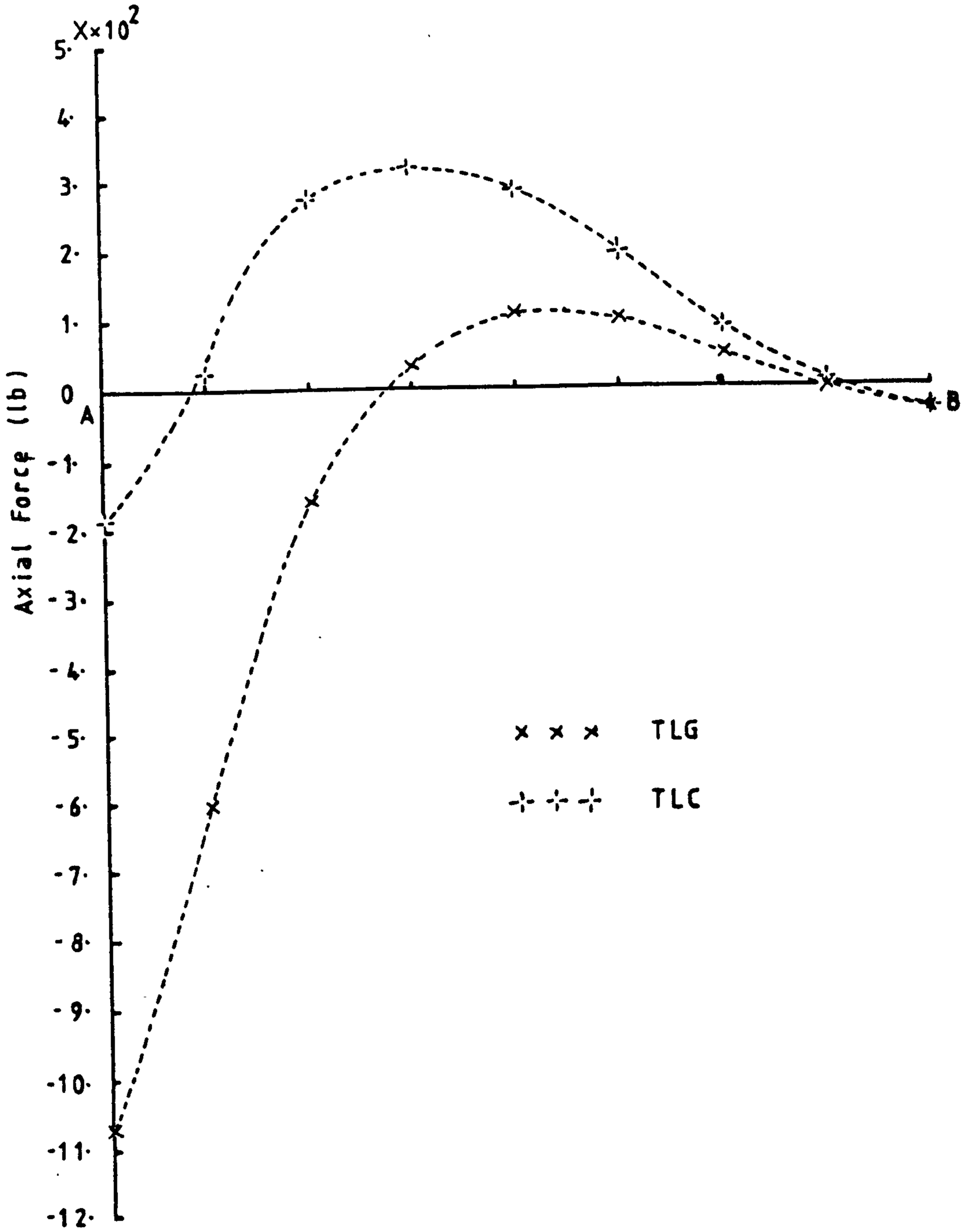

FIGURE 6.20e - 3-D 45° Bend - Variation of Axial Force along Length ($\frac{PL^2}{EI}$ = 3.6)

a. Beam Properties:

Thickness $t = 7.87$ mm

Depth $d = 7.72$ mm

Span $L = 495$ mm

Young's Modulus $E = 197400$ N/mm^2

Poisson's Ratio $= 0.3$

Yield stress $\sigma_y = 248$ N/mm^2

b. Finite Element Solution Results:

Applied Load (kN)	Central Deflection(mm)	Axial Force(kN)
0.100	1.0332	.2575
0.200	1.9767	.7101
0.300	2.8128	1.2758
0.350	3.1978	1.5648
0.400	3.5922	1.8658
0.450	3.9911	2.1803
0.475	4.2006	2.3465
0.500	4.4130	2.5255
0.525	4.6783	2.6551
0.550	4.9770	2.8449
0.575	5.2722	3.0564
0.600	5.5667	3.2517
0.625	5.8902	3.4453
0.650	6.2094	3.6644

TABLE 6.6 Fully-Encastre Beam Properties and Results. (6 Equal Length SEMILOOF Beam Elements for Half Span - 5 N-R Iterations per Increment).

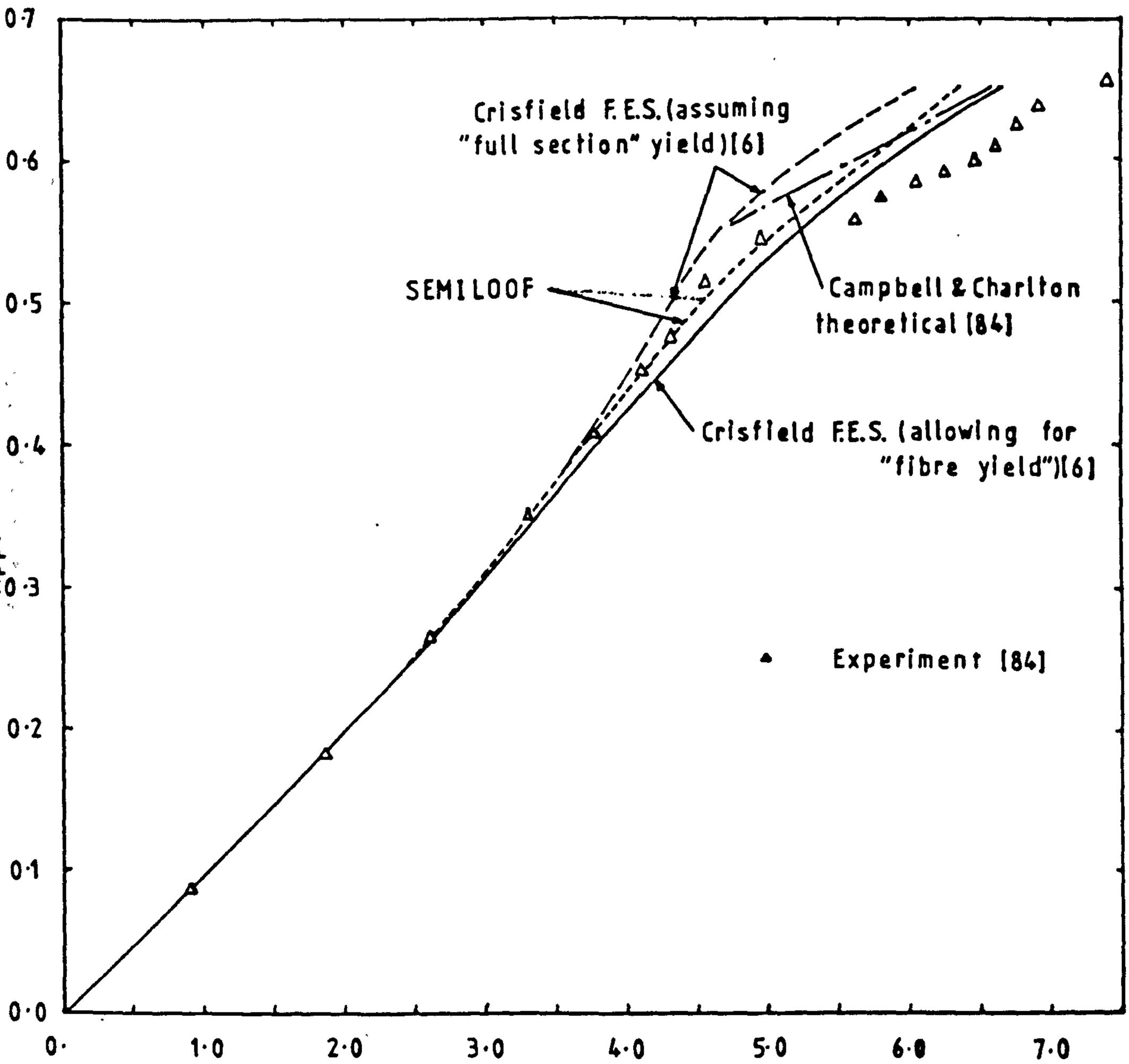

FIGURE 6.21 - Fully-Encastre Beam - Relationship Between Applied Load and Central Deflection

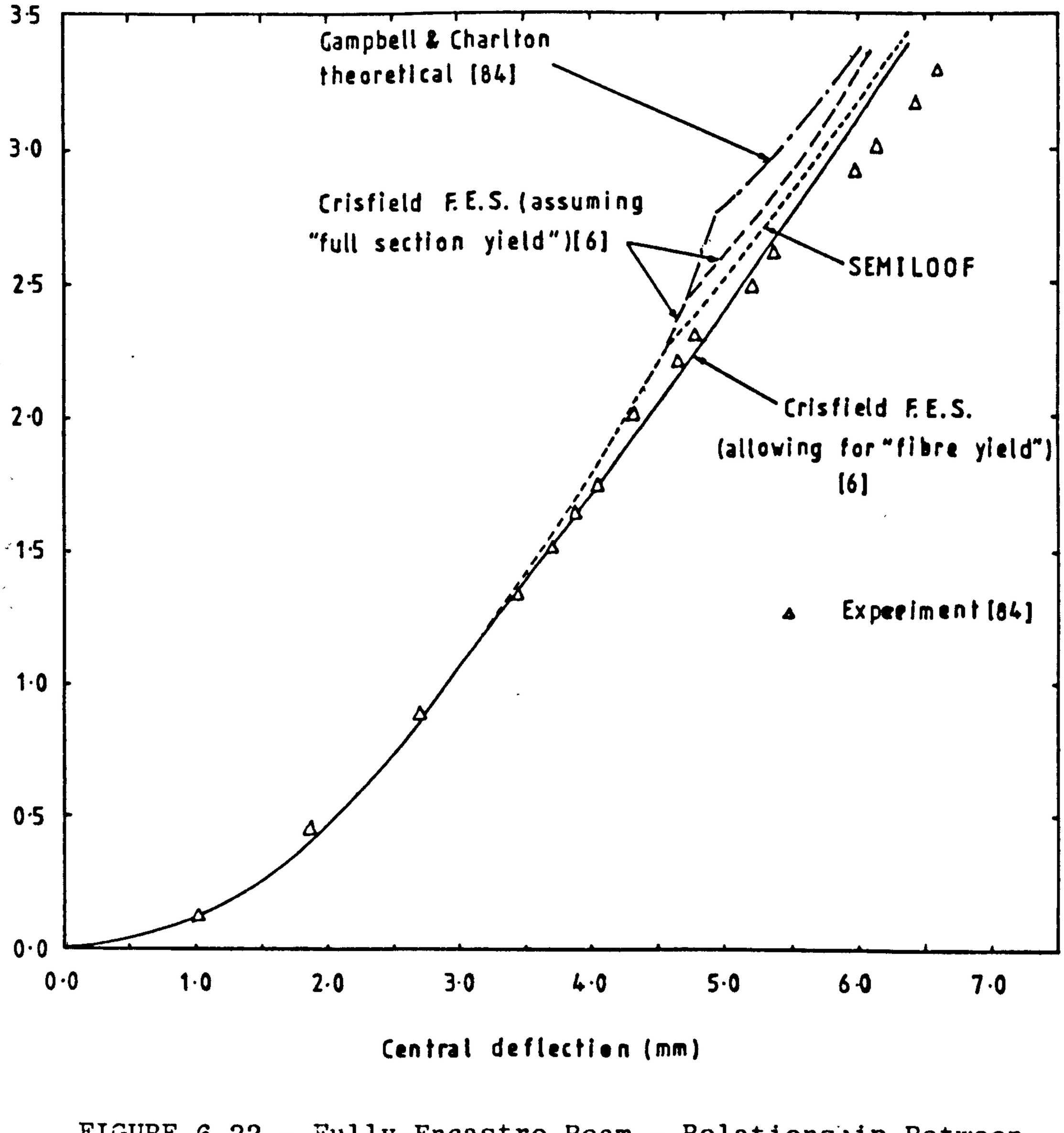

FIGURE 6.22 - Fully-Encastre Beam - Relationship Between Axial Force and Central Deflection

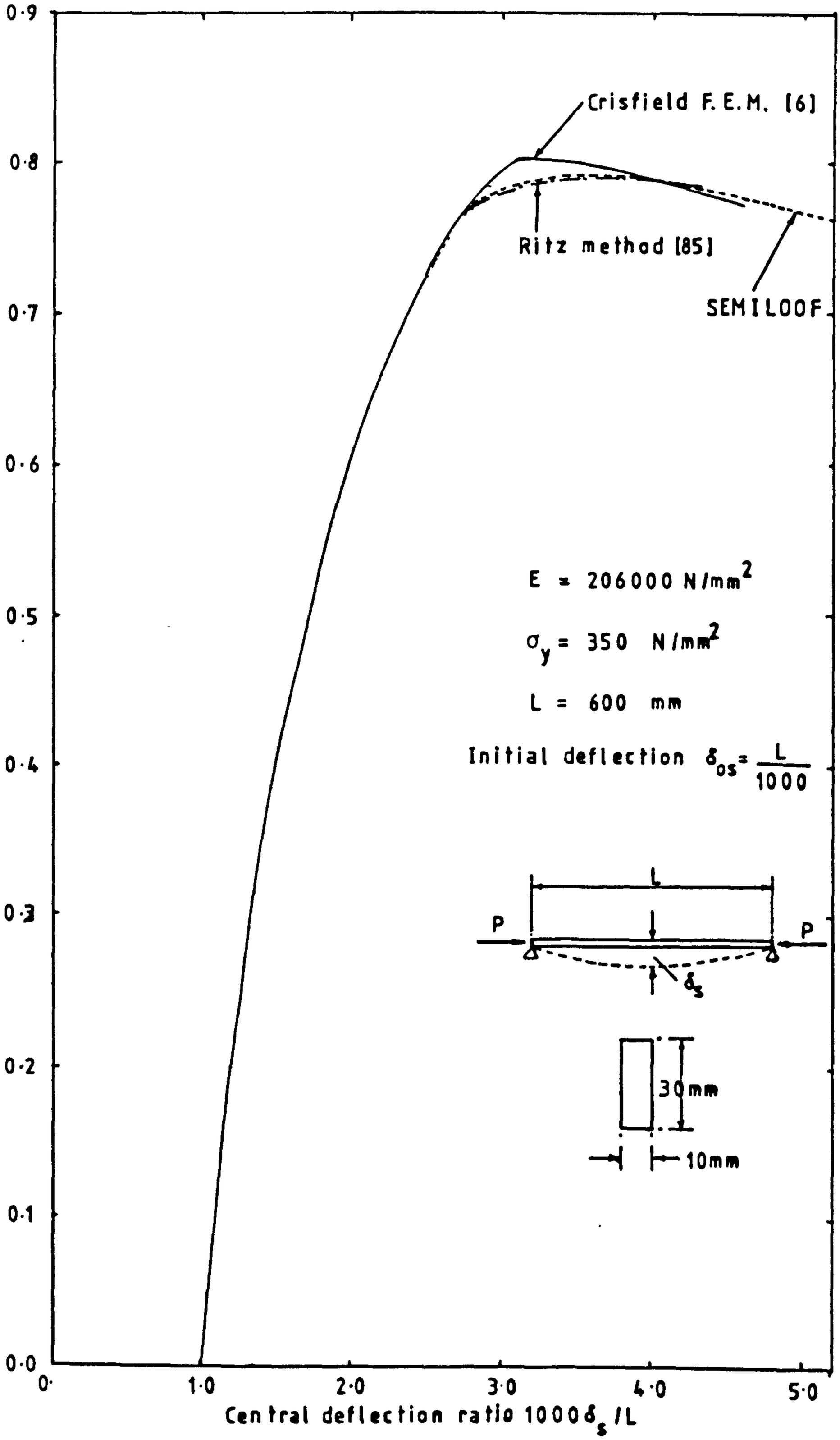

FIGURE 6.23 - Simply Supported Rectangular Strut - Relationship Between Load and Out-of-Plane Deflection

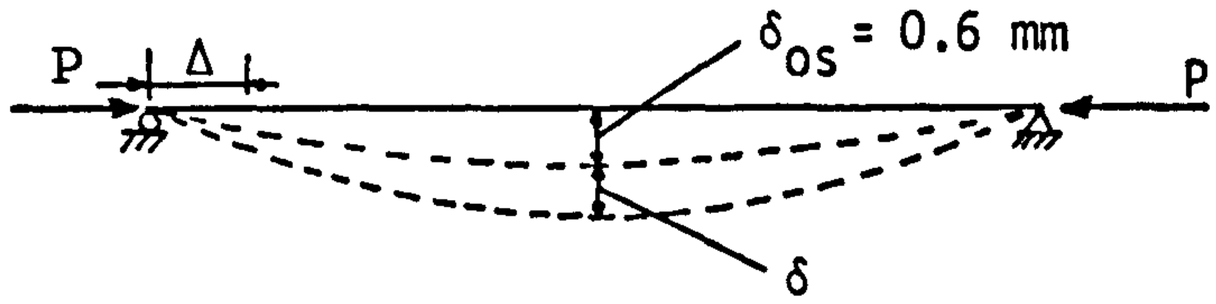

Axial Displacement Δ (mm)	Central Deflection δ (mm)	Axial Load P (kN)
0.01	0.0098	2.0549
0.02	0.0200	4.1092
0.03	0.0305	6.1632
0.04	0.0414	8.2166
0.05	0.0527	10.2695
0.06	0.0643	12.3218
0.07	0.0764	14.3736
0.08	0.0889	16.4249
0.09	0.1019	18.4754
0.10	0.1154	20.5254
0.14	0.1749	28.7180
0.18	0.2451	36.8966
0.22	0.3292	45.0570
0.26	0.4316	53.1923
0.30	0.5588	61.2915
0.32	0.6348	65.3219
0.34	0.7208	69.3354
0.335	0.7934	72.3315
0.365	0.8461	74.3208
0.375	0.9027	76.3026
0.385	0.9637	78.2757
0.395	1.0295	80.2389
0.405	1.1487	82.0374
0.415	1.4460	83.2024
0.425	2.6000	79.8677

TABLE 6.7 Simply Supported Rectangular Strut Results. (6 Equal Length SEMILOOF Beam Elements for Half Span-Solution obtained Incrementally with Residual Correction within Increment).

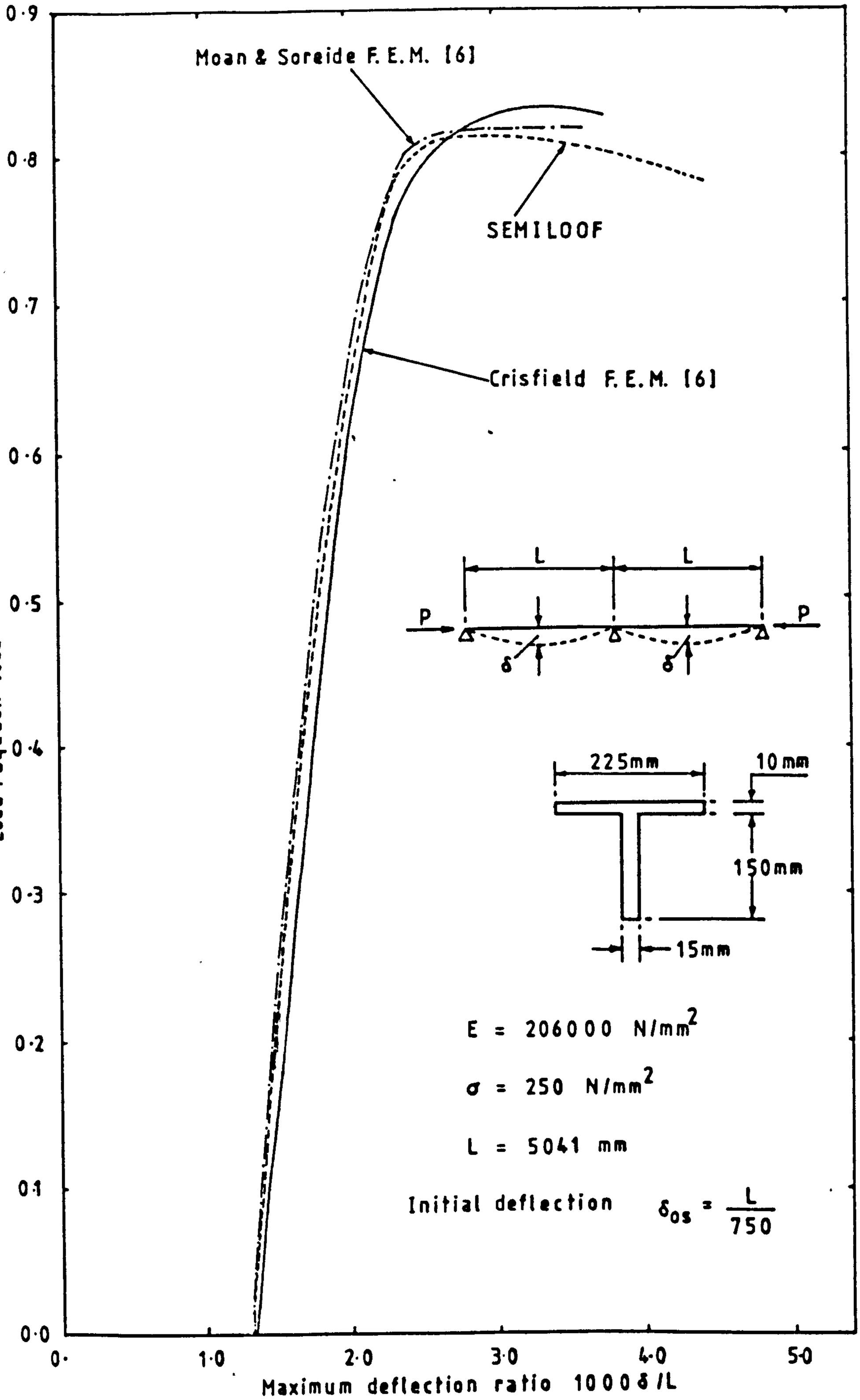

FIGURE 6.24 - Uniaxially Compressed Continuous T-Beam Strut - Relationship Between Load and Out-of-Plane Deflection

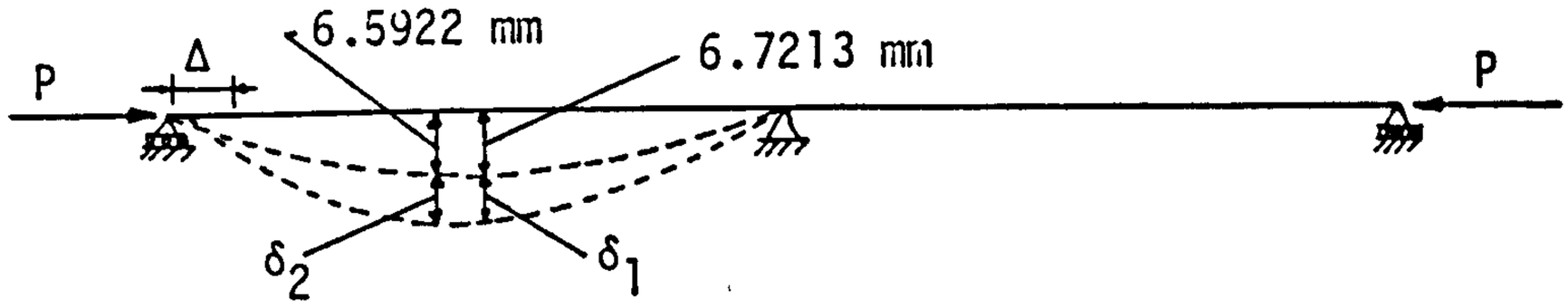

Axial Displacement Δ(mm)	Central Deflection δ_1(mm)	Maximum Deflection δ_2(mm)	Axial Load P (kN)
0.20	0.1124	0.1164	36.6450
0.40	0.2293	0.2374	73.2779
0.60	0.3507	0.3633	109.8980
0.80	0.4771	0.4944	146.5050
1.00	0.6088	0.6311	183.0970
1.20	0.7460	0.7736	219.6750
1.40	0.8891	0.9224	256.2360
1.60	1.0386	1.0779	292.7810
1.80	1.1949	1.2406	329.3070
2.00	1.3584	1.4109	365.8130
2.20	1.5297	1.5895	402.2990
2.40	1.7093	1.7769	438.7610
2.60	1.8980	1.9739	475.1990
2.80	2.0963	2.1811	511.6100
3.00	2.3051	2.3993	547.9910
3.20	2.5252	2.6296	584.3400
3.40	2.7575	2.8728	620.6550
3.60	3.0031	3.1301	656.9300
3.80	3.2632	3.4028	693.1620
4.00	3.5390	3.6922	729.3460
4.10	3.6833	3.8436	747.4180
4.20	3.8321	3.9998	765.4760
4.30	3.9856	4.1611	783.5190
4.40	4.1441	4.3275	801.5460
4.50	4.3077	4.4995	819.5570
4.60	4.4767	4.6772	837.5490
4.70	4.6515	4.3610	855.5230
4.80	4.8722	5.0975	873.2280
4.90	5.2042	5.4594	890.2550
5.00	5.8135	6.1340	905.3070
5.10	7.1606	7.6422	914.6800
5.20	9.7390	10.5461	911.4260
5.30	14.4070	15.8495	880.7250
5.40	18.7805	22.0139	827.8330
5.50	23.8545	26.7816	779.8350

TABLE 6.8 Uniaxially Compressed Continuous T-Beam Strut (2 Sets of Eccentric 8 SEMILOOF Beam Elements for Single Span).

CHAPTER 7

GENERAL CONCLUSIONS

7.1 SUMMARY OF WORK

The work described in this thesis has involved the development of the following:

(i) An exact large rotation two-dimensional theory for thin curved eccentric beams, its finite element formulations in a Lagrangian coordinate system and a family of two-dimensional beam elements that can accurately accommodate the theory.

(ii) A general Total Lagrangian formulation based on the geometric strains that has the capability of predicting the true stresses in large rotation and curvature problems.

(iii) A three-dimensional large rotation theory for thin curved eccentric beams, its finite element formulations in a Total Lagrangian coordinate system and a family of three-dimensional beam elements that can accurately accommodate the theory.

7.2 CONCLUDING REMARKS

The Total Lagrangian formulations have been proven to be numerically more effective than the Updated Lagrangian formulation. The large rotation Total Lagrangian formulation of thin curved beam finite elements in two- and three-dimensional space has been shown to be possible provided that the displacement derivatives, which are rotation measures, are used as degrees of freedom.

The constraint technique has been successfully used to develop the elements that are necessary for use with the theory. The completely conforming element developed by the technique has been found to be incapable of correctly reproducing axial force variations in very thin, deep structures in which the deformation is inextensional. The convergence of idealisations by this element of such structures is not monotonic. The element has been shown, however, to be effective in nonlinear applications. The "parent" element is a subparametric element in which the geometry is defined by three nodes and the variation of the displacements is defined by four nodes. The convergence of subparametric elements is monotonic. The variation of the variables in the "final" element, while being an exact cubic, is defined by two nodes only. Therefore, the "final" elenent may be considered to be a

superparametric element. This explains the peculiar element behaviour since the convergence of super-parametric elements is not always monotonic.

The only limitation of the exact large rotation theory which has been developed is that C^1 continuity of the in-plane displacement is essential. An approach that avoids this limitation needs to be considered. Such an approach will make the use of existing successful elements, such as the SEMILOOF shell element possible without having to modify the already complex shape function routines.

The C^1 continuity requirement has arisen from adopting the Kirchhoff hypothesis that plane sections before deformation remain plane and normal to the beam reference line after deformation. The strain-displacement terms that result in this requirement therefore can be eliminated by relaxing the condition of normality after deformation. Such a modification will, however, result in the introduction of nonlinear shear strain-displacement terms. Further investigation of this point is necessary.

The requirement of using the displacement derivatives as rotation measures in large rotation problems in which the deformation is in-extensional, however, still remains. The use of the Updated Lagrangian avoids this requirement. The serious disadvantage of an Updated

Lagrangian solution is that it requires a considerable amount of computer time. The combined formulation has been shown to retain most of the advantages of the Updated Lagrangian formulation while saving in computer time. Hence, the use of the combined formulation in the analysis of problems in which C^1 continuity of the in-plane displacement is objectionable could be considered. It has been shown, however, that the combined formulation needs to be modified for its results to be independent of the load increment size. The possibility of developing a combined formulation based on the conventional strains may be considered. This will combine the advantages of the Updated and Total Lagrangian formulations while being independent of the load increment size. It is important to realise that the limitation will then be on the rotation increment size rather than the total rotation size. The disadvantage of the combined formulation is that its computational implementation is complex and relatively difficult compared to the Updated and Total Lagrangian formulations.

The Total Lagrangian formulation based on the geometric strains is general. It has been demonstrated that the formulation can be successfully used with the versatile isoparametric elements. The additional advantage of this formulation is that it is applicable in large strain

problems. The three-dimensional version of the formulation in terms of continuum mechanics stresses and strains can be easily developed following the procedure used for the two-dimensional theory (Appendix II).

The materially nonlinear formulation has been based on the von-Mises yield criterion and the Prandtl-Reuss flow rule. The continuum mechanics strains required has been obtained from the generalised strain resultants and the local coordinates. Numerical integration, over the rectangular cross-section, has been used to evaluate the nonlinear modulus matrix. The shear stresses from such a formulation are, however, strictly correct only for a concentric square cross-section. Therefore, a modification of this materially nonlinear formulation is necessary. An alternative approach that may resolve the difficulty is the use of yield functions which are defined in terms of stress and strain resultants

The success of the large rotation theory can be primarily attributed to the use of an intrinsic (convective) local coordinate system. It is of the opinion of the author that the use of such a coordinate system in the isoparametric element formulation needs to be considered. The well known difficulties that arise when the isoparametric elements are used in

the analysis of very thin structures may be resolved by adopting this approach. Such a possibility arises because the use of a local coordinate system will eliminate the coupling between the terms in the Jacobian matrix. It is obvious that the success of a formulation of this kind will have great advantages in both linear and geometrically nonlinear structural analyses.

REFERENCES AND BIBLIOGRAPHY

(1) A. C. Walker, 'Some Uses of Small-scale Modelling in the Design of Steel Off-shore Structures', Seminar on the use of Physical Models in the Design of Off-shore Structures, 15th and 16th Nov. (1979), Building Research Station, Garston, Watford, England.

(2) L. H. Sobel and B. L. Agarwal, 'Buckling of Eccentrically Stringer-Stiffened Cylindrical Panels under Axial Compression', Computers and Structures, Vol. 6, pp. 193-198, (1976).

(3) A. C. Walker and S. Sridharan, 'Analysis of the Behaviour of Axially Compressed Stringer-Stiffened Cylindrical Shells', Proc. Instn. Civ. Engrs, Part 2, 69, pp. 447-472, June (1980).

(4) David Bushnell, 'BOSOR5 Program for Buckling of Elastic-Plastic Complex Shells of Revolution including Large Deflections', Computers and Structures, Vol. 6, pp. 221-239, (1976).

(5) David Bushnell, 'A Strategy for the Solution of Problems involving Large Deflections, Plasticity and Creep', Int. J. Num. Methods Engrg. Vol. 11, pp. 683-708, (1977).

(6) M. A. Crisfield, 'Large-Deflection Elastic-Plastic Buckling Analysis of Eccentrically Stiffened Plates using Finite Elements', TRRL REPORT 725, Transport and Road Research Laboratory, Crowthorne, Berkshire, (1976).

(7) S. E. Webb and P. J. Dowling, 'Large-Deflection Elastic-Plastic Behaviour of Discretely Stiffened Plates', Proc. Instn. Civ. Engrs, Part 2, 69, pp. 375-401, June (1980).

(8) Edwin H. Gaylord, Jr and Charles N. Gaylord (editors), Structural Engineering Handbook, McGraw-Hill, (1968).

(9) David Bushnell, 'Buckling of Elastic-Plastic Shells of Revolution with Discrete Elastic-Plastic Ring Stiffeners', Int. J. Solids Structures, Vol. 12, pp. 51-66, (1976).

(10) O. C. Zienkiewicz, The Finite Element Method, 3rd edition, McGraw-Hill, London, (1977).

(11) Klaus-Jürgen Bathe and Edward L. Wilson, Numerical Methods in Finite Element Analysis, Prentice-Hall, New Jersey, (1976).

(12) J. T. Oden, Finite Elements of Nonlinear Continua, McGraw-Hill, (1972).

(13) E. Hinton and D. R. J. Owen, An Introduction to Finite Element Computations , Pineridge Press, Swansea, (1979).

(14) K. C. Rockey, H. R. Evans, D. W. Griffiths and D. A. Nethercot, The Finite Element Method - A Basic Introduction, Crosby Lockwood Staples, London, (1975).

(15) Klaus-Jürgen Bathe and Said Bolourchi, 'A Geometric and Material Nonlinear Plate and Shell Element', Computers and Structures, Vol. 11, pp. 23-48, (1980).

(16) G. H. Ferguson and R. D. Clark, 'A Variable Thickness, Curved Beam and Shell Stiffening Element with Shear Deformation', Int. J. Num. Methods Engrg, Vol. 14, pp. 581-592, (1979).

(17) Ahmed K. Noor and Jeanne M. Peters, 'Mixed Models and Reduced/Selective Integration Displacement Models for Nonlinear Analysis of Curved Beams', Int. J. Num. Methods Engrg, Vol. 17, pp. 615-631, (1981).

(18) D. G. Ashwell, A. B. Sabir and T. M. Roberts, 'Further Studies in the Application of Curved Finite Elements to Circular Arches', Int. J. Mech. Sci., Vol. 13, pp. 507-517, (1971).

(19) Jan Bäcklund, 'Large Deflection Analysis of Elasto-Plastic Beams and Frames', Int. J. Mech. Sci., Vol. 18, pp. 269-277, (1976).

(20) Kluas-Jürgen Bathe and Said Bolourchi, 'Large Displacement Analysis of Three-Dimensional Beam Structures', Int. J. Num. Methods Engrg, Vol. 14, pp. 961-986, (1979).

(21) T. Belytschko, L. Schwer and M. J. Klein, 'Large Displacement, Transient Analysis of Space Frames', Int. J. Num. Methods Engrg, Vol. 11, pp. 65-84, (1977).

(22) D. J. Dawe, 'Curved Finite Elements for the Analysis of Shallow and Deep Arches', Computers and Structures, Vol. 4, pp. 559-580, (1974).

(23) D. J. Dawe, 'Numerical Studies Using Circular Arch Finite Elements', Computers and Structures, Vol. 4, pp. 729-740, (1974).

(24) D. J. Dawe, 'Some High-order Elements for Arches and Shells', Chapter 8, Finite Elements for Thin Shells and Curved Members, D. G. Ashwell and R. H. Gallgher (editors), John Wiley and Sons, (1977).

(25) Marcelo Epstein and David W. Murray, 'Large Deformation In-plane Analysis of Elastic Beams', Computers and Structures, Vol. 6, pp. 1-9, (1976).

(26) Marcelo Epstein and David W. Murray, 'Three-Dimensional Large Deformation Analysis of Thin Walled Beams', Int. J. Solids Structures, Vol. 12, pp. 867-876, (1976).

(27) F. Frey and S. Cescotto, 'Some New Aspects of the Incremental Total Lagrangian Description in Nonlinear Analysis', Int. Conf. on Finite Element in Nonlinear Solids and Structural Mechanics, Geilo, Norway, 29th August - 1st September, (1977).

(28) H. D. Hibbitt, E. B. Becker and L. M. Taylor, 'Nonlinear Analysis of Some Slender Pipelines', Computer Methods Appl. Mech. Engrg, 17/18, pp. 203-225, (1979).

(29) Cary K. Mak and Der-Wang Kao, 'Finite Element Analysis of Buckling and Post Buckling Behaviours of Archs with Geometric Imperfections', Computers and Structures, Vol. 3, pp. 149-161, (1973).

(30) Cenap Oran and Aslam Kassimali, 'Large Deformations of Framed Structures under Static and Dynamic Loads', Computers and Structures, Vol. 6, pp. 539-547, (1976).

(31) T. Y. Yang, 'Matrix Displacement Solution to Elastica Problems of Beams and Frames', Int. J. Solids Structures, Vol. 9, pp. 829-842, (1973).

(32) T. Y. Yang and Roger J. Wagner, 'Snap-Buckling of Nonlinearly-Elastic Finite Element Bars', Computers and Structures, Vol. 3, pp. 1473-1481, (1973).

(33) Paul Lyons, 'Large-Deflection Elasto-Plastic Analysis of Stiffened Shells Using Semiloof Elements', Numerical Methods for nonlinear Problems, Proc. Int. Conf. at University of Swansea, 2nd - 5th September, C. Taylor, E. Hinton and D. R. J. Owen (editors), Vol. 1, pp. 407-424, Pineridge Press, (1980).

(34) H. Javaherian, P. J. Dowling and L. P. R. Lyons, 'Nonlinear Finite Element Analysis of Shell Structures Using The Semiloof Element', Computers and Structures, Vol. 12, pp. 147-159, (1980).

(35) Bruce M. Irons, 'The Semiloof Shell Element', Chapter 11, Finite Elements for Thin Shells and Curved Members, D. G. Ashwell and R. H. Gallgher (editors), John Wiley and Sons, (1976).

(36) B. Kråkeland, 'Nonlinear Analysis of Shells Using Degenerate Isoparametric Elements', Finite Elements in Nonlinear Mechanics, Bergan et al (editors), Vol. 1, pp. 265-284, Tapir Press, Trondheim, (1978).

(37) Lawrence E. Malvern, 'Introduction to The Mechanics of a Continuous Medium, Prentice-Hall, New Jersey, (1969).

(38) L. P. R. Lyons, 'A General Finite Element System with Special Reference to the Analysis of Cellular Structures', Ph.D. Thesis, Imperial College, London, (1977).

(39) L. P. R. Lyons, The LUSAS Users Manual, The Stewart Lyons Partnership, London, England, (1980).

(40) R. M. McMeeking and J. R. Rice, 'Finite Element Formulations for Problems of Large Elastic-Plastic Deformation', Int. J. Solids Structures, Vol. 11, pp. 601-616, (1975).

(41) J. T. Oden, 'Some Results of Finite Element Applications in Finite Elasticity', Computers and Structures, Vol. 3, pp. 175-194, (1973).

(42) H. D. Hibbitt, P. V. Marcal and J. R. Rice, 'A Finite Element Formulation for Problems of Large Strain and Large Displacement', Int. J. Solids Structures, Vol. 6, pp. 1069-1086,(1970).

(43) Thomas J. R. Hughes,and James Winget, 'Finite Rotation Effects in Numerical Integration of Rate Constitutive Equations Arising in Large-Deformation Analysis', Int. J. Num. Methods Engrg, Vol. 15, pp. 1862-1867, (1980).

(44) Klaus-Jürgen Bathe, Ekkehard Ramm and Edward L. Wilson, 'Finite Element Formulations for Large Deformation Dynamic Analysis', Int. J. Num. Methods Engrg. Vol. 9, pp. 353-386, (1975).

(45) Klaus-Jürgen Bathe and Haluk Ozdemir, 'Elastic-Plastic Large Deformation Static and Dynamic Analysis', Computers and Structures, Vol. 6, pp. 81-92, (1976).

(46) G. A. Dupuis, H. D. Hibbitt, S. F. McNamara and P. V. Marcal, 'Nonlinear Material and Geometric Behaviour of Shell Structures', Computers and Structures, Vol. 1, pp. 223-239, (1971).

(47) Haluk Ozdemir, 'A Finite Element Approach for Cable Problems', Int. J. Solids Structures, Vol. 15, pp. 427-437, (1979).

(48) J. H. Argyris, H. Balmer, J. St. Doltsinis, P. C. Dunne, M. Haase, M. Kleiber, G. A. Malejannakis, H. P. Mlehnek, M. Muller and D. W. Scharpf, 'Finite Element Method - The Natural Approach', Computer Methods Appl. Mech. Engrg, 17/18, pp. 1-106, (1979).

(49) Kran S. Surana, 'Geometrically Nonlinear Formulation for the Axisymmetric Shell Elements', Int. J. Num. Methods Engrg, Vol. 18, pp. 477-502, (1982).

(50) Lloyd Hamilton Donnell, Beams, Plates and Shells, McGraw-Hill, (1976).

(51) P. V. Marcal and I. P. King, 'Elastic-Plastic Analysis of Two Dimensional Stress Systems by the Finite Element Method', Int. J. Mech. Sci., Vol. 9, pp. 143-155, (1967).

(52) G. C. Nayak and O. C. Zienkiewicz, 'Elasto-Plastic Stress Analysis - A Generalization for Various Constitutive Relations including Strain Softening', Int. J. Num. Methods Engrg, Vol. 5, pp. 113-135, (1972).

(53) Y. Yamada and N. Yoshimura, 'Plastic Stress-Strain Matrix and its Application for the Solution of Elastic-Plastic Problems by The Finite Element Method', Int. J. Mech. Sci., Vol. 10, pp. 343-354, (1968).

(54) O. C. Zienkiewicz, S. Valliappan and I. P. King, 'Elasto-Plastic Solutions of Engineering Problems 'Initial Stress' Finite Element Approach', Int. J. Num. Methods Engrg, Vol. 1, pp. 75-100, (1969).

(55) M. A. Crisfield, 'Large Deflection Elasto-Plastic Buckling Analysis of Plates Using Finite Elements', TRRL Report LR 393, Transport and Road Research Laboratory, Crowthorne, Berkshire, (1973).

(56) M. A. Crisfield, 'A Combined Rayleigh-Ritz/Finite Element Method for the Nonlinear Analysis of Stiffened Plated Structures', Computers and Structures, Vol. 8, pp. 679-689, (1978).

(57) Walter E. Haiseler, James A. Stricklin and Fredrick J. Stebbins, 'Development and Evaluation of Solution Procedures for Geometrically Nonlinear Structural Analysis', AIAA Journal, Vol. 10, pp. 264-272, March (1972).

(58) C. S. Desia and J. T. Abel, 'Techniques for Nonlinear Analysis', Chapter 7, Introduction to the Finite Element Method, Van Nostrand Reinhold.

(59) M. A. Crisfield, 'Iterative Solution Procedures for Linear and Nonlinear Structural Analysis', TRRL Report 900, Transport and Road Research Laboratory, Crowthorne, Berkshire, (1978).

(60) M. A. Crisfield, 'A Faster Modified Newton-Raphson Iteration', Computer Methods Appl. Mech. Engrg, Vol. 20, pp. 267-278, (1979).

(61) R. D. Wood and O. C. Zienkiewicz, 'Geometrically Nonlinear Finite Element Analysis of Beams, Frames, Arches and Axisymmetric Shells', Computers and Structures, Vol. 7, pp. 725-735, (1977).

(62) David Bushnell, 'Bifurcation Buckling of Shells of Revolution including Large Deformations, Plasticity and Creep', Int. J. Solids Structures, Vol. 10, pp. 1287-1305, (1974).

(63) Abdur Razzaque, 'Program for Triangular Bending Elements with Derivative Smoothing', Int. J. Num. Methods Engrg, Vol. 6, pp. 333-343, (1973).

(64) B. M. Irons and S. Ahmed, 'The Semiloof Beam and Shell', Chapter 18, Techniques of Finite Element Analysis, Ellis Harwood, Chichester, (1980).

(65) F. Albuquerque, 'A Beam Element for Use with the Semiloof Shell Element, MSc Thesis, University of Wales, (1973).

(66) A. R. E. Mohamed, 'A Finite Element Study of a Thin Curved Beam Element', MSc Thesis, The City University, London, (1978).

(67) E. P. Popov and P. Sharifi, 'A Refined Curved Element for Thin Shells of Revolution', Int. J. Num. Methods Engrg, Vol. 3, pp. 495-508, (1971).

(68) Ajaya K. Gupta and Paul S. Ma, 'Error in Eccentric Beam Formulation', Int. J. Num. Methods Engrg, Vol. 11. pp. 1473-1483, (1977).

(69) Hans A. Balmer, 'Another Aspect of the Error in Eccentric Beam Formulation', Int. J. Num. Methods Engrg, Vol. 12, pp. 1761-1771, (1978).

(70) S. Timoshenko, Strength of Materials - Part I Elementary, 3rd Edition, Van Nostrand Reinhold, (1955).

(71) S. Timoshenko, Strength of Materials - Part II Advanced, 3rd Edition, Van Nostrand Reinhold, (1956).

(72) L. M. Kachanov, Fundamentals of the Theory of Plasticity, Mir Publishers, Moscow, (1974).

(73) V. Z. Vlasov, Thin-Walled Elastic Beams, 2nd Edition, Israel Program for Scientific Translations, Jerusalem, (1961).

(74) K. Zbirohowski-Koscia, Thin Walled Beams from Theory to Practice, Crosby Lockwood and Son, London, (1967).

(75) Martin M. Black, The Analysis and Design of Thin Walled Opened-Section Beams, Symposium Pre-print, Thin Walled Steel Structures, University College Swansea, 11th-14th September, Crosby Lockwood and Son, (1968).

(76) Fathalla M. El-Amin and D. M. Brotton, 'Horizontally Curved Beam Finite Element including Warping', Int. J. Num. Methods Engrg, Vol. 10. pp. 1397-1428) (1976).

(77) Fathalla M. El-Amin and Mohamed A. Kasem, 'Higher Order Horizontally-Curved Beam Finite Element including Warping for Steel Bridges', Int. J. Num. Methods Engrg, Vol. 12, pp. 159-167, (1978).

(78) W. A. Thorton and R. T. Avis, 'Comment on Horizontally Curved Beam Finite Element including Warping', Int. J. Num. Methods Engrg, Vol. 14, pp. 621-623, (1979).

(79) J. W. Bunce and E. H. Brown, 'Non-linear Bending of Thin, Ideally Elastic Rods', Int. J. Mech. Sci., Vol. 18, pp. 435-441, (1976).

(80) K. Mattiasson, 'Numerical Results from Large Deflection Beam and Frame Problems Analysed by Means of Elliptic Integrals', Int. J. Num. Methods Engrg, Vol. 17, pp. 145-153, (1981).

(81) J. T. Holden, 'On the Finite Deflections of Thin Beams', Int. J. Solids Structures, Vol. 8, pp. 1051-1055, (1972).

(82) Murray R. Spiegel,Vector Analysis and an Introduction to Tensor Analysis, Schaum's Outline Series, McGraw-Hill, (1959).

(83) Shahram Nour-omid, A Finite Element Study Using the Semiloof Beam and Shell Elements, MSc Thesis, The City University, (1977).

(84) T. I. Campbell and T. M. Charlton, 'Finite Deformation of a Fully Fixed Beam Comprised of a Nonlinear Material', Int. J. Mech. Sci., Vol. 15, pp. 415-428, (1973).

(85) M. A. Crisfield, 'Full-Range Analysis of Steel Plates and Stiffened Plating under uniaxial Compression', Proc. Instn. Civ. Engrs., Part 2, 59, pp. 595-624, (1975),

(86) Subhash C. Anand and Hwei-Hwang Shaw, 'Elastic Plastic Analysis of a Rolling Disk by Finite Elements', Int. J. Mech. Sci., Vol. 19, pp. 37-44, (1977).

(87) J. W. Bunce and E. H. Brown, 'The Finite Deflection of Plane Frames', Int. J. Mech. Sci., Vol. 15, pp. 189-198, (1973).

(88) David Bushnell and Gerard D. Galletly, 'Comparisons of Test and Theory for Non-symmetric Elastic-Plastic Buckling of Shells of Revolution', Int. J. Solids Structures, Vol. 10. pp, 1271-1286, (1974).

(89) Kuo-Kuang Chen, 'A Triangular Plate Finite Element for Large Displacement Elastic Plastic Analysis of Automobile Structural Components', Computers and Structures, Vol. 10, pp. 203-215, (1979).

(90) Y. K. Cheung, P. M. Wong and H. C. Chan, 'Generation of Higher Order sub-parametric Bending Elements', Eng. Struct., Vol. 2, pp. 2-8, (1980).

(91) E. Hinton, A. Razzaque, O. C. Zienkiewicz and J. D. Davies, 'A Simple Finite Element Solution for Plates of Homogeneous, Sandwich and Cellular Construction', Proc. Instn. Civ. Engrs, Part 2, 59, pp. 43-65, (1975).

(92) J. Jirousek, 'A Family of Variable Section Curved Beam and Thick-Shell or Membrane-Stiffening Isoparametric Elements', Int. J. Num. Methods Engrg, Vol. 17, pp. 171-186, (1981).

(93) Peter C. Kohnke, 'Large Deflection Analysis of Frame Structures by Fictitious Forces', Int. J. Num. Methods Engrg. Vol. 12, pp. 1279-1294, (1978).

(94) Carl M. Larsen and Dag Kavlie, 'Nonlinear Analysis of Oil Pipelines by Potential Minimization',Computers and Structures, Vol. 8, pp. 733-743, (1978).

(95) S. Nagarajan and E. P. Popov, 'Plastic and Viscoplastic Analysis of Axisymmetric Shells', Int. J. Solids Structures, Vol. 11. pp. 1-19, (1975).

(96) S. Ranganath and R. J. Clifton, 'Finite Deflection Dynamics of Elastic Beams', Int. J. Solids Structures, Vol. 10. pp. 557-568, (1974).

(97) T. M. Roberts and D. G. Ashwell, 'The Use of Finite Element Mid-Increment Stiffness Matrices in the Post-Buckling Analysis of Imperfect Structures', Int. J. Solids Structures, Vol. 7, pp. 805-823, (1971).

APPENDIX I

EXPLICIT FORM OF THE CONSTRAINED DISPLACEMENT FIELD FOR THE 2-D STRAIGHT BEAM ELEMENT

The transvers displacement variation for a straight two dimensional beam element (Figure 3.4) is obtained by the constraint technique. It is possible to obtain either a non-conforming or an exactly conforming displacement field using alternative choices for the initial assumed variation of displacement. Two alternative approaches that give identical results are available. These are

(i) assuming the initial variation in terms of generalised variables

(ii) using independent interpolation of the initial vairables.

The first method can be used to formulate straight elements explicitly. The second method is best carried out numerically and is, therefore, suitable to be used in the development of curved elements.

I.1 INCOMPATIBLE DISPLACEMENT FIELD

The non-conforming displacement field is derived by each of the two methods for comparison.

I.1.1 GENERALISED VARIABLES

Consider that parabolic variations of the displacement v and its derivative θ for a straight beam element (Figure 3.4a) are defined in terms of the natural coordinate ξ and generalised variables α_i as follows

$$v = \alpha_1 + \alpha_2\xi + \alpha_3 \xi^2$$

$$\theta = \alpha_4 + \alpha_5\xi + \alpha_6 \xi^2 \quad \ldots \quad \ldots \quad \ldots \quad \ldots \quad (I.1)$$

The derivative of v with respect to the local x coordinate is then given by

$$\frac{dv}{dx} = \frac{dv}{d\xi}\frac{d\xi}{dx} = \frac{1}{c}(\alpha_2 + 2\alpha_3\xi) \quad \ldots \quad \ldots \quad \ldots \quad (I.2)$$

Four of the six equations required for a solution for α_i in terms of the nodal variables $(v_1, \theta_1, v_2, \theta_2)$ are obtained from the two end conditions as

$$v_1 = \alpha_1 - \alpha_2 + \alpha_3$$

$$v_2 = \alpha_1 + \alpha_2 + \alpha_3$$

$$\theta_1 = \alpha_4 - \alpha_5 + \alpha_6$$

$$\theta_2 = \alpha_4 + \alpha_5 + \alpha_6 \quad \ldots \quad \ldots \quad \ldots \quad \ldots \quad (I.3)$$

The two additional equations required are obtained by applying the condition $\theta = \frac{dv}{dx}$ at the two Gauss points $\xi = \pm 1/\sqrt{3}$. Therefore, from (I.1) and (I.2) we have

$$\alpha_4 - g\alpha_5 + \frac{1}{3}\alpha_6 = \frac{1}{c}(\alpha_2 - 2g\alpha_3)$$
$$\alpha_4 + g\alpha_5 + \frac{1}{3}\alpha_6 = \frac{1}{c}(\alpha_2 + 2g\alpha_3) \quad \ldots \quad \ldots \quad (I.4)$$

in which $g = 1/\sqrt{3}$

Equation (I.4) gives relations between the generalised variables for v and those for θ of the form

$$\alpha_2 = c\,\alpha_4 + \frac{c}{3}\alpha_6$$

$$\alpha_3 = \frac{c}{2}\alpha_5 \quad \ldots \quad \ldots \quad \ldots \quad \ldots \quad \ldots \quad \ldots \quad (I.5)$$

Solving the six equations (I.3) and (I.5) for α_i gives

$$\alpha_1 = \frac{1}{2} v_1 + \frac{1}{2} v_2 + \frac{c}{4} \theta_1 - \frac{c}{4} \theta_2$$

$$\alpha_2 = -\frac{1}{2} v_1 + \frac{1}{2} v_2$$

$$\alpha_3 = - \frac{c}{4} \theta_1 + \frac{c}{4} \theta_2$$

$$\alpha_4 = -\frac{3}{4c} v_1 + \frac{3}{4c} v_2 - \frac{1}{4} \theta_1 - \frac{1}{4} \theta_2$$

$$\alpha_5 = - \frac{1}{2} \theta_1 + \frac{1}{2} \theta_2$$

$$\alpha_6 = \frac{3}{4c} v_1 - \frac{3}{4c} v_2 + \frac{3}{4} \theta_1 + \frac{3}{4} \theta_2 \quad \ldots \quad \ldots \qquad (I.6)$$

The constrained displacement field is then obtained by substituting for α_i from (I.6) into (I.1), so that

$$v = (\frac{1}{2} - \frac{1}{2} \xi)v_1 + (\frac{1}{2} + \frac{1}{2} \xi)v_2 + \frac{c}{4}(1 - \xi^2)\theta_1 -$$

$$- \frac{c}{4}(1 - \xi^2)\theta_2$$

$$\theta = - \frac{3}{4c}(1 - \xi^2)v_1 + \frac{3}{4c}(1 - \xi^2)v_2 + \frac{1}{4}(- 1 - 2\xi + 3\xi^2)\theta_1 +$$

$$+ \frac{1}{4}(- 1 + 2\xi + 3\xi^2)\theta_2 \quad \ldots \quad \ldots \quad \ldots \quad \ldots \qquad (I.7)$$

I.1.2 Independent Interpolation

The displacement v and the derivative θ (Figure 3.4b) are defined by independint interpolation from the nodal values as follows

$$\begin{Bmatrix} v \\ \\ \\ \theta \end{Bmatrix} = \sum_{i=1}^{3} N_i \begin{Bmatrix} v \\ \\ \\ \theta \end{Bmatrix}_i \quad \ldots \quad \ldots \quad \ldots \quad \ldots \qquad (I.8)$$

where the hierarchical shape function N_i are given in terms of the natural coordinate ξ by

$$N_1 = \frac{1}{2} - \frac{1}{2}\xi \,,\; N_2 = \frac{1}{2} + \frac{1}{2}\xi \,,\; N_3 = 1 - \xi^2 \quad \ldots \qquad (I.9)$$

and the variables at the middle node are the departures from linearity Δv_3 and $\Delta \theta_3$.

The derivatives of N_i(Equation (I.9)) with respect to the local x are

$$\frac{dN_1}{dx} = -\frac{1}{2c} \,,\; \frac{dN_2}{dx} = \frac{1}{2c} \,,\; \frac{dN_3}{dx} = -\frac{2}{c}\xi \qquad \ldots \qquad (I.10)$$

in which $c = \frac{dx}{d\xi}$

The constraint equation to be applied at the two Gauss points $\xi = \pm 1/\sqrt{3}$ is defined from (I.8) as follows

$$- \theta + \frac{dv}{dx} = - \sum_{i=1}^{3} N_i \theta_i + \sum_{i=1}^{3} \frac{dN_i}{dx} v_i = 0 \quad \ldots \qquad (I.11)$$

Substituting from (I.9) and (I.10) into (I.11) and evaluating this at $\xi = \pm 1/\sqrt{3}$ gives

$$- \frac{1}{2} v_1 + \frac{1}{2} v_2 + 2g \, \Delta v_3 = c(\frac{1}{2} + \frac{g}{2})\theta_1 + $$

$$+ c(\frac{1}{2} - \frac{g}{2})\theta_2 + \frac{2c}{3} \Delta\theta_3$$

$$- \frac{1}{2} v_1 + \frac{1}{2} v_2 - 2g \, \Delta v_3 = c(\frac{1}{2} - \frac{g}{2})\theta_1 +$$

$$+ c(\frac{1}{2} + \frac{g}{2})\theta_2 + \frac{2c}{3} \Delta\theta_3 \quad \ldots \quad \ldots \quad \ldots \qquad (I.12)$$

where $g = 1/\sqrt{3}$

Solving (I.12) for the displacements to be eliminated Δv_3 and $\Delta\theta_3$ we have

$$\Delta v_3 = \frac{c}{4} \theta_1 - \frac{c}{4} \theta_2$$

$$\Delta\theta_3 = - \frac{3}{4c} v_1 + \frac{3}{4c} v_2 - \frac{3}{4} \theta_1 - \frac{3}{4} \theta_2 \quad \ldots \qquad (I.13)$$

The constrained displacement field is now obtained by substituting from (I.9) into (I.8) and using (I.13) to eliminate the unwanted variables Δv_3 and $\Delta\theta_3$. Therefore

$$v = (\frac{1}{2} - \frac{1}{2}\xi)v_1 + (\frac{1}{2} + \frac{1}{2}\xi)v_2 + \frac{c}{4}(1 - \xi^2)\theta_1 -$$

$$- \frac{c}{4}(1 - \xi^2)\theta_2$$

$$\theta = - \frac{3}{4c}(1 - \xi^2)v_1 + \frac{3}{4c}(1-\xi^2)v_2 + \frac{1}{4}(-1 - 2\xi + 3\xi^2)\theta_1 +$$

$$+ \frac{1}{4}(-1+ 2\xi + 3\xi^2)\theta_2$$

which is exactly the same as (I.7).

Differentiating v in (I.7) with respect to the local x gives

$$\frac{dv}{dx} = - \frac{1}{2c} v_1 + \frac{1}{2c} v_2 - \frac{1}{2}\xi\theta_1 + \frac{1}{2}\xi\theta_2 \qquad \ldots \qquad (I.14)$$

This "Smoothed" derivative is clearly incompatible with θ in Equation (I.7). The two derivatives are equal at the Gauss points $\xi = \pm 1/\sqrt{3}$ only.

It is possible, however, to obtain a completely compatible displacement field by assuming the original independent interpolation of both v and θ to be cubic and then eliminating the four internal degrees of freedom (Figure 3.4d).

I.2 CONFORMING DISPLACEMENT FIELD

Following the approach of using generalised variables the variation of v and θ is assumed to be

$$v = \alpha_1 + \alpha_2 \xi + \alpha_3 \xi^2 + \alpha_4 \xi^3$$

$$\theta = \alpha_5 + \alpha_6 \xi + \alpha_7 \xi^2 + \alpha_8 \xi^3 \quad \ldots \quad \ldots \quad (I.15)$$

The derivative of v with respect to the local x is given from (I.15) by

$$\frac{dv}{dx} = \frac{dv}{d\xi} \frac{d\xi}{dx} = \frac{1}{c}(\alpha_2 + 2\alpha_3 \xi + 3\alpha_4 \xi^2) \quad \ldots \quad \ldots \quad (I.16)$$

The four equations obtained from (I.15) by applying the end conditions are

$$v_1 = \alpha_1 - \alpha_2 + \alpha_3 - \alpha_4$$

$$v_2 = \alpha_1 + \alpha_2 + \alpha_3 + \alpha_4$$

$$\theta_1 = \alpha_5 - \alpha_6 + \alpha_7 - \alpha_8$$

$$\theta_2 = \alpha_5 + \alpha_6 + \alpha_7 + \alpha_8 \quad \ldots \quad \ldots \quad \ldots \quad (1.17)$$

The four additional equations required are given by applying the constraint condition $\frac{dv}{dx} = \theta$ at the four points $\xi = \mp \frac{3}{5}$, $\mp \frac{1}{5}$ as

$$\frac{1}{c}\alpha_2 - \frac{6}{5c}\alpha_3 + \frac{27}{25c}\alpha_4 = \alpha_5 - \frac{3}{5}\alpha_6 + \frac{9}{25}\alpha_7 - \frac{27}{125}\alpha_8$$

$$\frac{1}{c}\alpha_2 + \frac{6}{5c}\alpha_3 + \frac{27}{25c}\alpha_4 = \alpha_5 + \frac{3}{5}\alpha_6 + \frac{9}{25}\alpha_7 + \frac{27}{125}\alpha_8$$

$$\frac{1}{c}\alpha_2 - \frac{2}{5c}\alpha_3 + \frac{3}{25c}\alpha_4 = \alpha_5 - \frac{1}{5}\alpha_6 + \frac{1}{25}\alpha_7 - \frac{1}{125}\alpha_8$$

$$\frac{1}{c}\alpha_2 + \frac{2}{5c}\alpha_3 + \frac{3}{25c}\alpha_4 = \alpha_5 + \frac{1}{5}\alpha_6 + \frac{1}{25}\alpha_7 + \frac{1}{125}\alpha_8$$

$$\ldots \quad \ldots \quad \ldots \quad \ldots \quad (I.18)$$

which gives relations between the generalised variables for v and those for θ of the form

$$\alpha_2 = c\ \alpha_5$$

$$\alpha_3 = \frac{c}{2}\ \alpha_6$$

$$\alpha_4 = \frac{c}{3}\ \alpha_7$$

$$\alpha_8 = 0 \qquad \ldots\ \ldots\ \ldots\ \ldots\ \ldots\ \ldots \qquad (I.19)$$

Solving the eight equations (I.19) and (I.17) for α_i gives

$$\alpha_1 = \frac{1}{2} v_1 + \frac{1}{2} v_2 + \frac{c}{4} \theta_1 - \frac{c}{4} \theta_2$$

$$\alpha_2 = -\frac{3}{4} v_1 + \frac{3}{4} v_2 - \frac{c}{4} \theta_1 - \frac{c}{4} \theta_2$$

$$\alpha_3 = -\frac{c}{4} \theta_1 + \frac{c}{4} \theta_2$$

$$\alpha_4 = \frac{1}{4} v_1 - \frac{1}{4} v_2 + \frac{c}{4} \theta_1 + \frac{c}{4} \theta_2$$

$$\alpha_5 = -\frac{3}{4c} v_1 + \frac{3}{4c} v_2 - \frac{1}{4} \theta_1 - \frac{1}{4} \theta_2$$

$$\alpha_6 = -\frac{1}{2} \theta_1 + \frac{1}{2} \theta_2$$

$$\alpha_7 = \frac{3}{4c} v_1 - \frac{3}{4c} v_2 + \frac{3}{4} \theta_1 + \frac{3}{4} \theta_2$$

$$\alpha_8 = 0 \qquad \ldots\ \ldots\ \ldots\ \ldots\ \ldots\ \ldots \qquad (I.20)$$

The completely conforming constrained displacement field is then obtained by substituting from (I.20) into (I.15) as follows

$$v = (\frac{1}{2} - \frac{3}{4}\xi + \frac{1}{4}\xi^3)v_1 + (\frac{1}{2} + \frac{3}{4}\xi - \frac{1}{4}\xi^3)v_2 +$$

$$+ \frac{c}{4}(1 - \xi - \xi^2 + \xi^3)\theta_1 + \frac{c}{4}(-1 - \xi + \xi^2 + \xi^3)\theta_2$$

$$\theta = -\frac{3}{4c}(1 - \xi^2)v_1 + \frac{3}{4c}(1 - \xi^2)v_2 + \frac{1}{4}(-1 - 2\xi + 3\xi^2)\theta_1 +$$

$$+ \frac{1}{4}(-1 + 2\xi + 3\xi^2)\theta_2 \quad \ldots \quad \ldots \quad \ldots \quad \ldots \qquad (I.21)$$

A P P E N D I X II

TOTAL LAGRANGIAN MODIFIED INCREMENTAL EQUILIBRIUM EQUATIONS FOR A TWO-DIMENSIONAL STATE OF STRESS

The Total Lagrangian formulation for a general state of stress, in which isoparametric elements are used, is well established. Many investigators have demonstrated the accuracy and generality of such a formulation. All formulations that have been presented in literature are, however, based on the Green-Lagrange strains and direct proportionality is assumed between these strains and the 2nd Piola-Kirchhoff stresses in the internal virtual work expression. A formulation which is based on true stress measures will have obvious advantages especially for combined geometric and material nonlinearity solutions since the established flow rules are based on true stresses. The modified incremental equilibrium equations for a two-dimensional state of stress are developed here by using the conventional strain and the nominal stress as work conjugate variables in the virtual work expression. The formulation is suitable for use with the versatile isoparametric elements.

II.1 STRESS-STRAINS RELATIONS

The three stress components in two-dimensions are defined in terms of the strains as follows

$$\begin{Bmatrix} \sigma_x \\ \sigma_y \\ \tau_{xy} \end{Bmatrix} = [D] \begin{Bmatrix} \varepsilon'_{xx} \\ \varepsilon'_{yy} \\ \gamma'_{xy} \end{Bmatrix}$$

OR

$$\sigma = D\,\varepsilon' \qquad \ldots \quad \ldots \quad \ldots \quad \ldots \quad \ldots \qquad (II.1)$$

where σ is the nominal stress vector, ε' is the conventional strain vector and D is the modulus matrix.

II.2 STRAIN-DISPLACEMENT RELATIONS

The direct strains ε'_{xx} and ε'_{yy} are defined by the change in length per unit initial length of line elements originally oriented parallel to the X and Y axes respectively. The shear strain is the change in the right angle. This shear strain is assumed to be small so that $\sin\gamma'$ can be assumed to be equal to γ'. Convected coordinates and differentiation are to be used.

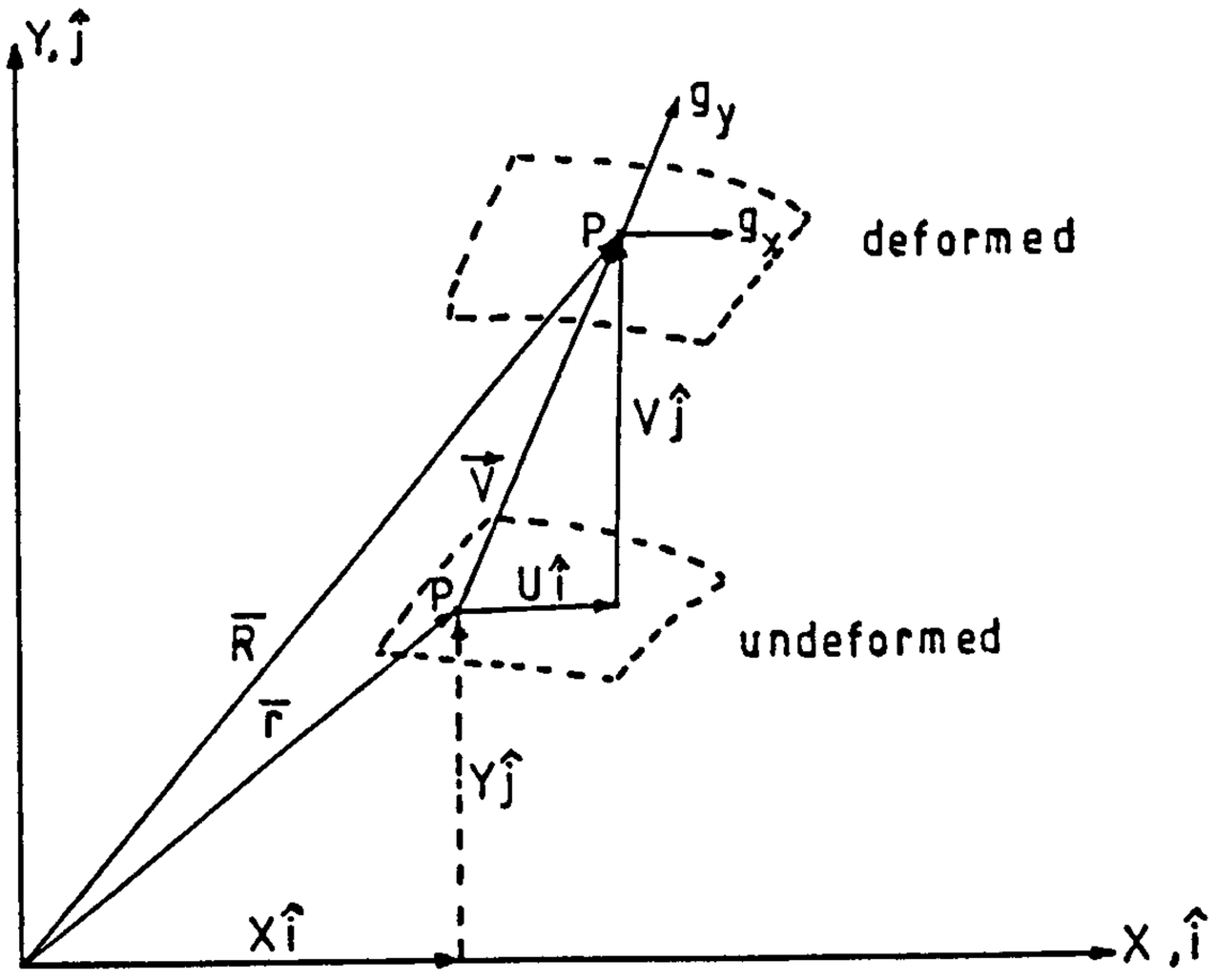

FIGURE II.1 - DEFORMATION GEOMETRY

Referring to Figure II.1, the position vector of a point P(x, y) after deformation is

$$\bar{R} = (X + U)\hat{i} + (Y + V)\hat{j} \qquad \ldots \quad \ldots \quad \ldots \qquad (II.2)$$

in which U and V are the components of displacement in the global axes directions.

The displacement gradient vectors are given from (II.2) by

$$\frac{\partial \bar{R}}{\partial X} = g_x = (1 + \frac{dU}{dx})\hat{i} + \frac{dV}{dx}\hat{j}$$

$$\frac{\partial \bar{R}}{\partial Y} = g_y = \frac{dU}{dY}\hat{i} + (1 + \frac{dV}{dY})\hat{j} \quad \ldots \quad \ldots \quad \ldots \quad \text{(II.3)}$$

from which the Green-Lagrange strains are obtained as follows

$$\varepsilon = \begin{Bmatrix} \varepsilon_{xx} \\ \varepsilon_{yy} \\ \gamma_{xy} \end{Bmatrix} = \begin{Bmatrix} \frac{1}{2}(\frac{\partial \bar{R}}{\partial X} \cdot \frac{\partial \bar{R}}{\partial X} - 1) \\ \frac{1}{2}(\frac{\partial \bar{R}}{\partial Y} \cdot \frac{\partial \bar{R}}{\partial Y} - 1) \\ \frac{\partial \bar{R}}{\partial X} \cdot \frac{\partial \bar{R}}{\partial Y} \end{Bmatrix}$$

$$= \begin{Bmatrix} \frac{dU}{dX} + \frac{1}{2}(\frac{dU}{dX})^2 + \frac{1}{2}(\frac{dV}{dX})^2 \\ \frac{dV}{dY} + \frac{1}{2}(\frac{dU}{dY})^2 + \frac{1}{2}(\frac{dV}{dY})^2 \\ \frac{dU}{dY} + \frac{dV}{dX} + \frac{dU}{dX}\frac{dU}{dY} + \frac{dV}{dX}\frac{dV}{dY} \end{Bmatrix} \quad \text{(II.4)}$$

Now defining the direct strains as change in length per unit initial length gives

$$\varepsilon'_{xx} = (\frac{\partial \bar{R}}{\partial X} \cdot \frac{\partial \bar{R}}{\partial X})^{1/2} - 1 = (1 + 2\varepsilon_{xx})^{1/2} - 1$$

$$\varepsilon'_{yy} = (\frac{\partial \bar{R}}{\partial Y} \cdot \frac{\partial \bar{R}}{\partial Y})^{1/2} - 1 = (1 + 2\varepsilon_{yy})^{1/2} - 1 \quad \text{(II.5)}$$

The shear strain is defined as the change in the right angle. Assuming that the shear angle is small we obtain

$$\gamma_{xy} = \frac{\partial \bar{R}}{\partial X} \cdot \frac{\partial \bar{R}}{\partial Y} = \left|\frac{\partial \bar{R}}{\partial X}\right| \times \left|\frac{\partial \bar{R}}{\partial Y}\right| \cos(90 - \gamma'_{xy})$$

$$\simeq (1 + 2\varepsilon_{xx})^{1/2} \times (1 + 2\varepsilon_{yy})^{1/2} \gamma'_{xy}$$

... ... (II.6)

which gives the shear strain as

$$\gamma'_{xy} = \frac{\gamma_{xy}}{(1 + 2\varepsilon_{xx})^{1/2} \times (1 + 2\varepsilon_{yy})^{1/2}} \quad \ldots \quad (II.7)$$

from (II.5) and (II.7) the variation in strain is

$$\delta\varepsilon' = \begin{Bmatrix} \delta\varepsilon'_{xx} \\ \delta\varepsilon'_{yy} \\ \delta\gamma'_{xy} \end{Bmatrix} \begin{bmatrix} \frac{1}{(1+2\varepsilon_{xx})^{1/2}} & , & 0 & , & 0 \\ 0 & , & \frac{1}{(1+2\varepsilon_{yy})^{1/2}} & , & 0 \\ \frac{-\gamma_{xy}}{(1+2\varepsilon_{xx})^{3/2}\,(1+2\varepsilon_{yy})^{1/2}} & , & \frac{-\gamma_{xy}}{(1+2\varepsilon_{xx})^{1/2}\,(1+2\varepsilon_{yy})^{3/2}} & , & \frac{1}{(1+2\varepsilon_{xx})^{1/2}\,(1+2\varepsilon_{yy})^{1/2}} \end{bmatrix} \begin{Bmatrix} \delta\varepsilon_{xx} \\ \delta\varepsilon_{yy} \\ \delta\gamma_{xy} \end{Bmatrix}$$

$$= H^{*}\ \delta\varepsilon \qquad \ldots\ \ldots\ \ldots\ \ldots\ \ldots\ \ldots\ \ldots\ \ldots \qquad \text{(II.8)}$$

The internal virtual work expression is written using (II.8) and (II.1) as follows

$$\delta W_{int} = \int_V \delta\varepsilon'^{T}\sigma\ dV = \int_V \delta\varepsilon^{T}\ H^{*T}\ D\ \varepsilon'\ dV \qquad \ldots\ \ldots\ \ldots\ \ldots\ \ldots\ \ldots\ \ldots\ \ldots \qquad \text{(II.9)}$$

The tangent stiffness matrix is obtained by taking variations of (II.9) with respect to the nodal variables provided that the applied loads are conservative. The variation of (II.9) is

$$d\,\delta W_{int} = \int_V \delta\varepsilon^T H^{*T} D\, d\varepsilon'\, dV + \int_V d\delta\varepsilon^T\, H^{*T}\sigma\, dV +$$

$$+ \int_V \delta\varepsilon^T dH^{*T}\sigma\, dV$$

$$= \delta a^T\left[(K_o + K_L)da + K_\sigma\, da + K_\sigma^*\, da\right]$$

... ... (II.10)

The first and second terms in (II.10) define the well known linear strain (infinitesimal strain and initial displacement) and geometric stiffness matrices respectively. The third term introduces an additional geometric stiffness matrix.

II.3 FINITE ELEMENT FORMULATION

The Green strains ε (Equation (II.4)) and their variations $\delta\varepsilon$ are defined in terms of the nodal variables in a finite element representation as follw follows

$$\varepsilon = \begin{Bmatrix} \frac{dU}{dX} \\ \frac{dV}{dX} \\ \frac{dU}{dY} + \frac{dV}{dX} \end{Bmatrix} + \frac{1}{2}\begin{bmatrix} \frac{dU}{dX} & \frac{dV}{dX} & 0 & 0 \\ 0 & 0 & \frac{dU}{dY} & \frac{dV}{dY} \\ \frac{dU}{dY} & \frac{dV}{dY} & \frac{dU}{dX} & \frac{dV}{dX} \end{bmatrix} \begin{Bmatrix} \frac{dU}{dX} \\ \frac{dV}{dX} \\ \frac{dU}{dY} \\ \frac{dV}{dY} \end{Bmatrix}$$

$$= B_o\, a + \frac{1}{2} A_\theta\, \theta = \left[B_o + \frac{1}{2} B_L(a)\right]\{a\} \qquad (II.11)$$

$$\theta = \{\frac{dU}{dx} , \frac{dV}{dx} , \frac{dU}{dY} , \frac{dV}{dY}\}^T = G\ a \quad \ldots \quad \ldots \quad (II.12)$$

$$\delta\varepsilon = [B_o + B_L(a)]\delta a = [B_o + A_\theta G]\delta a = B\,\delta a \quad \ldots \quad (II.13)$$

From (II.8) and (II.13) the variations in the geometric strains are now given by

$$\delta\varepsilon' = H^* \delta\varepsilon = H^* B\,\delta a = B^*\,\delta a \quad \ldots \quad \ldots \quad \ldots \quad (II.14)$$

The incremental equilibrium equations are obtained by substituting from (II.14) into (II.10) and equating the internal work to the external work. Since the applied loads are considered to be conservative we have

$$K_T \Delta a = R - \int_V B^T H^{*T} \sigma\ dV \quad \ldots \quad \ldots \quad \ldots \quad \ldots \quad (II.15)$$

where R is the vector of applied equivalent nodal forces. The tangent stiffness matrix K_T is given from (II.10) by

$$K_T = (K_o + K_L) + K_\sigma + K_\sigma^* \quad \ldots \quad \ldots \quad \ldots \quad \ldots \quad (II.16)$$

Therefore from (II.1), (II.10) and (II.14)

$$K_o + K_L = \int_V B^T\ H^{*T} D\ H^*\ B\ dV = \int_V B^{*T} D\ B^*\ dV \quad (II.17)$$

The geometric stiffness matrix K_σ is obtained from (II.10), (II.12) and (II.13) as follows

$$K_\sigma = \int_V \frac{dB^T}{da} H^{*T} \sigma \, dV = \int_V \frac{dB_L^T}{da} H^{*T} \sigma \, dV$$

$$= \int_V G^T \frac{dA_\theta}{da} H^{*T} \sigma \, dV = \int_V G^T S \, G \, dV \quad \ldots \quad (II.18)$$

where

$$S = \begin{bmatrix} \sigma^*_{xx} [I] & \tau^*_{xy} [I] \\ \tau^*_{xy} [I] & \sigma^*_{yy} [I] \end{bmatrix} \quad \ldots \quad \ldots \quad \ldots \quad \ldots \quad (II.19)$$

in which

$$\begin{Bmatrix} \sigma^*_{xx} \\ \sigma^*_{yy} \\ \tau^*_{xy} \end{Bmatrix} = H^{*T} \sigma \quad \ldots \quad \ldots \quad \ldots \quad \ldots \quad \ldots \quad (II.20)$$

and [I] is a 2 x 2 unit matrix

From (II.8), (II.1) and (II.11) we have

$$\delta H^{*T}\sigma = \begin{bmatrix} \dfrac{-\sigma_{xx}}{(1+2\varepsilon_{xx})^{3/2}} + \dfrac{3\gamma_{xy}\,\tau_{xy}}{(1+2\varepsilon_{xx})^{5/2}(1+2\varepsilon_{yy})^{1/2}} & \dfrac{\gamma_{xy}\,\tau_{xy}}{(1+2\varepsilon_{xx})^{3/2}(1+2\varepsilon_{yy})^{3/2}} & \dfrac{-\tau_{xy}}{(1+2\varepsilon_{xx})^{3/2}(1+2\varepsilon_{yy})^{1/2}} \\ & \dfrac{-\sigma_{yy}}{(1+2\varepsilon_{yy})^{3/2}} + \dfrac{3\gamma_{xy}\,\tau_{xy}}{(1+2\varepsilon_{xx})^{1/2}(1+2\varepsilon_{yy})^{5/2}} & \dfrac{-\tau_{xy}}{(1+2\varepsilon_{xx})^{1/2}(1+2\varepsilon_{yy})^{3/2}} \\ \text{Symm} & & 0 \end{bmatrix} \begin{Bmatrix} \delta\varepsilon_{xx} \\ \delta\varepsilon_{yy} \\ \delta\gamma_{xy} \end{Bmatrix}$$

$$= S^* \delta\epsilon = S^* B \delta a \qquad \ldots\ \ldots\ \ldots\ \ldots\ \ldots\ \ldots \qquad (II.21)$$

The additional geometric stiffness matrix K_σ^* is then obtained from (II.10) and (II.21) as

$$K_\sigma^* \int_V B^T \frac{dH^{*T}}{da}\sigma\, dV = \int_V B^T S^* B\, dV \qquad \ldots\ \ldots\ \ldots \qquad (II.22)$$

which is clearly a symmetrical matrix.